



UNIVERSITAT DE
BARCELONA

Sedimentology and sedimentary architecture of the Middle Ordovician Hawaz Formation in the subsurface of the Murzuq Basin (Libya)

Marc Gil Ortiz



Aquesta tesi doctoral està subjecta a la llicència **Reconeixement- NoComercial – SenseObraDerivada 4.0. Espanya de Creative Commons.**

Esta tesis doctoral está sujeta a la licencia **Reconocimiento - NoComercial – SinObraDerivada 4.0. España de Creative Commons.**

This doctoral thesis is licensed under the **Creative Commons Attribution-NonCommercial-NoDerivs 4.0. Spain License.**



UNIVERSITAT DE
BARCELONA



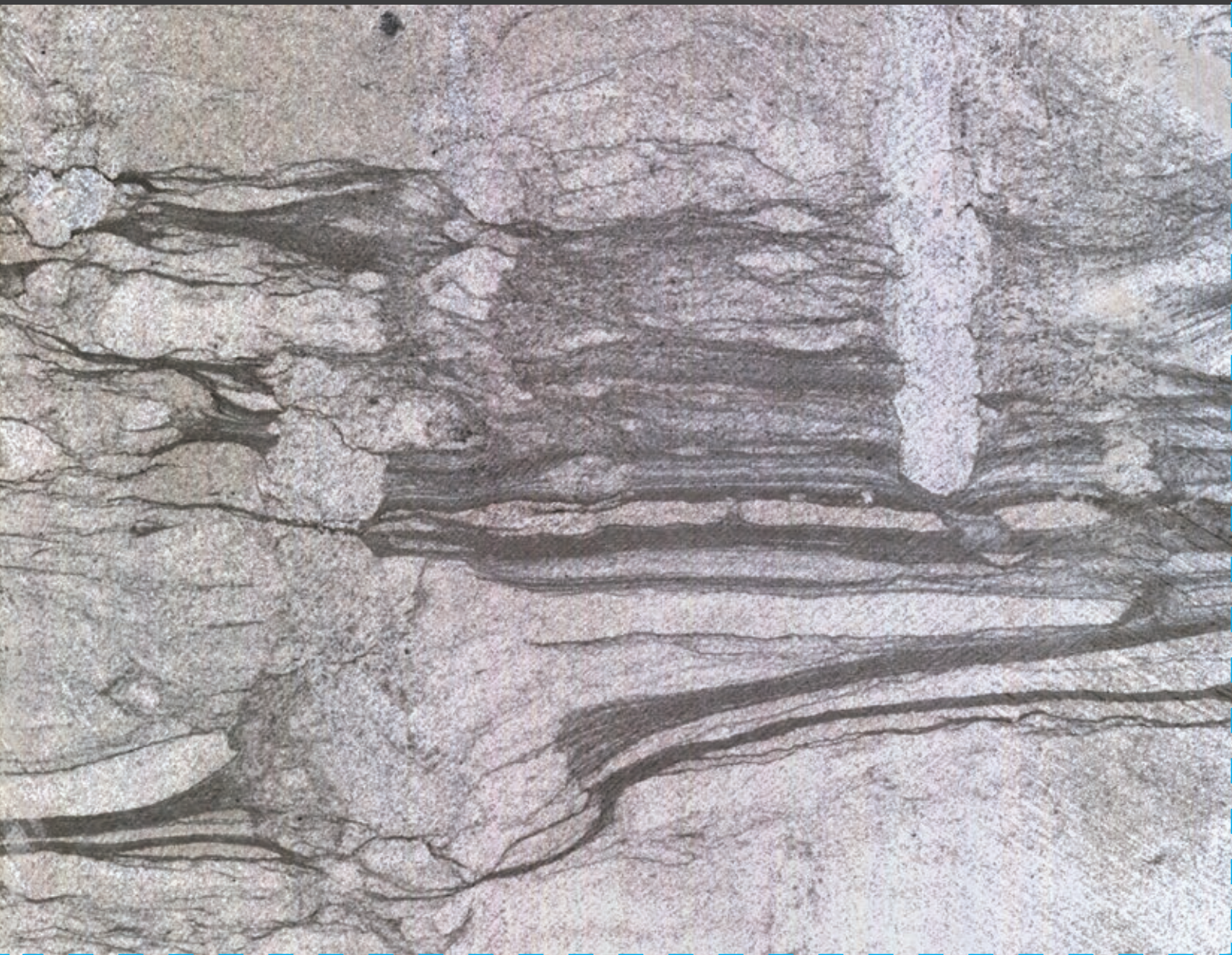
geomodels
institut de recerca

D O C T O R A L T H E S I S

SEDIMENTOLOGY AND SEDIMENTARY
ARCHITECTURE OF THE MIDDLE ORDOVICIAN
HAWAZ FORMATION IN THE SUBSURFACE
OF THE MURZUQ BASIN (LIBYA)

Marc Gil Ortiz

Barcelona, Juliol 2022





UNIVERSITAT DE
BARCELONA



geomodels
institut de recerca

Departament de Dinàmica de la Terra i de l'Oceà

Institut de Recerca Geomodels

Universitat de Barcelona

SEDIMENTOLOGY AND SEDIMENTARY
ARCHITECTURE OF THE MIDDLE ORDOVICIAN
HAWAZ FORMATION IN THE SUBSURFACE OF THE
MURZUQ BASIN (LIBYA)

Memòria de Tesi Doctoral presentada com a compendi d'articles per **Marc Gil Ortiz** per optar al grau de Doctor en Ciències de la Terra per la Universitat de Barcelona.

Aquesta memòria s'ha desenvolupat dins del Programa de Doctorat de Ciències de la Terra (Línia de recerca d'Estratigrafia i Anàlisi de Conques) i s'ha portat a terme sota la direcció de la **Dra. Patricia Cabello López** i el **Dr. Neil David McDougall**, i sota la tutela del **Dr. Mariano Marzo Carpio**.

Marc Gil Ortiz

Barcelona, Juliol 2022

Dra. Patricia Cabello López

Dr. Neil David McDougall

Dr. Mariano Marzo Carpio

This work has been carried out in the *Departament de Dinàmica de la Terra i de l'Oceà* and the *Institut de Recerca Geomodels (UB-Geomodels)*. The author received support from *Proyecto RTI2018-097312-A-I00 de investigación* financed by MCIN/ AEI /10.13039/501100011033/ FEDER “Una manera de hacer Europa” and *Grup de Recerca Consolidat de Geodinàmica i Anàlisi de Conques (GGAC)*, financed by the Generalitat de Catalunya (2017SGR596, 2014SGR467). *Repsol Exploración S.A.* provided the data for the development of this research with the endorsement of partners *TotalEnergies, Equinor, OMV* and the *Libyan National Oil Corporation*. This research project was also benefited from a private academic license of WellCAD 5.4 from *Advanced Logic Technology (ALT)*.

Als meus pares i a la Betlem

Agraïments/Agradecimientos/Acknowledgements

Són moltes les persones a les que voldria dedicar unes paraules i agrair la seva ajuda i col·laboració amb aquest doctorat.

En primer lloc, m'agradaria agrair als meus directors, a la Patricia Cabello i al Neil McDougall per la direcció d'aquesta tesi i tota la seva ajuda al llarg d'aquests 6 anys.

Patricia, d'una banda moltes gràcies per acceptar el repte de dirigir-me aquesta tesi. Sempre has estat disposada a ajudar-me, a escoltar-me i a aconsellar-me de la millor manera possible. Moltes gràcies per les teves idees, per trobar sempre un raconet per poder parlar, per discutir punts de vista, i fins i tot, per ajudar-me a crear noves figures. Tot i quan no tenies temps, tu sempre has trobat un moment per donar-me un cop de mà. Sento que he après molt sobre el món de la recerca durant els darrers anys, i sento que tot això ho he après de tu, t'estic profundament agraït.

Neil, mi referente y mentor desde que llegué a Repsol, e incluso antes. Cuando entré a trabajar en Repsol, solía pensar: "Me gustaría formar parte del equipo de especialistas y trabajar con Neil". Tras un tiempo en la compañía lo conseguí, lástima que no pudiéramos ser compañeros de trabajo durante poco más que tan solo unos meses, aunque fue por una buena causa y yo me alegré mucho por ti. A lo largo de estos años tu ayuda ha sido inefable. Tu me enseñaste a describir un testigo, a interpretar un log de imagen, a llevar a cabo un panel de correlación, a enseñarme lo valioso de la estratigrafía secuencial, por todo esto y mucho más, muchísimas gracias.

A Mariano Marzo, por sus grandes ideas y conocimientos. Recuerdo cuando me planteaba llevar a cabo la tesis doctoral y estaba en búsqueda de directores, Emilio me dijo: "Mariano tiene que formar parte de tu tesis, tiene unas ideas brillantes". A día de hoy, creo que el planteamiento que nos desvelaste al inicio de este doctorado sobre el "no-actualismo" y su aplicabilidad directa en este estudio, es uno de los pilares principales de esta tesis.

A Emilio Ramos, porque sin ti nada de esto hubiera sido posible. Gracias por "reclutarme" para aquel trabajo de final de máster al enterarte de que un estudiante había trabajado en Repsol el verano anterior con unos datos de la Cuenca de Murzuq que tú tan bien conocías. Recuerdo algunas de tus primeras palabras conmigo cuando acepté llevar a cabo el trabajo de TFM contigo: "Tú y yo no nos conocemos de nada, la confianza es algo que se gana con el tiempo", y tanto fue así que, con el tiempo..., me dejaste la llave de tu despacho para que yo pudiera

entrar a trabajar cuando quisiera, me prestaste tu ordenador portátil para que pudiera llevar a cabo un modelo con Petrel, incluso me animaste a publicar los resultados de lo que para mi tan solo era un mero trabajo de final de master. Aunque la hora de jubilarte llegó y no pudiste dirigirme esta tesis, yo te siento como un director más.

Gracias a Repsol, y en particular, a Repsol Exploración Murzuq S.A por prestarme los datos y permitirme llevar a cabo este estudio.

Thanks to partners TotalEnergies, Equinor and OMV, and also the Libyan National Oil Corporation for letting me publish the results of this PhD. Merci/Dakk/Danke/Shukran.

Gracias a Gessal por la ayuda con la digitalización de paneles de correlación que han sido la base de algunas figuras publicadas en nuestro segundo paper.

Thanks to Advanced Logic Technology (ALT) for the WellCAD 5.4 academic license, and special thanks to Mariano Rodríguez Andrino for making it happen.

A mis exjefes en Repsol Noemí Tur, Jean Hsieh y Gonzalo Zamora, porque desde su posición de managers me permitieron dedicar recursos y tiempo a elaborar la tesis en la oficina y compaginarlo con mi trabajo diario siempre y cuando las circunstancias lo permitían. Muchas gracias/Thank you.

Thanks are due to Lamin Abushaala for your support from the beginning, asking for all the requirements and permits to NOC and partners for publishing every single paper and abstract presented in this PhD.

A Alejandro Franco, gracias por toda tu ayuda y paciencia, así como el soporte para lanzar mi primer artículo. De corazón te digo, sos una persona maravillosa.

A Pedro Pulido por su ayuda incansable con la burocracia alrededor de los permisos de confidencialidad necesarios para llevar a cabo esta tesis, así como su predisposición para ayudarme siempre que lo he necesitado. Nunca te estaré lo suficientemente agradecido.

A Francisco J. Bataller, con quien hemos compartido muchos momentos de alegrías y miserias a lo largo de esta “cruzada” llamada doctorado. Todo ha resultado más sencillo con tu apoyo y con tu ayuda.

A Alexandre de Faría, por descubrirme el mundo de la geofísica, y concretamente de la interpretación sísmica. Juntos descubrimos misterios que entrañaba la Formación Hawaz,

muchos de ellos seguirán sin ver la luz, por el momento... Y yo que me pensaba que esto de interpretar sísmica iba solo de pintar horizontes y fallas. Obrigado.

Thanks are due to Edward Jarvis for that talk at the office and all your support. I remember when we met with Neil in that meeting room in Campus Repsol. I was sitting with two guys who had described several tens (possibly hundreds...) of metres of the Hawaz Fm., suggesting them a change of interpretation of the middle and upper Hawaz, after some preliminary observations. I remembered you said: "I always thought the same, but I never dared to change it". You encouraged me to keep my new interpretation and even made some research to share with me data that supported what I was thinking. For an inexperienced guy like me, that meant a lot and really empowered me to trust myself and keep believing in my ideas.

A l'Eduard Remacha, perquè em vas ensenyar a interpretar la geologia de camp amb uns altres ulls. Em vas donar una idea per reinterpretar seccions del meu doctorat que no acabava d'entendre i, a més, m'ho vas ensenyar al camp.

A Francisco Pángaro, por compartir su tiempo y experiencia conmigo que me hicieron entender mejor la posible distribución de algunos de los depósitos de shoreface presentes en este trabajo.

A mis excompañeros de Repsol, Rubén Loma y Laura Net. Gracias Rubén y Laura por esas charlas y cafés en la oficina, tan necesarios algunos días. Aún y cuando los tiempos no eran los mejores, vosotros siempre teníais dibujada una sonrisa en la cara, sois fuente de optimismo y alegría.

Al Joan Flinch, perquè res hagués estat igual sense tu. Una persona trempada amb els millors consells en els moments més indicats. Em vas ajudar des del principi, tant amb les gestions del meu doctorat a Repsol, com en allò més personal.

A Luz, gracias porque sin saberlo, fuiste tú la que me diste la idea de llevar a cabo un PhD.

Al Telm, moltes gràcies pel teu suport. Segur que penses que no has fet res per ajudar-me. A vegades, només unes paraules d'ànims en els moments que més ho necessites són l'ajuda més gran que un pot rebre.

A Alia, por tanto a lo largo de estos últimos años. Las hemos visto de todos colores, pero seguimos en pie. Gracias por tantas charlas y abrazos. Siempre hay luz al final del túnel.

Als meus pares, el Joan i la Núria, per l'estima tan gran i l'ajuda que m'heu donat al llarg de tota la vida, i especialment durant aquests darrers anys, així com per haver-me guiat per ser una

bona persona en aquest món tan difícil. Espero ser la meitat de bon pare del que heu sigut vosaltres amb mi.

A la Maggy, per ensenyar-me el significat de perseverança i estima incondicional.

A la Laura, perquè em dones força per aixecar-me cada dia i lluitar pel futur. Mai havia estimat tant a ningú en tant poc temps.

A Betlem, por todo tu amor y apoyo incondicionales, aún en los momentos más difíciles tú siempre estás ahí. Esto va dedicado especialmente para ti.

Als que ja no hi sou, i als que esteu per venir.

Per tots/es vosaltres, aquest treball també és vostre.

Table of contents

RESUM	1
ABSTRACT	7
PREFACE	13
Motivation and objectives.....	15
Description and structure of the thesis.....	18
CHAPTER 1. INTRODUCTION	23
1.1. Exploration in the Murzuq Basin.....	25
1.2. Sedimentology and sedimentary architecture of marginal to shallow marine tide-dominated environments	28
1.3. Previous studies and interpretations of the Hawaz Formation.....	31
CHAPTER 2. GEOLOGICAL SETTING	33
2.1. North Africa in the Lower Paleozoic – The Saharan Platform.....	35
2.2. The Murzuq Basin.....	38
2.3. The Hawaz Formation.....	43
CHAPTER 3. DATA AND METHODS	49
3.1. Study area and dataset.....	53
3.2. Sedimentological analysis: Methodology	56
3.2.1. Facies analysis.....	56
3.2.2. Hawaz Formation: Sequence stratigraphic-based zonation.....	57
3.3. Sedimentary architecture analysis: Methodology.....	58
3.3.1. Correlation panel construction.....	58
3.3.2. Gross Depositional Environment (GDE) map construction.....	61

CHAPTER 4. SUMMARY OF THE RESULTS	63
4.1. Sedimentology of the Hawaz Formation	65
4.1.1. Lithofacies	65
4.1.2. Facies associations.....	76
4.2. Sequence Stratigraphy of the Hawaz Formation	91
4.3. Sedimentary Architecture of the Hawaz Formation.....	94
4.3.1. Correlation panels.....	95
4.3.1.1. Dip-oriented correlations.....	95
4.3.1.2. Strike-oriented correlations	102
4.3.2. Paleogeographic reconstruction of the Hawaz Formation	108
4.3.2.1. Reservoir zone HWZ1 (TST-DS1).....	108
4.3.2.2. Reservoir zone HWZ2 (HST-DS1).....	108
4.3.2.3. Reservoir zone HWZ3 (TST-DS2).....	110
4.3.2.4. Reservoir zone HWZ4 (HST-DS2).....	112
4.4. Depositional model of the Hawaz Formation	113
 CHAPTER 5. DISCUSSION.....	 121
5.1. Factors controlling sedimentation in ancient marginal to shallow marine environments	123
5.2. A non-actualistic interpretation of the Hawaz Formation.....	128
 CHAPTER 6. CONCLUSIONS.....	 137
6.1. The sedimentology of the Hawaz Formation.....	139
6.2. The sedimentary architecture of the Hawaz Formation	140
6.3. General conclusions.....	141
6.4. Potential for future work	142
 REFERENCES	 145
 ANNEXES.....	 165

Figures and tables list

- Figure I.I. Geological map of Libya showing the main sedimentary basins. The Murzuq basin is bounded by the Atshan Arch to the northwest, the Gargaf High to the north, the Tihemboka High to the southwest and the Tibesti High to the southeast. The area of interest represented in **Fig. 2.4** is highlighted in the red box. Modified from Marzo and Ramos (2003).....16
- Figure 1.1. Proved reserves of crude oil and natural gas in Libya, North Africa (Algeria, Egypt, Libya, Sudan and Tunisia) and Africa. Crude oil reserves include gas condensates and natural gas liquids. Gas reserves measured in standard cubic metres (measured at 15 °C and 1013 mbar). From BP Statistical Review of World Energy (July, 2021). BBB=Thousands million barrels, TCM=Trillion cubic metres.27
- Figure 1.2. Common coastal depositional environments based on ratio of wave, tide and fluvial power. The deltas, strand plains, and open-coast tidal flats (lower half of diagram) are regressive coastal environments, whereas estuaries, barrier-lagoon systems, and open coast tidal flats (upper half of diagram) are transgressive coastal environments. Shelf environments are associated with both types of coast; shelf width increases during transgression and decreases during regression. Modified from Boyd et al. (1992) including modifications from James and Dalrymple (2010).30
- Figure 2.1. Middle Ordovician (Darriwilian – 460 Ma) tectonic plate distribution showing approximate plate boundaries, the principal emergent areas and oceans. The approximate location of the Murzuq Basin is represented with a red star. Note the wide extension of the shallow marine cratonic margin constituting all the north to north-western margin of Gondwana. Redrawn and modified from Cocks and Torsvik (2021).35
- Figure 2.2. African continent with the main four cratons and the Saharan Platform (Metacraton). Note the age of the crustal basement (after Gobanov and Mooney, 2009) differenced by colours from Archean to Cenozoic. The ages represent the time of crustal formation or thermal/tectonic crustal reworking. Note also the approximate location of the Murzuq Basin represented with a red star. The approximate area represented in **Fig. 2.3** is highlighted with a black rectangle. Redrawn and modified from Van Hinsbergen et al. (2011).36
- Figure 2.3. Regional map of North Africa and Iberia. The main Paleozoic sedimentary basins located onshore the Saharan Platform are, from west to east: the Essaouira, Doukkala and Rabt Basins on the western Moroccan margin; Tindouf and Bechar Basins between Morocco and Algeria; Reggane, Gourara, Ahnet, Oued Mya, and Illizi Basins in Algeria; Berkine-Ghadames and Hamra Basins partially between Algeria, Tunisia and Libya; Jefarah Basin in Tunisia; Murzuq, Sirte and Kufrah Basins in Libya and the Abu Gharadig Basin in north Egypt. These sedimentary basins are typically bounded by tectonic uplifts locally exposing the Paleozoic successions. The extent of **Fig. 2.4**. is also highlighted with a black square. After Boote et al. (1998).38
- Figure 2.4. Geological map and cross-section of the Murzuq Basin. Above, note the main structures forming the boundaries of this basin, the Atshan Arch to the northwest, the Gargaf High to the north and the Tihemboka and Tibesti (Dor el Gussa-Mourizidie) highs to the southwest and southeast respectively. Note also the main exploration concessions and the major hydrocarbon provinces in the Murzuq Basin after Hallet and Clark-Lowes (2016). The area of interest

represented in **Fig. 3.3** is highlighted by the red polygon. The outcrop area studied by Ramos et al. (2006), referred to in this paper is also highlighted with an orange arrow in the Gargaf High area. The location of the cross-section represented below is also represented in the map (A-A'). After Marzo and Ramos (2003) and Shalbak (2015). Below, see a regional cross-section of the Murzuq Basin from north to south (A-A'). After Davidson et al. (2000).....40

Figure 2.5. Murzuq Basin litho- and chronostratigraphy. A) Stratigraphic chart summarising the lithostratigraphy of the Murzuq Basin highlighting the main stratigraphic units and major basin-scale unconformities. 1 = Cambrian – Ordovician; 2 = Silurian; 3 = Devonian – Carboniferous; 4 = Mesozoic. B) Wheeler diagram showing the lithostratigraphic to chronostratigraphic relationships of the Ordovician and Lower Silurian succession in the area of study. The main petroleum systems elements are also represented.....42

Figure 2.6. Hawaz Formation thin sections. A) Detailed view of predominant monocrystalline quartz grains (MQ) and K-feldspars (F). See the intergranular macropores are totally infilled by clusters of kaolinite (K). K-feldspar grains are intimately related to kaolinite, this indicates that kaolinite is formed by the alteration of K-feldspar. Quartz grains have straight to concavo-convex contacts indicating that a moderate degree of compaction occurred.; B) General view of a moderately sorted, fine-grained sandstone. Detrital grains are predominantly composed of subangular monocrystalline quartz with subordinate K-feldspar (F) and micas. Detrital illite (DI) and indeterminate clays (IC) are present in compacted/crenulated laminae. Authigenic kaolinite derived from the alteration of K-feldspars is also present, and locally occludes intergranular pores. Pyrite is present in trace volumes. A and B thin sections from well W06; C) Very well sorted, massively structured, medium-grained quartz-arenite, with abundant monocrystalline quartz (MQ) displaying a moderately preserved intergranular pore network (IP). These pores are moderately well interconnected and supplemented by oversized grain dissolution pores (SP). Much of original porosity present at deposition has been reduced by compaction and significant authigenic quartz overgrowth cement (QO); D) A) Clean, very well sorted medium-grained sandstone consisting of abundant detrital quartz grains (MQ) displaying well developed, euhedral, pore-filling quartz overgrowths (QO). Moderate to strong compaction is indicated by the presence of straight to slightly sutured grain contacts. C and D thin sections from well W30. See **Fig. 3.3** for location of the wells.45

Figure 2.7. Paleocurrents measured in the Hawaz Formation. At the left, see the average paleocurrent trend measured by Ramos et al. (2006) at the Gargaf High in subtidal sandstones. Scale is 150 cm (Jacob's staff). Photo courtesy of Emilio Ramos. At the right, see also the paleocurrents measured in 3 m section from well W29 (see **Fig. 3.3** for location of the well) in equivalent subtidal complex deposits, with image log data (FMI), in the subsurface of the Murzuq Basin. Only large-scale or high-angle cross-bedding structures have been considered for paleocurrent analysis in this study, represented by red tad poles in the central track, compared to low-angle (green) laminations and high-angle (triangles) natural and induced fractures.46

Figure 2.8. Hawaz Formation architecture. A) Seismic section from the subsurface of the Murzuq Basin showing the typical geomorphological profile of the Ordovician succession in the form of paleohighs and paleovalleys. Note the deep incision corresponding to the Late Ordovician Glaciation Unconformity and the Upper Ordovician deposits infilling the paleovalleys, separated by Lower and Middle Ordovician Ash Shabiyat and Hawaz Formations. See also the high amplitude of the basal Tanezzuft Fm. corresponding to the Silurian hot shale, represented by a bright negative reflector; B) Dip parallel view along the axis of a major outcropping paleovalley in SE Algeria (Iherir area). The paleohighs are represented by Middle Ordovician In Tahouite Fm. (Unit III-3), lateral age-equivalent to the Hawaz Fm., and the paleovalley is filled with the Late Ordovician Tamadjert

Fm. (Unit IV), lateral age-equivalent to the Melaz Shuqran, Mamuniyat and Bir Tlacin Fms. Modified from McDougall, et al. (2008b).	47
Figure 3.1. Summary of the methodological workflow followed in this thesis.	52
Figure 3.2. Area of study and dataset location. See in the upper part of this figure a close-up view from Fig. 2.4 showing the main study area (NC186 concession) and two adjacent exploration concessions, NC115 and NC190, as well as the main discoveries made in this area classified by their main reservoir, Hawaz or Mamuniyat. Note the limit of the 3D seismic survey (“Megamerge 3D seismic survey”) available in both the area of study and surrounding concessions. The red polygon highlighted here corresponds to our area of study represented below with the location of the wells by availability of core data, expanded with further information in Fig. 3.3	55
Figure 3.3. Two-way time contour map representing an interpreted top Hawaz surface from Bataller et al. (2019), flattened on an intra-Silurian horizon in the area of study. Note also the superposition of the underlying basement-linked, apparently non-displacing, Cambro-Ordovician faults on this map and their relationship with paleovalley boundaries, interpreted from seismic data. Also shown are the locations of the 35 wells used in this study differentiated by the presence or absence of core data, together with the location of the correlation panels presented in this paper as well as the location of the seismic section shown in Fig. 3.4	59
Figure 3.4. Hawaz Formation subsurface architecture. This seismic section across the area of study highlights the remnant subsurface Hawaz paleotopography and infill geometries incised by multiple erosional events during the Late Ordovician glaciation. Note the interpreted base Tanezzuft Fm., which was the datum selected for the construction of the correlation panels presented in this paper. The gamma ray signature of the Hawaz Formation is shown aligned with wells intersecting this seismic line. See also the normal faults bounding many of the paleohighs and the paleovalleys, presumably active during the Cambro-Ordovician. Both the location of the wells and the position of this seismic line are shown in Fig. 3.3	60
Table 4.1. Summary of the lithofacies scheme for the Hawaz Formation. See description for more detail.	66
Figure 4.1. Summary of the main lithofacies identified in this study expressed in core sections (~90-cm length). Sx1 = large-scale cross-bedded sandstone (from well W09); Sx2 = small- to medium-scale cross-bedded sandstone (from well W09); Sl = parallel-laminated sandstone (from well W16); Sxl = cross-laminated sandstone (from well W16); Sr = ripple cross-laminated sandstone (from well W33); Sv = massive sandstone (from well W09); Sxb = burrowed cross-bedded sandstone (from well W33); Si = <i>Siphonichnus</i> . See Fig. 3.3 for the location of the corresponding wells and Table 4.1 for a summarised description.	73
Figure 4.1. (Continued) Summary of the main lithofacies identified in this study expressed in core sections (~90-cm length). Sxlb = burrowed cross-laminated sandstone (from well W33); Srb = burrowed ripple cross-laminated sandstone (from well W15); Sb = burrowed sandstone with <i>Siphonichnus</i> (from well W16); MSb = burrowed sandstone with feeding ichnofauna (from well W17); HS = sandy heterolithics (from well W19); HM = muddy heterolithics (from well W19); HSb = burrowed sandy heterolithics (from well W15); HMB = burrowed muddy heterolithics (from well W15); Pl = <i>Planolites</i> ; Si = <i>Siphonichnus</i> ; Sk = <i>Skolithos</i> ; Th = <i>Thalassionides</i> . See Fig. 3.3 for the location of the corresponding wells and Table 4.1 for a summarised description.	74

Figure 4.2. Summary of the equivalent lithofacies identified in the outcropping section of the Hawaz Formation in the Gargaf High by Ramos et al. (2006). A) Large-scale, sigmoidal cross-bedded sandstones. B) Medium-scale, sigmoidal cross-bedded sandstones. C) Parallel-laminated sandstones. D) Low angle, swaley to hummocky cross-stratified sandstones. E) Ripple cross-laminated sandstones. F) Massive sandstones. Scale is 150 cm (Jacob's staff), geologist hammer or a pencil. Photographs courtesy of Emilio Ramos.....75

Figure 4.2. (Continued) Summary of the equivalent lithofacies identified in the outcropping section of the Hawaz Formation in the Gargaf High by Ramos et al. (2006). G) Thick-bedded, massive, bioturbated sandstones. H) Heterolithic silty sandstones. Photographs courtesy of Emilio Ramos.76

Figure 4.3. Summary of facies associations and interpreted depositional settings. Description includes typical sections and thickness ranges (in metres) with the main lithofacies composing each facies association. Interpretation in terms of depositional environment is also included. See also the average conventional core analysis (CCA) values for porosity, permeability and gamma ray for each facies association. HWFA = Hawaz facies association; FWWB = mean fair-weather wave base; SWB = mean storm wave base; Cl = clay; si = silt; vfs = very fine sandstone; fs = fine sandstone; ms = medium sandstone; Sx1 = large-scale cross-bedded sandstone; Sx2 = small- to medium-scale cross-bedded sandstone; Sl = parallel-laminated sandstone; Sxl = cross-laminated sandstone; Sr = ripple cross-laminated sandstone; Sv = massive sandstone; Sxb = burrowed cross-bedded sandstone; Sxlb = burrowed cross-laminated sandstone; Srb = burrowed ripple cross-laminated sandstone; Sb = burrowed sandstone with *Siphonichnus*; MSb = burrowed sandstone with feeding ichnofauna; HS = sandy heterolithics; HM = muddy heterolithics; HSb = burrowed sandy heterolithics; HMb = burrowed muddy heterolithics.79

Figure 4.4. Detailed close-up views of some characteristic sedimentary structures and fabric of facies association HWFA1 Tidal flat. A) Modified lithological fabric due to the effect of both vertical and horizontal bioturbation. See the remnants of mud-draped lamination between burrows, from well W09. B) Remnants of rhythmic lamination preserved in the infilling of a *Siphonichnus* (Si) vertical burrow, from well W26. C) Mud-draped current ripples, from well W26. D) Combined current and wave ripples with mud drapes, from well W19. See **Fig. 3.3** for location of the wells.....79

Figure 4.4. (Continued) E) Flaser lamination in ripple cross-laminated sandstones, from well W26. F) Wavy to lenticular lamination in burrowed heterolithic sandstones, from well W16. G) Post-depositional local faulting, related to channel-bank collapse, from well W26. H) Base of an interpreted ephemeral channel displaying a lag of mud clasts and subsequent channel infilling with mud-draped ripple cross-laminated sandstones, from well W26. I) Core to image log calibration showing a 90 cm (aprox.) typical HWFA1 tidal flat section with an alternation of burrowed sandstones and sandy heterolithics. Note the typical low angle of sedimentary structures in these deposits associated with a generalised low energy setting and also the low rate of preservation of these structures due to an extended mixed *Cruziana* and *Skolithos* ichnofacies. Measured porosity and horizontal permeability in plugs from core analysis is also included, from well W09. See **Fig. 3.3** for location of the wells.....81

Figure 4.5. Detailed close-up views of some characteristic sedimentary structures and fabric of facies associations HWF2 Subtidal complex and HWFA3 Abandoned subtidal complex. A) Mudstone rip-up clasts from the base of a subtidal channel, from well W16. B) Mud-draped current ripples in clean sandstones of a subtidal complex, from well W33. Note the direction of the paleocurrent flow leftward. C) Cross-bedding with mud-draped tidal bundles eroded atop by an interpreted

reactivation surface, from well W16. D) Clean cross-bedded sandstones with occurrence of vertical *Siphonichnus* (Si) burrows, denoting a progressive abandonment of the subtidal complex and/or fringe zone of an active subtidal complex, from well W33. The location of the corresponding wells is in **Fig. 3.3**.....83

Figure 4.5. (Continued) E) Core to image log calibration showing a 90 cm (aprox.) typical HWFA2 subtidal complex section with a characteristic large-scale cross-bedded sandstones denoting the migration of bars and dunes under high to moderate energy conditions. Note the dominant direction of the paleoflow towards the north-northeast as interpreted from the right-hand side tadpoles track, from well W09. F) Core to image log calibration showing a 90 cm (aprox.) HWFA3 abandoned subtidal complex section with massive sandstones with scattered mud clasts and scarce *Siphonichnus* traces indicating lower energy conditions and an incipient abandonment or fringe zone of the subtidal complex, from well W33. Measured porosity and horizontal permeability in plugs from core analysis is also included. The location of the corresponding wells is in **Fig. 3.3**.....85

Figure 4.6. Detailed close-up views of some characteristic sedimentary structures and fabric of facies associations HWF4 Middle to lower shoreface, HWFA6 Burrowed inner shlef and HWFA7 Shelfal storm sheets. A) Characteristic view of burrowed cross-laminated sandstones with dominant suspension-feeding bioturbation from facies association HWFA4. B) Pervasive, mainly horizontal deposit-feeding bioturbation, in heterolithic sandstones and mudstones, from facies association HWFA6. C) Characteristic alternation of burrowed heterolithic sandstones and mudstones from distal facies association HWFA6. D) Mud-draped combined flow ripples from facies association HWFA7. Notice the direction of the paleocurrent flow rightward in the upper part and bidirectional in the lower part of the image. Four images extracted from core sections in well W15. See the location of the corresponding well in **Fig. 3.3**.....87

Figure 4.6. (Continued) E) Core to image log calibration showing a 90 cm (aprox.) HWFA4 middle to lower shoreface section with an alternation of burrowed cross-laminated sandstones and burrowed heterolithic sandstones with a prevalence of *Skolithos* ichnofacies. F) Core to image log calibration showing a 90 cm (aprox.) HWFA5 burrowed shelfal and lower shoreface section dominated by burrowed sandstones with a completely obliterated primary fabric by *Siphonichnus* traces. This core and image log section don't belong to the same part of the well due to lack of good quality comparative images for this facies association. G) Core to image log calibration showing a 90 cm (aprox.) HWFA6 burrowed inner shelf section with an alternation of burrowed heterolithic sandstones and mudstones with a mixed *Cruziana* and *Skolithos* ichnofacies. All sections extracted from well W15. See the location of the corresponding well in **Fig. 3.3**89

Figure 4.6. (Continued) H) Core to image log calibration showing a 90 cm (aprox.) HWFA7 shelfal storm sheets section with an alternation of heterolithic sandstones and mudstones. Section extracted from well W15. See the location of the corresponding well in **Fig. 3.3**90

Figure 4.7. Sequence stratigraphy framework of the Hawaz Formation in the study area. A) Composite section of well W19 showing a stratigraphic column of the Hawaz Formation, the associated wireline log responses, the suggested zonation for the reservoir based on the facies associations, and sequence stratigraphic framework. The transgressive and regressive stacking patterns are also represented on the figure together with the three main depositional sequences (DS1-3). B) Close-up view of a representative core section showing the main features of the maximum flooding surface of DS1, from well W15. C) Core section view of the erosive contact corresponding to the shoreline ravinement unconformity and sequence boundary of DS2, from well W15. D) Core

picture showing the main characteristics of the maximum flooding surface of DS2, from well W09.
 E) Core view highlighting the erosive character of the maximum regressive surface and sequence boundary of DS3, from well W19. The location of the corresponding wells is highlighted in **Fig 3.3**.93

Figure 4.8. Graph showing the relative proportions of Hawaz Facies Associations (HWFA) within each of the identified genetic sequences or Hawaz reservoir zones (HWZ) averaged from the 35 studied wells (values represented in percentages). The proportions shown in HWZ5 might well not be representative due to the lack of preserved section in most of the wells. HWFA1 = Tidal flat; HWFA2 = Subtidal complex; HWFA3 = Abandoned subtidal complex; HWFA4 = Middle to lower shoreface; HWFA5 = Burrowed shelfal and lower shoreface; HWFA6 = Burrowed inner shelf; HWFA7 = Shelfal storm sheets.....94

Figure 4.9. Correlation panel Dip 1. All the wells hang from the flattened base Tanezzuft Fm. datum. These are shown with their GR profile from 0 to 150 GAPI. Major transgressive and regressive cycles, systems tracts and Hawaz reservoir zones are also shown. A seismic section, oriented NW-SE around well W04, is also shown in the bottom left corner, highlighting the relationship of the paleohigh flank with respect to the bounding paleovalley normal fault and the Late Ordovician Glacial Unconformity. Also note the link between fault position and facies associations variations and slight variation in thickness represented above. DS = Depositional sequence; HST = Highstand systems tract; HWFA = Hawaz facies association; HWZ = Hawaz zone; MFS = Maximum Flooding Surface; MRS = Maximum Regressive Surface; TST = Transgressive systems tract.98

Figure 4.10. Correlation panel Dip 2. All the wells hang from the flattened base Tanezzuft Fm. datum. These are shown with their GR profile from 0 to 150 GAPI. Transgressive and regressive cycles corresponding to systems tracts and Hawaz reservoir zones are displayed. Note the enlargement of the stratigraphic correlation around wells W17 and W16 in the bottom left corner, showing an abrupt lateral facies change, specially for the middle section of the Hawaz Formation. DS = Depositional sequence; HST = Highstand systems tract; HWFA = Hawaz facies association; HWZ = Hawaz zone; TST = Transgressive systems tract.99

Figure 4.11. Correlation panel Dip 3. All the wells hang from the flattened base Tanezzuft Fm. datum. These are shown with their GR profile from 0 to 150 GAPI. Transgressive and regressive cycles corresponding to systems tracts and Hawaz reservoir zones are shown. See a close-up view of the stratigraphic correlation between wells W26 and W27 in the bottom left corner, showing a facies change, specially for the middle section of the Hawaz Formation, from subtidal complex deposits to the SE to abandoned subtidal complex deposits and thicker tidal flat deposits to the NW. DS = Depositional sequence; HST = Highstand systems tract; HWFA = Hawaz facies association; HWZ = Hawaz zone; TST = Transgressive systems tract. 100

Figure 4.12. Correlation panel Dip 4. All the wells hang from the flattened base Tanezzuft Fm. datum. These are shown with their GR profile from 0 to 150 GAPI. Principal transgressive and regressive cycles, corresponding to systems tracts and Hawaz reservoir zones are also displayed. An enlarged view of the correlation between wells W24 and W25 is presented in the bottom left corner, showing a distinctive lateral facies change from middle to lower shoreface deposits to the SE to burrowed shelfal and lower shoreface deposits to the NW in the lower section of the Hawaz Formation. Note also the significant accumulation of abandoned subtidal complex deposits in the middle Hawaz in well W25. DS = Depositional sequence; HST = Highstand systems tract; HWFA = Hawaz facies association; HWZ = Hawaz zone; TST = Transgressive systems tract..... 101

Figure 4.13. Correlation panel Strike 1. All the wells hang from the flattened base Tanezzuft Fm. datum. These are shown with their GR profile from 0 to 150 GAPI. The main transgressive and regressive cycles, systems tracts and Hawaz reservoir zones are shown. A close-up view of the stratigraphic correlation between wells W20 and W29 is included in the bottom left corner, showing the relationship between an inferred fault and its possible control on paleobathymetry. Note the lateral evolution from proximal HWFA4 to distal HWFA6 deposits in the HST of Depositional Sequence 1 and the growth in thickness of HWFA2 in the TST of Depositional Sequence 2 in the hanging wall of a Middle Ordovician active normal fault. DS = Depositional sequence; HST = Highstand systems tract; HWFA = Hawaz facies association; HWZ = Hawaz zone; TST = Transgressive systems tract. 104

Figure 4.14. Correlation panel Strike 2. All the wells hang from the flattened base Tanezzuft Fm. datum. These are shown with their GR profile from 0 to 150 GAPI. Transgressive and regressive systems tracts and Hawaz reservoir zones are shown. An extension of the stratigraphic correlation between wells W08 and W09 is presented in the bottom left corner, showing the characteristic extensive abandoned subtidal complex deposits appearing in the TST of DS1. DS = Depositional sequence; HST = Highstand systems tract; HWFA = Hawaz facies association; HWZ = Hawaz zone; TST = Transgressive systems tract. 105

Figure 4.15. Correlation panel Strike 3. All the wells hang from the flattened base Tanezzuft Fm. datum. These are shown with their GR profile from 0 to 150 GAPI. The main transgressive and regressive cycles, corresponding to systems tracts and Hawaz reservoir zones are shown. An enlarged view of the stratigraphic correlation between wells W23, W34 and W35 is included in the bottom left corner. Note the generally lower energy position of wells W35 and specially W34 with respect to W23 for the whole Hawaz section as shown by the presence of different facies associations in these wells. Note also the control on thickness associated with an apparently active normal fault to the SW of well W23 in the middle Hawaz. DS = Depositional sequence; HST = Highstand systems tract; HWFA = Hawaz facies association; HWZ = Hawaz zone; TST = Transgressive systems tract. 106

Figure 4.16. Correlation panel Strike 4. All the wells hang from the flattened base Tanezzuft Fm. datum. These are shown with their GR profile from 0 to 150 GAPI. Transgressive and regressive cycles, corresponding to systems tracts and Hawaz reservoir zones are also displayed. Also included is a seismic section, oriented SW-NE around wells W32 and W33 in the bottom left corner, showing the relationship of the paleohigh flank with respect to the normal fault bounding the paleovalley and the Late Ordovician Glacial Unconformity to the SW. Note how some of these faults appear to be connected to pre-existing basement structures. Also note the link between fault location and variations in character and thickness of facies associations. DS = Depositional sequence; HST = Highstand systems tract; HWFA = Hawaz facies association; HWZ = Hawaz zone; TST = Transgressive systems tract. 107

Figure 4.17. Gross Depositional Environment map corresponding to the transgressive systems tract (TST) of Depositional Sequence 1. Facies association proportions are posted next to their corresponding wells. W01, W12 and W21 are anomalies reflecting a reduced section associated with a shallower than normal Total Depth (TD); see **Annex 4** for details. 109

Figure 4.18. Gross Depositional Environment map corresponding to the highstand systems tract (HST) of Depositional Sequence 1. Facies association proportions are posted next to their corresponding wells. Note also the presence of apparently active normal faults, inferred from seismic and

correlation panels, which correspond with some of the faults picked in underlying Cambro-Ordovician sections from seismic data and shown in **Fig. 3.3**. 110

Figure 4.19. Gross Depositional Environment map corresponding to the transgressive systems tract (TST) of Depositional Sequence 2. Facies association proportions are posted next to their corresponding wells. Note also the presence of apparently active normal faults during the Middle Ordovician, which correspond with some of the faults picked in underlying Cambro-Ordovician sections from seismic data and shown in **Fig. 3.3**. Note also the paleocurrent directions inferred from image log data (FMI) and their principal orientation highlighted by black arrows. The interpretation in the north-western corner is purely speculative and driven by our depositional model, possibly beyond the limits of the study area. 111

Figure 4.20. Gross Depositional Environment map corresponding to the highstand systems tract (HST) of Depositional Sequence 2. Facies association proportions are posted next to their respective wells. Note also paleocurrent data associated with those wells intercepting ephemeral distributary channels in the tidal flat. The interpretation in the north-western corner is largely speculative and driven by our depositional model and outcrop data from the neighbouring Gargaf High zone, where Ramos et al. (2006) and Gibert et al. (2011) identified evidence of barrier island and tidal inlet facies and associated ichnofacies assemblages. 113

Figure 4.21. Conceptual depositional model for the Hawaz Formation in the Murzuq Basin. A) The interpretation of the depositional model corresponding to a typical early transgressive systems tract of the Hawaz Formation. B) The interpretation corresponding to a typical highstand or early regressive systems tract of this same lithostratigraphic unit. A synthetic stratigraphic column for each of the Hawaz Facies Associations, identified in the subsurface of the Murzuq Basin, together with their typical gamma ray (GR) response (left, low GR; right, high GR) and stacking pattern are also shown. Note the approximate limits and overlap of the main ichnofacies identified in this study are also included. Not to scale. Cl = clay, si = silt, vfs = very fine sandstone, fs = fine sandstone, ms = medium sandstone, msl = mean sea level. 118

Table 5.1. Comparative Table between key Actualistic (Present) and Non-actualistic (Early Paleozoic and older) main processes or controlling factors affecting the geological signature of tidal-influenced successions in the geological record. 124

Figure 5.1. Close-up view of the paleogeographic reconstruction of the north to north-western margin of Gondwana during the Middle Ordovician (Darriwilian – 460 Ma). Note the broad cratonic margin extending across the Saharan Platform with a dominated marginal to shallow marine setting. The approximate location of the area of study and the inferred main paleocurrent direction are represented with a red star and arrow, respectively. Redrawn and modified from Cocks and Torsvick (2021). 126

Figure 5.2. Three-dimensional conceptual sketch of a coastal, tidal-influenced environment analogue to the Hawaz Formation deposition during a highstand systems tract stage, grading from a prograding coastal plain in the most proximal part of the sedimentary system to intertidal and subtidal environments and lower shoreface to inner shelf settings. Note the clear relationship between the ichnofacies assemblage and the energy of the depositional environment. Volcanic ash deposits interpreted as a likely source for clay-fraction sediment in this environment. From left to right: (A) mixed *Cruziana* and *Skolithos* (Sk) ichnofacies assemblage with characteristic vertical suspension feeder burrows of Sk overprinting an ichnofabric comprising horizontal deposit feeders and miners

such as *Thalassionides* (Th) and *Planolites* (Pl) associated with tidal flat deposits, from well W09. (B) Characteristic Sk piperock ichnofacies with typical *Siphonichnus* (Si) burrows from lower shoreface to burrowed shelfal deposits, from well W15. (C) Mixed *Cruziana* and Sk ichnofacies assemblage, from burrowed inner shelf sediments with characteristic *Teichichnus* (Te), Th, and Sk burrows, from well W15. (D) Heterolithic mudstones belonging to the most distal storm deposits with *Chondrites* (Ch) burrows characteristic of the distal *Cruziana* ichnofacies, from well W15. See the location of the corresponding wells in **Fig. 3.3**..... 127

Figure 5.3. Regional map of North Africa (after Boote et al. (1998).) and Iberia showing the type section of the Hawaz Formation or lateral equivalent Middle Ordovician deposits in 5 different locations. 1) Middle Ordovician Upper Arenig to Llandeilo section mostly made of middle to lower shoreface and inner shelf deposits, with characteristic HCS and suspension feeding burrows in the outcropping section of Western Iberia (McDougall, 1988; unpublished results); 2) Hawaz type section from the outcropping succession in the Gargaf High, Murzuq Basin (modified from Ramos et al., 2006); 2) Hawaz type section from Well 19 in the subsurface of the Murzuq Basin (Gil-Ortiz et al., 2019, 2022). See **Fig. 3.3** for location of the well; 4) Hawaz type section from the outcropping succession in Jabal az-Zalmah, Kufrah Basin (modified from Le Heron et al., 2010); 5) Hawaz type section from the outcrops in Jabal Azbah, Kufrah Basin. See the fluvial influence in this last stratigraphic column, denoting a more proximal domain (modified from Le Heron et al., 2010). See the location of the type sections in the map above. 131

Figure 5.4. A) Map of the Gulf of Carpentaria and Arafura Sea between Australia and Papua New Guinea as a partial analogue of the Hawaz Formation depositional setting as a marginal to shallow marine cratonic margin. See also in the right part of the figure two close-up views images from Google Earth (© 2021 Google) showing along-strike variability of sub-environments; B) in the upper right image it can be seen braided rivers which rapidly evolve to meandering fluvial channels on a small delta plain, highly modelled by tides, whereas in C) tidal flat deposits domain the area, cross-cut by ephemeral tidal creeks and high sinuosity fluvio-tidal channels. Note in the lower part of the figure, a comparative scheme between the shoreface dip profile from the Gulf of Carpentaria, represented by line A-A', and the bathymetric profile off Bay City, Texas (Gulf of Mexico). The x-axis represents distance from shoreline and the y-axis, bathymetry. Note also the distance from shore at which the mean maximum Storm Wave Base (SWB) is reached in both types of basins (~80 m water depth). Location of shoreface profile A-A' and satellite close-up view images, B and C, are represented in map A (southern part of the map)..... 133

Figure 5.5. Hawaz Formation in the subsurface vs in the outcrop. Comparative summary of Hawaz type sections, in the studied area of the subsurface of the Murzuq Basin and their laterally equivalent deposits located 150 km to the N-NNE in the neighbouring Gargaf High, studied by Ramos et al. (2006). A synthetic stratigraphic column is shown both, for the subsurface as represented by well W19 (See **Fig. 3.3** for location), and in outcrop, each with their corresponding facies associations. Ichnofabric index is also shown together with the corresponding gamma ray profiles. See also the sequence stratigraphic framework discussed in this paper, which is also displayed for both locations, in order to compare in terms of genetic-based sedimentary packages or Hawaz zones. DS = Depositional sequence; HST = Highstand systems tract; HWFA = Hawaz facies association; HWZ = Hawaz zone; TST = Transgressive systems tract. 134

RESUM

La Formació Hawaz és una successió detrítica de composició majoritàriament silícica de l'Ordovicià Mitjà que s'estén centenars de quilòmetres a través del nord d'Àfrica. L'objectiu principal d'aquesta tesi és millorar el coneixement de la Formació Hawaz, important reservori de petroli a la província petrolera emergent de la Conca de Murzuq (Sud-Oest de Líbia), a partir de l'anàlisi de dades de subsol, principalment dades de pou, i complementades amb dades d'afloraments propers. La limitada continuïtat lateral d'aquesta formació, sovint truncada per les discordances glacials de l'Ordovicià Superior, ha presentat sempre un repte per a la interpretació d'aquest reservori en termes d'arquitectura sedimentària a gran escala i connectivitat lateral de fàcies.

Aquesta investigació ha requerit d'una descripció d'alta resolució i una interpretació de la sedimentologia i l'arquitectura sedimentària d'aquesta successió al subsol de la part nord-central de la Conca de Murzuq, en dues fases de treball ben diferenciades: 1) descripció sedimentològica i interpretació de litofàcies i associacions de fàcies juntament amb una anàlisi d'estratigrafia seqüencial de la successió; 2) caracterització del reservori a escala de conca en termes de continuïtat lateral i vertical de cinturons de fàcies, i reconstrucció paleogeogràfica d'aquesta unitat a l'àrea d'estudi.

Aquesta tesi ha permès la identificació i caracterització de quinze litofàcies característiques, definides en base a la seva litologia i fàbrica interna, principalment amb dades de testimoni i diagrames d'imatge de microresistivitat, agrupades en set associacions de fàcies correlacionables i distribuïdes en amples i extensos cinturons, interpretats com a dipositats en un ambient costaner marí transicional a marí proximal. Aquestes associacions de fàcies són: 1) plana mareal; 2) complex submareal; 3) complex submareal abandonat; 4) *shoreface* mitjà a inferior; 5) *shoreface* inferior i transició a plataforma bioturbada; 6) plataforma interna bioturbada; 7) tempestites de plataforma.

També s'han identificat tres seqüències deposicionals i els seus respectius tractes sedimentaris (*systems tracts*) que han estat interpretats com a representatius d'una sedimentació durant etapes de transgressió i nivell relatiu del mar alt. Aquesta subdivisió estratigràfica seqüencial ha permès proposar un esquema de zonació estratigràfica del reservori basat en processos genètics de formació. Per tant, aquesta zonació permet evitar qualsevol tipus de correlació litostratigràfica que indueixi a possibles errors, i serveix com a eina de millora de la gestió dels recursos del subsol presents en aquest reservori.

L'anàlisi de fàcies i la interpretació sedimentològica de la successió han servit com a base per a la reconstrucció de l'arquitectura sedimentària de la Formació Hawaz, mitjançant vuit panells

de correlació orientats paral·lels (NNO-SSE) i transversals (OSO-ENE) a la direcció principal de deposició i una sèrie de mapes deposicionals amb l'objectiu d'aportar nou coneixement sobre la distribució lateral dels cinturons d'associacions de fàcies i, per tant, la distribució de cossos amb potencial per tenir bones propietats de reservori, dins d'un marc de zonació d'estratigrafia seqüencial.

Els resultats d'aquest estudi suggereixen que la Formació Hawaz va ser dipositada en una línia de costa relativament protegida amb múltiples estuaris o badies que constituïen les principals entrades de sediment a la conca. La geomorfologia d'aquesta línia de costa estaria probablement parcialment influenciada pels efectes d'unes falles extensives preexistents, amb una orientació nord-nord-oest a sud-sud-est, d'edat Pan-Africana, que podrien haver controlat l'espai d'acomodació a l'àrea d'estudi, essent reactivades posteriorment durant l'Ordovicià.

Finalment, els factors principals que controlaren la sedimentació d'aquesta successió foren significativament diferents als proposats per models deposicionals actualístics en ambients deposicionals submareals i paràlics intermareals. Al menys, quatre processos podrien haver estat clau en la deposició de la Formació Hawaz, i ens permeten entendre millor la fàbrica, l'extensió lateral i distribució d'aquesta successió al llarg de la Plataforma Nord-Africana i a la nostre àrea d'estudi. Aquests factors són: 1) la manca generalitzada de flora terrestre durant l'Ordovicià Mitjà; 2) un escenari eustàtic global molt diferent a l'actual, considerant el present període d' "icehouse" en front del període de "greenhouse" de l'Ordovicià Mitjà, i la relació d'aquest fet amb el potencial erosiu en zones costaneres; 3) una possible variació del rang mareal producte d'una distància més petita entre la Terra i la Lluna durant el Paleozoic inferior, i finalment; 4) una icnofàbrica de tipus *Skolithos/Cruziana* producte de l'activitat biològica d'organismes marins extints, molt característica i present a la Formació Hawaz, i que no pot ser comparada amb les icnofàcies actuals de caire molt més diversificat i que trobem avui dia en ambients deposicionals similars.

ABSTRACT

The Hawaz Formation is a Middle Ordovician siliciclastic succession which extends for hundreds of kilometres across North Africa. This thesis uses a subsurface-based approach, mainly utilizing well data, complemented by data from nearby outcrops, with the aim of gaining new insight into the oil-prone Hawaz Formation in the emergent hydrocarbon province of the Murzuq Basin (SW Libya). The limited lateral continuity of this formation, often truncated by the Late Ordovician glaciation unconformities, has always presented a challenge to the interpretation of this reservoir in terms of large-scale sedimentary architecture and facies connectivity.

This investigation has required a high resolution description and interpretation of the sedimentology and sedimentary architecture of this succession in the subsurface of the north central part of the Murzuq Basin through two well-differentiated phases: 1) sedimentological description and interpretation of lithofacies and facies associations together with a sequence stratigraphic analysis of the succession; 2) basin-scale reservoir characterization in terms of vertical and lateral continuity of facies belts and paleogeographic reconstruction of this unit in the area of study.

This research has resulted in the identification and characterisation of fifteen distinctive lithofacies, defined on the basis of lithology and internal fabric, mainly using core and microresistivity image log data, grouped into seven correlatable facies associations distributed in broad and laterally extensive facies belts deposited in a shallow marine, intertidal to subtidal environment. These facies associations are: 1) tidal flat; 2) subtidal complex; 3) abandoned subtidal complex; 4) middle to lower shoreface; 5) burrowed shelfal and lower shoreface; 6) burrowed inner shelf and; 7) shelfal storm sheets.

Three main depositional sequences and their respective systems tracts have also been identified and interpreted as deposited mainly during transgressive and high relative sea level stages. On this basis, a genetic-based stratigraphic zonation scheme has been proposed as a tool to improve subsurface management of this reservoir unit.

Facies analysis and sedimentological interpretation provided the basis for the reconstruction of the sedimentary architecture of the Hawaz Formation by means of eight correlation panels oriented along both sedimentological dip (NNW-SSE) and strike (WSW to ENE) and a series of Gross Depositional Environment (GDE) maps with the aim of providing insight into the lateral distribution of facies association belts and hence, distribution of potential reservoir geobodies, within the framework of a sequence stratigraphic-based zonation.

The results of this study suggest that the Hawaz Formation was deposited in a relatively protected or embayed shoreline with multiple bays or estuaries as the main entry points for sediment into the basin, most likely partially influenced by the effects of pre-existing north-northwest to south-southeast Pan-African extensive faults controlling local accommodation space and reactivated during Ordovician times.

Finally, the principal factors controlling the deposition of this succession were significantly different from most actualistic depositional models for modern subtidal to intertidal paralic environments. At least four processes or factors were key for the deposition of the Hawaz Formation and permitted us to better understand the fabric, lateral extension and distribution of this succession across the North African Platform and, indeed, in our area of study. These factors were: 1) a generalised lack of land flora during the Middle Ordovician; 2) a different global eustatic sea level scenario, during much of the Middle Ordovician, differing substantially from present-day icehouse period in terms of relative sea level and erosive potential in coastal settings; 3) a likely higher variation in tidal ranges reflecting the shorter Earth-Moon distance associated with the Lower Paleozoic times and finally; 4) distinctive *Skolithos/Cruziana* ichnofabric present in the Hawaz Formation compared to broader and more diversified ichnofacies in equivalent depositional settings at present times, which are no longer preserved in modern coastal environments due to the extinction of most organisms causing these bioturbation traces.





PREFACE

Motivation and objectives

Description and structure of the thesis

The cover photo of the Preface shows a panoramic view of the tabular, thinly stratified and extremely bioturbated lower section of the Hawaz Formation taken from the exposed outcrops of the Gargaf High (Murzuq Basin, SW Libya).

Photograph courtesy of Emilio Ramos.

Motivation and objectives

The Murzuq Basin (**Fig. I.I**) is an emergent to mature hydrocarbon province in SW Libya where a number of significant commercial discoveries have been made, most notably from the late 1980's until the outbreak of civil war in 2011. The geological setting is near ideal, with a Silurian-age source rock, common traps of at least three types and two proven oil-bearing reservoir units belonging to the Lower Paleozoic succession of this basin, the Mamuniyat and the Hawaz Formations.

Much effort has been devoted to better understanding the reservoir architecture of the oil-prone glaciogenic Upper Ordovician Mamuniyat Formation (e.g. Blanpied et al., 2000; McDougall and Martin, 2000; Ghienne et al., 2003, 2010, 2012; Le Heron et al., 2003, 2004, 2006, 2010; Girard et al. 2012, 2015; Bataller et al., 2019, 2021, 2022), whilst the underlying, and also oil-bearing, Middle Ordovician Hawaz Formation has not received comparable attention and its subsurface character still remains, in a number of key respects, poorly understood. The Hawaz Formation constitutes one of the most important reservoirs in several producing fields in the central and northern part of the basin. The generally high reservoir quality and broadly sheet-like geometry, characteristic of the Hawaz, are key factors in the development and production of these accumulations. However, the limited lateral continuity of this formation, a reflection of the often-spectacular end-Ordovician glacial paleorelief, presents a challenge to the interpretation of this reservoir in terms of large-scale sedimentary architecture and facies connectivity.

The few published studies that have been carried-out to date are based mainly on outcrop data or very limited subsurface data (Vos, 1981; Anfray and Rubino, 2003; Ramos et al., 2006; Abouessa and Morad, 2009; Gibert et al., 2011; Abouessa, 2012; Franco et al., 2012). This limited database and the challenging subsurface expression of the Hawaz Formation, in the form of isolated paleohighs or “buried hills” (Khoja et al., 2000) highlights the necessity of generating large-scale, regional correlations based on a robust sedimentological model. In addition, subsurface interpretations of the Formation are based on inconsistent lithostratigraphic correlations unconstrained by a coherent, properly-defined sequence stratigraphic framework. As such, no genetic or sequence stratigraphy-based zonation exists. This limited database highlights the necessity of providing a sequence stratigraphic framework based on a robust sedimentological model of this succession. These issues are addressed in this thesis by means of the detailed study of a significant number of wells penetrating the Hawaz

Formation in a key study area, the results of which should be applicable across the Murzuq Basin and which can be interpreted within the framework of previous outcrop studies.

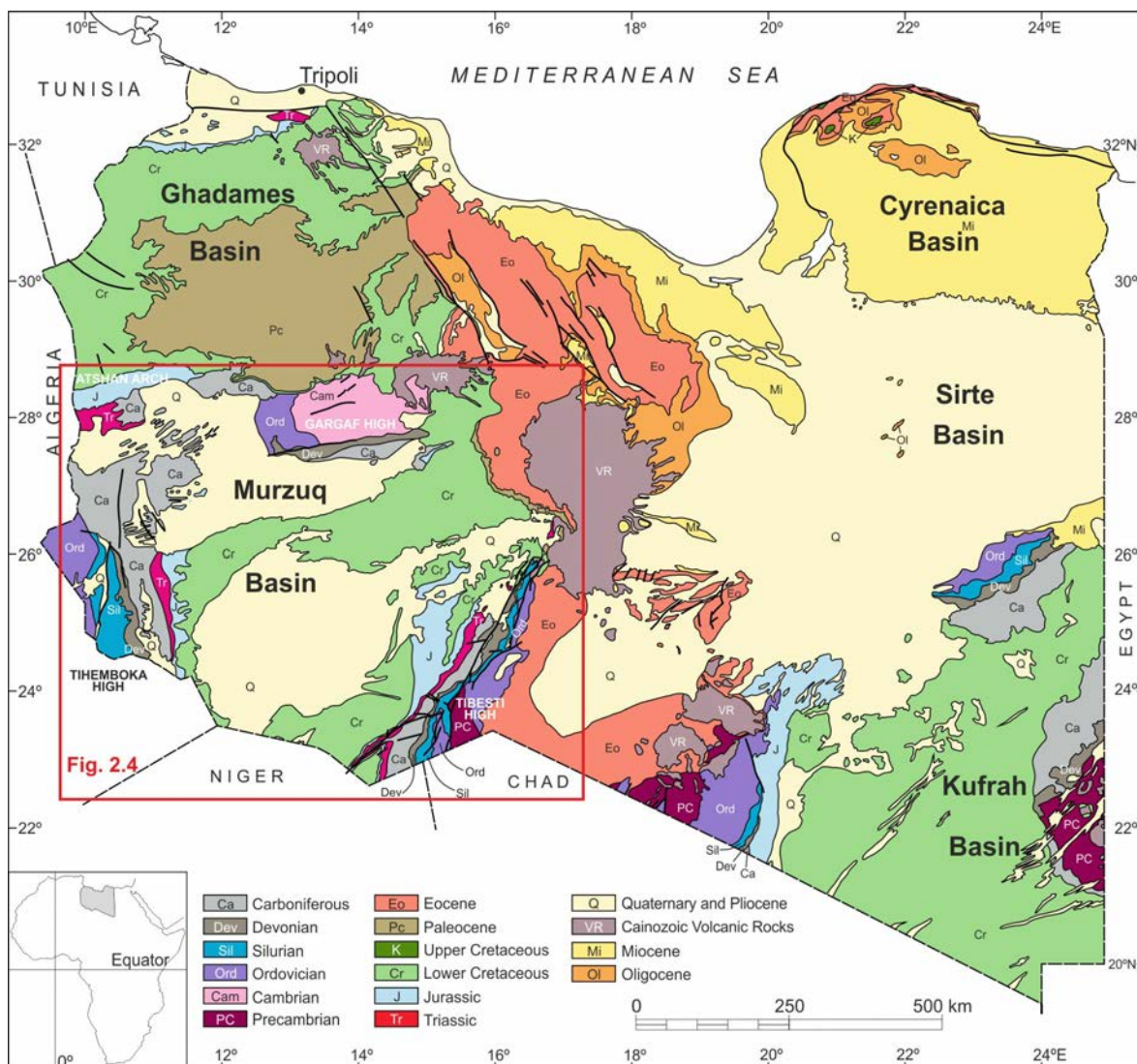


Figure I.I. Geological map of Libya showing the main sedimentary basins. The Murzuq basin is bounded by the Atshan Arch to the northwest, the Gargaf High to the north, the Tihemboka High to the southwest and the Tibesti High to the southeast. The area of interest represented in **Fig. 2.4** is highlighted in the red box. Modified from Marzo and Ramos (2003).

Thus, the main objectives of this thesis are:

- 1) to develop a consistent and uniformly applicable sedimentological characterisation of the Hawaz Formation, based on both core and image logs, leading to a detailed lithofacies description and interpretation, together with the subsequent development of a facies association scheme;
- 2) to build a genetically based reservoir zonation using a practical sequence stratigraphic approach;
- 3) to reconstruct the detailed sedimentary architecture of the Hawaz Formation in the selected study area, based both on the spatial distribution and vertical stacking of facies associations and the genetic or sequence stratigraphic-based zonation, capable of providing a robust tool for stratigraphic correlation;
- 4) to develop a depositional model, supported by large-scale, regional well correlations and Gross Depositional Environment (GDE) maps in order to justify the presence, stacking and spatial distribution of facies belts and to provide an efficient tool for future near-field exploration and production.

These sedimentological and stratigraphic models developed from the study area should offer a well-documented subsurface analogue for clastic reservoirs in similar settings of equivalent age. It is hoped that the results and conclusions of this study will hopefully prove useful in exploration and serve to improve management of the subsurface Hawaz reservoir in this highly productive basin, together with potential current strategic Carbon, Capture and Storage (CCS) portfolios in this area.

Description and structure of the thesis

This PhD thesis has been presented as a compilation of scientific articles published in indexed journals by the Journal Citation Report ® and organized based on the following chapters:

Chapter 1 aims to introduce the reader to the key points of this thesis highlighting the potential of the studied basin together with the scientific contribution of this study. Firstly, the importance of the Murzuq Basin, the focus of this research, is highlighted and the question of why it is worthy of the interest of energy companies is addressed as well as its direct impact on exploration and production of hydrocarbons and CO₂ storage. Secondly, this chapter also addresses some general issues surrounding the sedimentology and sedimentary architecture of marginal to shallow marine environments, which will allow the reader to become familiar with the main characteristics of these deposits and why they are of importance for the oil and gas industry. Finally, a review of several key publications focussed on the Hawaz Formation in outcrop close to our area of study, and which have been taken into consideration as starting points in our descriptions and interpretations of equivalent deposits further to the south in the subsurface of the Murzuq Basin.

Chapter 2 provides a geological framework for the area of study; first, by introducing the reader to the main features of North Africa, when it was part of the northern margin of Gondwana during the early Paleozoic, and secondly by reviewing the linked history of the Murzuq Basin within the framework of the notably stable African Saharan Platform. The Lower Paleozoic sedimentary infill of the Murzuq Basin contains several petroleum system elements represented by a number of detrital successions, amongst them the Middle Ordovician Hawaz Formation, which is the focus of this research and is introduced in this chapter.

Chapter 3 introduces the study area together with a summary of the available data used in this study, as well as the methodological workflow followed by several different techniques, which have been utilised in order to accomplish the objectives outlined in the first section of this Preface.

Chapter 4 presents the main results of the research, essentially comprising two, linked but clearly differentiated, parts:

The first and second sections (**Chapter 4.1 and 4.2**) presents the sedimentology and sequence stratigraphy of the Hawaz Formation in the subsurface of the central Murzuq Basin. The results of this section have been published in the journal of the *AAPG Bulletin* (see **Annex**

1). The aim of this first paper (Gil-Ortiz et al., 2019) was to present a sedimentological characterisation of the Hawaz Formation based on a detailed lithofacies description and interpretation together with the development of an interpretative facies association scheme. Moreover, a sequence stratigraphic framework based in the previous sedimentological analysis was presented, in order to build a genetically-based zonation that aims to improve reservoir management in the subsurface of the Murzuq Basin.

The third and fourth sections (**Chapters 4.3 and 4.4**) presents the results concerning the sedimentary architecture of the studied succession in the area of study and the depositional model of the Hawaz Formation, respectively. The outcome of this research has been published in the journal of *Marine and Petroleum Geology* (see **Annex 1**). The main objectives of this second paper (Gil-Ortiz et al., 2022) were the reconstruction of the detailed sedimentary architecture of the Hawaz Formation in the north central Murzuq Basin (SW Libya), based on the spatial distribution and vertical stacking of facies associations and a genetic or sequence stratigraphic-based zonation captured in the form of large-scale stratigraphic correlation panels and Gross Depositional Environment (GDE) maps, which allowed us to present an updated non-actualistic depositional model of the Hawaz Formation in accordance with plausible physical and chemical processes during the Middle Ordovician.

Chapter 5 includes a discussion of the main factors controlling the sedimentation and sedimentary architecture of coastal deposits in ancient marginal to shallow marine environments and how they apply to this specific case of study. This chapter also addresses the main limitations encountered in the interpretation of some of the results of this research.

Chapter 6 summarises the partial and general conclusions derived from this study concerning the principal sedimentary characteristics of the Hawaz Formation and how this succession evolves laterally and vertically in the subsurface of the central Murzuq Basin.

Finally, the **References** chapter gathers all the bibliographic research items cited throughout this thesis.

Annex 1: Publications in Science Citation Index Journals:

Gil-Ortiz, M., McDougall, N.D., Cabello, P., Marzo, M., Ramos, E. (2019). Sedimentology of a “nonactualistic” Middle Ordovician tidal-influenced reservoir in the Murzuq Basin (Libya). *American Association of Petroleum Geologists (AAPG) Bulletin* 103 (9), 2219–2246. <https://doi.org/10.1306/02151918138>

Gil-Ortiz, M., McDougall, N.D., Cabello, P., Marzo, M., Ramos, E. (2022). Sedimentary architecture of a Middle Ordovician embayment in the Murzuq Basin (Libya). *Marine and Petroleum Geology*, 135. <https://doi.org/10.1016/j.marpetgeo.2021.105339>

Annex 2: Abstracts presented in international congresses:

Gil-Ortiz, M.; McDougall, N.D.; Cabello, P.; Marzo, M.; Ramos, E. (2019). Sedimentology of the 'nonactualistic' Middle Ordovician Hawaz Formation in the Murzuq Basin (Libya). 34th IAS Meeting of Sedimentology, Rome, 10-13th September 2019. Conference paper.

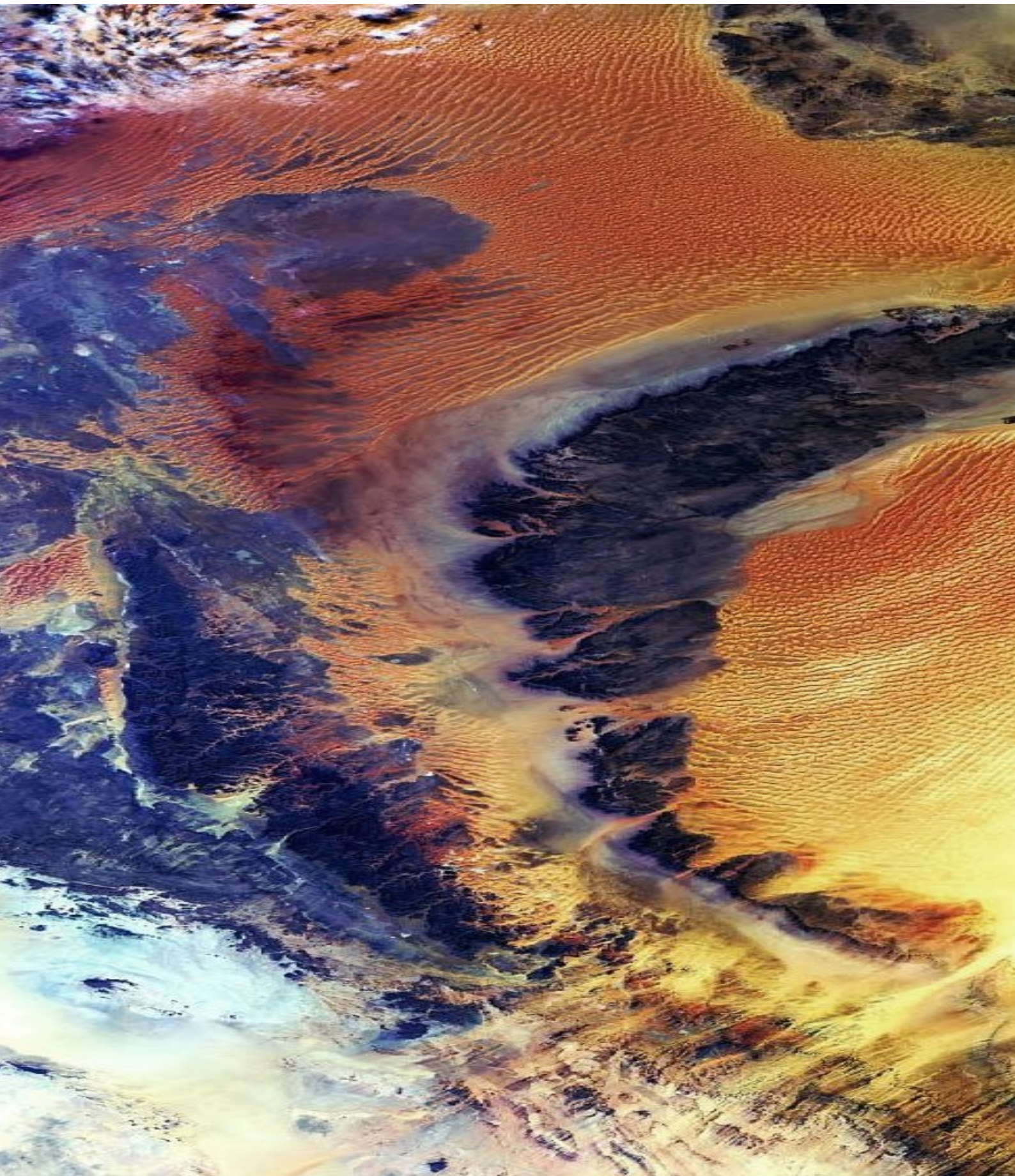
Gil-Ortiz, M.; McDougall, N.D.; Cabello, P.; Marzo, M.; Ramos, E. (2021). Sedimentary architecture of the Middle Ordovician Hawaz Formation in the Murzuq Basin (Libya). 35th IAS Meeting of Sedimentology, Prague, 21-25 th June 2021. Conference paper.

Annex 3: Other publications derived from presentations in national congresses:

Gil-Ortiz, M., Cabello, P., McDougall, N.D., Marzo, M., Ramos, E. (2021). Sedimentology and sedimentary architecture of the Hawaz Formation. The uniformitarian paradigm on the ropes; a Middle Ordovician case study. *GeoTemas*, 18, 156. X Congreso Geológico de España.

Annex 4: Summary table including Hawaz Formation thickness by reservoir zones and total accumulated thickness.

Annex 5: Well composites (W01-W35) including facies associations, conventional wireline logs, cored intervals and main transgressive/regressive cycles. Only included in the digital version of this thesis.





CHAPTER 1. INTRODUCTION

1.1. Exploration in the Murzuq Basin

1.2. Sedimentology and sedimentary architecture of marginal
to shallow marine tide-dominated environments

1.3. Previous studies and interpretations of the Hawaz Formation

The cover photo of the Chapter 1 shows an Environmental Satellite (Envisat) Medium Resolution Imaging Spectrometer (MERIS) image from the Murzuq Basin with the Ubari (north) and Murzuq (south) sand dune seas or ergs, from southwestern Libya. The image was taken by the European Space Agency on 24 November 2004.

Source: Photograph property of European Space Agency. © ESA, CC BY-SA 3.0 IGO

1.1. Exploration in the Murzuq Basin

Since the first discovery in 1953, more than 1100 new field wildcat wells have been drilled to test the Paleozoic basins of North Africa from Morocco to Egypt, discovering more than 46 billion barrels of oil equivalent (BBOE) in over 300 separate pools (Boote et al., 1998). The regionally extensive Lower Silurian (Rhuddanian-Telychian) “Hot Shale” (Lüning et al., 2000, 2003; Fello et al., 2006; Belaid et al., 2010) of the basal Tanezzuft Formation is a world-class source rock and the origin of most hydrocarbons, with a further contribution from the Late Devonian (Frasnian) shales, charging a significant number of intra-Paleozoic and basal Triassic reservoirs. The most important Paleozoic-sourced hydrocarbon accumulations of North Africa lie in southeast Algeria (Illizi and Berkine Basins) and western Libya (Ghadames-Murzuq Basins) and are mainly accumulated into Middle and Late Ordovician reservoirs.

Exploration in the Murzuq Basin began in the 1950’s with the first hydrocarbon discovery made by Esso (now Exxon) in 1957 with Atshan-B2.1 well. However, it was not until some 25 years later that the basin became an emerging hydrocarbon province after attention shifted to the northeast of Libya in the Sirte Basin, following several big discoveries before returning some years later. This was specially so from the late 1980’s to 1990’s when many significant discoveries were made such as the El Sharara fields in the mid 1980’s by Rompetrol and the Elephant Field (El Feel Field) in 1997 by LASMO (see **Chapter 2.2**). Repsol and partners took over the operatorship of Rompetrol’s licenses in 1997 and subsequently undertook an intensive exploratory program, mainly over the central Murzuq licenses (NC115 and NC186; see **Chapter 2.2**) focused on the most obvious and distinctive closures, making several significant discoveries, both in Upper and Middle Ordovician sandstones, between 1998 and 2006 (Ron Martín et al., 2016). The high exploration success rate encouraged a period of near-continuous exploration activity for Ordovician targets. However, despite the increasing maturity of the basin several key geological issues remain unresolved in both the Upper Ordovician Mamuniyat and Middle Ordovician Hawaz Formations. This is highlighted by the observation that, despite significant exploratory success, more than 20 dry holes have been drilled in the last 10 years (Ron Martín et al., 2016).

Oil and gas reserves and production in Libya are significant and largely associated with the onshore Sirte Basin. Volumetrically less important but growing in importance is the Murzuq Basin, whilst smaller contributions are associated with the under-developed Ghadames Basin (**Fig. I.I**).

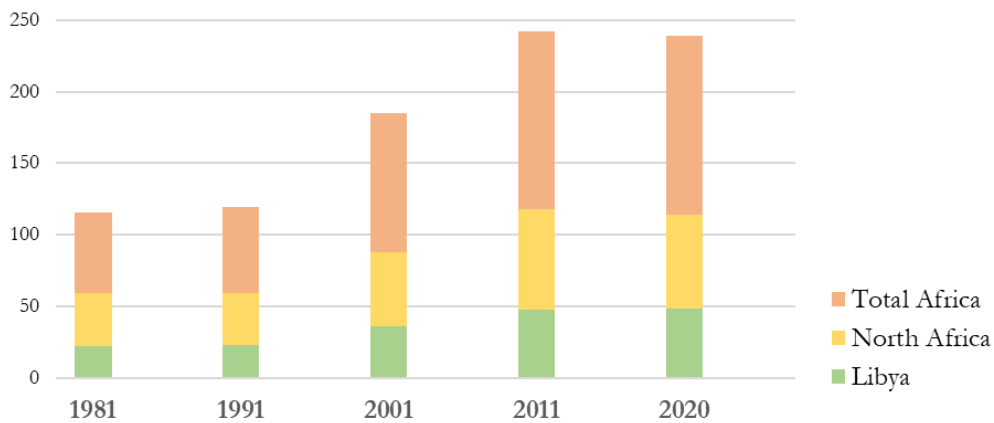
According to the most recent BP Statistical Review of World Energy (July, 2021), Libya holds 73.8% of the crude oil reserves of North Africa and 38.7% of total African oil reserves (**Fig. 1.1**), of which the Murzuq Basin accounts for around 7.4% of the Libya's reserves. The most recent oil-in-place estimation for this basin is about 7.3 billion barrels of oil and about 1.0 trillion cubic metres of gas (Shalbak, 2015).

The Murzuq Basin supplies around the 30% of Libya's current oil production. The principal contributors are the giant El Sharara Fields producing since 1996 at a current rate of 200,000 barrels per day (bopd) and the El Feel (Elephant) Field, which started production in 2004 at an initial rate of 10,000 bopd, rising to 125,000 bopd by 2007. In addition, main fields in Block NC186, which started production in 2003-2004, were supplying about 35,000 bopd in 2005 (Shalbak, 2015). These are, by any measure, impressive numbers (for perspective, Spain consumes approximately 1.3 million barrels per day, or about 2-3 days production from the Murzuq fields) considering the relative immaturity of this basin and the remaining exploration opportunities.

Furthermore, shallow reservoir depths and an absence of engineering challenges entail low drilling costs which, together with a broad knowledge of many current fields, it has led different operators to propose Carbon Capture and Storage projects in this basin in order to reduce their CO₂ emissions in efforts to reach their goal of zero emissions by 2050. The benefits of storing the CO₂, mostly associated with reservoir gas caps, will avoid venting and flaring and consequent emissions, whilst enhancing the recovery of oil in several producing fields.

	Proved reserves	Libya	North Africa	Total Africa
1981	Oil (BBB)	22,6	36,9	56,3
	Natural Gas (TCM)	0,6	4,2	5,7
1991	Oil (BBB)	22,8	36,2	60,4
	Natural Gas (TCM)	1,2	5,1	9,1
2001	Oil (BBB)	36,0	52,1	96,6
	Natural Gas (TCM)	1,2	7,1	12,5
2011	Oil (BBB)	48,0	69,9	124,6
	Natural Gas (TCM)	1,5	7,9	14,1
2020	Oil (BBB)	48,4	65,6	125,1
	Natural Gas (TCM)	1,4	5,8	12,9

Oil proved reserves (BBB)



Natural gas proved reserves (TCM)

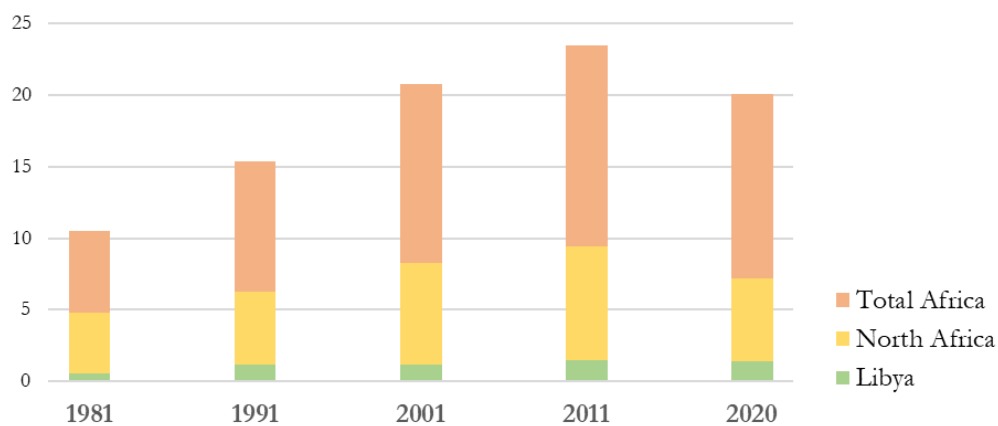


Figure 1.1. Proved reserves of crude oil and natural gas in Libya, North Africa (Algeria, Egypt, Libya, Sudan and Tunisia) and Africa. Crude oil reserves include gas condensates and natural gas liquids. Gas reserves measured in standard cubic metres (measured at 15 °C and 1013 mbar). From BP Statistical Review of World Energy (July, 2021). BBB=Thousands million barrels, TCM=Trillion cubic metres.

1.2. Sedimentology and sedimentary architecture of marginal to shallow marine tide-dominated environments

Stratigraphic implications and problems resulting from the evolution of clastic coastal systems, such as estuary infilling or delta progradation, mean that a process-based classification needs to be enlarged by an evolutionary classification. Coastal systems are very sensitive to changes in relative sea level and sediment supply amongst other factors and so should always be seen in 3 dimensions through time. In the context of coastal evolution, including estuary creation and infilling, relative time may be best expressed in terms of transgression and regression. This approach has the advantage of linking depositional environments with shoreline behaviour through time, but has two main problems: 1) firstly, depositional systems progress at different rates, depending on the ratio between sediment supply and accommodation space; 2) secondly, the relative intensity of river, wave and tidal processes is not an accurate guide to transgression or progradation, because shoreline migration is largely a function of sediment supply and relative sea level (Boyd et al., 1992). Thus, the best classification of clastic coastal environments is the one which combines both, the dominant process/es interacting in such a depositional setting (rivers, waves and tides) and the relative sea level variation through time (**Fig. 1.2**).

During progradation, when river deposition dominates over marine redistribution, deltas typically form elongate/lobate shorelines. During transgression, embayed river paleovalleys (incised valleys) become the sites of estuaries, which form under conditions of relative sea-level rise. Away from river mouths, coastlines tend to be more linear and during progradation or transgression, strand plains and tidal flat environments tend to develop alternating across the continental shelf (Boyd et al., 1992).

The classification followed in this study (**Fig. 1.2**) is entirely based on observations from modern coastal depositional environments and extensively developed in form of evolutionary ternary diagrams presented by Boyd et al. (1992) and Dalrymple et al. (1992).

Tidal dominance over other processes is most common in areas where the tidal range is large, resulting in strong tidal currents. Consequently, most microtidal (0-2 m tidal range) and mesotidal (2-4 m tidal range) areas are wave-storm dominated, whereas some mesotidal and most macrotidal (>4 m tidal range) areas are tide-dominated (Dalrymple, 1992). The potential sediment load of nearshore tidal currents and the effectiveness of the tides for sediment

deposition are related directly to tidal range (or maximum tidal height) and consequent current speed (Williams, 2000).

There are certain sedimentary and biogenic structures which are characteristic and sometimes diagnostic of tidal deposition (Nio and Yang, 1991; Davis, 2012). These include biogenic structures such as characteristic bioturbation or microbial mats and stromatolites; and physical structures such as desiccation or shrinkage (synaeresis) cracks, flaser, wavy and lenticular bedding (Reineck and Wunderlich, 1968), tidal bundles, reactivation surfaces (Klein, 1970), herringbone cross-stratification, inclined heterolithic stratification (IHS) (Bridges and Leeder, 1976; Thomas et al., 1987) mud-draped ripples and alternations of heterolithic deposits called tidal rhythmites (Reineck, 1967; Dalrymple et al., 1991; Williams, 1991; Kvale, 2003, 2012). Most of these physical structures reflect periodic changes in current speed and direction related to fluctuations in sea level produced by the differential gravitational attraction between the Moon and the Earth, which reflect the flood-, slack-, ebb- and slack-water periods of a complete tidal cycle.

With respect to specifically shallow marine, tide-dominated environments, these are typically represented by mixed sand- and mud-prone systems restricted to estuaries, tidal flats, or tide-dominated deltas (**Fig. 1.2**) (Boyd et al., 1992; Dalrymple, 1992; Dalrymple et al., 1992; Harris et al., 2002; Harris and Heap, 2003; Dalrymple and Choi, 2007; Dalrymple et al., 2012, 2015; Desjardins et al., 2012a) with their corresponding linked sub-environments such as tidal shelves, tidal/flood deltas or lagoons in tide-dominated-wave-modelled estuaries.

The combined effects of fluvial currents, waves and most notably tides, provide an effective system of sediment sorting and accumulation of sand-prone deposits in nearshore settings. These depositional environments offer notable reservoir potential for the oil and gas industry, which has devoted significant exploration effort in the search for incised valley fill and deltas in the subsurface, given the excellent reservoir quality properties and areal extension of the related delta front, subtidal and fluvio-tidal deposits.

Tidally-influenced shoreline and deltaic deposits form some of the largest and most architecturally complicated hydrocarbon fields in the world (Verdier et al., 1980; Carneiro de Castro, 1983; Higley, 1994; Ambrose et al., 1995; White et al., 1995; Marjanac and Steel, 1997; White and Barton, 1999; Martinius et al., 2000). Despite the highly prolific nature of reservoirs in these highly heterogeneous type of deposits (Tyler and Finley, 1991), ancient subsurface examples are poorly documented. In addition, although 8 of the 12 largest deltas in the modern world are either tide-dominated or show strong tidal influence (Middleton, 1991, after Milliman

and Meade, 1983), surprisingly little attention has been paid to characterizing tidally-influenced deltas or shorelines in the modern record (Wood, 2004). In addition, according to Bradley et al. (2018), an estimated 16000 Million Barrels of Oil Equivalent (MMBOE) and 16 trillion cubic feet (tcf) are reported to be contained only within Lower Paleozoic paralic reservoirs globally (Havord, 1993; Boote et al., 1998; Millson et al., 2008; Tamar-Agha, 2009).

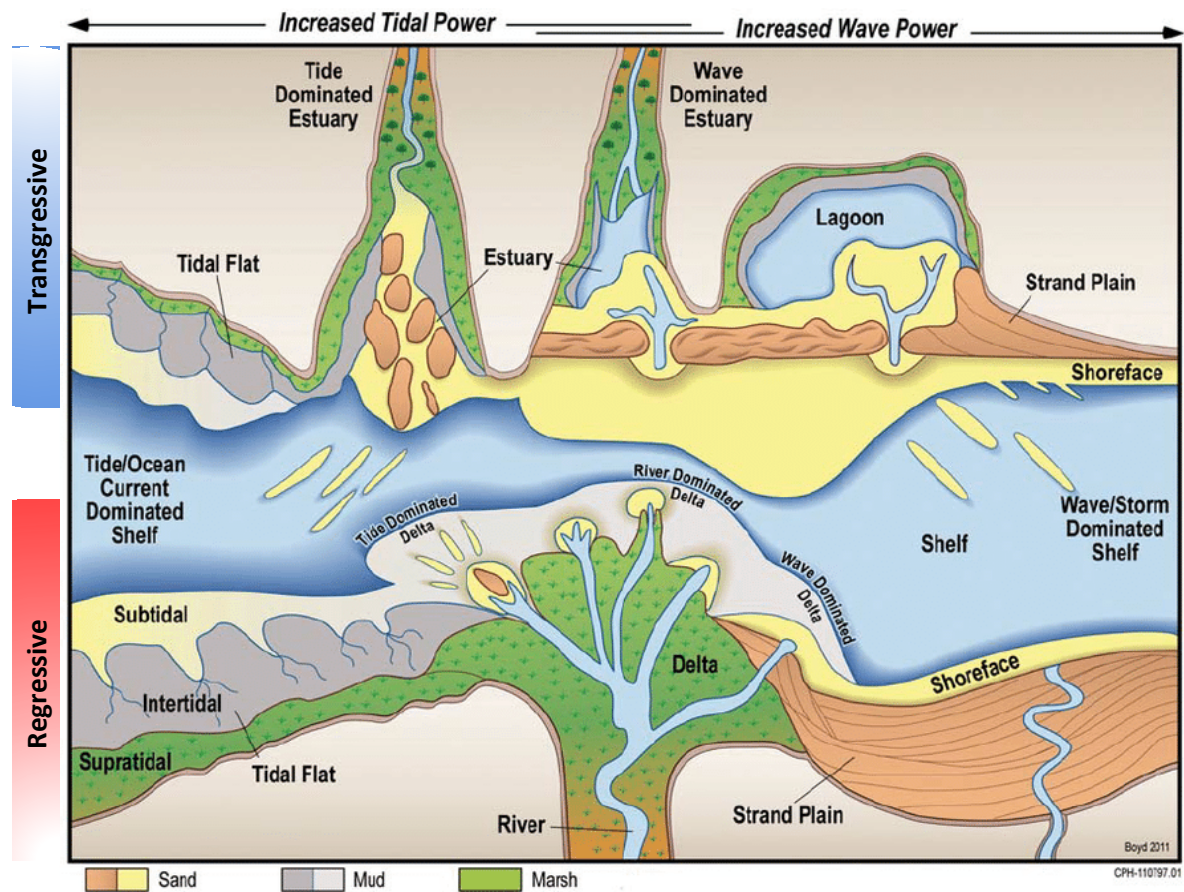


Figure 1.2. Common coastal depositional environments based on ratio of wave, tide and fluvial power. The deltas, strand plains, and open-coast tidal flats (lower half of diagram) are regressive coastal environments, whereas estuaries, barrier-lagoon systems, and open coast tidal flats (upper half of diagram) are transgressive coastal environments. Shelf environments are associated with both types of coast; shelf width increases during transgression and decreases during regression. Modified from Boyd et al. (1992) including modifications from James and Dalrymple (2010).

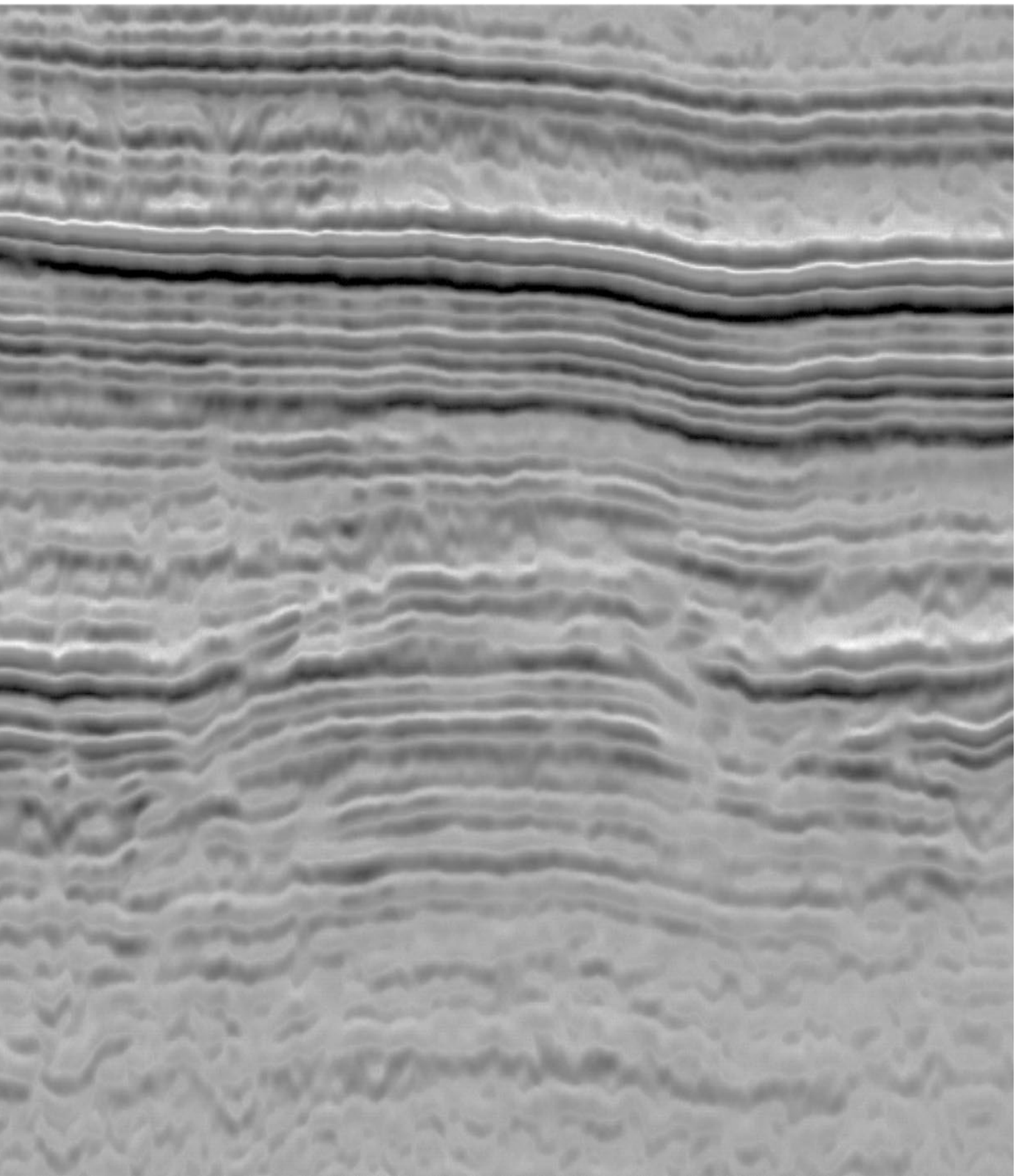
1.3. Previous studies and interpretations of the Hawaz Formation

To date, only a few sedimentological studies of the Hawaz Formation have been carried out, and all are almost exclusively based on surface geology (Vos, 1981; Anfray and Rubino, 2003; Ramos et al., 2006; Gibert et al., 2011). Other published works have focused on diagenesis (Abouessa and Morad, 2009; Abouessa, 2012) and trapping mechanisms (Franco et al., 2012).

Vos (1981) suggested that the Hawaz Formation was an example of a fan delta system principally comprising delta front deposits overlain by subaqueous distributary channels and distributary mouth shoals and swash bars. This delta front complex would be abruptly and erosively overlain by braided fluvial and distributary channels of the lower deltaic plain, sometimes overlain in turn by thin transgressive marine shelf sequences formed during periods of minimal detrital influx.

Other authors (i.e. Anfray and Rubino, 2003; Ramos et al., 2006) highlighted sedimentary structures suggestive of a strong tidal influence. Anfray and Rubino (2003) also identified tidal-dominated facies, including tidal bars, tidal inlets and ebb/flood deltas, and storm- and wave-dominated littoral facies – beach to shoreface. Ramos et al. (2006), also proposed a tide-dominated model with deposition in a low-gradient large-scale estuary where the morphology of the paleocoastline enhanced tidal action, specially during transgressive episodes, when the coastal embayment was flooded.

Given that the several interpretations suggested in these previous publications were based on an essentially limited database from the outcropping section of the Gargaf High (**Fig. I.I**), this thesis provides an entirely new state-of-the-art dataset from the subsurface of the Murzuq Basin, which aims to expand and complement the outcrop-based interpretation towards the South and to provide new insight of this clastic marginal to shallow marine succession.





CHAPTER 2. GEOLOGICAL SETTING

2.1. North Africa in the Lower Paleozoic –
The Saharan Platform

2.2. The Murzuq Basin

2.3. The Hawaz Formation

The cover photo of the Chapter 2 shows a seismic section from the subsurface of the Murzuq Basin showing the spectacular geomorphology produced by the Late Ordovician Glaciation in the form of paleohighs and paleovalleys. This section is interpreted in Fig. 2.8 of this chapter.

2.1. North Africa in the Lower Paleozoic – The Saharan Platform

During Early Paleozoic times, the African craton was part of the Gondwana supercontinent. Paleogeographic reconstructions (cf. Matte, 2001; Cocks and Torsvik, 2002, 2021; Kuhn and Barnes, 2005), suggest that what is today northwest Africa was located on the western-north-western margin of this supercontinent (**Fig. 2.1**). During this time, the Saharan region appears to have been a very low gradient, coastal plain to shallow marine platform or shelf located south of the Rheic Ocean and the Armorican microplate or Armorican Terrane Assemblage (**Fig. 2.1**). This region, also called “Saharan Platform”, was characterised by thick, near-continuous, sheet-like facies tracts deposited from at least the Mid-Late Cambrian to Middle Ordovician and can be observed across the larger North African cratonic margin (Boote et al., 1998).

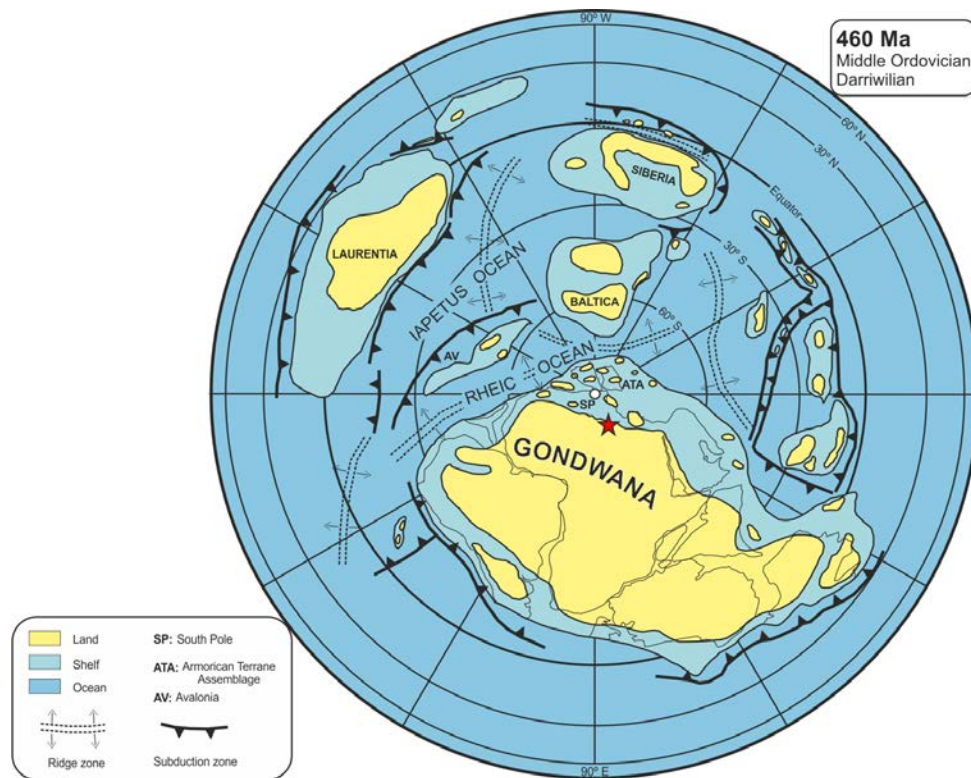


Figure 2.1. Middle Ordovician (Darrivilian – 460 Ma) tectonic plate distribution showing approximate plate boundaries, the principal emergent areas and oceans. The approximate location of the Murzuq Basin is represented with a red star. Note the wide extension of the shallow marine cratonic margin constituting all the north to north-western margin of Gondwana. Redrawn and modified from Cocks and Torsvik (2021).

Africa is broadly formed by cratons and mobile belts (Petters, 1991). The cratons are areas which have not been deformed since the Paleo – to the Mesoproterozoic or even younger times.

They include shields, comprising strongly deformed igneous–metamorphic basement complexes, and platforms, comprising less strongly deformed basement with a younger sedimentary cover (**Fig. 2.2**).

The African continent preserves a long geological record that covers almost 75% of Earth’s history, from at least Mid-Archean. For our study area, a key event was the so-called Pan-African orogeny (c. 600–500 Ma) which brought together several old continental kernels or cratons, such as the West African, Congo, Kalahari and Tanzanian (**Fig. 2.2**) thereby forming Gondwana and subsequently the supercontinent Pangea by the Late Paleozoic (Van Hinsbergen et al., 2011).

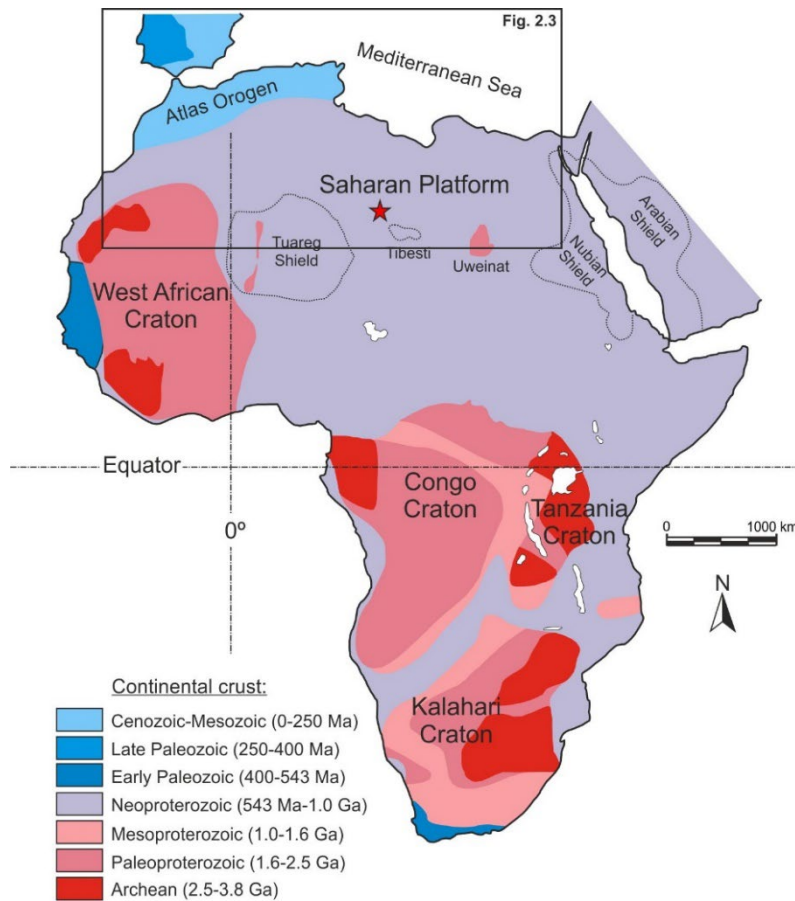


Figure 2.2. African continent with the main four cratons and the Saharan Platform (Metacraton). Note the age of the crustal basement (after Gobanov and Mooney, 2009) differentiated by colours from Archean to Cenozoic. The ages represent the time of crustal formation or thermal/tectonic crustal reworking. Note also the approximate location of the Murzuq Basin represented with a red star. The approximate area represented in **Fig. 2.3** is highlighted with a black rectangle. Redrawn and modified from Van Hinsbergen et al. (2011).

The North African or Saharan Platform lies between the North African shield zone in the south (Tuareg, Tibesti and Nubian-Arabian shields), and the Atlas fold belt and East Mediterranean Sea to the north (**Fig. 2.2**). Given this location, the North African Platform has experienced a complex and polyphase tectonic and sedimentary history.

The underlying Precambrian basement evolved from the collision and suturing of several cratons and intervening island arcs during the Pan-African orogeny. Subsequently, across a major unconformity, a regionally continuous, clastic-dominated passive margin developed on the northern margin of Gondwana (**Fig. 2.1**). This was progressively segmented into broad intracratonic basins bounded by tectonic highs, enlarged during the Devonian to Early Carboniferous. Subsequently, the Platform evolved into a stable Gondwana and later Tethyan passive margin, albeit interrupted by Hercynian deformation associated with the Late Carboniferous collision with Laurasia, rifting during the Mesozoic and the Atlassic-Maghrebian orogenesis in mid-late Tertiary (Boote et al., 1998).

The sedimentary cover of the Saharan Platform thus consists of a thick sequence of Cambrian to generally early Carboniferous (Viséan-Tournasian) largely clastic rocks covered locally by younger Mesozoic to Cenozoic sequences. These deposits are found in a series of shallow sag basins across the region, from the Kufra, Murzuq and Ghadames basins in the East to the Reggane and Tindouf Basins in the West (**Fig. 2.3**).

Many of these basins and surrounding outcrops have been extensively studied during the last few decades given the discovery of numerous major Paleozoic-sourced hydrocarbon accumulations, specially across the western part of the Saharan Platform in SW-W Libya and E-SE Algeria, in various sandstone reservoirs ranging in age from Cambro-Ordovician to basal Triassic (Boote et al., 1998).

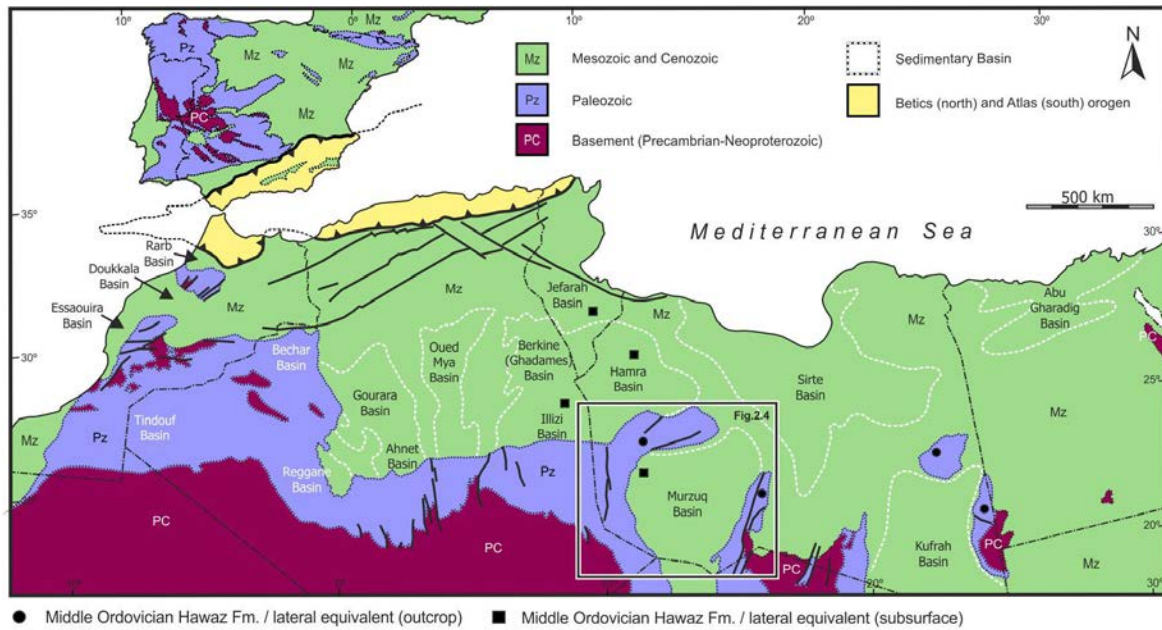


Figure 2.3. Regional map of North Africa and Iberia. The main Paleozoic sedimentary basins located onshore the Saharan Platform are, from west to east: the Essaouira, Doukkala and Rarb Basins on the western Moroccan margin; Tindouf and Bechar Basins between Morocco and Algeria; Reggane, Gourara, Ahnet, Oued Mya, and Illizi Basins in Algeria; Berkine-Ghadames and Hamra Basins partially between Algeria, Tunisia and Libya; Jefarah Basin in Tunisia; Murzuq, Sirte and Kufrah Basins in Libya and the Abu Gharadig Basin in north Egypt. These sedimentary basins are typically bounded by tectonic uplifts locally exposing the Paleozoic successions. The extent of **Fig. 2.4** is also highlighted with a black square. After Boote et al. (1998).

2.2. The Murzuq Basin

The Murzuq Basin lies in the central part of the Saharan Platform (**Fig. 2.2**), located in south-southwest Libya, covering an area of approximately 350,000 km². The estimated maximum sedimentary thickness is approximately 4000 m in its depocentre (Davidson et al., 2000), consisting mainly of Paleozoic and Mesozoic deposits, mostly covered by Holocene aeolian sand dunes forming the Libyan Desert (Ubari and Murzuq ergs or sand seas), to the north and south of the Messak Escarpment (**Fig. 2.4**).

An extensive collection of papers was reviewed by Sola and Worsley (2000) with the aim of summarising the state of knowledge in the Murzuq Basin. These were followed by a series of more recent publications, encouraged by the growing interest in this basin due to numerous hydrocarbon exploration discoveries (i.e. Davidson et al., 2000; McDougall and Martin, 2000; Hallet, 2002; Anfray and Rubino, 2003; Ghienne et al., 2003, 2012; Le Heron et al., 2004, 2006; Ramos et al., 2006; Boote et al., 2008; Abouessa and Morad, 2009; Gibert et al., 2011; Abouessa,

2012; Franco et al., 2012; Shalbak, 2015; Ron Martín, 2016; Bataller et al., 2019, 2021, 2022; Gil-Ortiz et al., 2019, 2022).

Its present-day geometry bears little relation to the broader and larger pre-existing sedimentary basin that existed during the Paleozoic. The Paleozoic succession of this basin is an erosional remnant of an areally extensive continental margin (Saharan Platform) which originally extended along the north-western margin of the Gondwana supercontinent (Davidson et al., 2000).

Its present extent reflects several periods of uplift and unroofing during the late Paleozoic, Mesozoic, and Cenozoic, which, together, are responsible for its modern architecture and present basin geometry, which according to Boote et al. (1998) was formed mostly by mid-Cretaceous Austrian tectonism followed by intra-Cenozoic uplift/exhumation that exposed the pre-existing basin.

The current basin is composed of a central Cretaceous depression bounded to the northwest by the Atshan Arch, the Gargaf High to the north, and the Tihemboka and Tibesti (Mourizidie-Dor el Gussa) highs to the southwest and southeast, respectively (**Fig. 2.4**). These structural highs were formed by multiphase tectonic uplifts ranging in age from the middle Paleozoic to Cenozoic and the main periods of uplift and erosion occurred during the late Carboniferous (Hercynian), mid-Cretaceous (Austrian), early Cenozoic (Alpine) orogenic cycles (**Fig. 2.5-A**) and subsequent intra-Cenozoic exhumation.

Several geological events are imprinted on the stratigraphic record of the Murzuq Basin and some of them can be recognised as basin-scale unconformities within the sedimentary infill. Most of these were tectonically-controlled (Craig et al., 2008) and correspond to the Pan-African, Caledonian, Austrian and Hercynian tectonic phases (**Fig. 2.5-A**). The Taconic unconformity is also widely recognised and corresponds to the remarkable basal glacial erosional surface marking the base of the Late Ordovician glaciation (**Fig. 2.5-A**). Other unconformities can also be recognised within the sedimentary record and mainly correspond to a younger Alpine cycle, with only a minor impact on the Paleozoic section in the central Murzuq Basin.

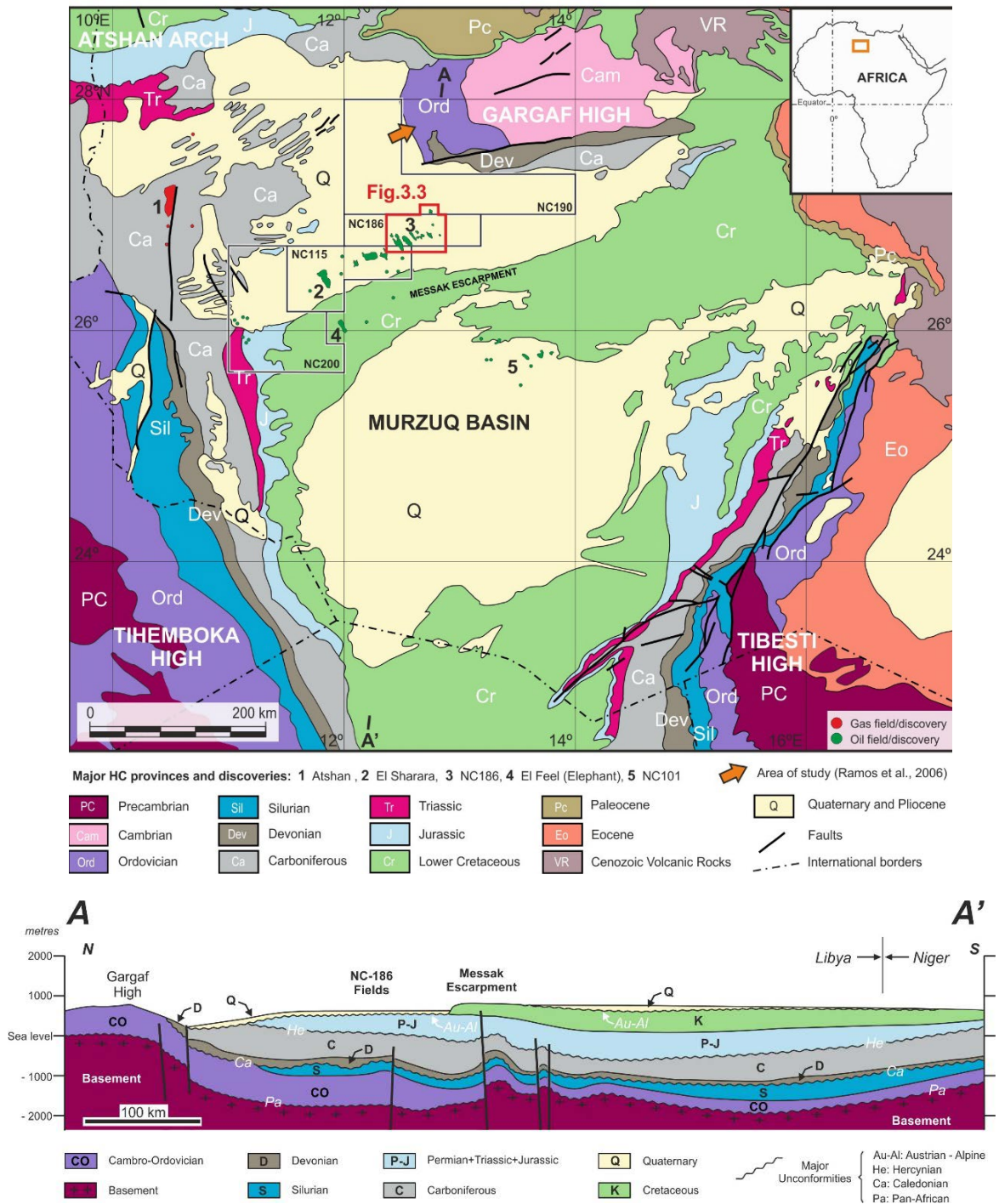


Figure 2.4. Geological map and cross-section of the Murzuq Basin. Above, note the main structures forming the boundaries of this basin, the Atshan Arch to the northwest, the Gargaf High to the north and the Tihemboka and Tibesti (Dor el Gussa-Mourizidie) highs to the southwest and southeast respectively. Note also the main exploration concessions and the major hydrocarbon provinces in the Murzuq Basin after Hallet and Clark-Lowes (2016). The area of interest represented in **Fig. 3.3** is highlighted by the red polygon. The outcrop area studied by Ramos et al. (2006), referred to in this paper is also highlighted with an orange arrow in the Gargaf High area. The location of the cross-section represented below is also represented in the map (A-A'). After Marzo and Ramos (2003) and Shalbak (2015). Below, see a regional cross-section of the Murzuq Basin from north to south (A-A'). After Davidson et al. (2000).

Within this framework, Boote et al. (2008), comment on the implications for the Paleozoic petroleum system elements, such as overburden removal, source rock maturity and reservoir quality due to diagenesis triggered by successive uplift events and unroofing of Mesozoic series and should be considered in future opportunities for hydrocarbon exploration. This combination of major tectonic events, key regional unconformities and the lithostratigraphic sub-division of the Murzuq Basin succession is reflected in **Fig. 2.5-A**, which is a data synthesis derived from Bellini and Massa (1980); Aziz (2000), Davidson et al. (2000), Echikh and Sola (2000), Craik et al. (2001) and Ramos et al. (2006).

The basement of the Murzuq Basin is composed of high-grade metamorphic and plutonic rocks, as well as low-grade metamorphic rocks of Precambrian age (Mourizidie Formation). The top of the basement is typically recognised and bounded by the Pan-African unconformity, which is overlain by the first main sedimentary unit of the Lower Paleozoic (**Fig. 2.5-A**).

Above the Pan-African unconformity, the sedimentary infill of the Murzuq Basin can be subdivided into four main units: (1) Cambrian–Ordovician, (2) Silurian, (3) Devonian–Carboniferous and (4) Mesozoic (**Fig. 2.5-A**), which commonly are covered by large Quaternary aeolian deposits in the central part of the basin. The Cambrian-Ordovician succession or main sedimentary unit 1, also known as the Gargaf Group (after Burollet, 1960), comprises, from bottom to top, the Hasawnah, Ash Shabiyat, Hawaz, Melaz Shuqran, Mamuniyat and Bir Tlacin Formations (**Fig. 2.5-A**), including the two most important oil-bearing reservoirs in the Murzuq Basin.

There are two petroleum systems in the Murzuq Basin (Boote et al., 1998; Davidson et al., 2000; Shalbak, 2015) both involving the basal Silurian hot shales source rock of the Tanezzuft Formation (Lüning et al., 2000; Lüning et al., 2003, Fello et al., 2006; Belaid et al., 2010; Hall et al., 2012; Meinhold et al., 2013). The main petroleum system is associated with the Middle and Upper Ordovician sandstones of the Hawaz and Mamuniyat reservoirs respectively, separated by a deeply incised unconformity related to the Late Ordovician glaciation (**Fig. 2.5-B**); both sealed by a thick succession of the Tanezzuft Formation shales (**Fig. 2.5**). The other petroleum system, considered as secondary, due to the non-commercial discoveries made to date, is composed of the basal Devonian sandstones as reservoirs and the intra-Devonian shales as the seal (Hallet, 2002; Shalbak, 2015).

Proven hydrocarbon distribution in the basin reflects the interaction of several factors such as regional structural evolution, trap geometry and age, reservoir quality both in terms of lateral

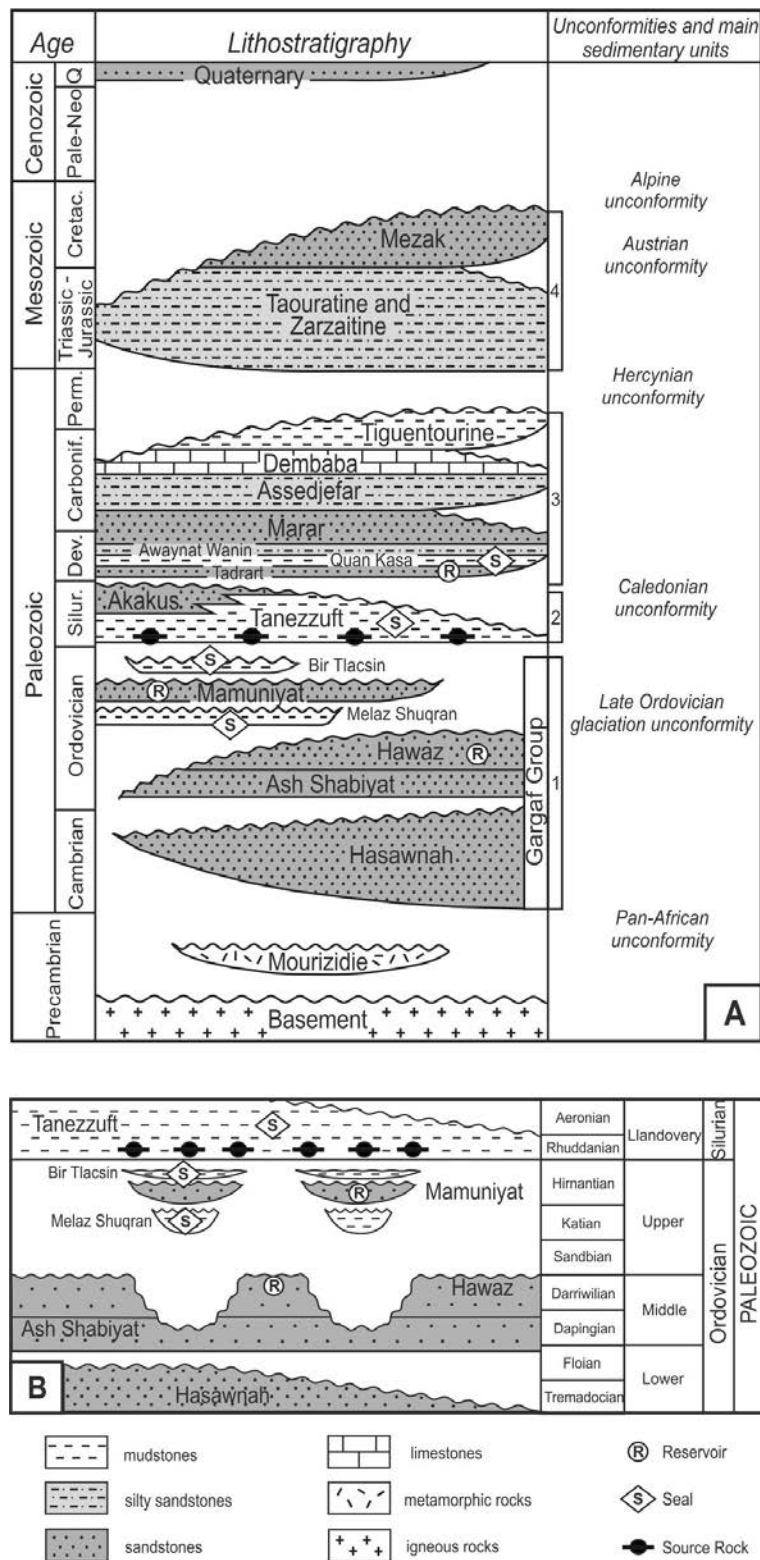


Figure 2.5. Murzuq Basin litho- and chronostratigraphy. A) Stratigraphic chart summarising the lithostratigraphy of the Murzuq Basin highlighting the main stratigraphic units and major basin-scale unconformities. 1 = Cambrian – Ordovician; 2 = Silurian; 3 = Devonian – Carboniferous; 4 = Mesozoic. B) Wheeler diagram showing the lithostratigraphic to chronostratigraphic relationships of the Ordovician and Lower Silurian succession in the area of study. The main petroleum systems elements are also represented.

facies variations and diagenetic changes and source rock quality and maturity. Migration pathways are controlled by reservoir facies variations, the character and continuity of Tanezzuft seals facies and by the fault system distribution. It is also significant that in areas where the shaly Bir Tlacsin Formation is developed, it appears to act as a barrier, or waste zone, for effective and direct communication between source rock and reservoir (Echikh and Sola, 2000).

2.3. The Hawaz Formation

The Hawaz Formation was originally defined by Massa and Collomb (1960) as the entire sandy Ordovician succession outcropping in the Gargaf High area (**Fig. 2.4**), bounded by two unconformities, above the top of the Hasawnah Formation and below the Melaz Shuqran or the Mamuniyat Formations. Later, Collomb (1962) subdivided the Hawaz Formation into three members: a) “Tigillites inferieurs”, b) “Gres intermediaries” and c) “Tigillites superieurs”, referring to highly bioturbated basal and upper successions (a and c) with *Skolithos* traces (Droser, 1991) separated by a cross-bedded sandstone member (b). Subsequently, Havlicek and Massa (1973) introduced the term Ash Shabiyat Formation for the lower and part of the middle member from the former subdivision by Collomb (1962) creating the current lithostratigraphic sub-division for the Middle Ordovician succession (**Fig. 2.5-A**).

The age of the Hawaz Formation is defined by reference to the acritarch and chitonozoan data of Molyneux et al. (1996) and Paris (1990, 1996), complemented by data from Tunisia and Algeria (Vecoli, 1999). An internal study by Robertson Research International Limited from a limited number of wells (see more details in **Chapter 3.1**) (Miles (2001, 2003)), confirms the best evidence for the age of the Hawaz Formation comes from the lower part of the unit where top *Stelliferidium striatulum* and *S. cortinulum* indicate an age no younger than the Llandeilo stage. Other acritarch datums within the Hawaz Formation suggest a Llanvirnian or older age, justified by the tops of *Dicrodiacrodium ancoriforme* and *Frankea longiuscula*. The bases of *Villosacapsula irrorata* and *V. setosapellicula* indicate an age no older than the upper Arenig, Fenn stage, on the basis of extensive data from the neighbouring Algerian basins. This is supported by the bases of *Frankea breviscula* and *Frankea sarthernardensis*. Thus, we can assume an Upper Arenig to Upper Llanvirn range (according to the traditional Ordovician British series), for the Hawaz Formation, which correlates with the late Dapingian to Late Darriwilian stages (**Fig. 2.5-B**) of the current International Chronostratigraphic Chart (Cohen et al., 2021).

The Hawaz Formation is recorded in the subsurface of the Murzuq Basin as a siliciclastic dominated succession, slightly more than 200 m in thickness, mainly composed of fine-grained quartz arenites and arkosic arenites with subordinate sub-lithic arenites (Gil-Ortiz et al., 2019). It is considered as an excellent reservoir, with mean measured porosities of up to 25.7% and modal values of 15 to 16% in the most sand-prone sections of the middle Hawaz. Horizontal permeabilities can reach 900–1000 mD, although values are most commonly between 0.2 and 150 mD (Shalbak, 2015). Sedimentation rates for this succession can be estimated as less than 26.9 m/my calculated for the whole Hawaz Formation, in equilibrium with the total subsidence (Ramos et al., 2006). Depositional facies, together with diagenesis, have an important impact on reservoir quality (Abouessa and Morad, 2009; Morad et al., 2010). Some of these diagenetic processes are related to near-surface eogenetic alterations, mediated by meteoric pore waters resulting in kaolinization of framework silicates (**Fig. 2.6-A**) and formation of small amounts of pyrite by marine pore waters. Subsequently, sandstones were also affected by deeper diagenetic processes related to the presence of feldspar, illite and high dickite/kaolinite ratios (**Fig. 2.6-B**), which are considerably higher in the subsurface than in outcrops probably due to a longer residence time and/or deeper burial conditions before final exhumation. In addition, there was also a significant phase of quartz overgrowth cementation (**Fig. 2.6-C and D**) in response to pressure dissolution of quartz grains, mechanical and chemical compaction (mesogenetic conditions). Finally, sandstones were affected by telogenetic alterations related to calcitization of mesogenetic siderite, oxidation of pyrite and formation of goethite, only identified in outcrop samples by Abouessa and Morad (2009) in this last case.

Several depositional models have been proposed for the Hawaz Formation (Vos, 1981; Anfray and Rubino, 2003; Ramos et al., 2006; Abouessa and Morad, 2009; Gil-Ortiz et al., 2019) all within a transitional to shallow marine setting. Gibert et al. (2011) identified up to 11 ichnogenera in the outcropping series of the Hawaz Formation on the Gargaf High, which are closely linked with both lithofacies and depositional environments. In broad terms, nearshore to shoreface facies are characterised by a dense ‘Pipe rock’ fabric dominated by *Skolithos* and *Siphonichnus* fossil traces, whereas storm-dominated heterolithics are characterised by horizontal deposit-feeding *Cruziana* ichnofacies traces.

Paleocurrents interpreted from image log tools suggest that there is a dominant flow direction toward the north-northwest with certain subordinate paleocurrents in the opposite direction related to tidal-flood currents effect (Gil-Ortiz et al., 2019, 2022). This trend would be mostly in accordance with large-scale sedimentary structures measured by Ramos et al. (2006) from outcrops of the Gargaf High (**Fig. 2.7**).

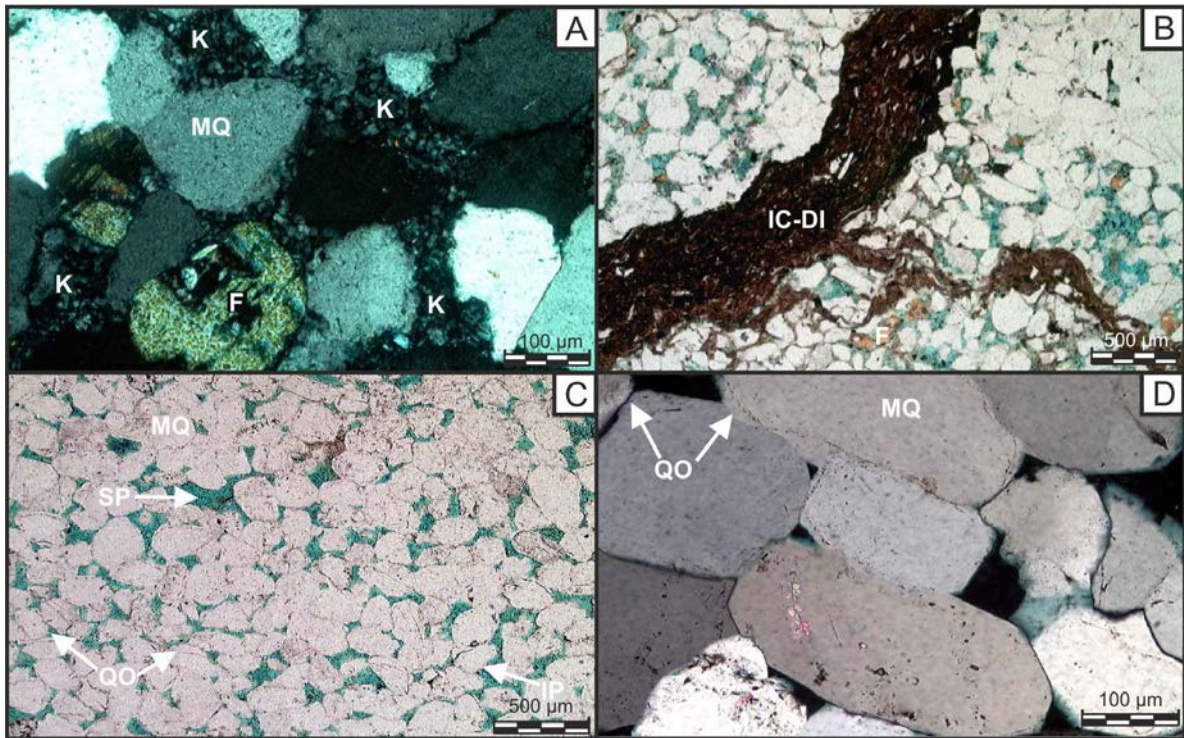


Figure 2.6. Hawaz Formation thin sections. A) Detailed view of predominant monocrySTALLINE quartz grains (MQ) and K-feldspars (F). See the intergranular macropores are totally infilled by clusters of kaolinite (K). K-feldspar grains are intimately related to kaolinite, this indicates that kaolinite is formed by the alteration of K-feldspar. Quartz grains have straight to concavo-convex contacts indicating that a moderate degree of compaction occurred.; B) General view of a moderately sorted, fine-grained sandstone. Detrital grains are predominantly composed of subangular monocrySTALLINE quartz with subordinate K-feldspar (F) and micas. Detrital illite (DI) and indeterminate clays (IC) are present in compacted/crenulated laminae. Authigenic kaolinite derived from the alteration of K-feldspars is also present, and locally occludes intergranular pores. Pyrite is present in trace volumes. A and B thin sections from well W06; C) Very well sorted, massively structured, medium-grained quartz-arenite, with abundant monocrySTALLINE quartz (MQ) displaying a moderately preserved intergranular pore network (IP). These pores are moderately well interconnected and supplemented by oversized grain dissolution pores (SP). Much of original porosity present at deposition has been reduced by compaction and significant authigenic quartz overgrowth cement (QO); D) A) Clean, very well sorted medium-grained sandstone consisting of abundant detrital quartz grains (MQ) displaying well developed, euhedral, pore-filling quartz overgrowths (QO). Moderate to strong compaction is indicated by the presence of straight to slightly sutured grain contacts. C and D thin sections from well W30. See **Fig. 3.3** for location of the wells.

The architecture of the Hawaz Formation and lateral age-equivalents observed in both, the subsurface (**Fig. 2.8-A**) and outcrop (**Fig. 2.8-B**), reflects often spectacular Late Ordovician erosional incision by north-northwest to west-flowing glaciers during the Hirnantian (Ghienne et al., 2003; Le Heron et al., 2004; Ramos et al., 2012; Bataller et al., 2021), eroding deeply down into the Hawaz and even the underlying Ash Shabiyat Formation. This event generated a distinctive Middle to Upper Ordovician architecture comprising a series of paleovalleys filled by

Katian-Hirnantian glaciogenic sediments, and remnant Middle Ordovician paleohighs (**Fig. 2.8**).

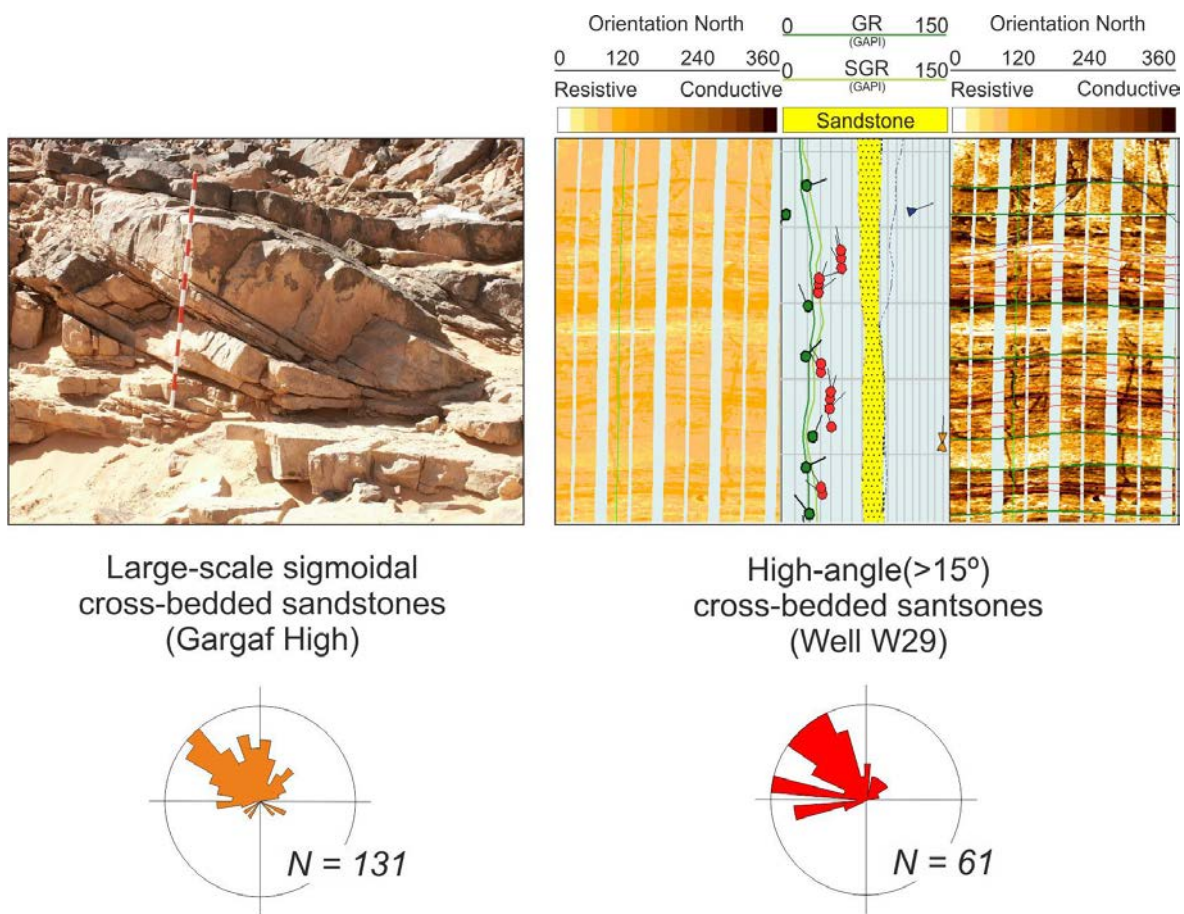


Figure 2.7. Paleocurrents measured in the Hawaz Formation. At the left, see the average paleocurrent trend measured by Ramos et al. (2006) at the Gargaf High in subtidal sandstones. Scale is 150 cm (Jacob’s staff). Photo courtesy of Emilio Ramos. At the right, see also the paleocurrents measured in 3 m section from well W29 (see **Fig. 3.3** for location of the well) in equivalent subtidal complex deposits, with image log data (FMI), in the subsurface of the Murzuq Basin. Only large-scale or high-angle cross-bedding structures have been considered for paleocurrent analysis in this study, represented by red tad poles in the central track, compared to low-angle (green) laminations and high-angle (triangles) natural and induced fractures.

This erosional paleorelief constitutes the main stratigraphic trapping mechanism for the Hawaz Formation in the Murzuq Basin, in form of typically isolated Hawaz paleohighs.

The Middle Ordovician Hawaz succession is well represented in the Murzuq Basin although its lateral equivalents extend for hundreds of kilometres across North Africa into Arabia and can most definitely be recognised in the neighbouring areas of the Kufrah Basin to the east (Seilacher et al., 2002; Le Heron et al., 2010), in the Jefarah and Berkine-Ghadames basins to the north (Dardour et al., 2004; Jabir et al., 2021) and in the Illizi Basin to the west (McDougall

et al., 2008a, 2008b, 2011), where the equivalent is known as the In Tahouite Formation (or Unit III-3 in the subsurface), on the basis of published data (**Fig. 2.3**).

This study is thus focused on only a small part of a broader and widespread facies complex deposited during the Middle Ordovician in the north-western part of the Gondwana cratonic margin.

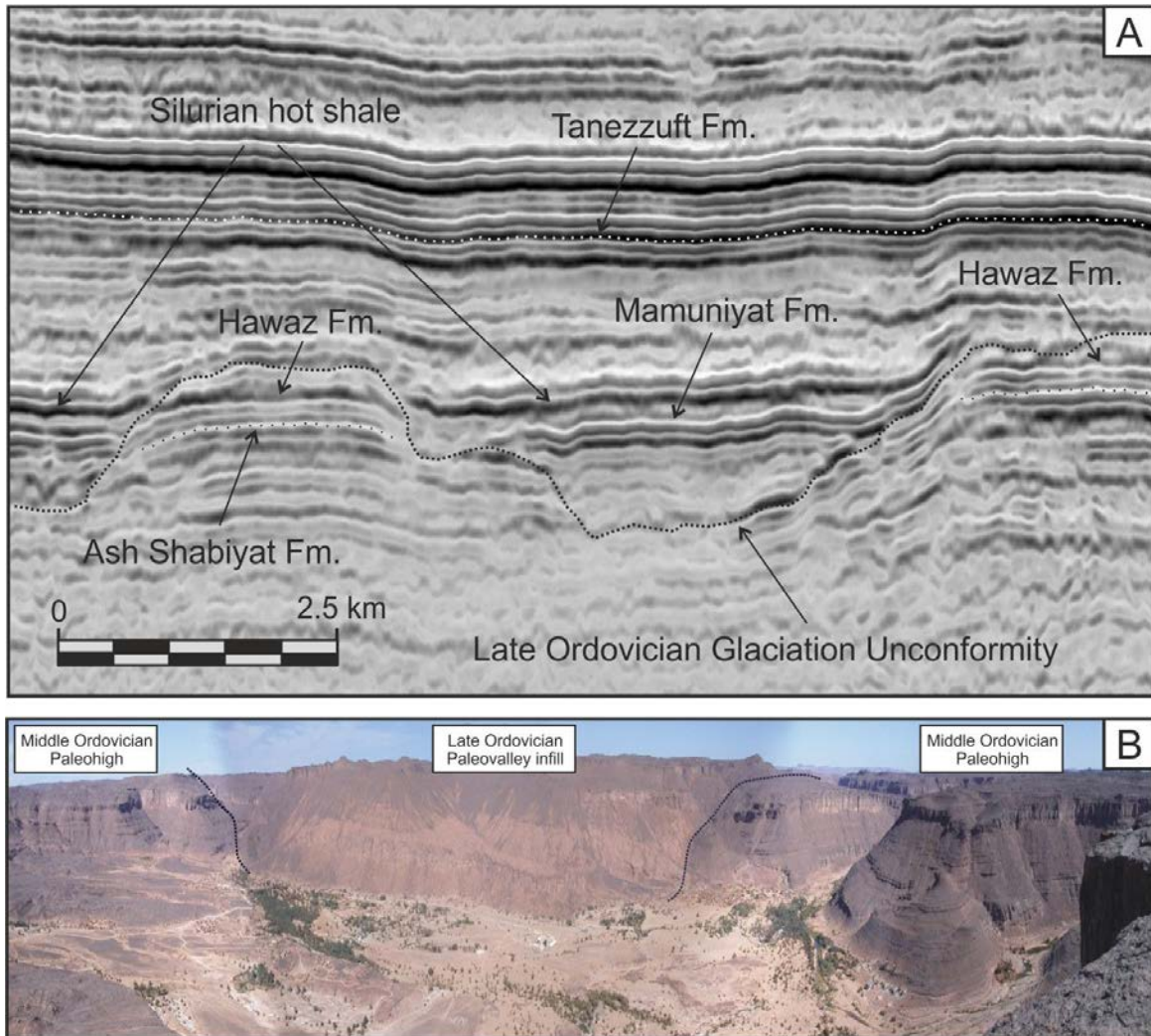


Figure 2.8. Hawaz Formation architecture. A) Seismic section from the subsurface of the Murzuq Basin showing the typical geomorphological profile of the Ordovician succession in the form of paleohighs and paleovalleys. Note the deep incision corresponding to the Late Ordovician Glaciation Unconformity and the Upper Ordovician deposits infilling the paleovalleys, separated by Lower and Middle Ordovician Ash Shabiyat and Hawaz Formations. See also the high amplitude of the basal Tanezzuft Fm. corresponding to the Silurian hot shale, represented by a bright negative reflector; B) Dip parallel view along the axis of a major outcropping paleovalley in SE Algeria (Iherir area). The paleohighs are represented by Middle Ordovician In Tahouite Fm. (Unit III-3), lateral age-equivalent to the Hawaz Fm., and the paleovalley is filled with the Late Ordovician Tamadjert Fm. (Unit IV), lateral age-equivalent to the Melaz Shuqran, Mamuniyat and Bir Tlacin Fms. Modified from McDougall, et al. (2008b).





CHAPTER 3. DATA AND METHODS

3.1. Study area and dataset

3.2. Sedimentological analysis: Methodology

3.3. Sedimentary architecture analysis: Methodology

The cover photo of the Chapter 3 shows several amalgamated and vertically stacked massive, lenticular sand bodies belonging to a subtidal complex in the middle section of the Hawaz Formation. The picture was taken in the outcrops of the Gargaf High (Murzuq Basin, SW Libya).

Photograph courtesy of Emilio Ramos.

This section introduces the study area and summarises the input data and the methodological workflow (**Fig. 3.1**) followed in this thesis.

The main dataset used in this research is represented by subsurface data, mainly core, image log and conventional wireline log data, but also geological field data collected by Ramos et al. (2006) in the neighbouring area of the Gargaf High, which has been used as a comparative tool along the first descriptive sedimentological phase (see **Chapter 3.1**).

The methodological workflow can be separated in two well-defined phases: 1) Phase I: sedimentological analysis (see **Chapter 3.2**) and 2) Phase II: sedimentary architecture analysis (see **Chapter 3.3**). In summary, the overall methodological workflow is as follows:

- 1) Phase I: Characterisation of lithofacies with core and image log (FMI) data in a purely first descriptive phase.
- 2) Phase I: Interpretation of facies associations at each control point (wells), from stacking patterns observed in core, image log and conventional wireline log data.
- 3) Phase I: Building of a sequence stratigraphic framework for each well, identifying potential correlatable systems tracts/stratigraphic reservoir zones.
- 4) Phase II: Correlation of these sedimentary packages throughout the study area with a set of eight correlation panels constructed along both depositional dip and strike directions, according to an idealized preliminary conceptual sedimentary model.
- 5) Phase II: Calculation of the relative proportions of facies associations for every well and systems tract and extrapolation of these data from wells to surrounding areas together with paleocurrents, insights from the conceptual sedimentary model and interpreted correlation panels for each systems tract or zone, within four different Gross Depositional Environment (GDE) maps.
- 6) Building of an updated depositional model on the basis of the outputs from the correlation panels and GDE maps for our area of study.

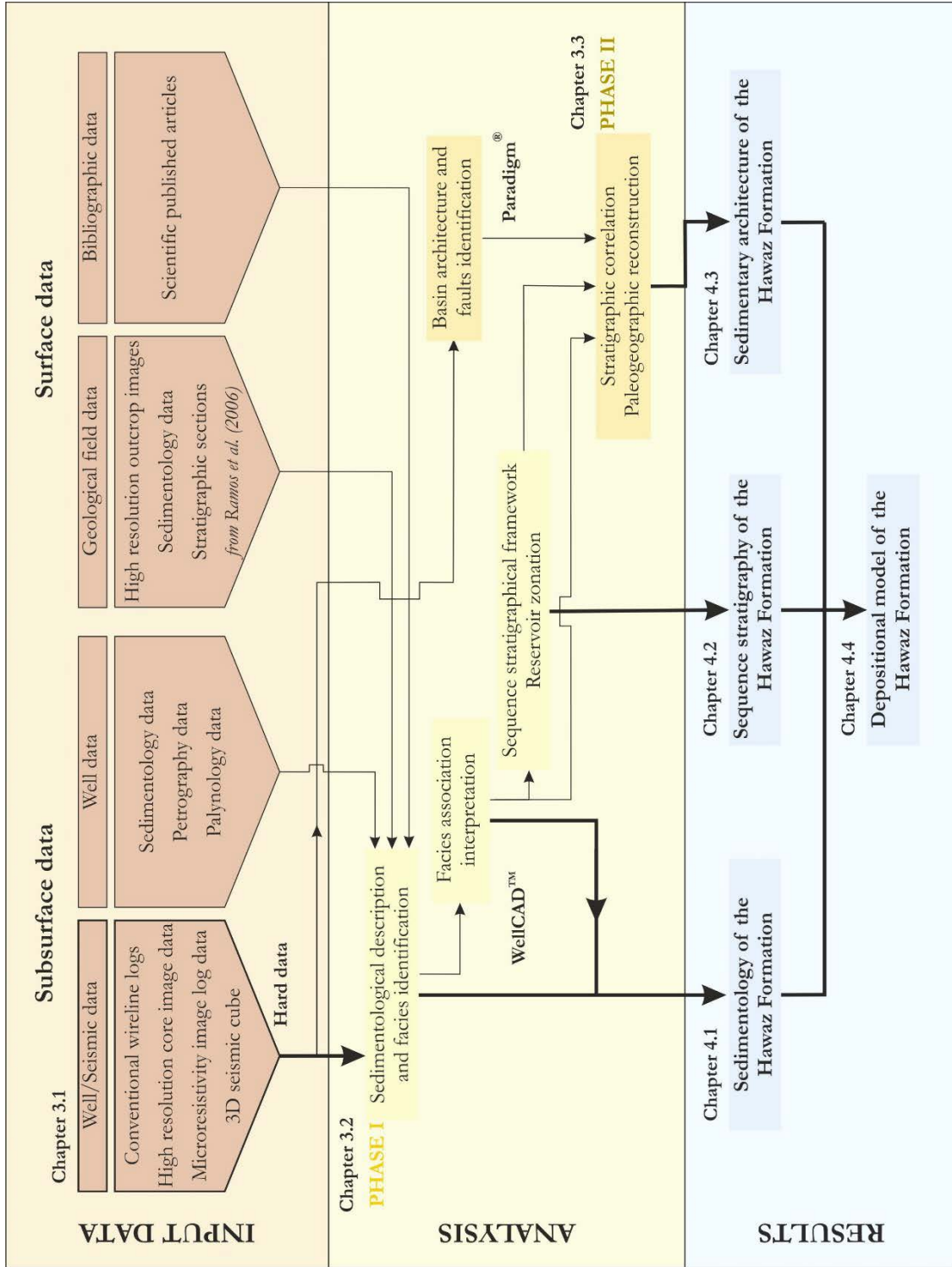


Figure 3.1. Summary of the methodological workflow followed in this thesis.

3.1. Study area and dataset

The current study area lies within the north central part of the Murzuq Basin (SW Libya), mostly covered by Quaternary aeolian deposits associated with two major ergs (Ubari and Murzuq) or sand seas and only at the margins (Gargaf, Atshan, Tihemboka and Tibesti Highs), or along the central Messak Escarpment, are the Paleozoic and Mesozoic deposits observed outcropping (**Fig. 2.4**).

This thesis was principally based on well data after synthesis and standardization from 35 exploration and appraisal wells, drilled by Repsol Exploración Murzuq SA (REMSA), located across the north-central sector of the Murzuq Basin, mainly in Concession or Block NC186 (**Fig. 3.2**), covering an approximate area of 1600 km². The average distance between wells is about 5 km, although wells belonging to the same field can be much closer up to a few hundreds of metres apart. The maximum distance of separation between wells is slightly more than 15 km.

Most of the wells drilled the four main sedimentary units of the Murzuq Basin (**Fig. 2.5-A**) up to the Lower Ordovician Ash Shabiyat Fm. reaching depths up to 1600 m. The top of the Hawaz Formation is encountered between 830 and 1500 m KB (below Kelly Bushing – Driller's Depth) in the studied area.

These data included a broad spectrum of data types including:

- 1) Conventional wire-line logs (Gamma Ray, Density, Neutron and Sonic). The logs were acquired mostly in 12.25" and 8.5" vertical boreholes, using Water Base Mud (WBM) at a standard vertical sample rate of 0.1524 m, which can be considered as the vertical resolution of these tools.
- 2) Slabbed core descriptions and high resolution core images by Robertson Research International Limited as internal study for Repsol Murzuq S.A. and partners Equinor, TotalEnergies and OMV.
- 3) Microresistivity image logs (Fullbore Formation Microimager Image - FMI) for most of the wells with approximately 60% to 80% radial borehole coverage (depending on the hole size) and 0.5 cm vertical resolution.
- 4) Seismic 3D data (**Fig. 3.2**), used to provide insight about the basin architecture of this Formation in the area of study, as well as identification of main faults bounding paleohighs.

- 5) Sedimentology and petrography data interpreted for most of the wells in the area of study by Robertson Research International Limited.
- 6) Palynology interpreted data from six wells in the present area of study (i.e. W04, W28, W29, W27, W32 and W35; **Fig. 3.3**) by Robertson Research International Limited (Miles, 2001, 2003).
- 7) Comparisons to outcropping equivalents studied by Ramos et al. (2006) on the Gargaf High (**Fig. 2.4**), in further detail in Marzo and Ramos (2003) confidential report.
- 8) Other bibliography from public domain (scientific published articles).

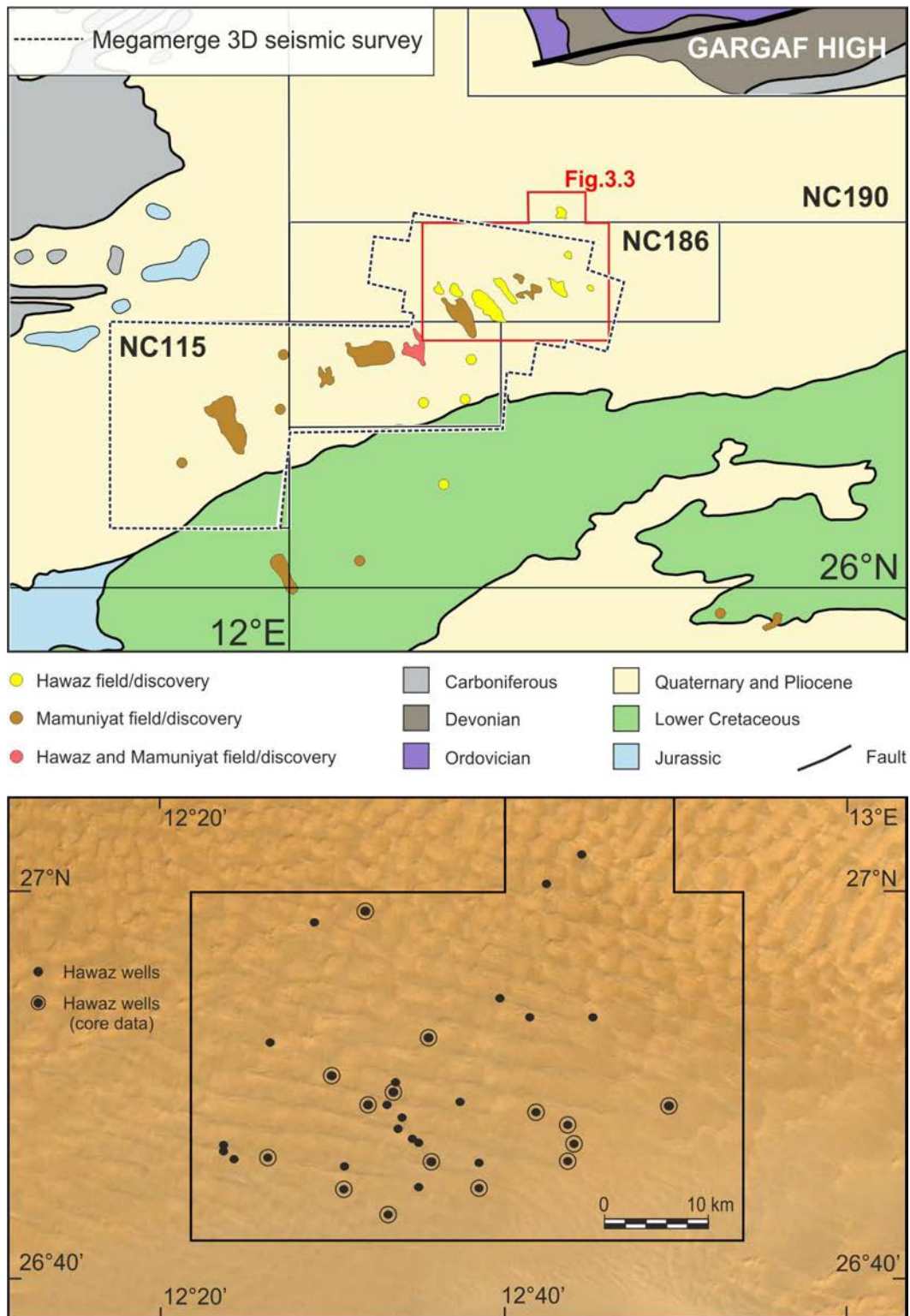


Figure 3.2. Area of study and dataset location. See in the upper part of this figure a close-up view from **Fig. 2.4** showing the main study area (NC186 concession) and two adjacent exploration concessions, NC115 and NC190, as well as the main discoveries made in this area classified by their main reservoir, Hawaz or Mamuniyat. Note the limit of the 3D seismic survey (“Megamerge 3D seismic survey”) available in both the area of study and surrounding concessions. The red polygon highlighted here corresponds to our area of study represented below with the location of the wells by availability of core data, expanded with further information in **Fig. 3.3**.

3.2. Sedimentological analysis: Methodology

3.2.1. Facies analysis

Description and interpretation of the sedimentary facies is largely based on fourteen 1:50 scale well core descriptions and image log data, defined on the basis of lithologies and internal fabric. For this study a review and re-interpretation of lithofacies was made, using both the original descriptions and high-resolution core images, considering the impossibility of getting access to the physical slabbed core data due to ongoing security issue in Libya. For this reason, the high-resolution micro-resistivity image logs (FMI) constituted a key piece of information for describing lithofacies at this stage.

The Formation Micro Imager (FMI) tool was acquired by *Schlumberger* and the processing of raw data was made by petrophysical specialists team in Repsol following these steps: 1) navigation quality control through the magnetometer and accelerometer data assuring tool orientation centralization and stick and pull effects, 2) speed correction assuring correct depth using stick and pull effects through the cable tension; and 3) generation of the final static track (constant values for the colour scale end-points) and dynamic track images (changing end-point values for the colour scale aiming to maximize contrast between resistive and conductive features) for an interpretation purpose.

Conventional wireline logs (GR, Sonic, Density and Neutron), whilst available for all study wells, were not used to define lithofacies at this stage because the typical thickness of most lithofacies units is typically below the vertical resolution of these tools (0.1524 m).

The main elements considered in the facies description include lithology, grain size, sorting, sedimentary structures, type and degree of bioturbation, bed thickness and accessory elements such as diagenetic nodules, mud clasts, mud drapes and cracks. The resultant lithofacies scheme was compared with equivalent deposits in outcrop studied by Ramos et al. (2006), complemented with valuable observations on ichnofacies made by Gibert et al. (2011), both in the same area of the Gargaf High (**Fig. 2.4**), approximately 120 km distant from our area of study, and then used as an analogue for subsurface correlations (see **Chapter 4.1.1**).

Based on this lithofacies scheme, a group of facies associations was characterised based on vertical evolution of lithofacies, interpreted mainly on high resolution image logs (FMI) calibrated with available core data. Core-to-image log shift and stretch was a common process to properly fit the studied sections as they rarely perfectly coincided.

Support from complementary conventional wireline logs provided valuable data on stacking patterns and clay content (see **Chapter 4.1.2**), which was specially helpful in those sections without core and, less commonly, without image log data.

3.2.2. Hawaz Formation: Sequence stratigraphic-based zonation

Based on the vertical changes observed in facies associations and their stacking patterns, some depositional trends and genetic stratigraphic units can be clearly identified in the Hawaz Formation. These patterns defined correlatable system tracts bounded by high frequency sequence boundaries and flooding surfaces, which in turn reflect changes in sediment supply, relative sea level and accommodation. Following an adapted sequence stratigraphic approach based on the methodology of Embry (2009), a series of consistent, genetically-based sedimentary packages were identified in the Hawaz Formation (Gil-Ortiz et al., 2019).

Although a number of high-frequency sequences can be identified in all wells, a simplified scheme of three major, possibly 3rd order, depositional sequences (DS1-DS3) was preferred. Each of these sequences is composed of two systems tracts (TST and HST) bounded by key surfaces. These were then used to create a five-fold reservoir zonation scheme (HWZ1 to HWZ5) (see **Chapter 4.2**), each zone equivalent to an individual systems tract, considering that the last depositional sequence (DS3) is rarely present due to the Late Ordovician glaciation unconformity only preserving the remnants of the early transgressive systems tract, with the main objective of providing a more robust genetic correlation and so avoid a tempting, but purely lithostratigraphic correlation in an apparent Hawaz “layer cake” succession.

The key bounding surfaces defining the limits of the genetic sedimentary packages were recognised using a material-based sequence stratigraphic approach (Embry, 2009). The defined surfaces are the following.

- Maximum regressive surface, in which a conformable horizon marks a change from coarsening- and shallowing-upward to fining- and deepening-upward.
- Maximum flooding surface, in which a conformable horizon marks a change from fining- and deepening-upward to coarsening- and shallowing-upward and is normally represented by the most mud-rich horizon in the succession.

- Shoreline ravinement unconformity, in which a clear erosive surface is overlain by brackish marine deposits, and which represents erosion in the stratigraphic unit produced by wave and tidal currents during an early transgressive stage just after a base level fall.

- Regressive surface of marine erosion, in which, in an overall regressive succession, a clear change exists in depositional trend with shelfal deposits abruptly overlain by prograding shoreface deposits. As suggested by Embry (2009), this last surface is not a suitable surface for correlation because of its highly diachronous nature. As such it has not been used as a main bounding surface for our sequence stratigraphic framework. However, locally, it may be of use in explaining trend changes in the facies succession observed in some wells.

3.3. Sedimentary architecture analysis: Methodology

3.3.1. Correlation panel construction

The large-scale geometry of the present day Hawaz Formation, in both outcrop and subsurface, bears little relation to its original configuration and depositional profile. Its current gross architecture or geometry is characterised by a number of paleohighs separated by a set of northwest to southeast or west-east aligned paleovalleys in the area of study, generated by multiple erosive episodes associated with the Late Ordovician Hirnantian glaciation (**Fig. 3.3** and **3.4**). This remnant sub-glacial paleorelief was subsequently infilled with Late Ordovician glaciogenic sediments, locally in excess of 500 m thick, associated with a complex series of erosive and deposition events related to the advance and retreat of ice sheets (**Fig. 2.8** and **3.4**). The resultant paleotopography has remained largely unchanged since the late Ordovician, with only slight modifications during subsequent major tectonic events (**Fig. 2.5-A**).

Many of the paleohighs in this “buried” paleorelief are notably bounded by faults (**Fig. 3.4**), which follow a north-northwest to south-southeast trend, linked to Pan-African basement structures, apparently connected to lower intervals within the Cambro-Ordovician succession. It is suggested by some authors that the structural weaknesses and/or distribution of Pan-African fault-bounded basins in the zone might have acted as guides for the glacial erosion and

also local glacio-isostatic fault reactivation during the Late Ordovician (Ghienne et al., 2003, 2012).

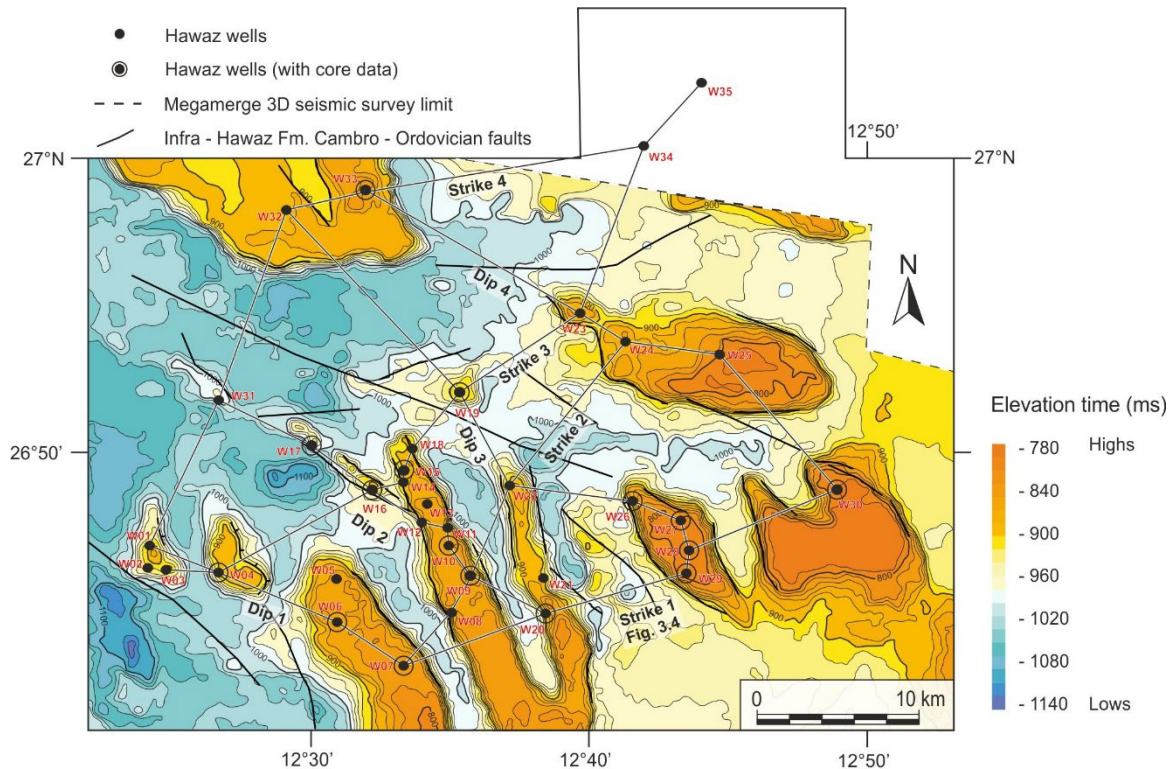


Figure 3.3. Two-way time contour map representing an interpreted top Hawaz surface from Bataller et al. (2019), flattened on an intra-Silurian horizon in the area of study. Note also the superposition of the underlying basement-linked, apparently non-displacing, Cambro-Ordovician faults on this map and their relationship with paleovalley boundaries, interpreted from seismic data. Also shown are the locations of the 35 wells used in this study differentiated by the presence or absence of core data, together with the location of the correlation panels presented in this paper as well as the location of the seismic section shown in **Fig. 3.4**.

Although the separation between some paleohighs is barely a few kilometres (**Fig. 3.3 and 3.4**), others are ten or more kilometres apart, which makes any stratigraphic correlation a challenging task in this particular area of study.

After Gil-Ortiz et al. (2019) and supported by paleocurrent data obtained from image logs, the sedimentological model suggested for the Hawaz is a depositional system evolving from the south-southeast (proximal) to north-northwest (distal). With this as a framework, we have generated a series of eight correlation panels (**Fig. 3.3**), four along the direction of depositional dip to capture the main depositional changes across the study area as the system evolved, and four along the depositional strike to better capture lateral, alongshore variations within systems tracts (see **Chapter 4.3.1**).

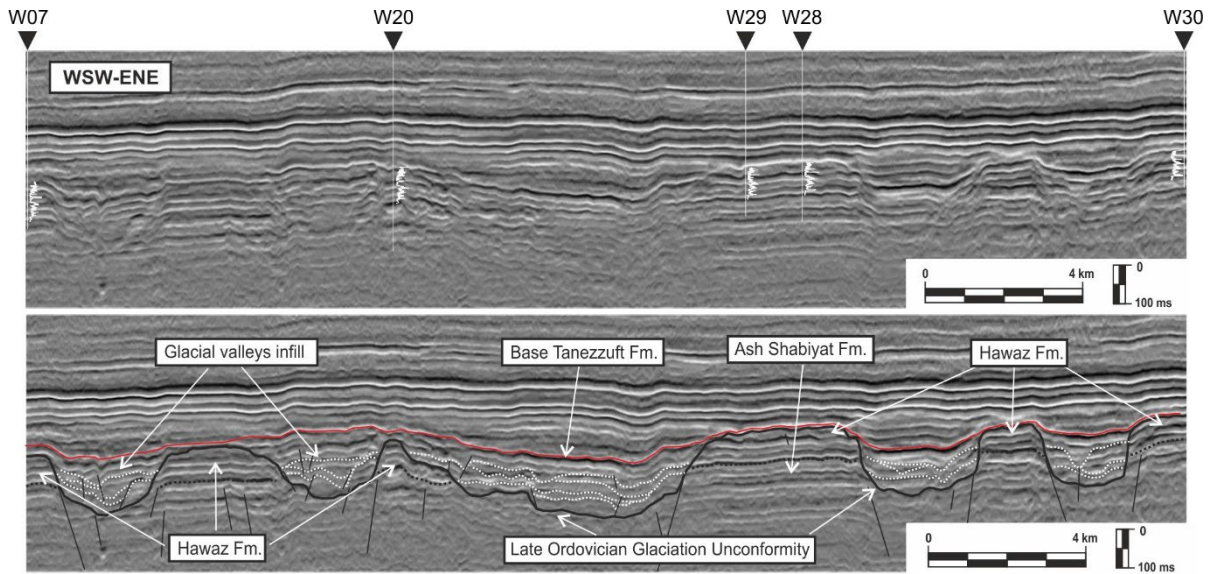


Figure 3.4. Hawaz Formation subsurface architecture. This seismic section across the area of study highlights the remnant subsurface Hawaz paleotopography and infill geometries incised by multiple erosional events during the Late Ordovician glaciation. Note the interpreted base Tanezzuft Fm., which was the datum selected for the construction of the correlation panels presented in this paper. The gamma ray signature of the Hawaz Formation is shown aligned with wells intersecting this seismic line. See also the normal faults bounding many of the paleohighs and the paleovalleys, presumably active during the Cambro-Ordovician. Both the location of the wells and the position of this seismic line are shown in **Fig. 3.3**.

Given the deeply incised character of the top Hawaz, we chose the base of the Silurian Tanezzuft Fm. as a regional stratigraphic datum, when constructing the stratigraphic correlation sections. The Tanezzuft is, however, diachronous in character, overlapping the incised Hawaz paleotopography. As such, the age of this horizon may be Rhuddanian, Aeronian or even younger, so that at least two stages may be missing locally, constituting a hiatus of up to 7 my (**Fig. 2.5-B**). However, despite this limitation, the base of Tanezzuft Fm. is a distinctive, commonly well-preserved surface represented by a bright negative reflector in seismic (**Fig. 2.8-A**) covering the entire underlying Ordovician succession (**Fig. 3.4**). This datum was flattened across all wells in order to obtain a detailed, consistent picture of Hawaz Formation architecture at the time of deposition and to correlate facies belts more easily across the study area. Only the more complete Hawaz sections preserved on the paleotopographic highs were correlated, whereas the erosional gaps caused by subsequent Late Ordovician glaciation, filled with the Upper Ordovician lithostratigraphic units (Melaz Shuqran, Mamuniyat and Bir Tlacin Formations), were deliberately ignored, in order to avoid gaps in the Hawaz interpretation between wells in the correlation panels.

3.3.2. Gross Depositional Environment (GDE) map construction

In addition, a series of Gross Depositional Environment (GDE) maps were also created to illustrate the lateral extent of facies belts within the framework of sequence stratigraphic-based zones. These maps merge data from the isolated control points to predict the pre-erosional distribution of facies associations, depositional environments, and the presence of reservoir facies by describing the sedimentological evolution of the studied area, extrapolating the facies associations between wells, on the basis of their relative proportions within genetic sequences or reservoir zones (See **Annex 4**). Thus, following the sequence stratigraphic framework presented in Gil-Ortiz et al. (2019), a GDE map was created for each systems tract and its corresponding Hawaz zone except for the last transgressive systems tract (TST-DS3) (see **Chapter 4.3.2**), which was excluded, through being partially or totally eroded by the Late Ordovician glacial unconformities in the studied area. In addition, it is important to note that some of the limits between depositional environments represented in these maps are likely to be somewhat speculative considering that our area of study forms only a small part of a much larger and widespread regional facies complex deposited during the Middle Ordovician age, across a very low gradient cratonic margin. Nevertheless, we have opted to represent some of these changes in depositional environment on the margins of these maps, despite the lack of well data, provided that we had a regional insight from the variations in the proportions of facies associations in wells, suggesting a change in the trend of dominant facies belts, and/or complementary information from neighbouring areas. These maps are not a representation of a specific time but a synthesis of depositional trends during the period of time represented by each systems tract, with the aim of summarising the main paleogeographic relationships found in each sequence stratigraphic package.



CHAPTER 4. SUMMARY OF THE RESULTS

- 4.1. Sedimentology of the Hawaz Formation
- 4.2. Sequence Stratigraphy of the Hawaz Formation
- 4.3. Sedimentary architecture of the Hawaz Formation
- 4.4. Depositional model of the Hawaz Formation

The cover photo of the Chapter 4 shows a core photograph with mud-draped current ripples denoting high energy fluctuations over these deposits. Core photograph belongs to subtidal complex deposits from Well 26 of the present study.

4.1. Sedimentology of the Hawaz Formation

The results obtained from the sedimentological description of the Hawaz Formation in the subsurface of the central Murzuq Basin have been published in the following scientific paper of the journal of the American Association of Petroleum Geologists (AAPG) Bulletin:

- Gil-Ortiz, M., McDougall, N.D., Cabello, P., Marzo, M., Ramos, E. (2019). Sedimentology of a “nonactualistic” Middle Ordovician tidal-influenced reservoir in the Murzuq Basin (Libya). *American Association of Petroleum Geologists (AAPG) Bulletin* 103 (9), 2219–2246. <https://doi.org/10.1306/02151918138> (**Annex 1**).

In addition to this article, these results have been also presented at the international conference of the 34th IAS Meeting of Sedimentology, Rome (2019):

- Gil-Ortiz, M., McDougall, N.D., Cabello, P., Marzo, M., Ramos, E. (2019). Sedimentology of the ‘nonactualistic’ Middle Ordovician Hawaz Formation in the Murzuq Basin (Libya). Conference paper (**Annex 2**).

4.1.1. Lithofacies

Fifteen Hawaz lithofacies were defined in the subsurface of the central Murzuq Basin based upon their lithology and internal fabric, including sedimentary structures and bioturbation (**Table 4.1**). These include sandstones (S), muddy sandstones (MS), heterolithic sandstones (HS), and heterolithic mudstones (HM), with a high density and diverse assemblage of sedimentary structures and variation in the degree and types of bioturbation. Each of the lithofacies is described and interpreted as follows:

Table 4.1. Summary of the lithofacies scheme for the Hawaz Formation. See description for more detail.

Code	Texture	Sedimentary structures & main features	Interpretation
Sx1	Fine sand	High-angle (>15°) cross-bedding with local mud drapes and rare mudstone intraclasts. Unbioturbated.	Migration of dune bedforms.
Sx2	Fine to medium sand	Low-angle (5-15°) cross-bedding with local planar lamination, ripple cross-lamination, mud drapes and mudstone intraclasts. Absent to weak bioturbation, with rare <i>Planolites</i> .	Migration of medium-scale dunes, ripples and megaripples, or toesets of previous Sx1.
Sl	Fine sand	Parallel lamination (<5°).	Net sedimentation under upper-flow regime.
Sxl	Fine sand	Low-angle cross-lamination with occasional climbing ripples and mud drapes. Absent to weak bioturbation, with rare <i>Skolithos</i> .	Storm events (swaley-hummocky cross-stratification?).
Sr	Fine sand	Current ripple cross-lamination with occasional mud drapes and intraclasts. Sometimes bimodal coupling. Unbioturbated.	Migration of current ripples.
Sv	Fine sand	Massive with local poorly defined planar lamination and cross-bedding. Unbioturbated.	Early post-depositional dewatering and partial fluidization.
Sxb	Fine sand	Small- to medium-scale cross-bedding with local mudstone intraclasts. Moderately bioturbated with common <i>Skolithos</i> and <i>Siphonichnus</i> .	Migration of dune and bar bedforms in a high-energy shallow marine environment.
Sxlb	Fine sand	Low-angle cross-lamination and local mud laminae and mudstone intraclasts. Moderately bioturbated with common <i>Skolithos</i> and <i>Siphonichnus</i> .	Subtidal sand sheets or low relief sand bars in a lower shoreface and/or intertidal environment.
Srb	Very fine to fine sand	Current ripple cross-lamination and subordinate planar lamination. Locally argillaceous. Moderately bioturbated with common <i>Skolithos</i> and <i>Siphonichnus</i> .	Migration of current ripples in a shallow marine environment.

Code	Texture	Sedimentary structures & main features	Interpretation
Sb	Fine sand	Massive with local mud laminae. Highly bioturbated dominated by <i>Siphonichnus</i> (“Pipe rock” fabric).	Moderate- to low-energy restricted to shallow marine environment.
MSb	Shaly fine sand	Massive and argillaceous. Highly bioturbated with common <i>Teichichnus</i> and <i>Thalassinoides</i> .	Low-energy marginal marine or open-marine environment.
HS	Heterolithic very fine to fine sand and shaly-silt	Common flaser structures, combined current and wave ripple cross-lamination and planar lamination. Absent to weak bioturbation, with rare <i>Chondrites</i> and <i>Planolites</i> .	Storm events deposition in a fluctuating, generally low-energy, open-marine environment, below fair-weather wave base.
HSb	Heterolithic shaly-very fine sand and shaly-silt	Combined current and wave ripple cross-lamination and planar lamination. Moderately bioturbated with mixed <i>Skolithos</i> and <i>Cruziana</i> ichnofacies.	Migration of combined current and wave ripples in the transition from a high-energy to low-energy setting.
HM	Heterolithic clay, shaly-silt and very fine sand	Planar lamination and lenticular bedding. Unbioturbated.	Fairly distal marine environment or restricted and stressed marginal marine environment.
HMb	Heterolithic shaly-silt and fine sand	Planar lamination and lenticular bedding with local shrinkage cracks. Variably bioturbated with common <i>Siphonichnus</i> , <i>Skolithos</i> and <i>Planolites</i> .	Relatively distal marine environment or restricted intertidal environment.

Large-Scale Cross-Bedded Sandstones (Sx1)

Lithofacies Sx1 are fine-grained, well-sorted, and cross-bedded sandstones with high-angle foresets (>15° dip) (**Fig. 4.1**) characterised by a north-northwest-directed paleoflow derived from image log dip picking. Locally, mud drapes, and rare mudstone intraclasts line set bases and foresets. No evidence of bioturbation exists. Typically, these sandstones form sets more than 50 cm thick and cosets up to 10 m thick. The cross-bedding is interpreted as a response to the migration of dune bedforms under conditions of net sedimentation. The mud-draped foresets reflect alternating periods of slack water in a tidal regime. The lack of detrital clays and bioturbation suggests moderate- to high energy conditions, under which the fines were carried off in suspension. Equivalent lithofacies have been described by Ramos et al. (2006) in outcrops

as large-scale, sigmoidal cross-bedded sandstones with occasional horizontal trace fossils (*Cruziana* ichnofacies) (**Fig. 4.2-A**).

Small- to Medium-Scale Cross-Bedded Sandstones (Sx2)

Lithofacies Sx2 comprises fine- to medium-grained, well-sorted, and cross-bedded sandstones with low-angle (5°–15° dip) foresets (**Fig. 4.1**) again characterised by a north-northwest-directed paleoflow as suggested by image log interpretation. Planar lamination, current ripple cross-lamination, mud drapes, and mudstone intraclasts also occur locally. The degree of bioturbation ranges from absent to weak with rare *Planolites*. It forms sets up to 50 cm thick. The cross stratification and cross-lamination record the migration of medium-scale dunes and ripples and megaripples, respectively, under the influence of unidirectional current flow. This lithofacies could also be interpreted as corresponding to toesets of the previously described large-scale cross-bedded sandstones (i.e. lithofacies Sx1). Most probably, deposition occurred within a high-energy, tidally-influenced environment. Equivalent lithofacies have been described by Ramos et al. (2006), outcropping as medium-scale, sigmoidal cross-bedded sandstones with occasional horizontal trace fossils (*Cruziana* ichnofacies) (**Fig. 4.2-B**).

Parallel Laminated Sandstones (Sl)

Lithofacies Sl comprises fine-grained sandstones with parallel lamination (<5°) (**Fig. 4.1**). Bioturbation was not recognised. The lithofacies is organized in sets 10–100 cm thick. It is interpreted to record sand deposition from nearshore currents under a moderate- to high-energy, upper-flow regime. A similar lithofacies has been described by Ramos et al. (2006) in outcrops as parallel-laminated sandstones with occasional parting lineation and very scarce bioturbation (**Fig. 4.2-C**).

Cross-Laminated Sandstones (Sxl)

Lithofacies Sxl comprises fine-grained sandstones with low-angle (5°–15° dip) cross-lamination (**Fig. 4.1**). Climbing ripple lamination and mud drapes are also occasionally present. In general, it is a non-bioturbated lithofacies, although sparse *Skolithos* were occasionally observed. The set thicknesses range from 10 to 140 cm. This lithofacies is interpreted as the deposits of storm events in a nearshore environment. When climbing ripples are present, a high rate of sedimentation under unidirectional flows is inferred. Similar lithofacies are described by Ramos et al. (2006) outcropping in the Gargaf High as low angle, swaley to hummocky cross-stratified sandstones (**Fig. 4.2-D**).

Ripple Cross-Laminated Sandstones (Sr)

Lithofacies Sr comprises fine-grained, very well-sorted sandstones with ripple cross-lamination and occasional intraclasts. Locally, the current ripples display bimodal foreset directions. Bedset or coset thickness does not exceed 50 cm, whilst individual sets are up to 3 cm thick, typically associated with very thin clay drapes (**Fig. 4.1**). This is an unbioturbated lithofacies. The cross-lamination records the migration of current ripples under low to moderate velocity currents. The presence of clay drapes and the bimodal foreset directions, observed in some sets, would suggest deposition in a subtidal setting. Equivalent ripple cross-laminated sandstones with occasional horizontal trace fossils (*Cruziana* ichnofacies) have also been identified in outcrop by Ramos et al. (2006) characterised by a dominantly north-northwest paleoflow direction, locally bimodal toward south-southeast (**Fig. 4.2-E**).

Massive Sandstones (Sv)

Lithofacies Sv comprises fine-grained, clean, generally well-sorted sandstones with poorly defined planar lamination and cross-bedding (**Fig. 4.1**). Locally, mud intraclasts and basal erosive surfaces were identified. This lithofacies is characterised by the absence of bioturbation. It is organized into beds or bedsets 30–100 cm thick. The massive appearance of this facies could be interpreted as the result of early post-depositional processes involving dewatering and partial fluidization suggestive of a high sedimentation rate in the depositional system. This lithofacies can be easily misinterpreted as Sx1 in cores when the clean nature of the sandstones, reflecting the lack of micas and fine-grained sedimentary layers, obscures the boundaries between cross-bed sets. The lack of detrital clays and micas in these sandstones suggests deposition in a relatively high-energy environment where fines were carried off in suspension. Equivalent lithofacies have been observed by Ramos et al. (2006) outcropping in the northern margin of the basin as apparently massive sandstones (**Fig. 4.2-F**).

Burrowed Cross-Bedded Sandstones (Sxb)

Lithofacies Sxb comprises clean, fine-grained sandstones displaying small- to medium-scale cross-bedding with local mudstone intraclasts. It has a moderate degree of bioturbation dominated by *Skolithos* and *Siphonichnus* burrows (**Fig. 4.1**). It is typically organized into 30- to 200-cm thick beds. The clean nature of the sandstones and the presence of mudstone intraclasts suggest moderate- to high-energy conditions in which fines were carried off in suspension. The cross-bedding records the migration of dune and bar bedforms, whereas the vertical to oblique burrows suggest a shallow, high-energy marine environment.

Burrowed Cross-Laminated Sandstones (Sxlb)

Lithofacies Sxlb comprises fine-grained, variably argillaceous, and micaceous sandstones with low-angle (5–15° dip) cross-lamination and local mud laminae and mudstone intraclasts. This lithofacies is moderately bioturbated with an ichnofabric dominated by *Skolithos* and *Siphonichnus*, indeterminate burrows and meniscate-backfilled burrows (**Fig. 4.1**). The minimum thickness observed for this lithofacies is 70 cm. The moderately intense bioturbation, dominated by mainly vertical, suspension-feeding burrows suggests a shallow, high-energy subtidal environment. However, the mud laminae also reflect low-energy conditions. Thus, depending on the context, this lithofacies may have different interpretations ranging from a lower shoreface to an intertidal environment. The low-angle cross-lamination is interpreted as reflecting deposition from subtidal sand sheets or low relief sand bars.

Burrowed Ripple Cross-Laminated Sandstones (Srb)

Lithofacies Srb comprises very fine- to fine-grained sandstones, locally argillaceous, and micaceous characterised by current ripple cross-lamination and planar lamination. A moderate degree of bioturbation characterises this lithofacies (**Fig. 4.1**), with an ichnofabric dominated by *Skolithos* (6–8 mm diameter and maximum length of 30 cm), *Siphonichnus*, and local indeterminate burrows. This lithofacies forms packages 15–170 cm thick. The fine grain size and the locally argillaceous composition of this lithofacies imply deposition in a relatively low-energy environment. The cross-lamination records the migration of current ripples under conditions of net sedimentation and implies that the sand was transported by a unidirectional current of low to moderate velocity. The ichnofauna (mostly represented by vertical burrows) suggests a shallow marine environment dominated by suspension-feeding benthonic fauna.

Burrowed Sandstones with *Siphonichnus* (Sb)

Lithofacies Sb comprises fine-grained, well-sorted sandstones locally with mud laminae. This lithofacies is highly bioturbated, with an ichnofauna dominated by *Siphonichnus* burrows, locally up to 100 cm in length, giving rise to a distinctive “Pipe rock” fabric. The minimum bed thickness appears to be approximately 20 cm, although bed boundaries are typically obscured by bioturbation (**Fig. 4.1**). This lithofacies is volumetrically very abundant, and continuous sections of up to 20 m have been identified in some wells. The occurrence of vertical burrows (*Skolithos* ichnofacies) suggests a moderate- to low-energy restricted to shallow marine environment, and the presence of mud laminae (mud drapes) implies fluctuating energy levels. Equivalent lithofacies have been described by Ramos et al. (2006) in outcrops as thick-bedded, massive, bioturbated sandstones (**Fig. 4.2-G**).

Burrowed Sandstones with Feeding Ichnofauna (MSb)

Lithofacies MSb comprises argillaceous fine-grained sandstones characterised by moderately intense bioturbation dominated by horizontal, deposit-feeding burrows (**Fig. 4.1**), notably *Teichichnus* and *Thalassinoides*. Individual beds range in thickness from 10 to 270 cm. The moderately high detrital clay content of these sandstones and the characteristic low-energy ichnofauna suggests a relatively protected depositional setting or open-marine conditions.

Sandy Heterolithics (HS)

Lithofacies HS comprises interbedded very fine- to fine-grained sandstones and argillaceous siltstones (>50% sand content). This lithofacies displays flaser structures together with combined current and wave ripple cross-lamination and also planar lamination (**Fig. 4.1**). Only a limited amount of bioturbation with rare *Chondrites* and *Planolites* burrows exists. The thickness of this lithofacies ranges between 1 cm sets up to an accumulated bedset thickness of 5 m. The interbedding of sandstone and argillaceous siltstone implies fluctuating energy levels. Sands were transported and deposited by both unidirectional and oscillatory (wave-generated) flows. Unidirectional current flow was mostly of low to moderate velocity, resulting in the formation of current ripples. By contrast, the presence of cross-bedding (recording the migration of dune and bar bedforms) and mudstone intraclasts indicates higher current velocities. The presence of *Chondrites* indicates that burrowing took place under marine conditions; the remaining burrows, *Planolites* and indeterminate horizontal tubes, also suggest a marine environment. The low bioturbation index together with the local occurrence of *Chondrites* (generally considered to be characteristic of low oxygen conditions), suggests that oxygenation levels were low. Wave, current, and combined flow cross-lamination suggests sands were deposited during storm events below fair-weather wave base (FWWB). Equivalent lithofacies have been observed by Ramos et al. (2006) outcropping as heterolithic silty sandstones (**Fig. 4.2-H**).

Burrowed Sandy Heterolithics (HSb)

Lithofacies HSb comprises thinly interbedded, very fine-grained, micaceous, argillaceous sandstone and micaceous, argillaceous siltstone (>50% sand content). Locally, the argillaceous siltstones display planar lamination and the sandstones current and wave ripple cross-lamination. Bioturbation is moderately intense, characterised by overprinted *Skolithos* and *Cruziana* ichnofacies (*Siphonichnus* burrows, with subordinate *Planolites* and indeterminate burrows) (**Fig. 4.1**). Minimum bed thickness is 1 cm, whereas accumulated bedset thickness can reach 4 m. The interbedding of sandstone and siltstone suggests fluctuating energy conditions,

with the sandstones representing higher energy levels. The cross-lamination within the sandstones records the migration of combined current and wave ripples under conditions of net sedimentation and low to moderate current velocities. The mixed assemblage of ichnofauna suggests the transition from a high-energy to a low-energy setting, from an open-marine inner shelf up to a lower shoreface setting. A variation of this lithofacies in the upper part of the Hawaz Formation exists, interpreted as sedimentation in a mixed to sandy tidal flat. Locally, the base of the most sandy intervals displays rip-up mudstone clasts and a rhythmic alternation of thin, inclined mud drapes and sandstones. In this case, the interpretation corresponds to inclined heterolithic stratification (IHS) associated with minor channels or tidal creeks in a sandy to mixed intertidal sub-environment.

Muddy Heterolithics (HM)

Lithofacies HM comprises mudstones interbedded with micaceous argillaceous siltstone and very fine-grained sandstone (>50% clay content). The mudstone and argillaceous siltstone display planar lamination and lenticular bedding (current and wave-rippled sand lenses). The sandstone contains current ripples and rare wave ripples (**Fig. 4.1**). Occasional shrinkage cracks are also present. Individual lithofacies packages have a minimum thickness of 5 cm but may reach an accumulated bedset thickness up to 3.5 m. The sandstone beds and lenses represent energetic pulses in an overall low energy setting where mud settled out of suspension. During the higher-energy pulses, sand was moved by both unidirectional and oscillatory (wave-generated) flows. The lack of burrows indicates anoxic conditions in a fairly distal marine setting or a restricted and stressed sub-environment, such as a tidal mudflat or lagoon.

Burrowed Muddy Heterolithics (HMb)

Lithofacies HMb comprises argillaceous siltstone interbedded with minor fine-grained sandstone layers and sandstone laminae (>50% clay content). It is characterised by a variable degree of bioturbation with *Siphonichnus*, *Skolithos*, *Planolites*, and indeterminate vertical burrows (**Fig. 4.1**). Shrinkage cracks may occur locally. The minimum thickness of individual beds is 7 cm, whereas the accumulated bedset thickness is up to 3.8 m. The interbedding of argillaceous siltstone and very fine- to fine-grained sandstone suggests fluctuating energy conditions in an overall low-energy setting. The shrinkage cracks are most probably related to variations in salinity and temperature when present. The depositional setting of this lithofacies ranges from a relatively distal, inner shelf sub-environment to a restricted intertidal flat sub-environment.



Figure 4.1. Summary of the main lithofacies identified in this study expressed in core sections (~90-cm length). Sx1 = large-scale cross-bedded sandstone (from well W09); Sx2 = small- to medium-scale cross-bedded sandstone (from well W09); Sl = parallel-laminated sandstone (from well W16); Sxl = cross-laminated sandstone (from well W16); Sr = ripple cross-laminated sandstone (from well W33); Sv = massive sandstone (from well W09); Sxb = burrowed cross-bedded sandstone (from well W33); Si = *Siphonichnus*. See **Fig. 3.3** for the location of the corresponding wells and **Table 4.1** for a summarised description.

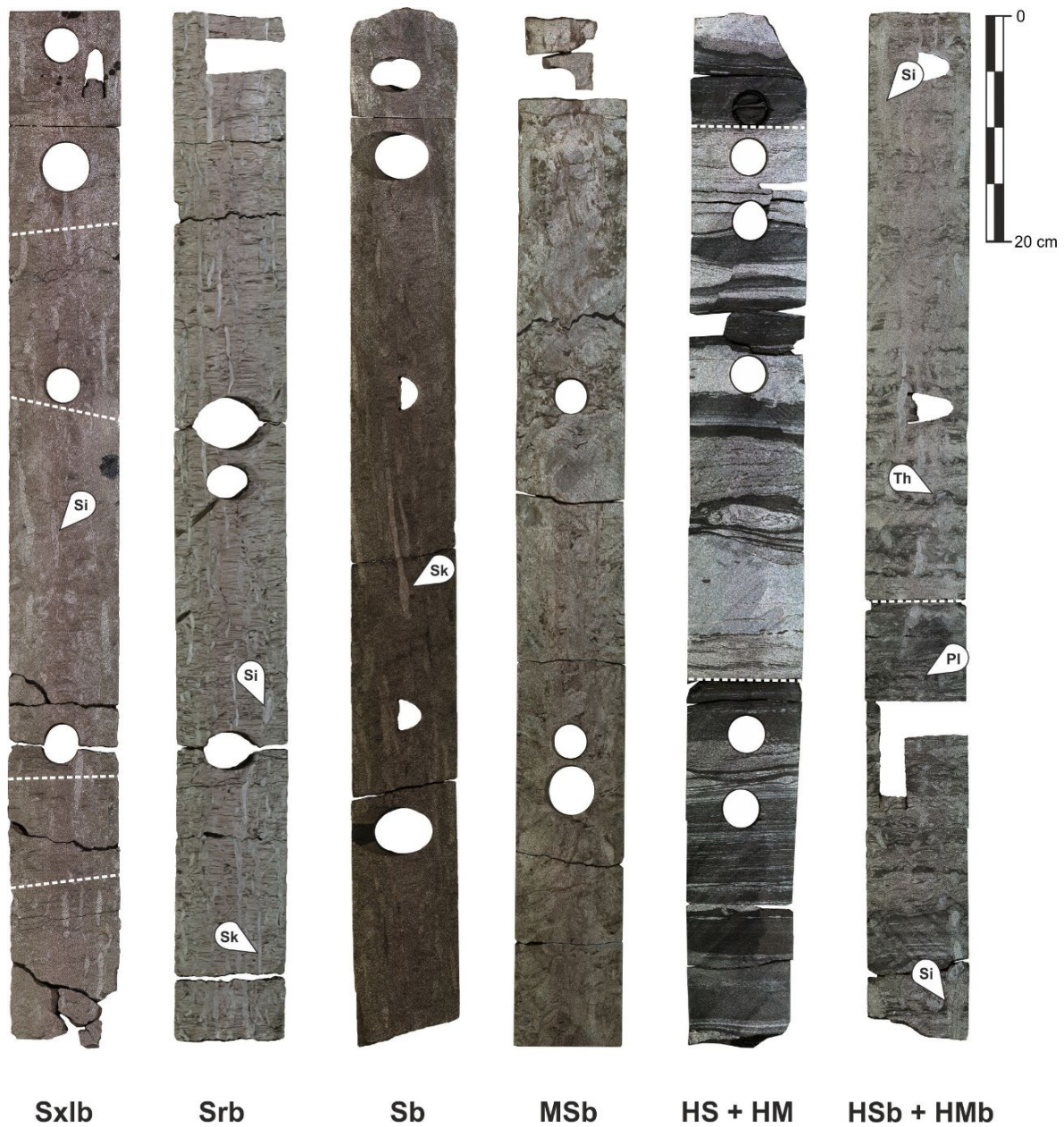


Figure 4.1. (Continued) Summary of the main lithofacies identified in this study expressed in core sections (~90-cm length). Sxlb = burrowed cross-laminated sandstone (from well W33); Srb = burrowed ripple cross-laminated sandstone (from well W15); Sb = burrowed sandstone with *Siphonichnus* (from well W16); MSb = burrowed sandstone with feeding ichnofauna (from well W17); HS = sandy heterolithics (from well W19); HM = muddy heterolithics (from well W19); HSb = burrowed sandy heterolithics (from well W15); HMb = burrowed muddy heterolithics (from well W15); Pl = *Planolites*; Si = *Siphonichnus*; Sk = *Skolithos*; Th = *Thalassionides*. See **Fig. 3.3** for the location of the corresponding wells and **Table 4.1** for a summarised description.

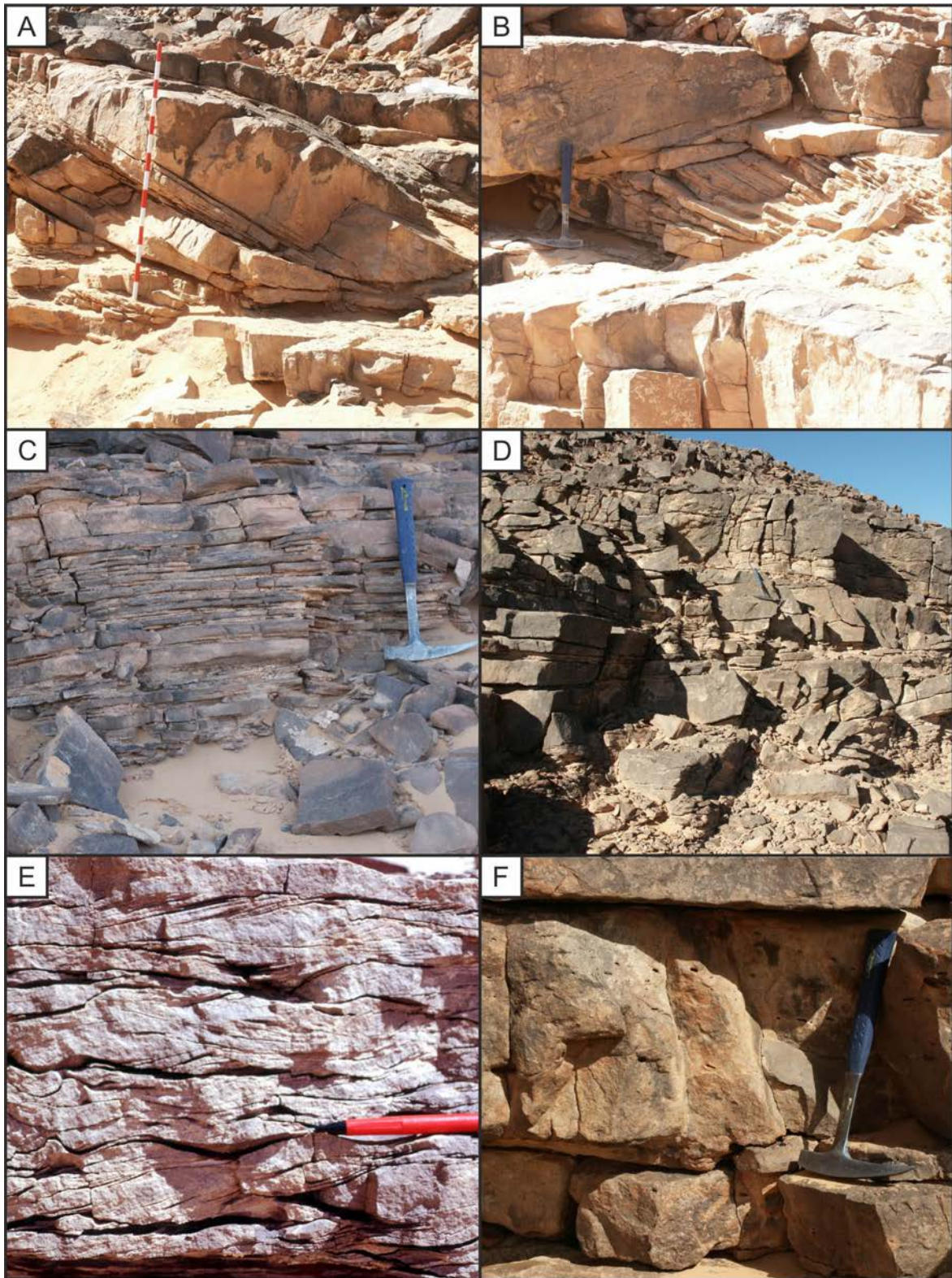


Figure 4.2. Summary of the equivalent lithofacies identified in the outcropping section of the Hawaz Formation in the Gargaf High by Ramos et al. (2006). A) Large-scale, sigmoidal cross-bedded sandstones. B) Medium-scale, sigmoidal cross-bedded sandstones. C) Parallel-laminated sandstones. D) Low angle, swaley to hummocky cross-stratified sandstones. E) Ripple cross-laminated sandstones. F) Massive sandstones. Scale is 150 cm (Jacob's staff), geologist hammer or a pencil. Photographs courtesy of Emilio Ramos.

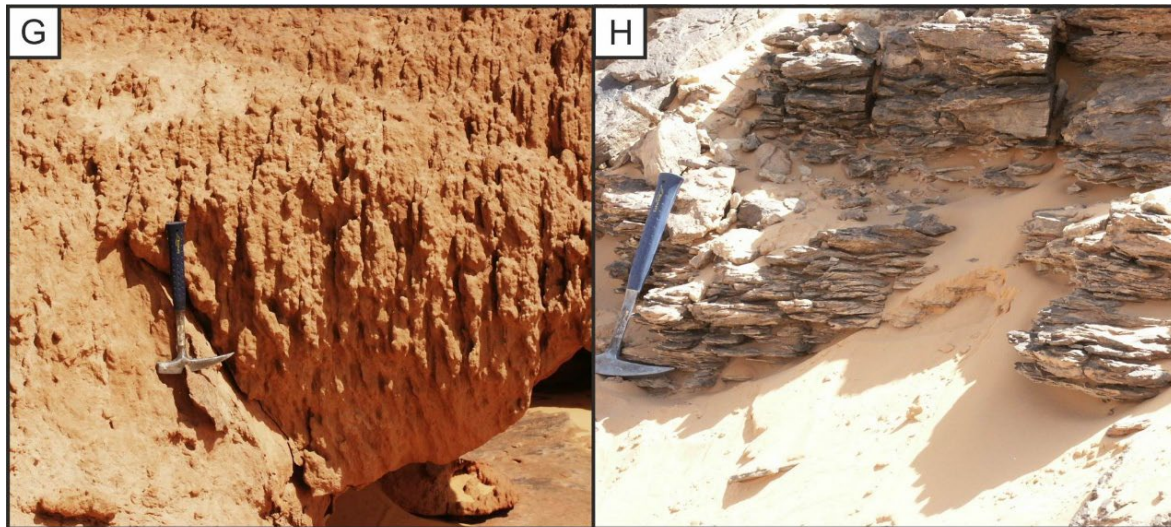


Figure 4.2. (Continued) Summary of the equivalent lithofacies identified in the outcropping section of the Hawaz Formation in the Gargaf High by Ramos et al. (2006). G) Thick-bedded, massive, bioturbated sandstones. H) Heterolithic silty sandstones. Photographs courtesy of Emilio Ramos.

4.1.2. Facies associations

The proposed scheme, based on the previously described lithofacies, establishes seven facies associations designated as Hawaz Facies Association (HWFA1 to HWFA7), associated with proximal and increasingly distal environments (**Fig. 4.3**).

Hawaz Facies Association 1: Tidal Flat

Facies association HWFA1 mainly consists of lithofacies Sxlb, MSb, Sb, HMb, and HSb with subordinate Srb and Sv (**Fig. 4.3**). The thickness of individual packages of this facies association is very variable, ranging from 30 to 60 m as a direct consequence of the downcutting associated with the Upper Ordovician glaciogenic unconformities. The GR log response ranges widely from 30 to 140 API units in a characteristic fining-upward succession. The intensity of bioturbation is moderate to very high, characterised by a mixed low diversity *Skolithos* and *Cruziana* ichnofacies assemblage indicative of a relatively high-energy environment grading toward a more protected and restricted low-energy setting. It is also characterised by an upward-increasing detrital clay content typical of tidal flat environments.

Furthermore, the low diversity of acritarch assemblages and the strong predominance of leiospheres, characteristic of a marginal marine setting, identified in palynological studies of some wells (Miles, 2001, 2003), suggests a relatively protected tidal sand to mixed flat environment grading normally from the underlying HWFA3 or HWFA2 (see below). Some ichnogenera identified as *Planolites*, *Siphonichnus*, and *Thalassinoides* are strongly associated with tidal flat deposits (Gingras et al., 2012). The primary fabric of this facies association was completely modified (**Fig. 4.4-A**) by immediate early post-depositional processes related to colonization of benthic paleofauna, which very often co-existed with low to moderate sedimentation rates in these environments, as seen in some tidal rhythmites partially preserved in the infilling of vertical burrows in a few core sections (**Fig. 4.4-B**). There is also a common occurrence of mud drapes (**Fig. 4.4-C and D**) and flaser to lenticular bedding (**Fig. 4.4-E and F**). The sporadic occurrences of individual massive to rippled sandstone levels (Sv and Srb) and the presence of rip-up mudstone clasts at the base of these units in the heterolithic intervals (locally associated with small post-depositional faults) are interpreted in terms of bank collapse in tidal creeks on the sand flat (**Fig. 4.4-G and H**). The same package in the Gargaf High was described as an upper shoreface wave dominated facies assemblage by Ramos et al. (2006), which probably would represent a beach to barrier island setting, a laterally distal equivalent to this facies association HWFA1.

The most frequent response of this facies association in image logs is an alternation of low-angle cross-laminated resistive (sand-prone) and conductive (silt-/clay-prone) beds/laminae with presence of both extensive vertical suspension-feeding and horizontal deposit-feeding bioturbation traces (**Fig. 4.4-I**). Whereas in core sections is often difficult to discern individual layers, image log constitutes a key piece of information in order to infer the remnants of the primary fabric of these deposits, frequently strongly modified, where primary sedimentary structures have been obliterated by the action of extensive bioturbation activity.

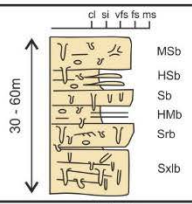
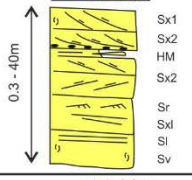
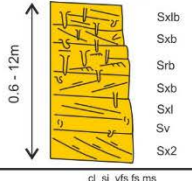
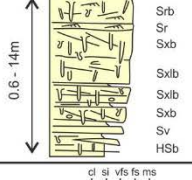
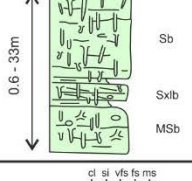
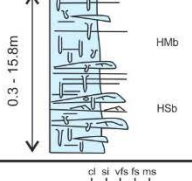
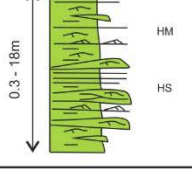
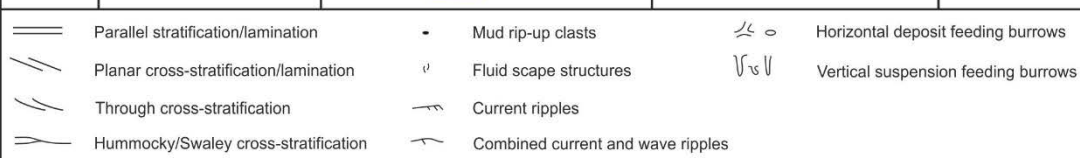
Depositional setting	Facies association	Description (Typical section with lithofacies & thickness ranges)	Interpretation	CCA average Ø / K Gamma Ray
FORESHORE Intertidal zone	HWFA1 Tidal flat	 30 - 60m MSb HSb Sb HMb Srb Sxlb	Tidal sand to mixed flat deposited during high relative sea levels in an embayed tidal-influenced setting	13% / 30.4 mD 30 - 140 GAPI
	HWFA2 Subtidal complex	 0.3 - 40m Sx1 Sx2 HM Sx2 Sr Sxl Sl Sv	Amalgamated complex of sand bars, dunes and channel deposits deposited in a subtidal setting	11% / 125 mD 25 - 65 GAPI
MIDDLE SHOREFACE Subtidal zone	HWFA3 Abandoned subtidal complex	 0.6 - 12m Sxlb Sxb Srb Sxb Sxl Sv Sx2	Distal equivalent of the subtidal complex product of the abandonment of previously active subtidal channels	14% / 152 mD 25 - 70 GAPI
	HWFA4 Middle to lower shoreface	 0.6 - 14m Srb Sr Sxb Sxlb Sxb Sv HSb	Prograding middle to lower shoreface related to regressive sand belts during highstand sea level conditions	14% / 56 mD 30 - 80 GAPI
LOWER SHOREFACE below FWFB	HWFA5 Burrowed shelfal and lower shoreface	 0.6 - 33m Sb Sxlb MSb	Deposition in a relatively protected to more open lower shoreface to inner shelf setting	14% / 3.5 mD 30 - 80 GAPI
	HWFA6 Burrowed inner shelf	 0.3 - 15.8m HMb HSb	Deposition in an open-marine inner shelf setting	9% / 0.2 mD 60 - 120 GAPI
INNER SHELF above SWB	HWFA7 Shelfal storm sheets	 0.3 - 18m HM HS	Distal mixed sand to mud rich deposits product of waning storm events in an open-marine shelf setting	5% / 0.2 mD 80 - 160 GAPI
		 <ul style="list-style-type: none"> Parallel stratification/lamination Planar cross-stratification/lamination Through cross-stratification Hummocky/Swaley cross-stratification Mud rip-up clasts Fluid scape structures Current ripples Combined current and wave ripples Horizontal deposit feeding burrows Vertical suspension feeding burrows 		

Figure 4.3. Summary of facies associations and interpreted depositional settings. Description includes typical sections and thickness ranges (in metres) with the main lithofacies composing each facies association. Interpretation in terms of depositional environment is also included. See also the average conventional core analysis (CCA) values for porosity, permeability and gamma ray for each facies association. HWFA = Hawaz facies association; FWWB = mean fair-weather wave base; SWB = mean storm wave base; Cl = clay; si = silt; vfs = very fine sandstone; fs = fine sandstone; ms = medium sandstone; Sx1 = large-scale cross-bedded sandstone; Sx2 = small- to medium-scale cross-bedded sandstone; Sl = parallel-laminated sandstone; Sxl = cross-laminated sandstone; Sr = ripple cross-laminated sandstone; Sv = massive sandstone; Sxb = burrowed cross-bedded sandstone; Sxlb = burrowed cross-laminated sandstone; Srb = burrowed ripple cross-laminated sandstone; Sb = burrowed sandstone with *Siphonichnus*; MSb = burrowed sandstone with feeding ichnofauna; HS = sandy heterolithics; HM = muddy heterolithics; HSb = burrowed sandy heterolithics; HMb = burrowed muddy heterolithics.

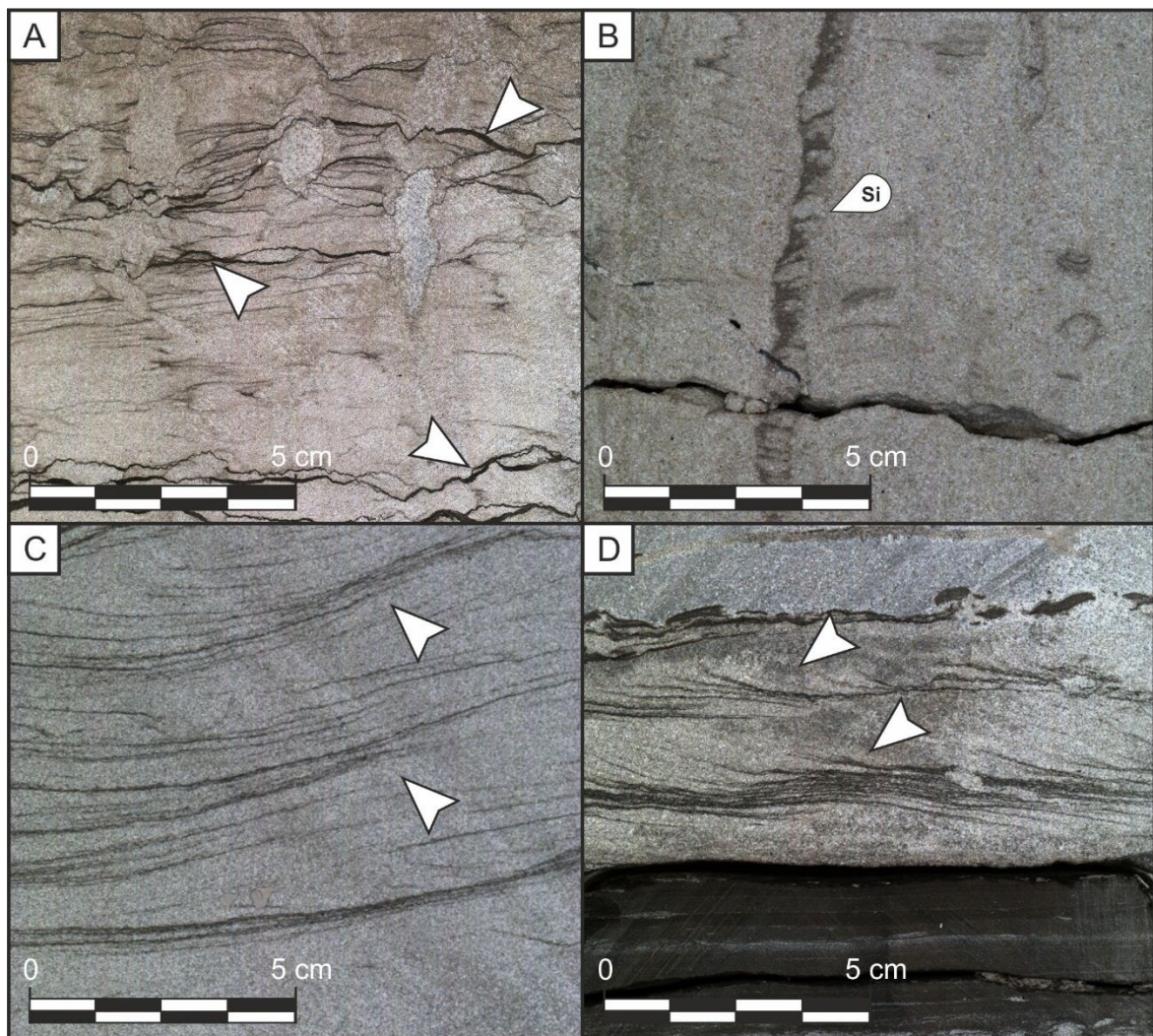


Figure 4.4. Detailed close-up views of some characteristic sedimentary structures and fabric of facies association HWFA1 Tidal flat. A) Modified lithological fabric due to the effect of both vertical and horizontal bioturbation. See the remnants of mud-draped lamination between burrows, from well W09. B) Remnants of rhythmic lamination preserved in the infilling of a *Siphonichnus* (Si) vertical burrow, from well W26. C) Mud-draped current ripples, from well W26. D) Combined current and wave ripples with mud drapes, from well W19. See **Fig. 3.3** for location of the wells.

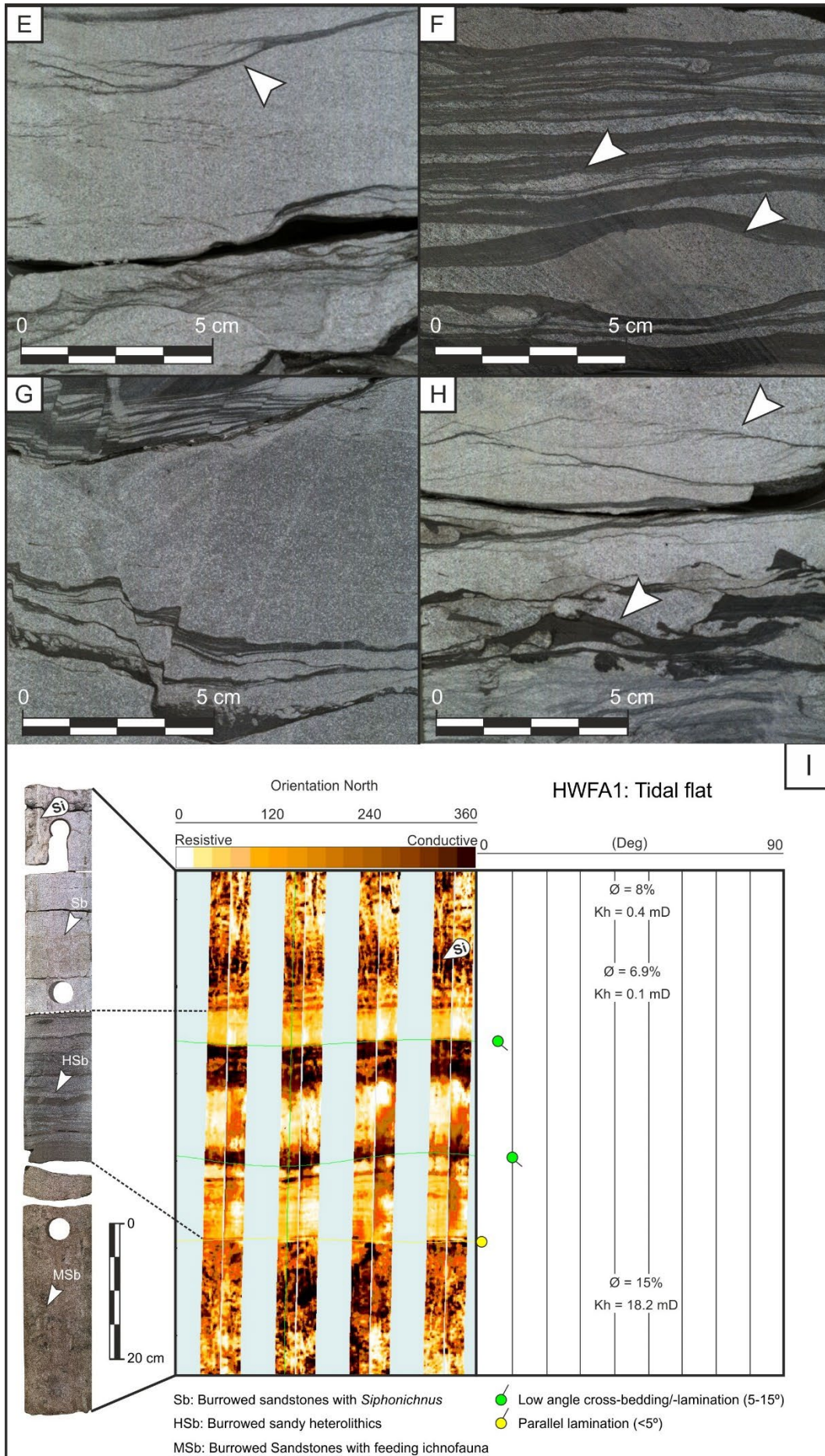


Figure 4.4. (Continued) E) Flaser lamination in ripple cross-laminated sandstones, from well W26. F) Wavy to lenticular lamination in burrowed heterolithic sandstones, from well W16. G) Post-depositional local faulting, related to channel-bank collapse, from well W26. H) Base of an interpreted ephemeral channel displaying a lag of mud clasts and subsequent channel infilling with mud-draped ripple cross-laminated sandstones, from well W26. I) Core to image log calibration showing a 90 cm (aprox.) typical HWFA1 tidal flat section with an alternation of burrowed sandstones and sandy heterolithics. Note the typical low angle of sedimentary structures in these deposits associated with a generalised low energy setting and also the low rate of preservation of these structures due to an extended mixed *Cruziana* and *Skolithos* ichnofacies. Measured porosity and horizontal permeability in plugs from core analysis is also included, from well W09. See **Fig. 3.3** for location of the wells.

Hawaz Facies Association 2: Subtidal Complex

Facies association HWFA2 is mainly composed of lithofacies Sx2, Sx1, Sxl, Sr, Sl, and Sv with subordinate HM (**Fig. 4.3**). It is organized into stacked packages 0.3–40 m thick. The basal contact of these packages is typically erosive, locally marked by the presence of mud clasts (**Fig. 4.5-A**), and the GR response is both clean and blocky (GR values ~25 API units) locally marked by peaks (up to 65 API units) related to the presence of thin mud drapes, concentrations of mica or mud clasts. These values are within the established range for micaceous sandstones, which could have values of up to 80 API units (Rider, 2004). Bioturbation is scarce to absent, probably related to a very high sediment supply in a relatively short period of time. Paleocurrents, measured in this facies association from image logs, indicate a dominant trend toward the north-northwest with some bidirectionality, most likely related to tidal effects as indicated by the mud drapes in lithofacies Sx1, Sx2, and Sr (**Fig. 4.5-B**). However, an additional secondary trend has also been identified, indicating flow toward the northeast. The reservoir quality of this facies association is the best of the entire Hawaz Formation, with an average porosity of 11% and an average horizontal permeability of 125 mD.

Facies association HWFA2 is interpreted as an amalgamated complex of sand bars and dunes (slightly coarsening-upward profile with lithofacies Sx1, Sx2, Sxl and Sr) and channel deposits (slightly finning-upward profile with lithofacies Sv, Sl, and Sr) influenced by the tidal action and associated with common reactivation surfaces (**Fig. 4.5-C**). The interpretation is a laterally extensive fluvio-tidal to subtidal complex deposited in a nearshore setting. Subordinate heterolithic intervals are also found intercalated with the cross-stratified sand bars, possibly related to periods of slack water and deposition in relatively protected lagoonal or interbar sub-environments. The features of this facies association are very similar to those described by Ramos et al. (2006) as subtidal deposits, from the Gargaf High 100 km to the north. They are almost equivalent in depositional environment; although in the subsurface of the northern

Murzuq Basin, HWFA2 would represent a shallower lateral equivalent with higher fluvial influence because of the general absence of bioturbation reflecting higher energy and sedimentation rates.

Hawaz Facies Association 3: Abandoned Subtidal Complex

Facies association HWFA3 is primarily characterised by lithofacies Sxlb, Sxb, Srb, Sxl, Sv, and Sx2 (**Fig. 4.3**). It forms packages ranging in thickness from 0.6 to 12 m. Facies packages are distinguished by a fining-upward succession of fine-grained sandstones represented by a distinctive upward increase in the GR characterised by API values between 25 and 70. Bioturbation is moderate, typically becoming more abundant toward the upper part of these successions with common *Skolithos* and *Siphonichnus* burrows (**Fig. 4.5-D**).

This facies association is interpreted to represent the progressive abandonment of the associated subtidal complex (HWFA2) after a general rise in relative sea level and a cessation or major decrease in sediment supply, promoting colonization of marine fauna in a subtidal setting. An alternative but complementary possible interpretation corresponds to the lower energy fringe zones surrounding the former HWFA2. It is quite common to find this facies association gradationally intercalated with the subtidal complex, reflecting a transgressive trend and/or fluctuations in energy in a relatively protected environment.

Considering the often-uniform fabric of these facies associations (HWFA2 and HWFA3), with a generalised lack of clay content, it makes difficult to differentiate first occurrences of bioturbation traces indicating a waning energy event and progressive abandonment of the subtidal complex. In this respect, image logs provide an essential tool to differentiate between unburrowed high energy cross-bedded sandstones in an active subtidal complex (**Fig. 4.5-E**) from a progressively abandoned subtidal complex (**Fig. 4.5-F**) with presence of scarce suspension-feeding *Skolithos* and *Siphonichnus* traces, indicating a subsequent colonization of the area in a still high to moderate energy setting.

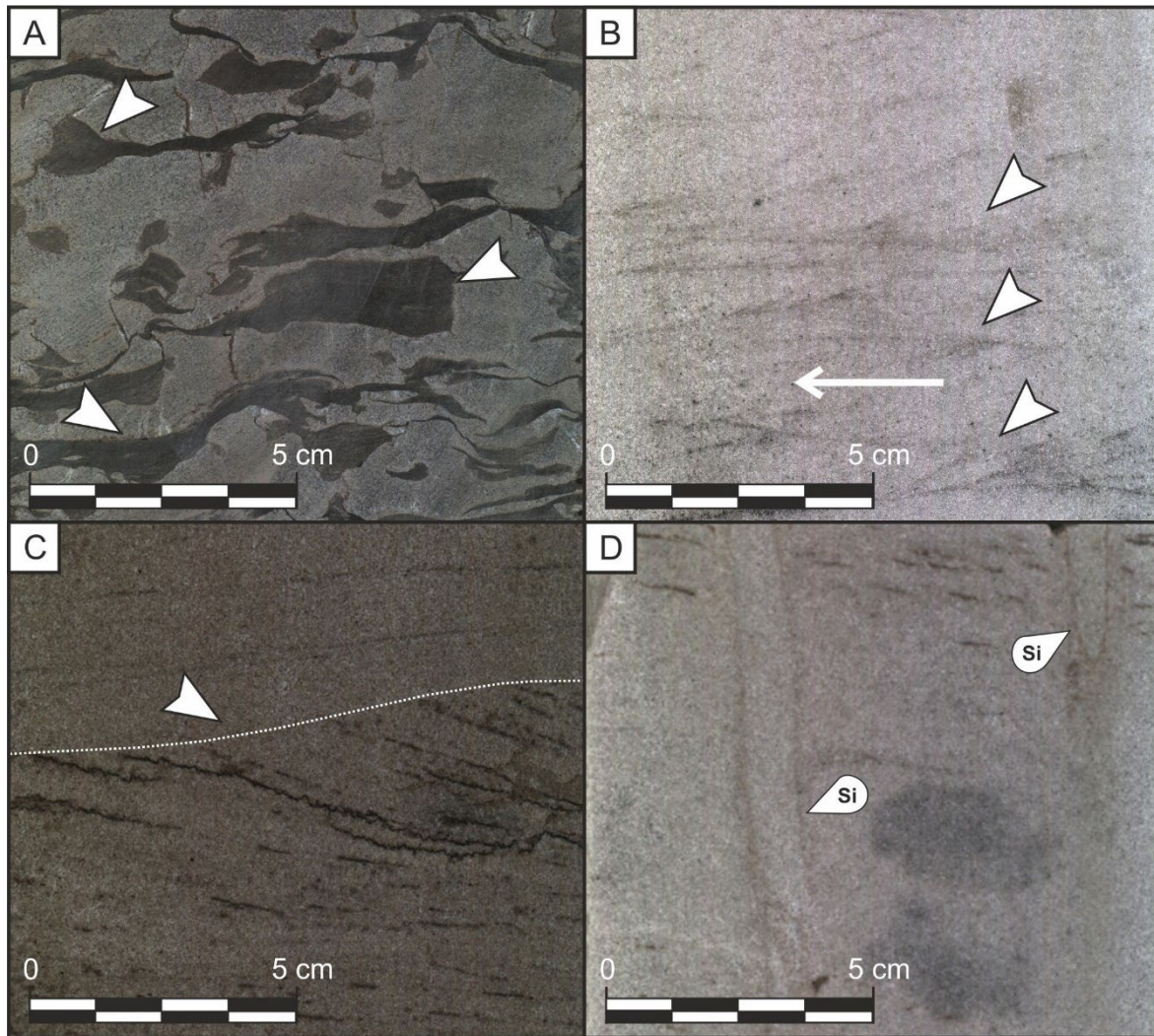


Figure 4.5. Detailed close-up views of some characteristic sedimentary structures and fabric of facies associations HWF2 Subtidal complex and HWFA3 Abandoned subtidal complex. A) Mudstone rip-up clasts from the base of a subtidal channel, from well W16. B) Mud-draped current ripples in clean sandstones of a subtidal complex, from well W33. Note the direction of the paleocurrent flow leftward. C) Cross-bedding with mud-draped tidal bundles eroded atop by an interpreted reactivation surface, from well W16. D) Clean cross-bedded sandstones with occurrence of vertical *Siphonichnus* (Si) burrows, denoting a progressive abandonment of the subtidal complex and/or fringe zone of an active subtidal complex, from well W33. The location of the corresponding wells is in **Fig. 3.3**.

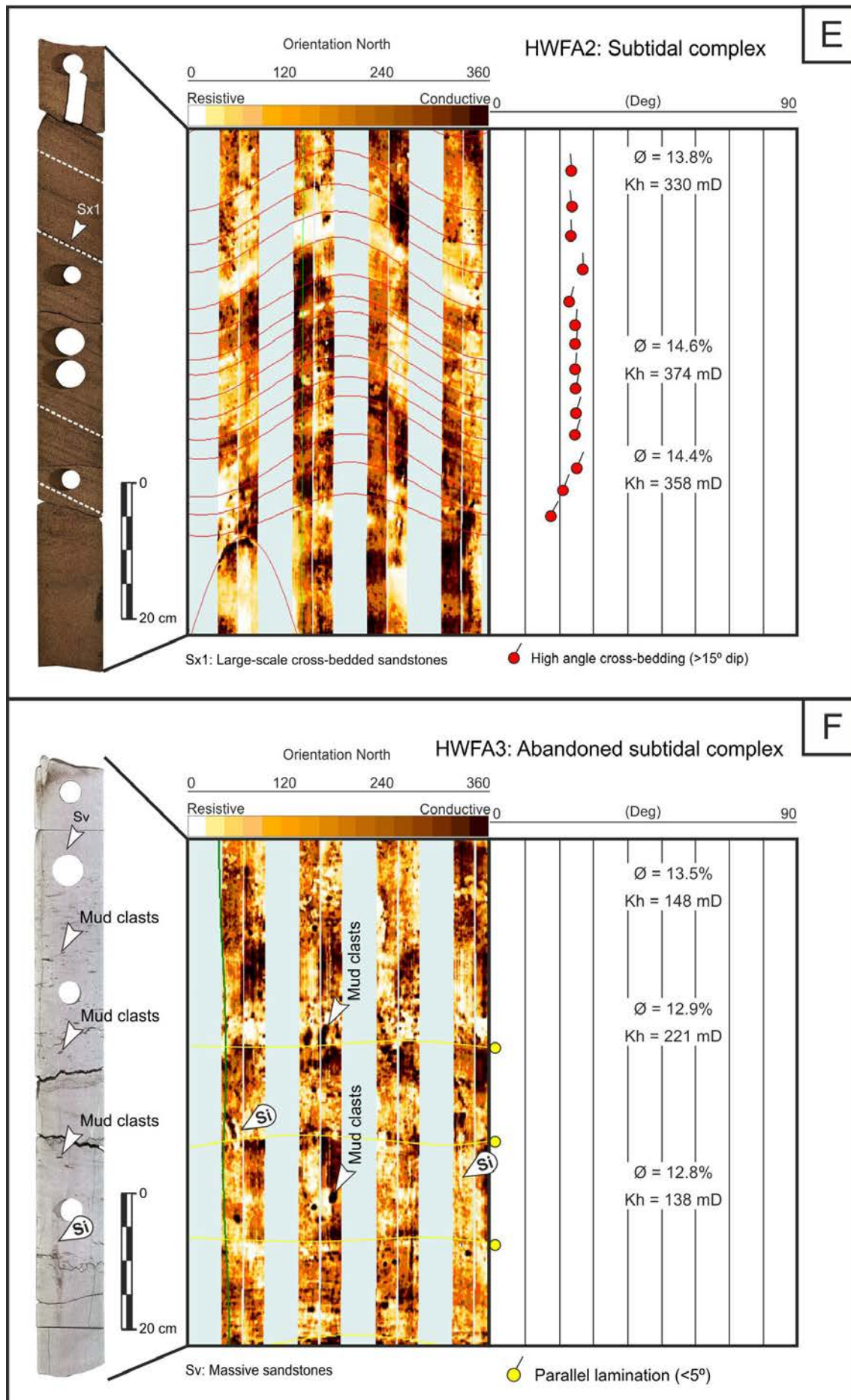


Figure 4.5. (Continued) E) Core to image log calibration showing a 90 cm (aprox.) typical HWFA2 subtidal complex section with a characteristic large-scale cross-bedded sandstones denoting the migration of bars and dunes under high to moderate energy conditions. Note the dominant direction of the paleoflow towards the north-northeast as interpreted from the right-hand side tadpoles track, from well W09. F) Core to image log calibration showing a 90 cm (aprox.) HWFA3 abandoned subtidal complex section with massive sandstones with scattered mud clasts and scarce *Siphonichnus* traces indicating lower energy conditions and an incipient abandonment or fringe zone of the subtidal complex, from well W33. Measured porosity and horizontal permeability in plugs from core analysis is also included. The location of the corresponding wells is in **Fig. 3.3**.

Hawaz Facies Association 4: Middle to Lower Shoreface

Facies association HWFA4 is mainly composed of lithofacies Sr, Srb, Sxlb, Sxb, Sv, and HSb (**Fig. 4.3**). The thickness of individual packages ranges between 0.6 and 14 m. The GR response is typically a serrate, coarsening-upward succession with values ranging between 30 and 80 API units. Bioturbation ranges from scarce to moderate. Overall packages of this facies association form clear, coarsening-upward successions with a characteristic *Skolithos* ichnofacies (**Fig. 4.6-A**) related to regressive sand belts prograding during highstand sea-level conditions (Gibert et al., 2011).

On this basis, the interpretation proposed is of a low- to moderate-energy, middle to lower shoreface setting prograding in a relatively high-energy subtidal environment.

Hawaz Facies Association 5: Burrowed Shelfal and Lower Shoreface

Facies association HWFA5 mainly consists of lithofacies Sb, MSb, and Sxlb (**Fig. 4.3**). Thickness of individual packages ranges between 0.6 and 33 m. The typical GR log response of this facies association is irregularly serrate, with values between 30 and 80 API units, reflecting a relative increase in the detrital clay content. Bioturbation is moderate to very abundant, tending to overprint and obscure all primary sedimentary structures.

This facies association is interpreted to have been deposited in a lower shoreface to shelf environment as suggested by the variably clean to argillaceous nature of the sandstones and ubiquitous bioturbation with a well-developed *Skolithos* ichnofacies, frequently mixed with the common occurrence of deposit-feeding bioturbation traces characteristic of the *Cruziana* ichnofacies.

Hawaz Facies Association 6: Burrowed Inner Shelf

Facies association HWFA6 comprises lithofacies HMB and HSb (**Fig. 4.3**). The minimum thickness of individual packages is approximately 30 cm, whereas the maximum value is 15.8 m. It may be considered as the distal equivalent of HWFA5 distinguished by a spiky GR response characterised by notably higher values ranging from 60 to 120 API units. Bioturbation intensity is moderate, with an ichnofaunal assemblage dominated by the *Cruziana* ichnofacies.

This facies association is interpreted as having been deposited in a distal burrowed lower shoreface to inner shelf setting based on its heterolithic lithology, a *Cruziana* ichnofacies (**Fig. 4.6-B and C**), and the occurrence of combined current and wave ripples. This suggests a low-energy, open-marine environment in moderate water depths above storm wave base (SWB).

Hawaz Facies Association 7: Shelfal Storm Sheets

Facies association HWFA7 is mostly composed of lithofacies HS and HM (**Fig. 4.3**). The thickness of these facies packages ranges from 0.3 to 18 m. It is characterised by a continuously high GR response with values of up to 150 API units or even higher. Where notably high GR peaks occur, these may represent local flooding events interrupting a shallower depositional sequence. This facies association has the lowest reservoir quality in the formation with an average porosity of approximately 5% and an average horizontal permeability of 0.2 mD.

It is interpreted to have been deposited in a distal shelf environment on the basis of a high detrital clay content and the occurrence of combined wave and current ripples (**Fig. 4.6-D**). These suggest fluctuating energy levels in broadly very low-energy environment between the FWFB and SWB. This is supported by the generally very low intensity of bioturbation, the occasional occurrence of *Chondrites* burrows, and shrinkage cracks indicating deposition in a fairly distal, poorly oxygenated setting, perhaps associated with distal waning storm events capable of transporting sand to the open-marine shelf.

Image logs have been proved to be an efficient tool to distinguish between different subenvironments into shoreface and inner shelf settings. The ichnofacies evolution, from the HWFA4 middle to lower shoreface (**Fig. 4.6-E**), characteristic for presenting a *Skolithos* ichnofacies, passing through a lower energy HWFA5 burrowed shelfal and lower shoreface (**Fig. 4.6-F**) with a mixed *Cruziana/Skolithos* ichnofacies, up to the HWFA6 burrowed inner shelf (**Fig. 4.6-G**), characteristic for its *Cruziana* ichnofacies, can be frequently recognised with image logs. The identification of these biogenic structures together with fabric, stacking patterns

and increase in clay content, provided by core and conventional wireline logs, permitted us to identify main boundaries between these subenvironments, often disrupted by HWFA7 shelfal storm sheet deposits (**Fig. 4.6-H**).

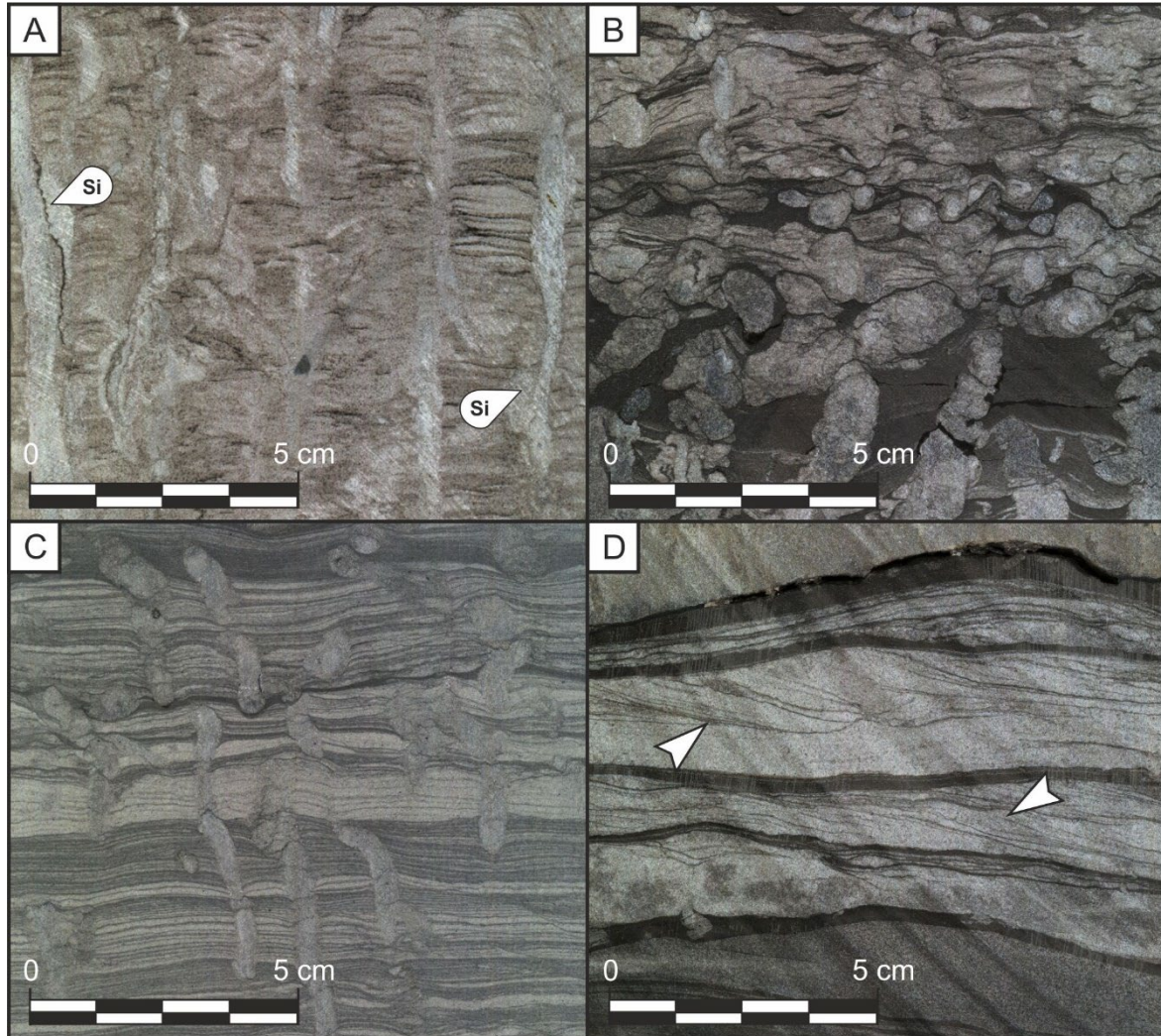
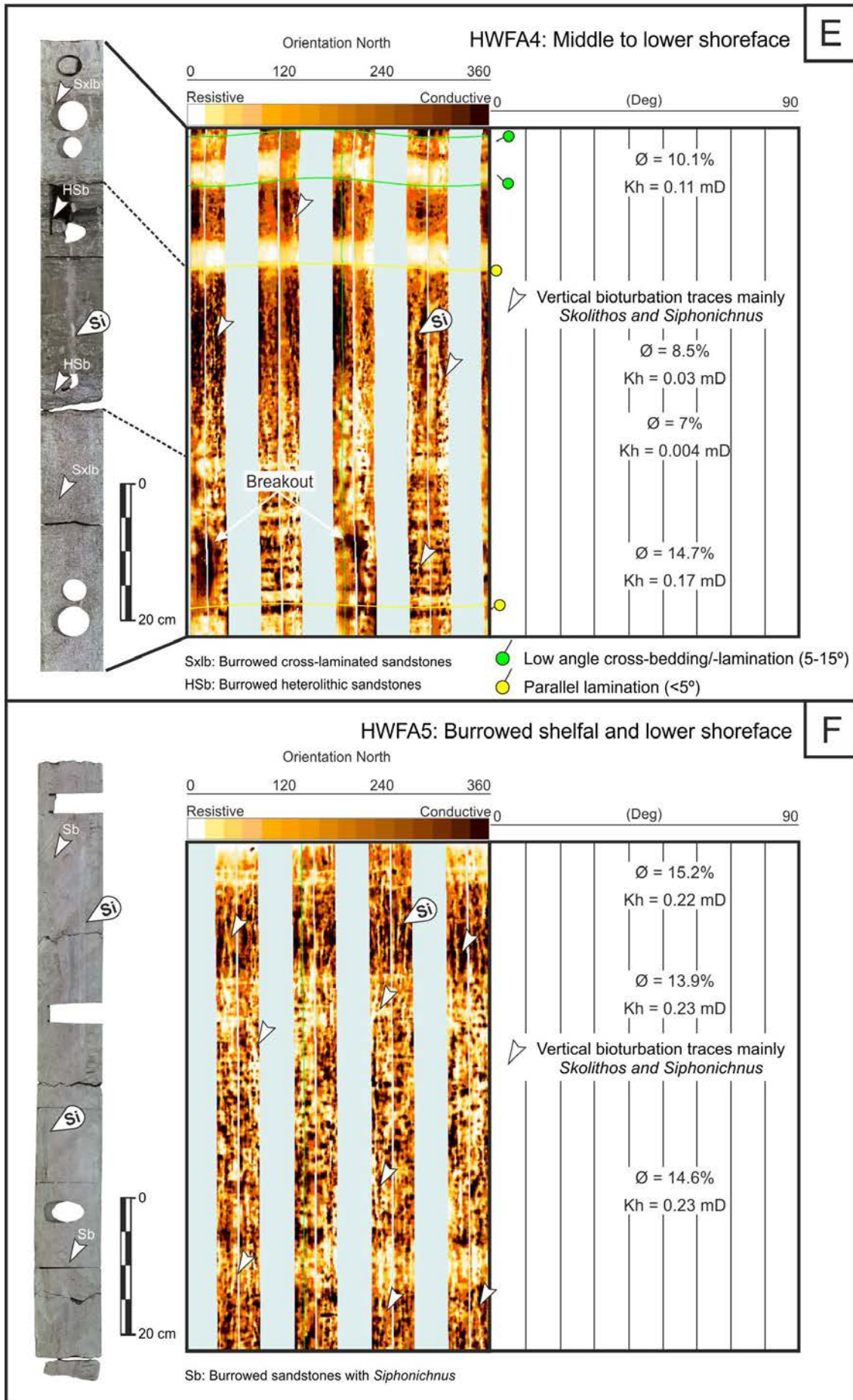


Figure 4.6. Detailed close-up views of some characteristic sedimentary structures and fabric of facies associations HWFA4 Middle to lower shoreface, HWFA6 Burrowed inner shelf and HWFA7 Shelfal storm sheets. A) Characteristic view of burrowed cross-laminated sandstones with dominant suspension-feeding bioturbation from facies association HWFA4. B) Pervasive, mainly horizontal deposit-feeding bioturbation, in heterolithic sandstones and mudstones, from facies association HWFA6. C) Characteristic alternation of burrowed heterolithic sandstones and mudstones from distal facies association HWFA6. D) Mud-draped combined flow ripples from facies association HWFA7. Notice the direction of the paleocurrent flow rightward in the upper part and bidirectional in the lower part of the image. Four images extracted from core sections in well W15. See the location of the corresponding well in **Fig. 3.3**.



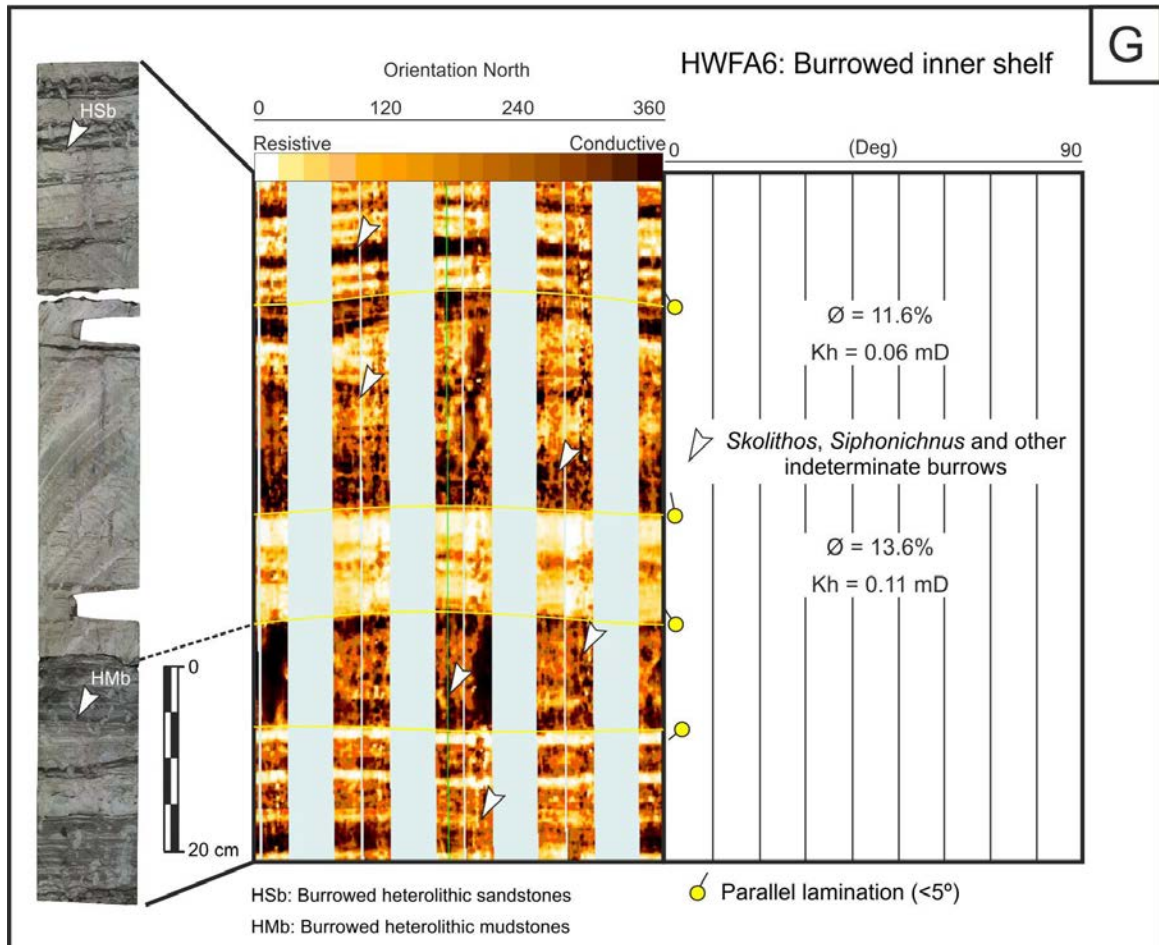


Figure 4.6. (Continued) E) Core to image log calibration showing a 90 cm (aprox.) HWA4 middle to lower shoreface section with an alternation of burrowed cross-laminated sandstones and burrowed heterolithic sandstones with a prevalence of *Skolithos* ichnofacies. F) Core to image log calibration showing a 90 cm (aprox.) HWA5 burrowed shelfal and lower shoreface section dominated by burrowed sandstones with a completely obliterated primary fabric by *Siphonichnus* traces. This core and image log section don't belong to the same part of the well due to lack of good quality comparative images for this facies association. G) Core to image log calibration showing a 90 cm (aprox.) HWA6 burrowed inner shelf section with an alternation of burrowed heterolithic sandstones and mudstones with a mixed *Cruziana* and *Skolithos* ichnofacies. All sections extracted from well W15. See the location of the corresponding well in **Fig. 3.3**.

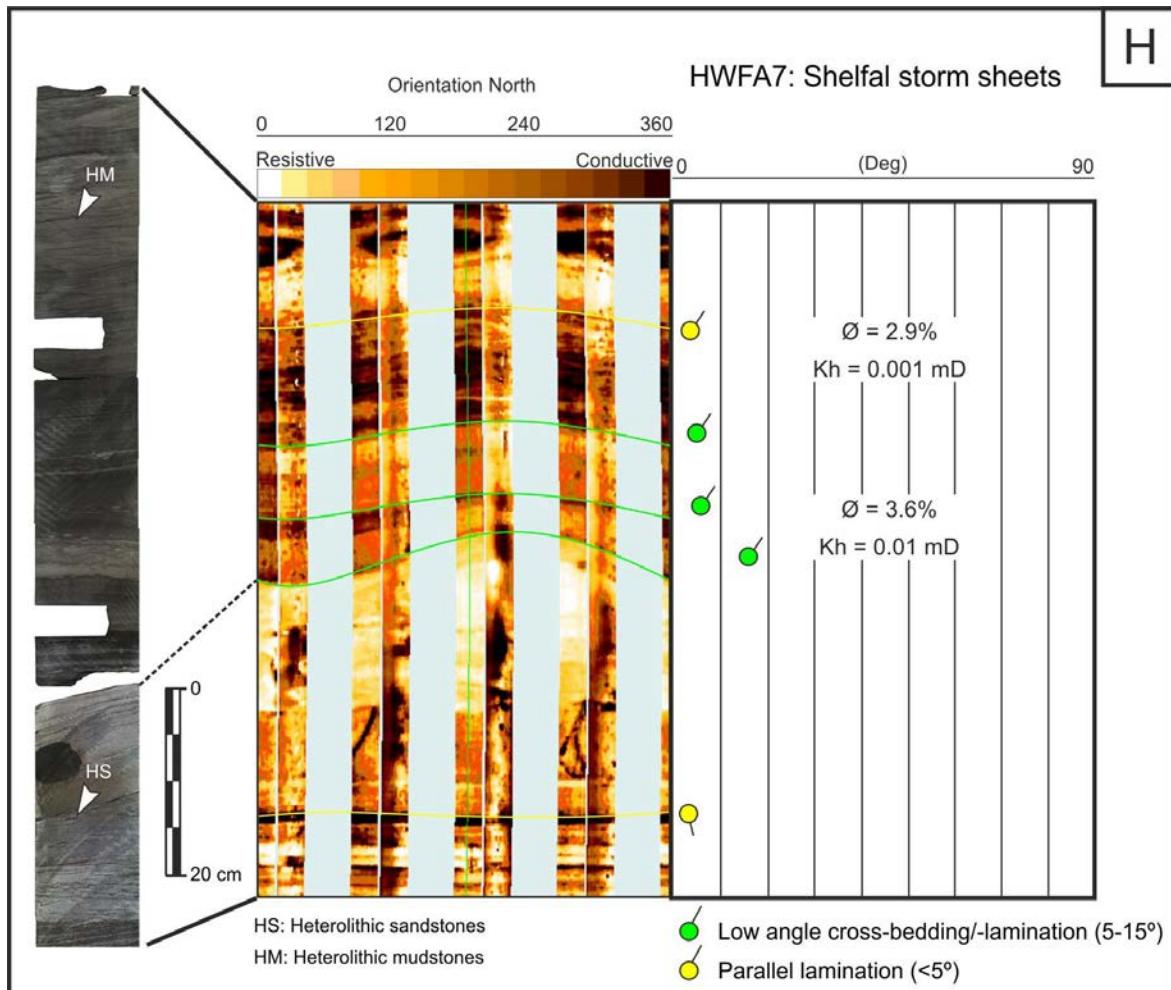


Figure 4.6. (Continued) H) Core to image log calibration showing a 90 cm (aprox.) HWFA7 shelfal storm sheets section with an alternation of heterolithic sandstones and mudstones. Section extracted from well W15. See the location of the corresponding well in **Fig. 3.3**.

4.2. Sequence Stratigraphy of the Hawaz Formation

The purpose of this section is to recognise and correlate stratigraphic surfaces representing changes in depositional trends and to interpret the resulting stratigraphic units bounded by these surfaces.

Taking into account this framework, several low-order and numerous high-order sequences can be recognised in the stratigraphic record of the Hawaz Formation (**Fig. 4.7**); but, after analysing the evolution or stacking of the facies associations in each well, it is possible to erect a simplified scheme with three major depositional sequences (DS1–DS3) and five Hawaz reservoir zones (HWZ1–HWZ5), each defined by key, correlatable, genetic, material-based surfaces (**Fig. 4.7-A – E**).

The top of the Ash Shabiyat Formation is marked by a sharp or slightly more gradational shift from the blocky, low GR response, characteristic of this formation, to a notably more spiky or serrate GR response typical of much of the lower Hawaz. This shift is interpreted not only as a maximum regressive surface, but also as a sequence boundary. As such, it is a compound surface and might be considered in terms of marine erosion as a ravinement, which marks the base of DS1 (**Fig. 4.7-A**).

The first and oldest depositional sequence (DS1) is widely preserved across the study area and corresponds to a transgressive systems tract (TST) defined as reservoir zone 1 (HWZ1). It comprises several stacked fining-upward parasequences overlying the contact with the underlying Ash Shabiyat Formation (**Fig. 4.7-A**). This sedimentary package is dominated by retrogradational shelfal and lower shoreface deposits (**Fig. 4.8**) commonly interlayered within a higher order progradational package but culminating with an abrupt lithological change to argillaceous facies representing a regionally extensive flooding surface associated with shelfal storm deposits (**Fig. 4.7-A**). This flooding surface is commonly represented by the highest GR peak in the entire Hawaz succession and is interpreted as a maximum flooding surface (MFS), normally represented by black shales, moderately rich in organic matter, and with evidence of anoxic conditions as represented by pyritic nodules and ichnofossils such as *Chondrites*, characteristic of low-oxygen environments (**Fig. 4.7-B**). This MFS represents a major shift in stacking patterns and the beginning of a regressive package dominated by inner shelf to middle shoreface deposits, interpreted as the highstand systems tract (HST) of DS1 and reservoir zone 2 (HWZ2). This package can commonly be divided into two sub-zones (HWZ2a and HWZ2b) separated by a regressive surface of marine erosion (RSME) representing a sharp shift in relative

sea level and shallowing of facies associations, interpreted as a response to a forced regression and consequently a shallower wave base (**Fig. 4.7-A**).

The base of the second depositional sequence (DS2) is commonly marked by a sharp erosive surface interpreted as a shoreline ravinement unconformity and sequence boundary (**Fig. 4.7-C**), generated during early transgressive stages by the action of tides and waves just after relative sea level fall and possibly enhanced by an allocyclic trigger mechanism, perhaps related to tectonic activity. This surface also constitutes the base of the TST (**Fig. 4.7-A**) and reservoir zone 3 (HWZ3). This package is commonly dominated by subtidal complex deposits (**Fig. 4.8**) and constitutes the main reservoir of the Hawaz Formation. The DS2 package continues with a marked change in depositional environment, from subtidal complex or abandoned subtidal complex, to tidal flat deposits (**Fig. 4.7-A**). This change is interpreted in terms of a MFS in a nearshore environment and is commonly represented by thin, condensed, argillaceous deposits (**Fig. 4.7-D**). Above, the remainder of the package is dominated by tidal flat deposits (**Fig. 4.8**) with common intercalated ephemeral distributary channels and constitutes the HST of this DS2, and reservoir zone 4 (HWZ4) (**Fig. 4.7-A**). This HST is interpreted to represent a bay infilling with prograding sand to mixed tidal flat deposits during a period of early falling relative sea level. The upwards increase in shale content is typical for the low energy conditions associated with these tide-dominated environments together with a parallel decrease in the diversity of ichnofossils and the increased abundance of marginal marine palynofossils (Miles, 2001, 2003; Abuhmida and Wellman, 2017), both suggesting a more proximal domain.

The third depositional sequence (DS3) is rarely preserved after being typically stripped away during the Late Ordovician glaciation, and only the basal part is sometimes preserved locally (See **Annex 4**). The onset of DS3 is marked by a change in depositional trend, from the underlying low energy mixed-argillaceous tidal flat deposits of the HST-DS2, to slightly higher energy and cleaner deposits of the same facies association (**Fig. 4.7-A**). No major unconformities are preserved although the contact between the underlying clay-rich tidal flat deposits and the subsequent cleaner sandstones tends to be erosive in character (**Fig. 4.7-E**) and is interpreted in terms of maximum regressive surface (MRS) and sequence boundary (**Fig. 4.7-A**). Commonly, subtidal complex deposits can be recognised in the uppermost section of some wells suggesting a slight deepening, and a new TST and reservoir zone 5 (HWZ5) (**Fig. 4.7-A**).

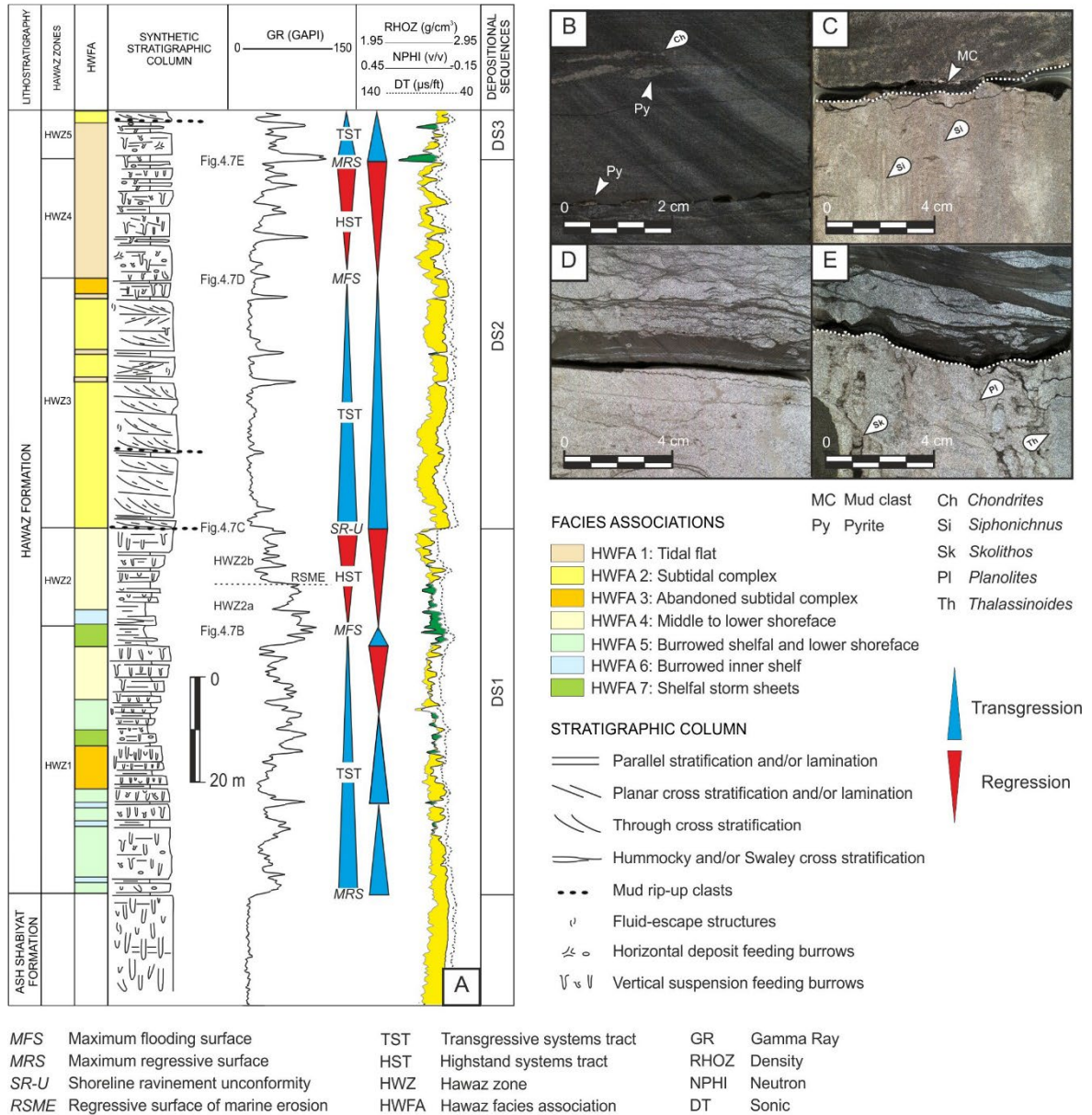


Figure 4.7. Sequence stratigraphy framework of the Hawaz Formation in the study area. A) Composite section of well W19 showing a stratigraphic column of the Hawaz Formation, the associated wireline log responses, the suggested zonation for the reservoir based on the facies associations, and sequence stratigraphic framework. The transgressive and regressive stacking patterns are also represented on the figure together with the three main depositional sequences (DS1-3). B) Close-up view of a representative core section showing the main features of the maximum flooding surface of DS1, from well W15. C) Core section view of the erosive contact corresponding to the shoreline ravinement unconformity and sequence boundary of DS2, from well W15. D) Core picture showing the main characteristics of the maximum flooding surface of DS2, from well W09. E) Core view highlighting the erosive character of the maximum regressive surface and sequence boundary of DS3, from well W19. The location of the corresponding wells is highlighted in **Fig 3.3**.

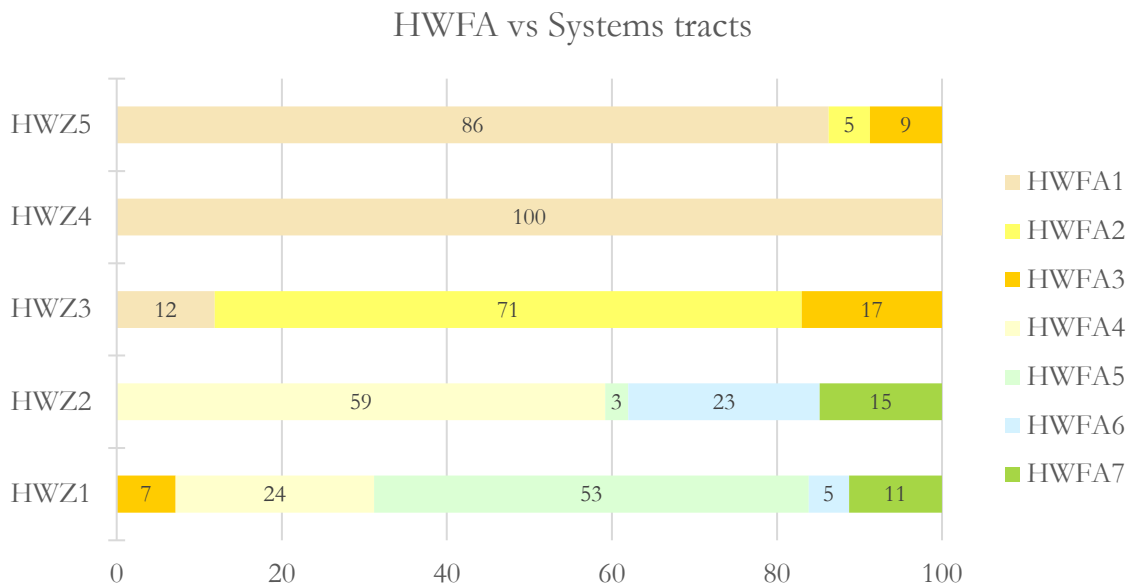


Figure 4.8. Graph showing the relative proportions of Hawaz Facies Associations (HWFA) within each of the identified genetic sequences or Hawaz reservoir zones (HWZ) averaged from the 35 studied wells (values represented in percentages). The proportions shown in HWZ5 might well not be representative due to the lack of preserved section in most of the wells. HWFA1 = Tidal flat; HWFA2 = Subtidal complex; HWFA3 = Abandoned subtidal complex; HWFA4 = Middle to lower shoreface; HWFA5 = Burrowed shelfal and lower shoreface; HWFA6 = Burrowed inner shelf; HWFA7 = Shelfal storm sheets.

4.3. Sedimentary Architecture of the Hawaz Formation

The results obtained from the reconstruction of the sedimentary architecture of the Hawaz Formation in the subsurface of the central Murzuq Basin have been published in the following scientific paper of the journal of the Marine and Petroleum Geology:

- Gil-Ortiz, M., McDougall, N.D., Cabello, P., Marzo, M., Ramos, E. (2022). Sedimentary architecture of a Middle Ordovician embayment in the Murzuq Basin (Libya). *Marine and Petroleum Geology*, 135. <https://doi.org/10.1016/j.marpetgeo.2021.105339> (**Annex 1**)

Furthermore, the results have also been presented at the international conference of the 35th IAS Meeting of Sedimentology, Prague (2021) and at the national conference of the X Congreso Geológico de España, Vitoria-Gasteiz (2021):

- Gil-Ortiz, M., McDougall, N.D., Cabello, P., Marzo, M., Ramos, E. (2021). Sedimentary architecture of the Middle Ordovician Hawaz Formation in the Murzuq basin (Libya). Conference paper (**Annex 2**).

- Gil-Ortiz, M., Cabello, P., McDougall, N.D., Marzo, M., Ramos, E. (2021). Sedimentology and sedimentary architecture of the Hawaz Formation. The uniformitarian paradigm on the ropes; a Middle Ordovician case study. Conference paper (**Annex 3**).

4.3.1. Correlation panels

The results of this work show that, in most wells, at least four sedimentary packages can be recognised across the study area. Although an initial impression might suggest a “layer-cake” architecture, the correlations reveal that the Hawaz does in fact show a significant degree of internal heterogeneity. These four packages are related to several transgressive and regressive systems tracts, grouped into two depositional sequences (DS1-2) introduced in the previous section, which correspond to well-defined reservoir zones (HWZ1-4) (**Fig. 4.7**). In addition, the remnants of a fifth package corresponding to the last transgression into the Hawaz Formation (HWZ5) in DS3, are hardly preserved due to the Late Ordovician glaciation unconformities.

Based on key observations from correlations, we outline here the principal interpretations derived from first, dip correlation panels (**Figs. 4.9 – 4.12**) and second, strike-oriented correlation panels (**Figs. 4.13 – 4.16**). For position of the panels, refer to **Chapter 3.3.1 - Fig. 3.3**.

4.3.1.1. Dip-oriented correlations

From dip-oriented correlations, several key observations can be made. Firstly, from the lowermost HWZ1 reservoir zone (**Fig. 4.7**) it is apparent that there was a subtle deepening of the basin towards the NW inferred from the occurrence and increase in thickness of the most distal burrowed shelfal and lower shoreface (HWFA5), burrowed inner shelf (HWFA6) and shelfal storm sheets (HWFA7) facies associations in this direction. This is best developed in correlation panel Dip 3 between wells W32 and W19 (**Fig. 4.11**) and in correlation panel Dip 4 between wells W24 and W25 (**Fig. 4.12**), where a lateral facies change is observed, from shallower middle to lower shoreface (HWFA4) to burrowed shelfal and lower shoreface (HWFA5) deposits in a SE-NW trend, with an increased abundance of burrowed inner shelf (HWFA6) and also shelfal storm sheet deposits (HWFA7) towards the northwest. Also worthy of note is the presence of a distinctive and extensive (more than 15 km down dip) abandoned

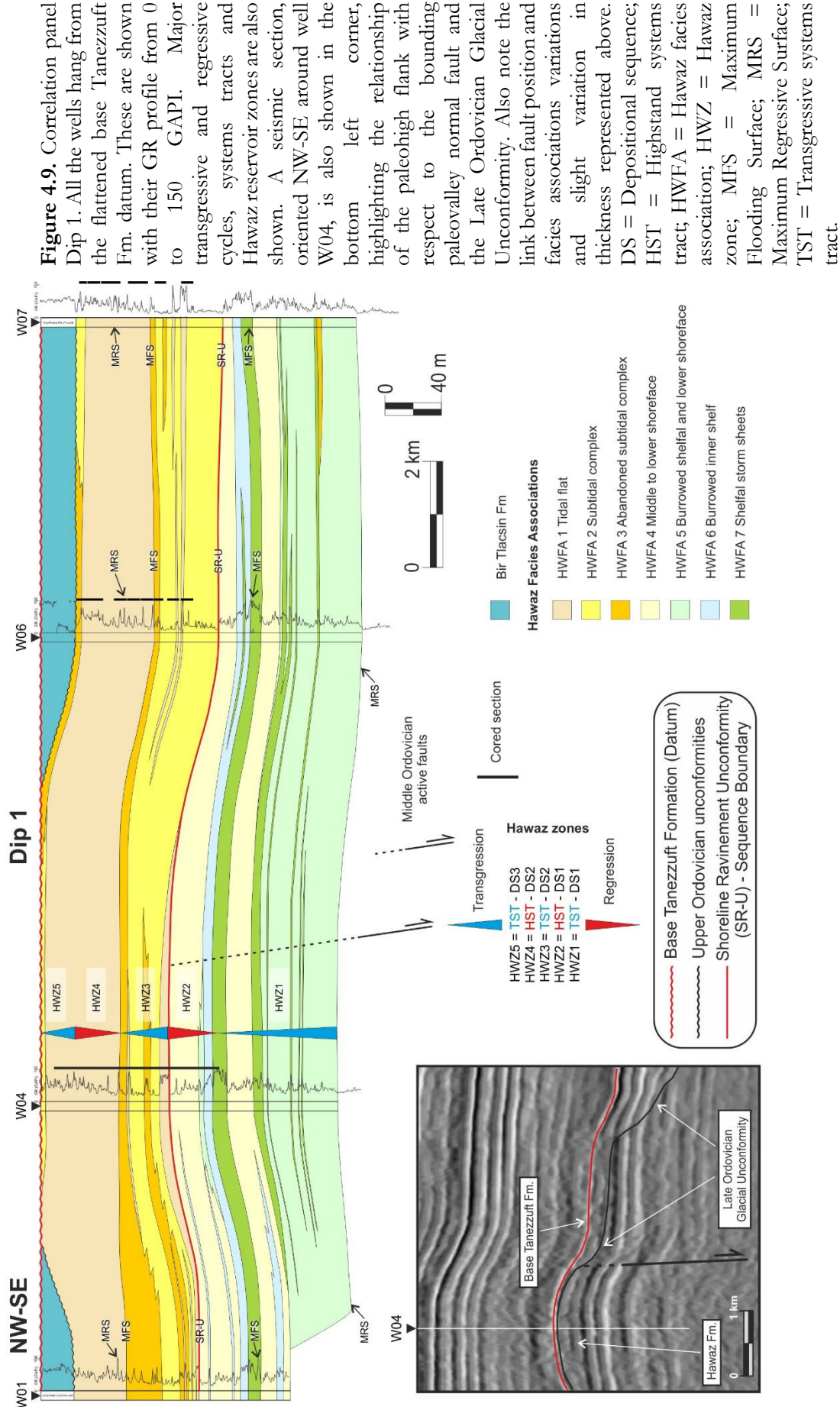
subtidal complex (HWFA3) towards the central and south-eastern part of the study area as seen in correlation panels Dip 2, 3 and 4 (**Figs. 4.10 – 4.12**) during the first main transgression of DS1. In addition, shelfal storm sheet deposits are present across the area, intercalated with shallower, burrowed shelfal and lower shoreface deposits, some of them forming relatively thick packages (around 15-20 m) in the lowermost part of the succession in the south-eastern sector and pinching-out towards the NW, likely representing tempestite lobes connected to shallower shoreface areas (**Figs. 4.10 and 4.12**).

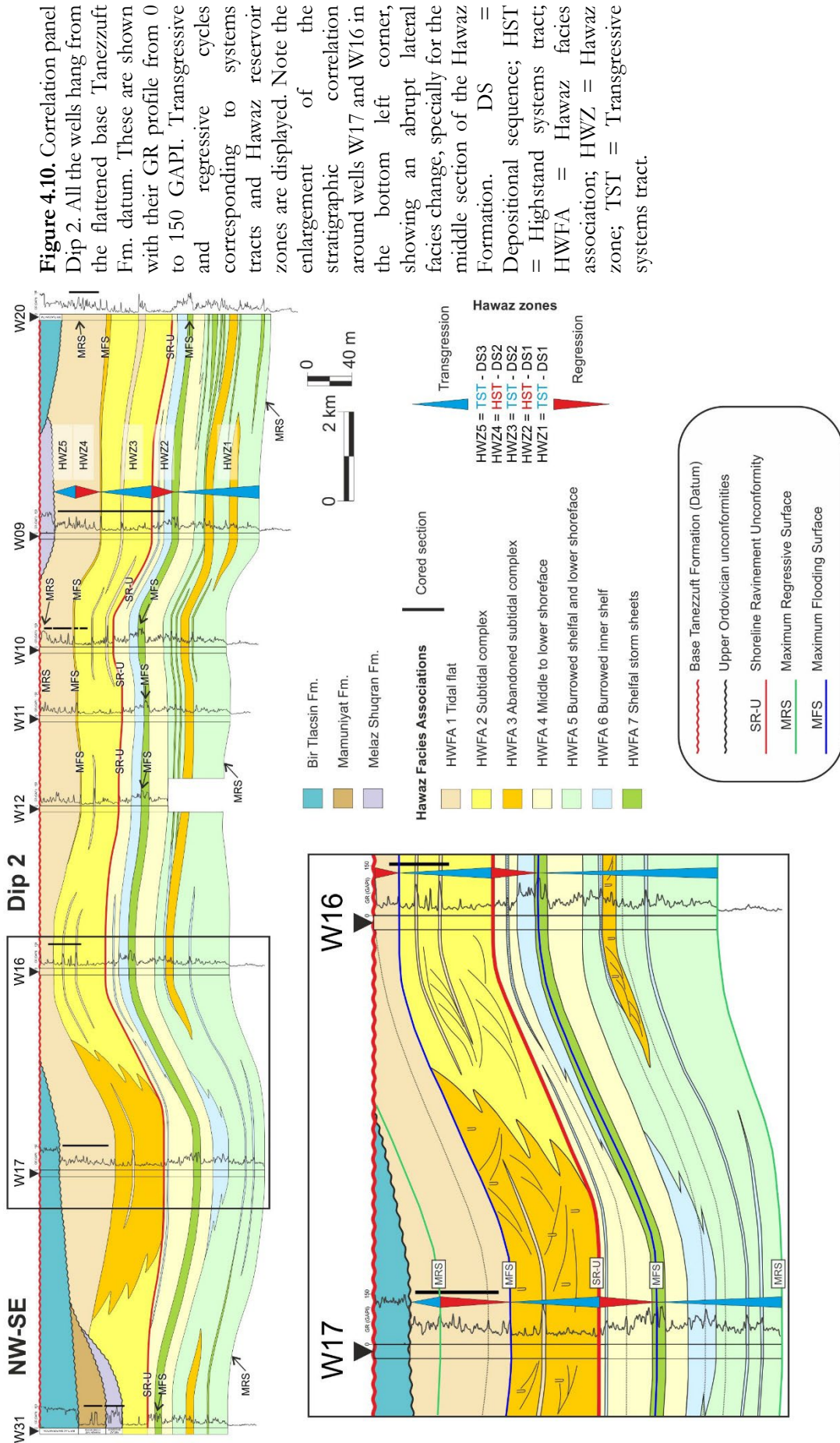
The overlying package, corresponding to zone HWZ2 (**Fig. 4.7**), comprises three main facies belts; shelfal storm sheets (HWFA7), burrowed inner shelf (HWFA6) and middle to lower shoreface (HWFA4), respectively. Despite the significant areal extent of this package and its apparent high continuity over the entire area, internal differences are observed, which demonstrate deepening towards the NW with a progradational trend from SSE to NNW as can be seen in the north-western part of panels Dip 3 and 4 (**Figs. 4.11 and 4.12**), where burrowed inner shelf (HWFA6) and shelfal storm sheets (HWFA7) become more common and relatively thicker towards the NW.

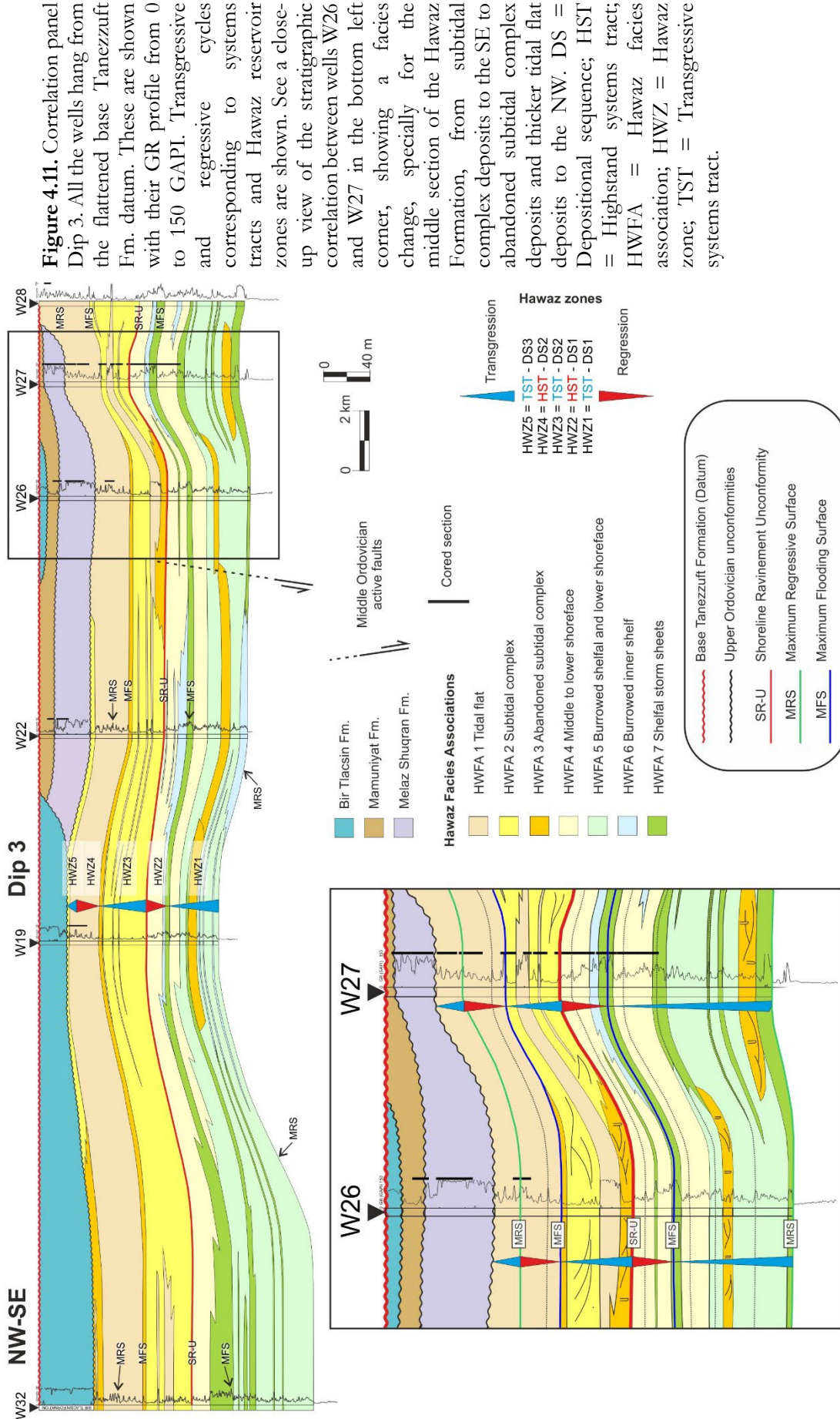
Depositional Sequence 2 begins above a major shoreline ravinement surface with a relative sea level rise and deposition of the main reservoir of the Hawaz Formation in zone HWZ3 (**Fig. 4.7**), mainly comprising subtidal complex deposits (HWFA2). Firstly, correlation panel Dip 1 (**Fig. 4.9**) shows an abrupt decrease in depositional energy toward the western part of the studied area represented by wells W01 and W04, where a characteristic high energy, subtidal environment evolved to a lower energy abandoned subtidal setting. This trend is also apparent in the area of wells W17 (**Fig. 4.10**), W26 (**Fig. 4.11**) and, quite notably, W25 (**Fig. 4.12**). These lateral facies changes might be explained within the framework of distal, but active subtidal complexes, and/or their abandonment due to seasonal fluctuations in sediment supply and/or changes in accommodation space by oscillations in relative sea level (Dalrymple et al., 1992; Cattaneo and Steel, 2003; Dalrymple and Choi, 2007). Even major storms might play an important role in triggering subtidal channel switching and consequent abandonment (Dalrymple et al., 2012).

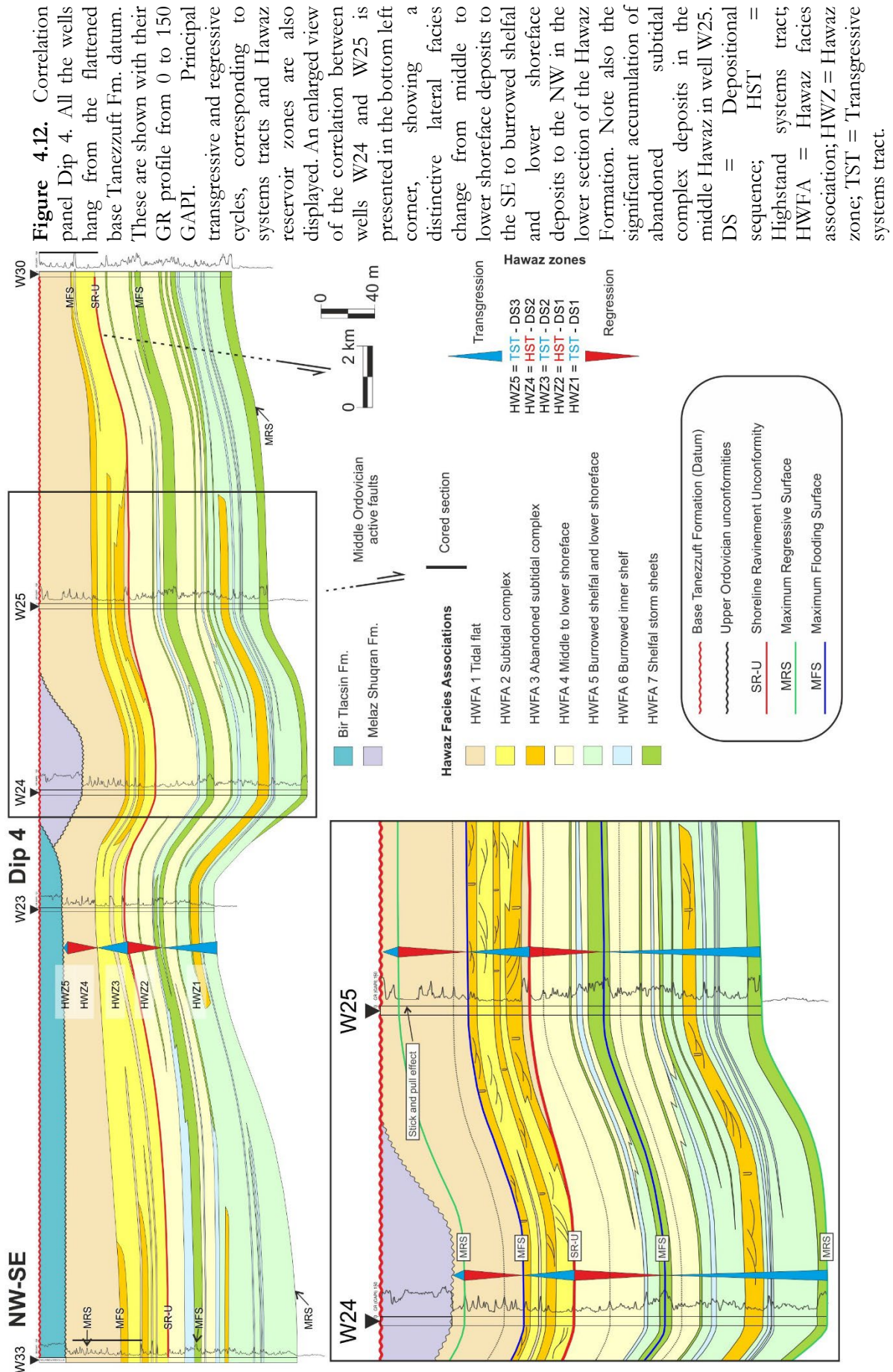
Depositional Sequence 2 culminates with a regressive section of tidal flat deposits (HWFA1) widely present across the entire study area. This section corresponds to reservoir zone HWZ4 (**Fig. 4.7**) and is extremely uniform in character, interrupted only by some ephemeral distributary channels and tidal creeks cutting the tidal flat deposits and embedded within this major facies association HWFA1.

Depositional Sequence 3 and reservoir zone HWZ5 (**Fig. 4.7**), which is often partially or totally eroded by the Late Ordovician unconformities, has not been evaluated here due to the limited preserved thickness and restricted lateral extent.









4.3.1.2. Strike-oriented correlations

Along strike, correlations show lateral facies changes within time-equivalent deposits. Some of the most remarkable observations are the significant variations in thickness and facies associations, presumably related to alongshore differences in accommodation space and sediment supply ratios. Many of these variations may well be related to the presence of a series of high angle extensional normal faults, the traces of which often coincide with the erosional limits of Late Ordovician paleovalleys as identified in seismic (See **Chapter 3.3.1 - Fig. 3.4**). Whether these faults were active during deposition of the Hawaz is difficult to confirm but along strike changes in thickness and facies patterns are certainly suggestive.

These changes mainly occur in reservoir zones HWZ2 and HWZ3, corresponding to the HST-DS1 and TST-DS2 (**Fig. 4.7**), although the most significant variations appear in the main reservoir or zone HWZ3, characterised not only by lateral facies changes but also thickness variations presumably linked to the above-mentioned faults.

Specifically, in the hanging wall of these potentially active faults, the HWZ3 succession is dominated by high energy, thicker subtidal complex deposits (HWFA2), whereas, in the footwall of these faults the equivalent succession tend to be more frequently represented by less energetic and thinner abandoned subtidal complex (HWFA3) and tidal flat (HWFA1) deposits. These variations in thickness and/or lateral facies changes can be seen in correlation panels Dip 1, between wells W04 and W06 (**Fig. 4.9**); Dip 3, between wells W22 and W26 (**Fig. 4.11**); Dip 4, between wells W25 and W30 (**Fig. 4.12**); in Strike 1 between wells W07 and W29, and between W29 and W30 (**Fig. 4.13**); in panel Strike 2, between wells W22 and W24, and specially between W07 and W22 (**Fig. 4.14**); in the central part of Strike 3, between wells W04 and W23 (**Fig. 4.15**); and finally, between W01 and W33 in correlation panel Strike 4 (**Fig. 4.16**). It is also possible that these faults were active during earlier periods of Hawaz deposition, at least since reservoir zone HWZ2. This is suggested by the relationship between deposition of more distal and thicker burrowed inner shelf (HWFA6) deposits in the hanging wall of these faults, compared to shallower and thicker middle to lower shoreface (HWFA4) deposits present in the footwall. This relationship can be seen in correlation panels Strike 1 between wells W20 and W29, and between wells W28 and W30 (**Fig. 4.13**), Strike 2 between wells W22 and W24 (**Fig. 4.14**) and Strike 3 between wells W19 and W23 (**Fig. 4.15**).

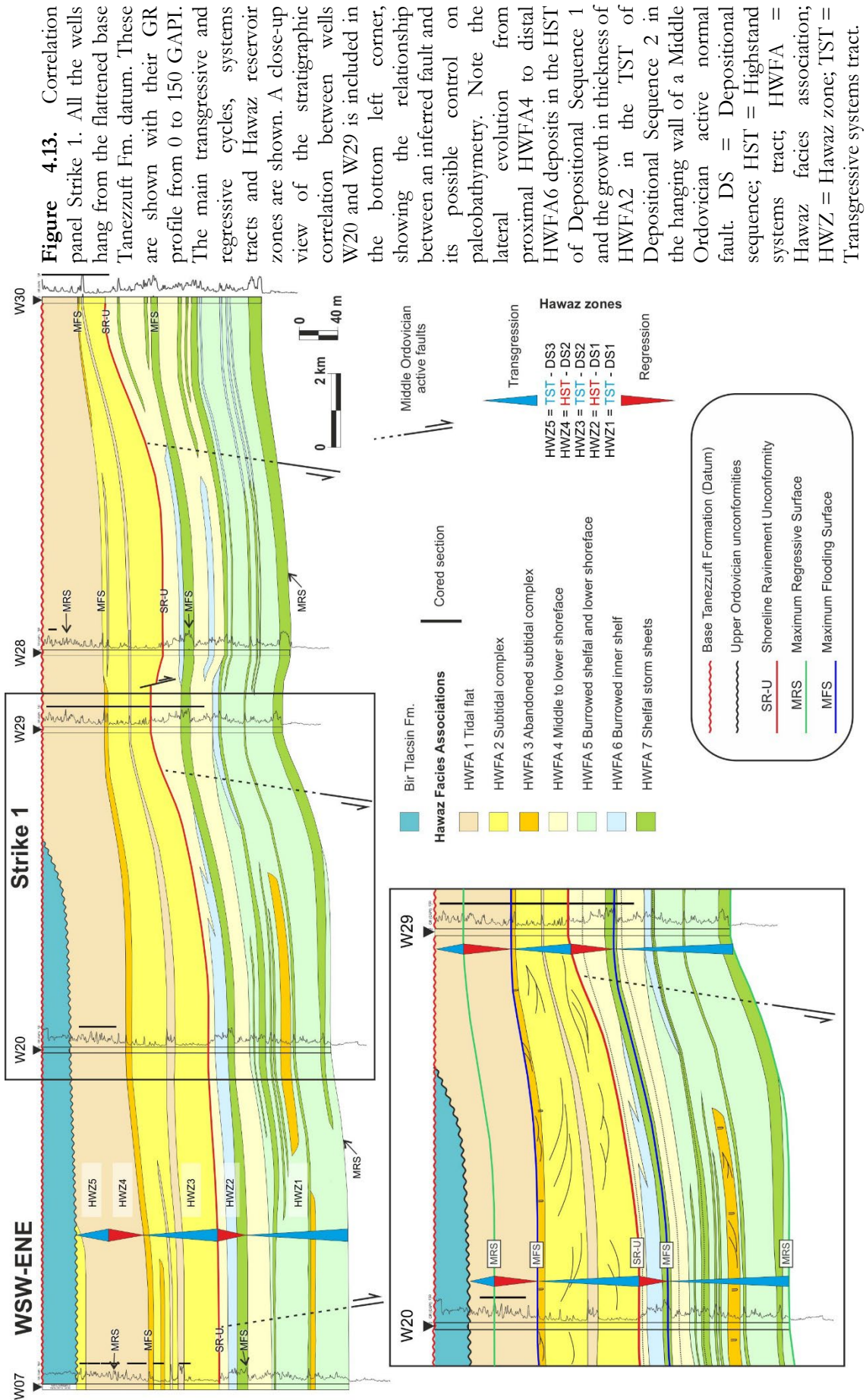
Several additional key observations from strike correlations are outlined as follows. Reservoir zone HWZ1 (**Fig. 4.7**) is dominated by burrowed shelfal to lower shoreface deposits (HWFA5)

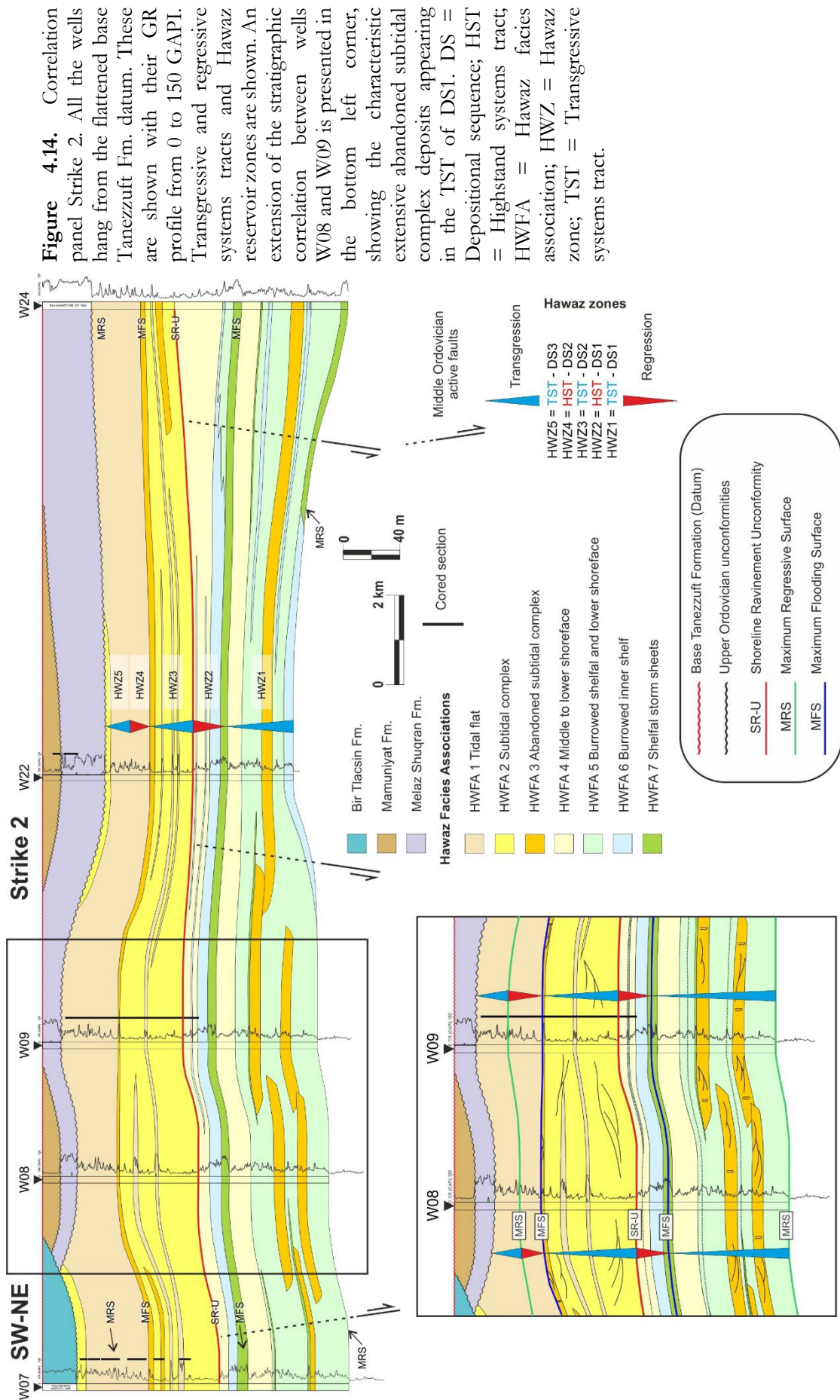
with a characteristic interlayered abandoned subtidal complex (HWFA3) present in the central and south-eastern part of the area of study, most probably related to distal subtidal complex deposits sourced from the SE, most notably in correlation panels Strike 2 and 3 (**Figs. 4.14 and 4.15**). Also, a characteristic interval of storm sheet deposits, in the lowermost Hawaz, immediately overlying the Ash Shabiyat Fm., can be observed in the most eastern part of the study area (**Figs. 4.13 and 4.14**) as previously inferred from Dip correlation panels 3 and 4 (**Figs. 4.11 and 4.12**).

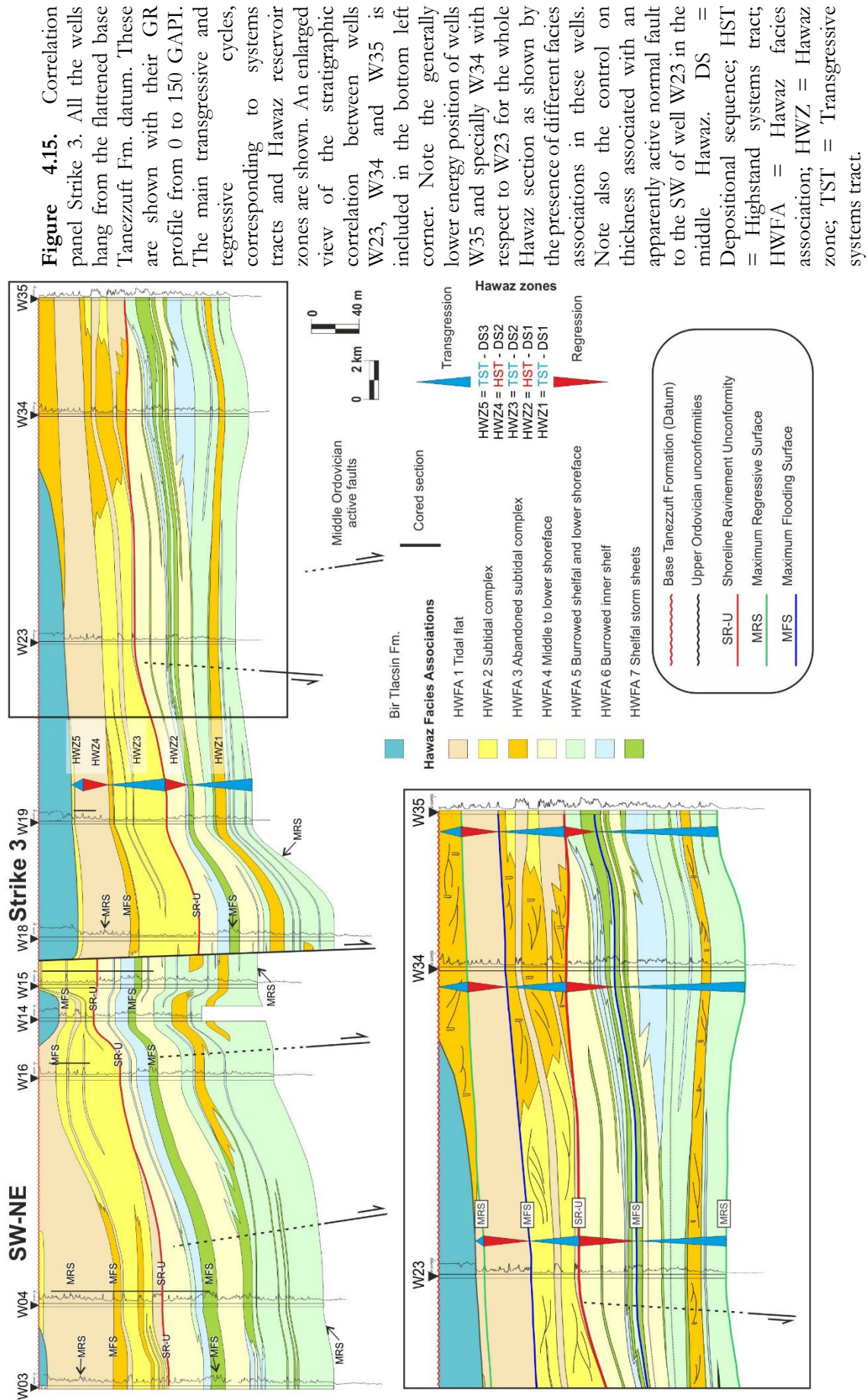
Reservoir zone HWZ2 (**Fig. 4.7**) shows important differences in thickness as observed in Strike panels 1, 2 and 3 (**Figs. 4.13 – 4.15**), presumably related to the activity of normal faults highlighted above. In contrast, whilst the thickness and occurrence of middle to lower shoreface (HWFA4) deposits is notably higher in the west-southwest and central-eastern part of the study area, in the central to north-western areas the succession is dominated by distal burrowed inner shelf deposits (HWFA6) and shelfal storm sheets (HWFA7). Hence, active faulting may have controlled the spatial distribution of facies associations locally and perhaps slightly determine the shoreface profile.

As an alternative explanation to these alongshore variations, local differences in accommodation and/or energy in a broad exposed low gradient tidal shelf could have facilitated these lateral facies associations changes as well. The trigger for these variations in accommodation space and energy of the sedimentary system could be attributed to thermal subsidence and/or alongshore lateral migration of entry points of sediment into the basin.

Additional key observations of reservoir zone HWZ3 in Strike correlation panels 3 and 4 (**Figs. 4.15 and 4.16**) show, not only variations in thickness, possibly linked to fault-generated accommodation space, but also a transition from subtidal complex deposits to lower energy abandoned subtidal complex and tidal flat deposits in footwall positions, as shown in panel Strike 3 in the area of wells W03, W04 and W34 (**Fig. 4.15**) and in panel Strike 4 around wells W01 and W34 (**Fig. 4.16**). A subtle increase in the abundance of abandoned subtidal complex deposits from south to north within HWZ3 zone may also suggest a slight deepening trend towards the north.







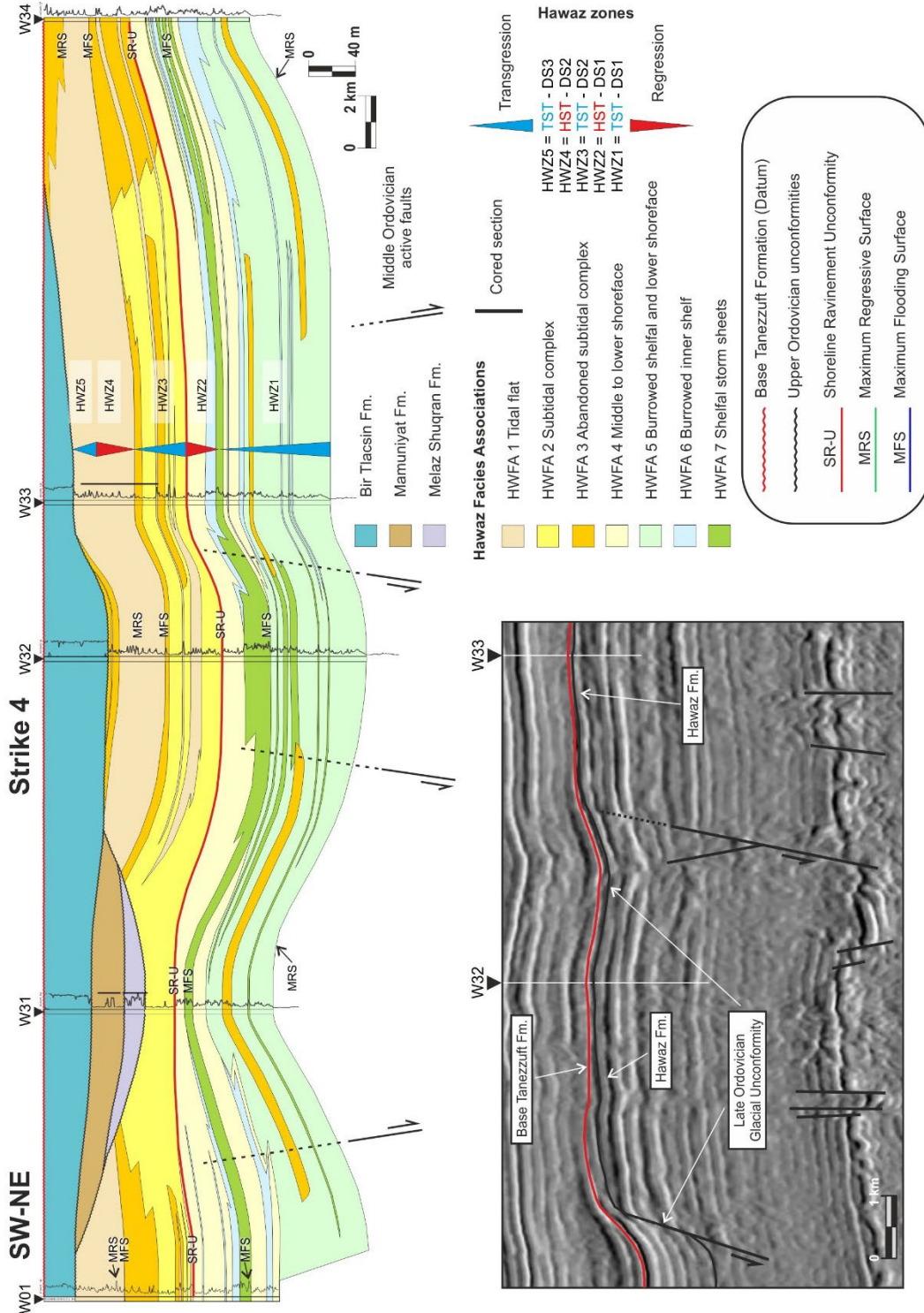


Figure 4.16. Correlation panel Strike 4. All the wells hang from the flattened base Tanezzuft Fm. datum. These are shown with their GR profile from 0 to 150 GAPI. Transgressive and regressive cycles, corresponding to systems tracts and Hawaz reservoir zones are also displayed. Also included is a seismic section, oriented SW-NE around wells W32 and W33 in the bottom left corner, showing the relationship of the paleohigh flank with respect to the normal fault bounding the paleovalley and the Late Ordovician Glacial Unconformity to the SW. Note how some of these faults appear to be connected to pre-existing basement structures. Also note the link between fault location and variations in facies character and thickness of facies associations. DS = Depositional sequence; HST = Highstand systems tract; HWFA = Hawaz facies association; HWZ = Hawaz zone; TST = Transgressive systems tract.

4.3.2. Paleogeographic reconstruction of the Hawaz Formation

A series of Gross Depositional Environment (GDE) maps (**Figs. 4.17 – 4.20**) were generated with the aim of providing insight into the lateral distribution of facies belts within the framework of a sequence stratigraphic-based reservoir zonation (**Fig. 4.7**), following the methodology explained in the previous **Chapter 3.3.2**.

4.3.2.1. Reservoir zone HWZ1 (TST-DS1)

The HWZ1 reservoir unit comprises a 3rd order transgressive sequence, including two higher order transgressive cycles capped by a regressive sequence and culminating with a new transgressive cycle (**Fig. 4.7**). The proportion of facies associations calculated for this zone in each well, as well as the lateral distribution of these facies associations proved by the correlation panels, shows that there is a deepening trend from southeast to northwest based on the occurrence of shallower abandoned subtidal complex deposits (av. 7%) in the central to southeast areas evolving to distal burrowed inner shelf deposits (av. 5%) to the northwest, within a dominant background of a burrowed shelfal and lower shoreface environment (av. 53%) mostly dominating the area of study (**Fig. 4.17**). In addition, tempestites or storm sheets are generally widely present across the study area (av. 11%). Most of these storm deposits were most probably supplied to the shelf through subtidal channels as suggested by **Fig. 4.17**, although the exact location and geometries of such bodies are speculative as none have been drilled by any of the wells in this study. The wells W01, W12 and W21 (**Fig. 4.17**) did not penetrate the full interval and so are not representative.

4.3.2.2. Reservoir zone HWZ2 (HST-DS1)

The overlying zone is characterised by an overall regressive sequence (**Fig. 4.7**) and dominated by middle to lower shoreface deposits grading upwards from areally extensive shelfal storm sheets and burrowed inner shelf packages. In fact, in terms of facies abundance, the middle to lower shoreface deposits are predominant (av. 59%) and significantly thicker prevailing over the shelfal storm sheets (av. 15%) and burrowed inner shelf (av. 23%) in the area of study. The lateral distribution of facies associations again suggests a deepening trend from the southeast toward the northwest. However, the presence of possible active normal faults, inferred from correlation panels and seismic data, might have played a significant role in

the control of the lateral distribution of facies as shown in the lower central part of the map (Fig. 4.18), and in correlation panels strike 1, 2 and 3 (Figs. 4.13 – 4.15). These faults may have also influenced the paleobathymetric profile of the area, by creating accommodation space and allowing deeper water facies associations to dominate in the lows created by these structures. In marked contrast, shallower water locations in the west-southwest and central-eastern areas accumulated thicker successions of prograding middle to lower shoreface deposits (Fig. 4.18). As before, storm sheets are present across much of the studied area for this zone although they become more important towards the distal north-western areas. For example, in well W32 storm sheets form a 60 m thick package (Fig. 4.18). As in the case of zone HWZ1, it is assumed that the storm sands accumulated in lobes, were fed by subtidal channels connected to the middle and upper shoreface, although the exact location of these geobodies can only be speculatively represented in this map.

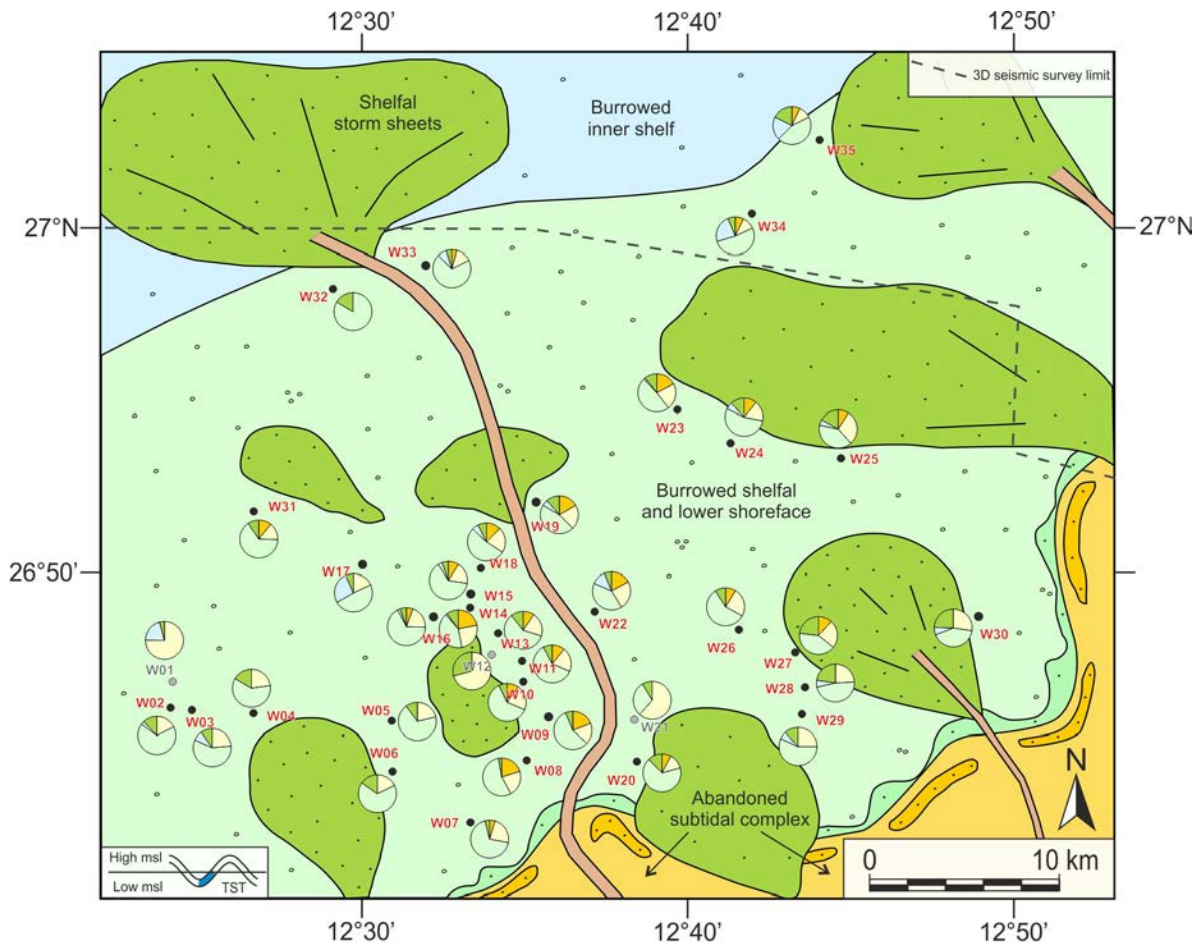


Figure 4.17. Gross Depositional Environment map corresponding to the transgressive systems tract (TST) of Depositional Sequence 1. Facies association proportions are posted next to their corresponding wells. W01, W12 and W21 are anomalies reflecting a reduced section associated with a shallower than normal Total Depth (TD); see Annex 4 for details.

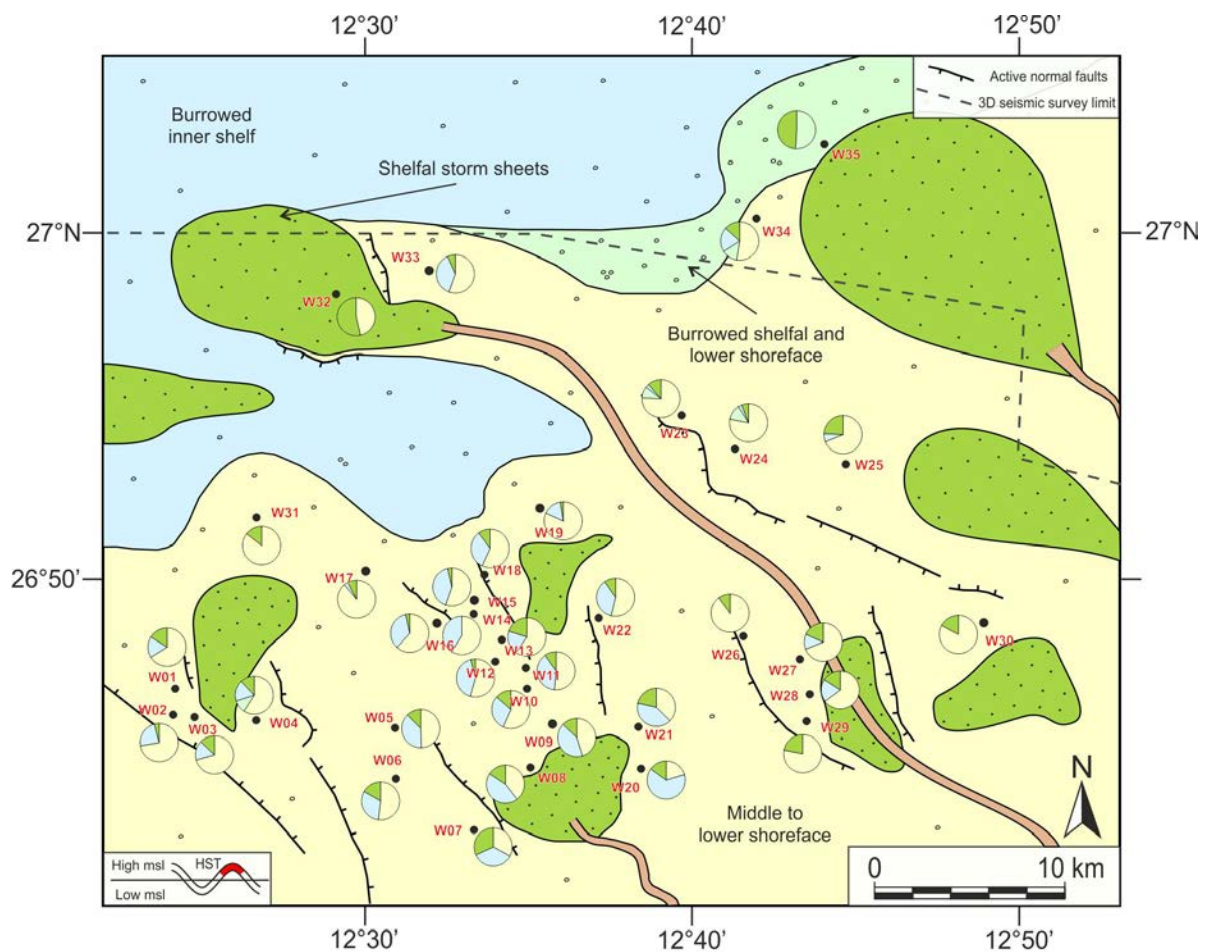


Figure 4.18. Gross Depositional Environment map corresponding to the highstand systems tract (HST) of Depositional Sequence 1. Facies association proportions are posted next to their corresponding wells. Note also the presence of apparently active normal faults, inferred from seismic and correlation panels, which correspond with some of the faults picked in underlying Cambro-Ordovician sections from seismic data and shown in **Fig. 3.3**.

4.3.2.3. Reservoir zone HWZ3 (TST-DS2)

The succeeding zone was deposited during a transgressive stage dominated by subtidal complex deposits (**Fig. 4.7**) in a protected to semi-protected nearshore environment. From the proportions of facies associations and the interpretation of correlation panels, it is apparent that the zone comprises three main facies belts; the dominant subtidal complex (av. 71%), the subordinate abandoned subtidal complex (av. 17%) and tidal flat deposits (av. 12%). Within this broad framework, the boundary between the subtidal and the intertidal zones may well have been conditioned by the presence and activity of NNW to SSE-trending normal faults as interpreted in **Fig. 4.19**. The thickness of the main reservoir facies may also have been controlled by both syn-depositional activity on these faults and compensation associated with the pre-existing paleorelief left after deposition of underlying HST-DS1. This is demonstrated

in correlation panels Strike 1, 2 and 3 (**Figs. 4.13 – 4.15**) where thicker sections of HWZ2 are sometimes associated with a notably thinner HWZ3 above.

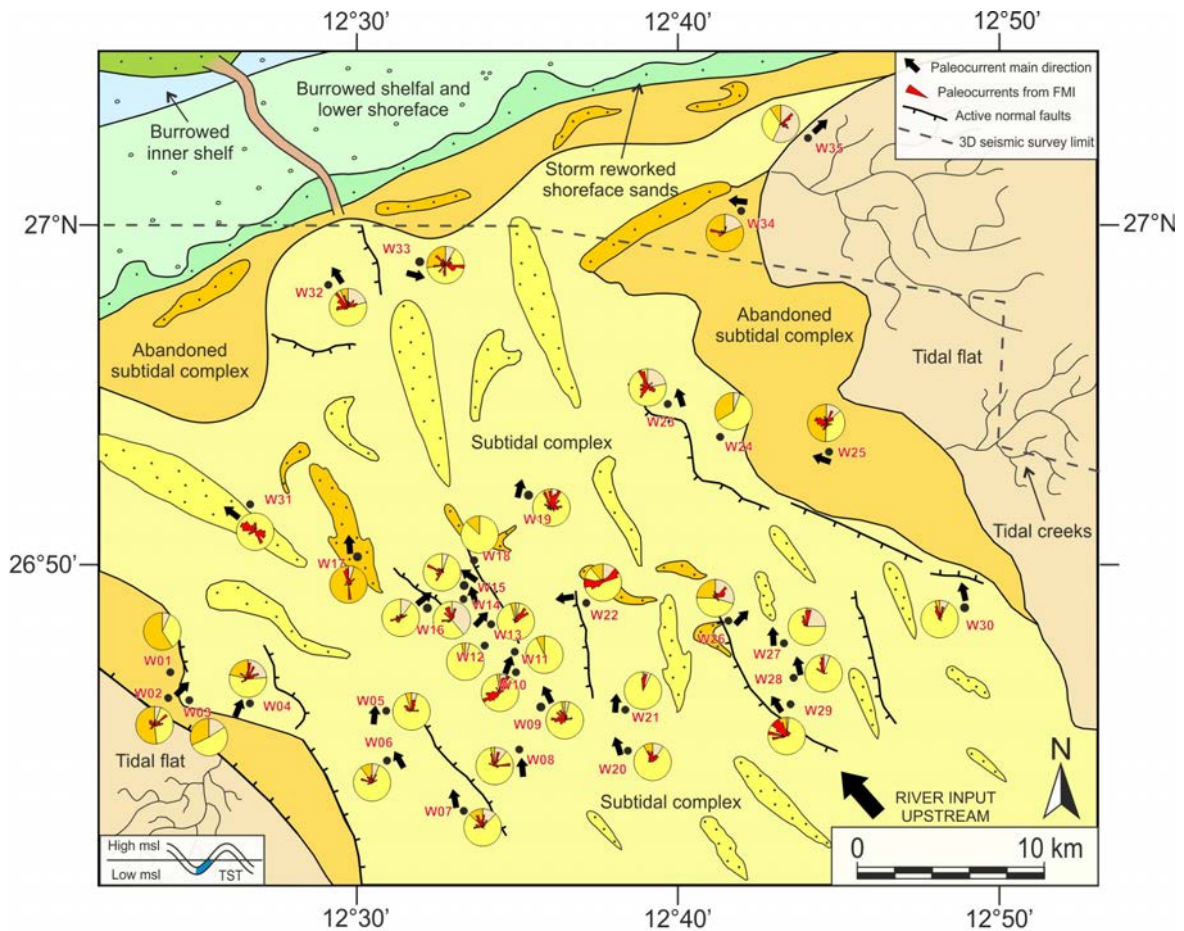


Figure 4.19. Gross Depositional Environment map corresponding to the transgressive systems tract (TST) of Depositional Sequence 2. Facies association proportions are posted next to their corresponding wells. Note also the presence of apparently active normal faults during the Middle Ordovician, which correspond with some of the faults picked in underlying Cambro-Ordovician sections from seismic data and shown in **Fig. 3.3**. Note also the paleocurrent directions inferred from image log data (FMI) and their principal orientation highlighted by black arrows. The interpretation in the north-western corner is purely speculative and driven by our depositional model, possibly beyond the limits of the study area.

Another key observation is the apparent existence of two areas dominated by the lower energy abandoned subtidal complex and tidal flat deposits, respectively towards the SW and the NE (**Fig. 4.19**). These deposits may represent the margins of a bay or estuary, although neither major scours or incised valleys were observed in seismic nor more obviously proximal, fluvial deposits were identified in the studied area, although the presence of such features further to the SE is entirely possible. From paleocurrent data we infer a mean dominant flow towards the NNW, across most of the wells, most likely associated with the main sediment input and ebb tidal direction. Paleocurrent data also shows that wells in the north-western half of the study

area show an increase in bi-directionality of sedimentary structures, which suggests an increase in the power of the subordinate flow, considered here as the effect of flood tides. Finally, it should be emphasized that the interpretation proposed for the north-western corner of this GDE map is purely speculative and driven, in the absence of any well data, by our sedimentary model (See Chapter 4.4). Accordingly, it is entirely possible that the suggested shoreface deposits may occur much further towards the NW given that none of the wells found evidence of such distal facies associations within this unit in the studied area.

4.3.2.4. Reservoir zone HWZ4 (HST-DS2)

This reservoir zone is mainly characterised by sandy to mixed tidal flat deposits across the whole area of study. It corresponds to the HST of the second 3rd order depositional sequence and shows a marked prograding trend from distal sandy tidal flat deposits to proximal mixed sandy and shaly tidal flat deposits (Fig. 4.7). The very low gradient of the Middle Ordovician cratonic margin facilitated the progradation of these deposits for hundreds of kilometres across the studied area. This facies association was drilled by all the wells in the study area, only interrupted by thin ephemeral distributary channels and tidal creeks embedded in an overall intertidal setting (Fig. 4.20). Some of these ephemeral distributary channels were identified in wells as 1–2 m thick, erosively-based, fining-upwards bodies comprising clean, cross-laminated to heterolithic sandstones. From image log data (FMI), paleocurrent directions were obtained for these channels and plotted in this GDE map (Fig. 4.20). The interpretation suggested for the north-western corner of this map, it should be emphasized, is largely speculative. It is driven by the depositional model (See Chapter 4.4), but also by the evidence for barrier island and tidal inlets, based on sedimentological and ichnofacies assemblages, found by Ramos et al. (2006) and Gibert et al. (2011) for laterally equivalent deposits in the neighbouring Gargaf High.

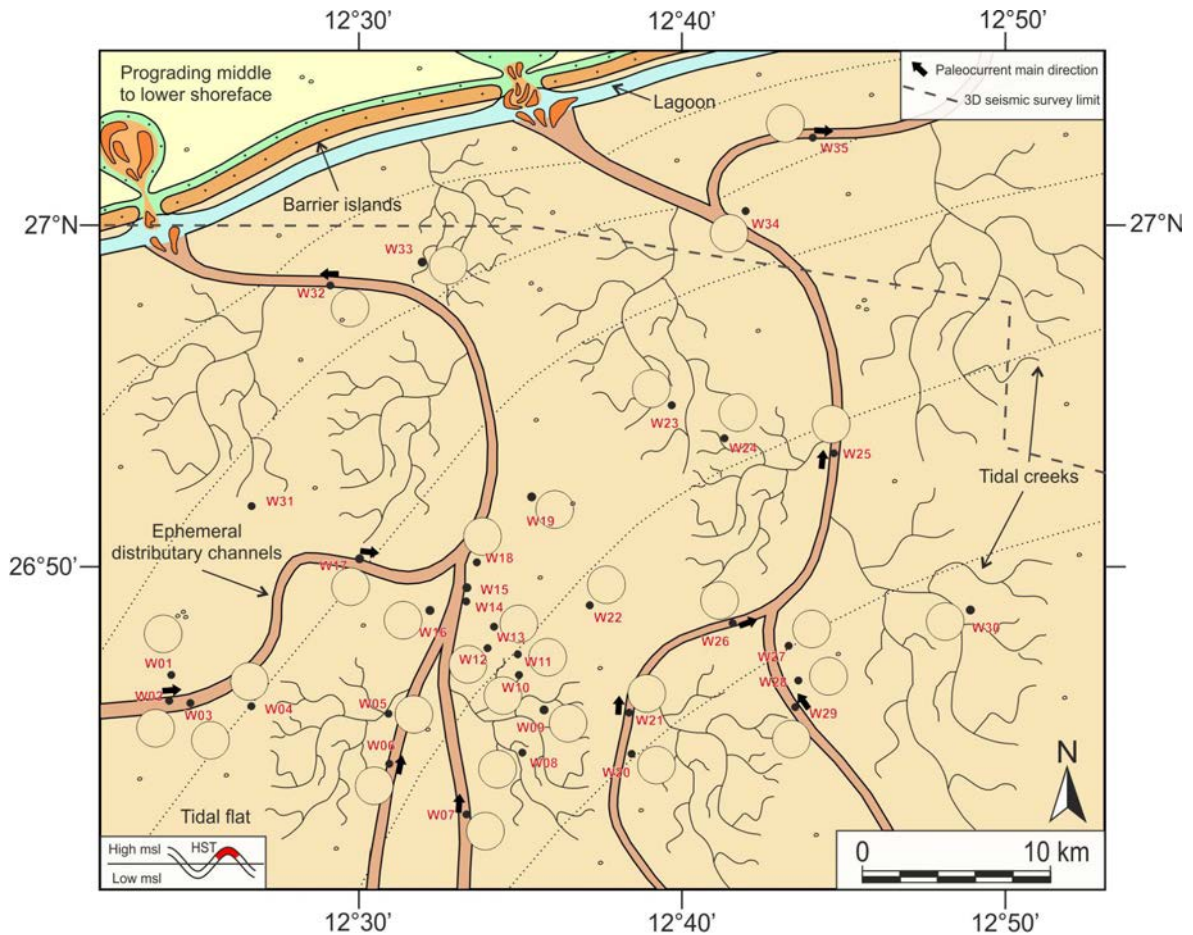


Figure 4.20. Gross Depositional Environment map corresponding to the highstand systems tract (HST) of Depositional Sequence 2. Facies association proportions are posted next to their respective wells. Note also paleocurrent data associated with those wells intercepting ephemeral distributary channels in the tidal flat. The interpretation in the north-western corner is largely speculative and driven by our depositional model and outcrop data from the neighbouring Gargaf High zone, where Ramos et al. (2006) and Gibert et al. (2011) identified evidence of barrier island and tidal inlet facies and associated ichnofacies assemblages.

4.4. Depositional model of the Hawaz Formation

The Hawaz Formation could be classified as a lithostratigraphic unit deposited in a clastic coastal depositional environment mainly controlled by tidal processes. From classifications of major coastal depositional environments, developed by both Boyd et al. (1992) and Dalrymple et al. (1992) and based upon a comparison with modern coastal environments, the Hawaz Formation could also be considered a composite sequence of transgressive tide dominated bay/estuarine facies and regressive tidal flats. However, this comparison assumes that modern fluvial, wave and tidal processes were similar to those in the past. Thus, there may be some limitations in the application of this approach when comparing Cambro-Ordovician or older

systems with most present day nearshore depositional environments (Eriksson et al., 1998; Clifton, 2006; Eriksson and Simpson, 2012).

These limitations and differences derive from observations made in this study, where the factors controlling the sedimentation and the architecture of the Hawaz Formation might have been significantly influenced by at least four processes (Gil-Ortiz et al., 2019) discussed in **Chapter 5.2**.

Several key observations made from the correlation panels and gross depositional environment maps allowed us to improve upon the conceptual depositional models suggested for the Hawaz Formation in previous works (Vos, 1981; Anfray and Rubino, 2003; Ramos et al., 2006; Abouessa and Morad, 2009; Gibert et al., 2011), which helped to define the relationships between the facies associations and the paleogeographic implications of their lateral distribution patterns in the north central part of the Murzuq Basin.

Given the significant differences between the factors controlling modern and ancient Ordovician environments, the Hawaz Formation is best described by an updated conceptual depositional model based on both, a complete sedimentological study (Gil-Ortiz et al., 2019) and the results obtained from correlations and GDE maps presented before (Gil-Ortiz et al., 2022).

The Hawaz Formation comprises two, well-distinguished, sedimentary domains; an open shallow marine setting represented by DS1 (HWZ1 and HWZ2 reservoir zones) and a transitional marginal marine unit represented by DS2 (HWZ3 and HWZ4 reservoir zones) and DS3 (HWZ5 reservoir zone) (**Fig. 4.7**). Our conceptual depositional model reflects variations in the presence and abundance of the facies associations and dominant ichnofacies across both depositional dip and strike with changing relative sea level, during transgressive (**Fig. 4.21-A**) and highstand regressive stages (**Fig. 4.21-B**).

The early stages of transgression (**Fig. 4.21-A**) are dominated by shallow water, open marine facies represented by a transition from inner shelf to burrowed shelfal to lower shoreface deposits with common interlayered storm deposits. In shallower, marginal marine subtidal to intertidal environments, subtidal complex deposits developed in relatively protected nearshore areas associated with dominant ebb tides and further fluvial discharge directed from SSE to NNW, along an embayed coastline surrounded by bounding lower energy tidal flats (**Fig. 4.21-A**).

The trace fossil assemblages associated with these environments show a characteristic lateral evolution down depositional dip within the framework of a dominant low energy *Cruziana* ichnofacies, represented here by a high diversity and degree of horizontal deposit-feeding traces, very characteristic of low energy open marine settings (Seilacher, 1970, 2000, 2007; Droser and Bottjer, 1986; Bottjer and Droser, 1991; Mángano et al., 1996; Pemberton et al., 2001, 2012; Seilacher et al., 2002; Gingras et al., 2012; Gingras and MacEachern, 2012; Pemberton et al. 2012). In some areas there is overlap with a mixed *Cruziana* and *Skolithos* ichnofabric (Gingras et al., 1999; Buatois et al., 2005), which coexisted, both in the deeper open marine lower shoreface but also in shallower marginal marine settings under mixed marine and brackish water conditions (**Fig. 4.21-A**).

In contrast, as relative sea level dropped, regressive middle to lower shoreface deposits were dominant. In this context, the shoreline migrated seaward under tidal-wave influence possibly developing barrier island systems protecting extensive backshore intertidal flat areas favoured by the embayed morphology of the shoreline but also by the very low gradient (possibly much less than 1°) of the Middle Ordovician cratonic margin (**Fig. 4.21-B**). Similar processes have been presented by Desjardins et al. (2012b) for the lower Cambrian Gog Group of the Canadian Rocky Mountains where tidal flats were forced to prograde in response to falling sea level in tide-dominated settings.

In addition, a transition is again observed from a dominant *Cruziana* ichnofacies, in low energy shelfal deposits, to a predominant *Skolithos* ichnofacies, in higher energy middle to lower shoreface deposits with common *Skolithos* and *Siphonichnus* suspension-feeding trace fossils. In contrast, a lower diversity but still high bioturbation index *Cruziana* ichnofacies is present in the shallowest section of the Hawaz Formation (**Fig. 4.21-B**).

Despite the typical linkage of *Cruziana* trilobite traces with open-marine and nearshore settings, some authors have proved the presence of traces of this paleofauna as also very common in intertidal environments during the Early Paleozoic (Mángano et al., 2014). Trilobite trace fossils from tidal-flat strata, with desiccation cracks and other structures indicative of very shallow conditions (e.g., flat-topped ripples) are also known from the Lower and Middle Cambrian deposits of western and north-western Argentina (Astini et al., 2000; Mángano and Astini, 2000; Mángano and Buatois, 2003, 2004).

Another example is the Middle Cambrian Bright Angel Shale of Arizona, which has recently been re-interpreted as representing sedimentation in a marginal marine environment, most likely

an un-incised, low-relief estuary, in contrast to the previous open-marine environment interpretation (Baldwin et al., 2004).

According to Buatois et al. (2005), during the Early Paleozoic, trilobites, eurypterids, and other trilobitomorph arthropods were key characters in the process of colonization of brackish-water settings. In tide-dominated systems, where salinity stress was probably attenuated by tidal mixing, salinity-tolerant arthropods could migrate from the open sea into estuaries and bays, most likely following salt-water wedges, whereas in high- to moderate-energy sandy environments the most common ichnofacies is characterised by vertical suspension-feeding burrows, typically *Skolithos*. In particular, Ordovician assemblages present some degree of landward expansion within brackish-water ecosystems, although the intensity of bioturbation and specially ichnodiversity levels were relatively low during this phase.

On the basis of this work, the Hawaz Formation was interpreted as deposited in a tide-dominated environment on the margins of an epeiric sea characterised by very shallow water that is unlikely to have exceeded some tens of metres in depth, with the sea floor above storm wave-base at most locations. The succession evolves from a shallow open-marine setting, characterised by both storm- and tide-influenced facies, to a relatively protected subtidal to intertidal setting on an embayed shoreline.

The lower section is characterised by moderate and diverse acritarch assemblages, including a number of complex acanthomorph taxa (Miles, 2001, 2003), sphaeromorph acritarchs and rare chitinozoans and cryptospores (Abuhmida and Wellman, 2017), typical of shallow inner shelf marine environments. In marked contrast, the upper section of the Hawaz is distinguished by a low diversity assemblage of acanthomorphic and sphaeromorphic acritarchs (rare to absent), absence of chitinozoans and high recovery of leiospheres and cryptospores, a characteristic palynoflora of marginal marine settings (Miles, 2001, 2003; Abuhmida and Wellman, 2017).

Hence, the Hawaz Fm. can be summarised as a broadly shallowing-upward succession, from nearshore marine inner shelf to marginal marine tidal flat deposits (Gil-Ortiz et al., 2019, 2022). This interpretation is also supported by palynological data, which distinguish different assemblages in the lower and upper part of the succession, grading from distal to proximal from bottom to top of this lithostratigraphic unit.

Based on paleocurrent data interpreted from image logs in the study area, the depositional system appears to have shifted from proximal coastal environments in the south-southeast to

open marine settings toward the north-northwest. This trend was also in agreement with observations made by Ramos et al. (2006) in the outcrops of the Gargaf High.

The controlling factors influencing the vertical stacking of facies associations were mainly changes in relative sea level (Dalrymple, 1992; Dalrymple et al., 1992; Walker and Plint, 1992; Johnson and Baldwin, 1996), possibly also affected by local tectonic subsidence as inferred from lateral changes in both facies associations and relative thickness (**Figs. 4.9 – 4.16**), which controlled the accommodation and sediment supply in the study area.

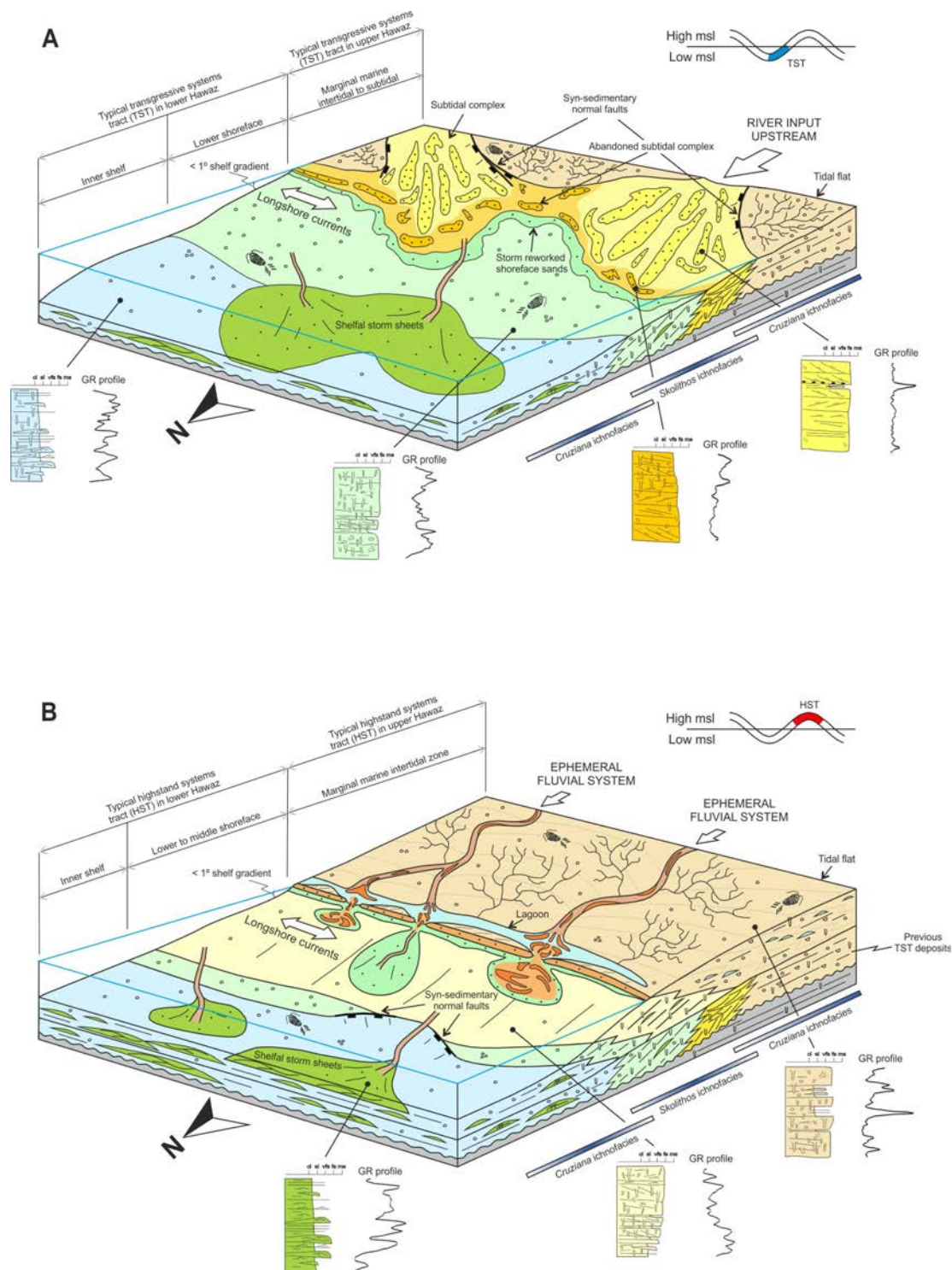


Figure 4.21. Conceptual depositional model for the Hawaz Formation in the Murzuq Basin. A) The interpretation of the depositional model corresponding to a typical early transgressive systems tract of the Hawaz Formation. B) The interpretation corresponding to a typical highstand or early regressive systems tract of this same lithostratigraphic unit. A synthetic stratigraphic column for each of the Hawaz Facies Associations, identified in the subsurface of the Murzuq Basin, together with their typical gamma ray (GR) response (left, low GR; right, high GR) and stacking pattern are also shown. Note the approximate limits and overlap of the main ichnofacies identified in this study are also included. Not to scale. Cl = clay, si = silt, vfs = very fine sandstone, fs = fine sandstone, ms = medium sandstone, msl = mean sea level.



CHAPTER 5. DISCUSSION

5.1. Factors controlling sedimentation in ancient marginal to shallow marine environments

5.2. A non-actualistic interpretation of the Hawaz Formation

*The cover photo of the Chapter 5 shows a characteristic *Skolithos* (left) and *Cruziana* (right) ichnofacies in the Middle Ordovician Hamax Formation. The pictures were taken in the outcrops of the Gargaf High (Murzuq Basin, SW Libya).*

Photographs courtesy of Emilio Ramos.

5.1. Factors controlling sedimentation in ancient marginal to shallow marine environments

The present-day geomorphology of clastic coastal depositional environments is closely linked to the relative influence of waves and tides along the shoreline (Harris and Heap, 2003) whilst their evolution is controlled by three main factors: sediment supply, physical processes (river currents, tidal currents, and waves), and relative sea-level variation (Boyd et al., 1992; Dalrymple, 1992; Dalrymple et al., 1992; Harris et al., 2002).

Ever since James Hutton's key observations in the late eighteenth century (modified by the work of John Playfair) and, critically, Lyell's (1832) development of the concept of uniformitarianism in his *Principles of Geology*, geologists have sought to explain ancient processes by reference to actualistic processes to better understand the sedimentary record.

However, Earth has changed significantly through geological history. Indeed, even from the Early Paleozoic until present day, some processes and depositional environments simply cannot be directly compared, because conditions were significantly different. As Nichols (2017) certainly points out, if choosing a "present" to be the "key of the past," probably choosing the most recent present is not the best idea.

First, the absence of vegetation in subaerial settings during the Middle Ordovician and more ancient times must have constituted a key controlling factor on depositional processes operating in marginal marine and coastal environments (Kenrick et al., 2015, 2016; Bradley et al., 2018). Land flora constitutes a fixing element within the substrate, allowing the stabilization of floodplains and the control of lateral river channel migration in modern coastal plain settings (Davies and Gibling, 2010; Davies et al., 2011; Gibling and Davies, 2012), generally lowering the energy and net sediment throughput of the environment. Whereas fluvial meandering systems can be considered a general pattern in continental to marine transitional zones for most present-day cases (with the notable exception of glacial-influenced settings or short distance to high-relief source areas), the lack of vegetation in the Middle Ordovician would have almost certainly contributed to maintaining high-energy levels in the sedimentary system as far as the coastal plain, characterised by laterally extensive mixed aeolian and braided floodplains (**Table 5.1**).

Table 5.1. Comparative table between key Actualistic (Present) and Non-actualistic (Early Paleozoic and older) main processes or controlling factors affecting the geological signature of tidal-influenced successions in the geological record.

Processes / Controlling factors	Actualistic (Present)	Non-Actualistic (Early Paleozoic and older)
Land flora	Vegetation in continental to transitional environments helps to stabilize river banks limiting channel shifting, changing river style from braided to meandering in low gradient systems.	The lack of vegetation in subaerial conditions led to the development of high energy fluvial systems (mainly braided style) characterised by rapid channel shifting of rivers even in very low gradient systems.
	Chemical weathering and related clay generation.	Lack of clay generation by induced chemical weathering due to the absence of vegetation in subaerial environments. Clay-size particles alternatively sourced from volcanic ash, hydrothermalism, diagenesis, etc.
Greenhouse / Icehouse	Incision of valleys during sea level fall in recent Icehouse periods and subsequent development of estuarine environments with marine transgressions. Fluvial sediments are common in proximal parts of the systems and related hyperpycnal deposits in more distal settings during lowstand stages.	Epeiric seas in large cratonic basins during Greenhouse periods developing areally extensive paralic environments. Very difficult to identify lowstand deposits due to very limited incision in proximal environments. Very low gradients imply major paleoshoreline shifts with only limited relative sea level rises.
Tidal range	Lower tidal range caused by tidal energy dissipation due to larger distance between the Earth and the Moon with time. Maximum known current tidal range is about 12m.	Higher tidal range due to the reduced distance between the Earth and the Moon (unknown maximum tidal range at Early Paleozoic times).
Ichnofacies	Broader and more diversified ichnofacies at present times. Characteristic <i>Skolithos</i> and <i>Cruziana</i> ichnofacies found in Hawaz Formation have different signature due to the presence of different fauna in present depositional environments.	Characteristic, often low diversity, mix of <i>Skolithos</i> and <i>Cruziana</i> ichnofacies is largely confined to the Early Paleozoic, often occurring in the form of ichnofabrics characterised by a distinctive “Pipe Rock” texture and trilobite traces.

The other remarkable aspect worthy of note is the effect of vegetation on the generation of clay minerals (**Table 5.1**). Many Precambrian to Ordovician clastic deposits are characterised by their low claystone or detrital clay content. One of the reasons for this may be the absence of vegetation and the resultant enhanced chemical weathering on land surfaces before the “greening” of the continents, from the Early Paleozoic to the end of the Devonian (Davies and Gibling, 2010; Davies et al., 2011; Gibling and Davies, 2012; Ielpi et al., 2018). The generation of clays by weathering was significantly less than at the present time, and therefore, the availability of clays in the source areas, including potentially erodible rocks, was also less for the same reason. Other mechanisms for inputting a clay fraction into the depositional environment may be associated with hydrothermal processes, diagenesis, or volcanic ash deposits.

Second, in line with Nichols (2017), the climate factor related to periods of greenhouse and icehouse is also key in understanding how coastal environments have evolved. Given that the last few million years of geological history are considered as an icehouse period, some processes related to the characteristic low relative sea levels are clearly not equivalent to those produced during greenhouse periods, such as those corresponding to much of the Cambrian–Ordovician (**Table 5.1**). The eustatic sea level, during much of the Ordovician (at least until the onset of the Hirnantian glaciation), was probably tens of metres higher than at the present time (Haq and Al-Qahtani, 2005; Videt et al., 2010; Dabard et al., 2015) due to a much warmer climate and the generalized absence of ice caps at the poles, framed in a global Greenhouse period.

In the case of the Saharan Platform, located at relatively high paleolatitudes in Gondwana during the middle Ordovician (Dapingian-Darwillian), there is no evidence for ice. Consequently, the study area represented a very extensive and low relief flooded cratonic margin (**Fig. 5.1**). Accordingly, potential for significant erosion in coastal settings, as marginal marine or paralic environments, was highly limited. Thus, confined estuary systems, produced by incision of valleys during sea-level drops, are neither expected nor indeed identified in this setting. In addition, the shape and extent of the shoreface depends on the interaction of sediment supply and wave energy expended at the coast (Walker and Plint, 1992), but in mesotidal or macrotidal settings, tidal process may mask the effects of waves (Bhattacharya, 2006).

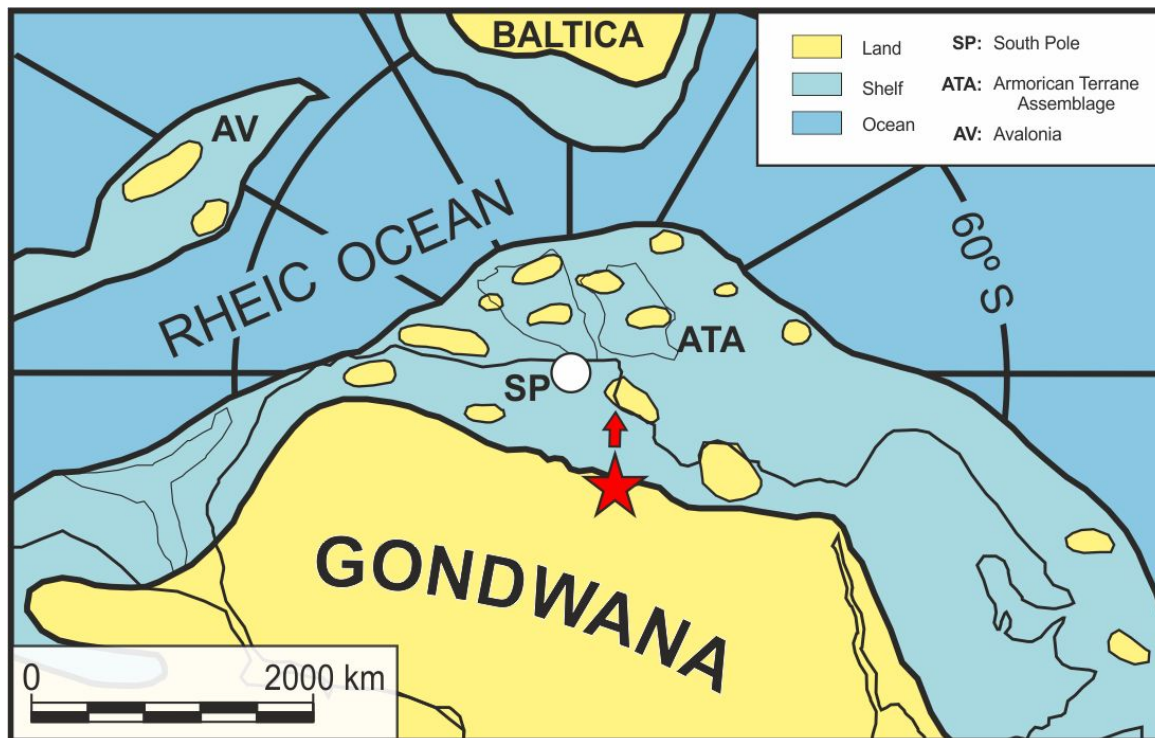


Figure 5.1. Close-up view of the paleogeographic reconstruction of the north to north-western margin of Gondwana during the Middle Ordovician (Darriwilian – 460 Ma). Note the broad cratonic margin extending across the Saharan Platform with a dominated marginal to shallow marine setting. The approximate location of the area of study and the inferred main paleocurrent direction are represented with a red star and arrow, respectively. Redrawn and modified from Cocks and Torsvick (2021).

Third, it is also relevant to our study that tidal range has not been constant throughout the whole of Earth's history. Tides are largely controlled by differential gravitational forces exerted between Earth and the Moon, but the distance between both bodies has changed through time at a currently calculated rate of 3.8 cm/yr (1.5 in./yr) (Odenwald, 2018), entailing an average Earth–Moon distance of 367,000 km as opposed to 384,000 km today. Tidal-energy dissipation over time is thus a well-established process reflected in the increasing length of the day and thus number of days per year. This appears to be a purely linear process reflecting the progressive slowing of Earth's rotation and the associated outward spiralling of the Moon. Thus, a day in the Ordovician is calculated to have been 21 hr long and the year 414 days long. For our purposes, it is also true that the potential sediment load of nearshore tidal currents together with their depositional effectiveness are related directly to the tidal range or maximum tidal height (Williams, 2000), itself, controlled by global tidal forces, water depths, and local topography. In general, therefore, we can assume notably higher tidal ranges, independent of the tidal setting (micro-, meso- or macrotidal) and more powerful tidal currents during the Middle Ordovician (Table 5.1).

Fourth, ichnofacies are commonly related to sedimentary environments and, particularly in tidal settings, specific parameters exist such as salinity, depositional energy, sediment grain size, and sedimentation rates that control fauna colonization (Gingras et al., 2012). However, some ichnological assemblages may also have a relative chronostratigraphic value when looked at on the basis of bioturbation intensity and lateral extent (**Fig. 5.2**). A couple of very good examples of this concept are the characteristic, low diversity “Pipe rock” *Skolithos* (Droser, 1991) and *Cruziana* ichnofacies (Seilacher, 1970; Mángano et al., 1996, 2014; Seilacher et al., 2002; Gibert et al., 2011) unknown from any modern analogue, and the result of an already extinct marine paleofauna (**Table 5.1**).

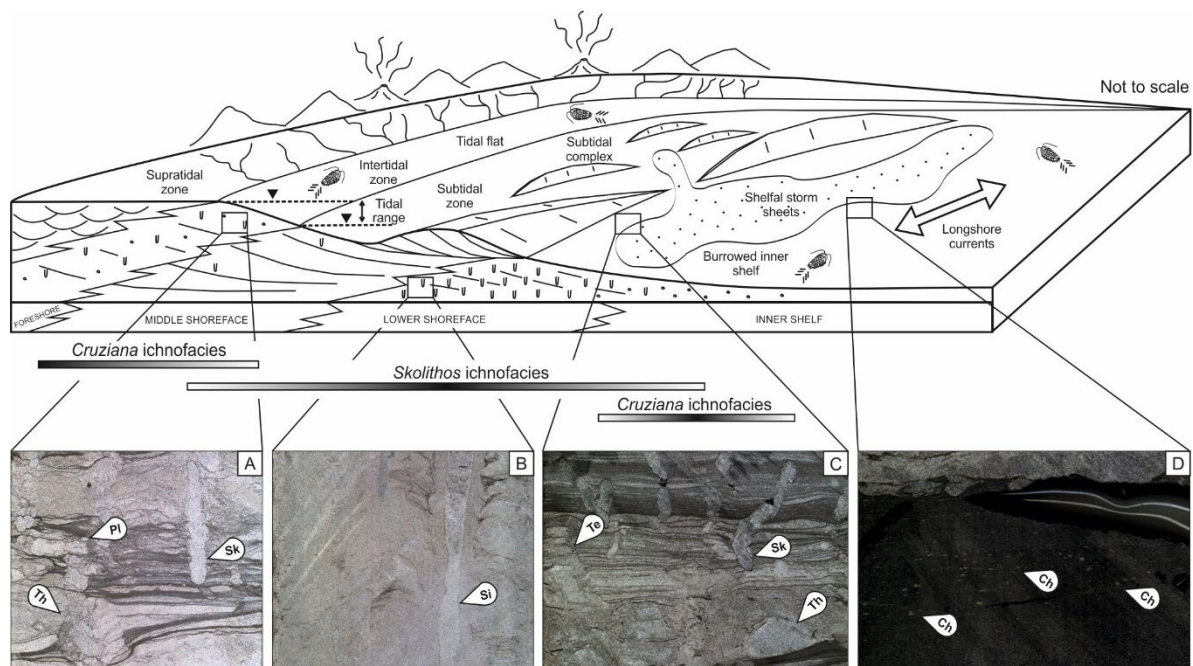


Figure 5.2. Three-dimensional conceptual sketch of a coastal, tidal-influenced environment analogue to the Hawaz Formation deposition during a highstand systems tract stage, grading from a prograding coastal plain in the most proximal part of the sedimentary system to intertidal and subtidal environments and lower shoreface to inner shelf settings. Note the clear relationship between the ichnofacies assemblage and the energy of the depositional environment. Volcanic ash deposits interpreted as a likely source for clay-fraction sediment in this environment. From left to right: (A) mixed *Cruziana* and *Skolithos* (Sk) ichnofacies assemblage with characteristic vertical suspension feeder burrows of Sk overprinting an ichnofabric comprising horizontal deposit feeders and miners such as *Thalassionides* (Th) and *Planolites* (Pl) associated with tidal flat deposits, from well W09. (B) Characteristic Sk piperock ichnofacies with typical *Siphonichnus* (Si) burrows from lower shoreface to burrowed shelfal deposits, from well W15. (C) Mixed *Cruziana* and Sk ichnofacies assemblage, from burrowed inner shelf sediments with characteristic *Teichichnus* (Te), Th, and Sk burrows, from well W15. (D) Heterolithic mudstones belonging to the most distal storm deposits with *Chondrites* (Ch) burrows characteristic of the distal *Cruziana* ichnofacies, from well W15. See the location of the corresponding wells in **Fig. 3.3**.

5.2. A non-actualistic interpretation of the Hawaz Formation

After careful study of the Hawaz Formation and the sedimentary processes involved in its deposition, several significant concepts have been developed which require further discussion in this respect (**Table 5.1**). The previously discussed controlling factors or processes affecting Middle Ordovician and older coastal dynamics can be directly applied to the case study and are discussed here.

The Hawaz Formation is a sandy detrital succession with very few true interlayered argillaceous or heterolithic intervals. From a purely lithological perspective, the facies identified were very sand-prone, with just the exception of lithofacies MSb, HS, HSb, HM and HMb (see **Chapter 4.1 - Table 4.1 and Fig. 4.1**), characterised by higher clay content, although argillaceous siltstones and sandstones are by far the most common lithologies, even within heterolithic intervals. This is indeed what can be observed in the upper part of the Hawaz Formation (Reservoir zone HWZ4 or HST-DS2; **Fig. 4.7-A**), which typically comprises a package of sand-prone tidal flat deposits (HWFA1; **Fig. 4.3**) with very few clear significant claystone intervals. These accumulated in a restricted low-energy environment where, in modern depositional systems, finer clay-rich sediments are commonly fixed by vegetation at the very top of this kind of succession. The origin and provenance of clays in the Hawaz certainly requires further research. The possibility of a clay input from a volcanoclastic origin for instance, should not be ruled out, since Ramos et al. (2006) highlight the presence of K-bentonite layers within the Hawaz Formation as observed in outcrops.

As discussed in the previous section, the Middle Ordovician was framed in a generalized Greenhouse period with much warmer climate with respect to present day, providing a globally higher eustatic sea level. Furthermore, the area of study constituted a nearshore environment on a very low gradient cratonic margin (**Fig. 5.1**). This discussion can be applied to the depositional model of the Hawaz Formation (**Fig. 4.21**). As such, classical fluvio-tidal dominated, confined estuarine environments are inherently unlikely. Hence, the presence of prominent unconformities, delimiting incised valleys, is also improbable as demonstrated by both the interpreted strike correlation panels (**Figs. 4.13 – 4.16**) and indeed across the basin and its outcropping margins. Thus, conventional lowstand systems tracts would be, in any case, extremely difficult to identify, as major erosive features related to sea-level drop would be neither produced nor preserved in this low-gradient, cratonic transitional setting. Available seismic data in the area didn't provide insight about the presence of these architectural features

such as incised valleys or clinoforms, confirming the extremely flat, low gradient bathymetric profile of the platform or epeiric sea where the Hawaz Formation was deposited.

Going further, we may also assume that, in the case of the upper Hawaz Formation (Reservoir zones HWZ4 and HWZ5; **Fig. 4.7-A**), for example, even very small variations in high water level in such a low-gradient depositional environment (**Fig. 4.21-B**) would result in a significant increase in the areal extension of marginal or paralic, tidally influenced environments (**Table 5.1**). Also, the higher tidal ranges and stronger tidal currents, characteristic of Lower Paleozoic times, may well have offered a notably more effective way of transporting sediment across this marginal and shallow marine environment. This is indeed suggested by the interpreted dip correlation panels (**Figs. 4.9 – 4.12**) and notably the Gross Depositional Environment maps (**Figs. 4.17 – 4.20**) which clearly demonstrated the existence of very wide facies belts extending for tens to hundreds of kilometres in the studied zone from the subsurface of the central Murzuq Basin to, at least, the outcropping section of the Gargaf High.

With respect to this key discussion point, the Hawaz Formation and its lateral equivalents occur over hundreds of kilometres across the Saharan Platform in both Libya, Algeria and southern Tunisia, and certainly extend across the Murzuq, Illizi and southern Berkine-Ghadames basins (Dardour et al., 2004; Jabir et al., 2021) (**Fig. 5.3**). Age-equivalent and, in some respects, broadly similar deposits, can also be identified further to the northwest into the Iberian Peninsula (**Fig. 5.3**), which as the Iberian Craton, formed part of the ancient Armorican plate (**Fig. 5.1**).

However, there are certain significant differences which must be considered when comparing this lithostratigraphic unit in the Murzuq Basin with equivalent lateral deposits in, for example, the neighbouring Illizi Basin (Middle Ordovician Unit III-3 or In Tahouite Formation). Most notably, the middle Hawaz reservoir zone HWZ3 (**Fig. 4.7-A**), mainly comprising characteristic high energy subtidal complex deposits, present in our study area, is apparently largely missing from the Illizi succession, implying non-deposition or significant condensation in laterally equivalent lower energy deposits, with the only scarce occurrence of local sandy packages known as “Grès de Castelet” or “Grès de Oued Saret” (McDougall et al., 2008a, 2008b, 2011).

From this observation, we may infer that the subtidal complex deposits of our study area, represent the distal expression of a main entry point of sediment into the basin, located further to the SE, compared to contiguous areas, such as the SE Illizi Basin. This inferred sediment entry point is characteristic of our area of study but most definitely is not unique, as similar

features can be observed in the middle Hawaz in nearby areas of Block NC115 or in outcrops of the Gargaf High (See **Chapter 2.2 - Fig. 2.4**), also possibly further to the east in the Kufrah Basin (Seilacher et al., 2002; Le Heron et al., 2010) (**Fig. 5.3**), and even further to the east into southern Jordan and Saudi Arabia, with the nearshore age-equivalent Hiswah/Dubaydib (Turner et al., 2012) and Qasim Formations (Senalp and Al-Duaiji, 2001; McDougall et al., 2008b), respectively. In this respect, active faulting may have contributed to the deposition of the Hawaz Formation, in the study area, by controlling local accommodation space, but also the location and width of the main entry points for sediment into the basin, defining a non-linear shoreline with multiple un-incised, low relief estuaries or bays during Middle Ordovician times (**Fig. 4.21-A**).

Although some faults clearly affect the overlying Upper Ordovician, it is notably more difficult to confirm whether most of the faults observed in seismic created significant offset in the displacement of syn-tectonic deposits during Hawaz deposition. It is also possible that faults only created local accommodation related to deeper basement-linked structures, during Hawaz succession sedimentation.

Finally, distinctive ichnofacies such as *Skolithos* and *Cruziana*, which are typical from Middle Ordovician and older deposits and not found in present-day nearshore successions with the same characteristics. A very good example is the lower part of the Hawaz Formation (Reservoir zone HWZ1; **Fig. 4.7-A**) and the underlying Lower Ordovician Ash Shabiyat Formation, which are characterised by their distinctive “Pipe rock” or high-density burrowed *Skolithos* ichnofabric, dominated by lithofacies Sb, MSb and Sxlb (see **Chapter 4.1 - Table 4.1 and Fig. 4.1**) in an interpreted burrowed shelfal and lower shoreface environment (HWFA5; **Fig. 4.3**). Similarly, the association of this suspension-feeding fabric, commonly overprinting a deposit feeding burrowing characterised by common trilobite traces, and thus a “true” *Cruziana* ichnofacies is distinctive (**Figs. 4.21 and 5.2**). Some, if not many or even all, of the organisms responsible for these ichnofabrics are already extinct (**Table 5.1**). Thus, the occurrence of these ichnofacies in such a very low gradient, cratonic platform is highly unlikely in the present day.

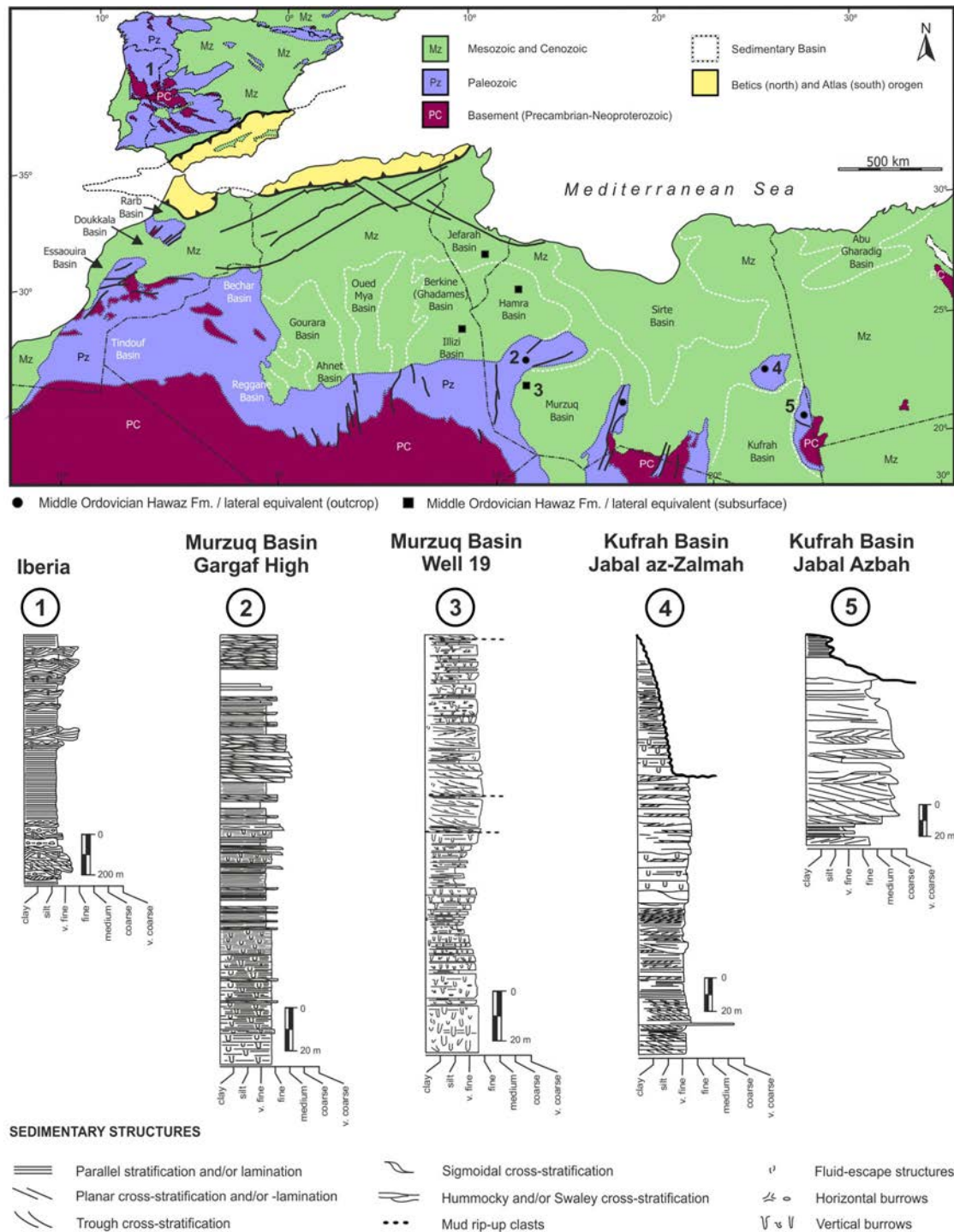


Figure 5.3. Regional map of North Africa (after Boote et al. (1998).) and Iberia showing the type section of the Hawaz Formation or lateral equivalent Middle Ordovician deposits in 5 different locations. 1) Middle Ordovician Upper Arenig to Llandeilo section mostly made of middle to lower shoreface and inner shelf deposits, with characteristic HCS and suspension feeding burrows in the outcropping section of Western Iberia (McDougall, 1988; unpublished results); 2) Hawaz type section from the outcropping succession in the Gargaf High, Murzuq Basin (modified from Ramos et al., 2006); 2) Hawaz type section from Well 19 in the subsurface of the Murzuq Basin (Gil-Ortiz et al., 2019, 2022). See **Fig. 3.3** for location of the well; 4) Hawaz type section from the outcropping succession in Jabal az-Zalmah, Kufrah Basin (modified from Le Heron et al., 2010); 5) Hawaz type section from the outcrops in Jabal Azbah, Kufrah Basin. See the fluvial influence in this last stratigraphic column, denoting a more proximal domain (modified from Le Heron et al., 2010). See the location of the type sections in the map above.

Within the context of the results of this study there are several additional points worthy of discussion. Most notably, a key limitation on the interpretation of both the correlation panels and GDE maps was the difficulty encountered in representing lateral facies variations, particularly in a down dip direction, within the framework of a single map of the study area as well as interpreting the exact location of the contacts bounding facies belts. It is suggested that, in large measure, this may be related to the very low gradient, typical of the cratonic margin across which the Hawaz was deposited, and which considerably affected the width of facies belts (very likely more than 100 km from subtidal middle shoreface to open marine shelfal settings) and enlarged the transitional zones between depositional environments.

In such circumstances, it would be appropriate to appeal to modern analogues but, as it is often the case in Lower Paleozoic and Precambrian successions, the Hawaz Formation may have very few present-day analogues. Some possibilities could be the Gulf of Carpentaria – Arafura Sea (**Fig. 5.4**), which may be a partial modern analogue (Edgar et al., 2003), or perhaps the Kara, Laptev and East Siberian Seas, or Hudson Bay, in Canada, all of which could be seen as similar to shallow marine cratonic margins or epeiric seas, broadly comparable, in some key respects, to the Middle Ordovician Hawaz Formation depositional environment.

Also significant in understanding the limitations of the conclusions drawn from the correlation panels and maps is the distance between many of the well data available in this study, which in many cases, might be several kilometres apart and thus too distant to precisely locate lateral facies changes. Accordingly, we believe that the area of study considered here, despite of covering an approximate area of 1600 km², might be too small to capture the full range of heterogeneities associated with the depositional environments of the Hawaz Formation. In this respect, we should consider the similarities and differences within the Hawaz Formation of this study area when compared with the laterally equivalent outcrop sections in the Gargaf High (**Fig. 5.5**) described by Ramos et al. (2006).

Although, the outcrops of the Gargaf High are approximately at 100–150 km distant from the current area of study and may constitute a slightly distal lateral equivalent to the section found in the subsurface, they nonetheless show similar and/or identical sedimentological and ichnological assemblages. Only in the reservoir zone HWZ4 (HST-DS2; **Fig. 4.7-A**), there are significant differences, high energy shoreface-beach barrier island and tidal inlet deposits in Gargaf outcrops, compared to more proximal, protected inter-bay tidal flat deposits further to the south. We should also consider that the present day Hawaz architecture, in the form of paleohighs often separated by large continuous paleovalleys, filled with Upper Ordovician

deposits, will inevitably introduce uncertainties into the correlations and maps. Despite these inherent difficulties it has nevertheless proved possible to demonstrate important lateral sedimentological heterogeneities within the Hawaz Formation and to infer paleogeographies across the area of study.

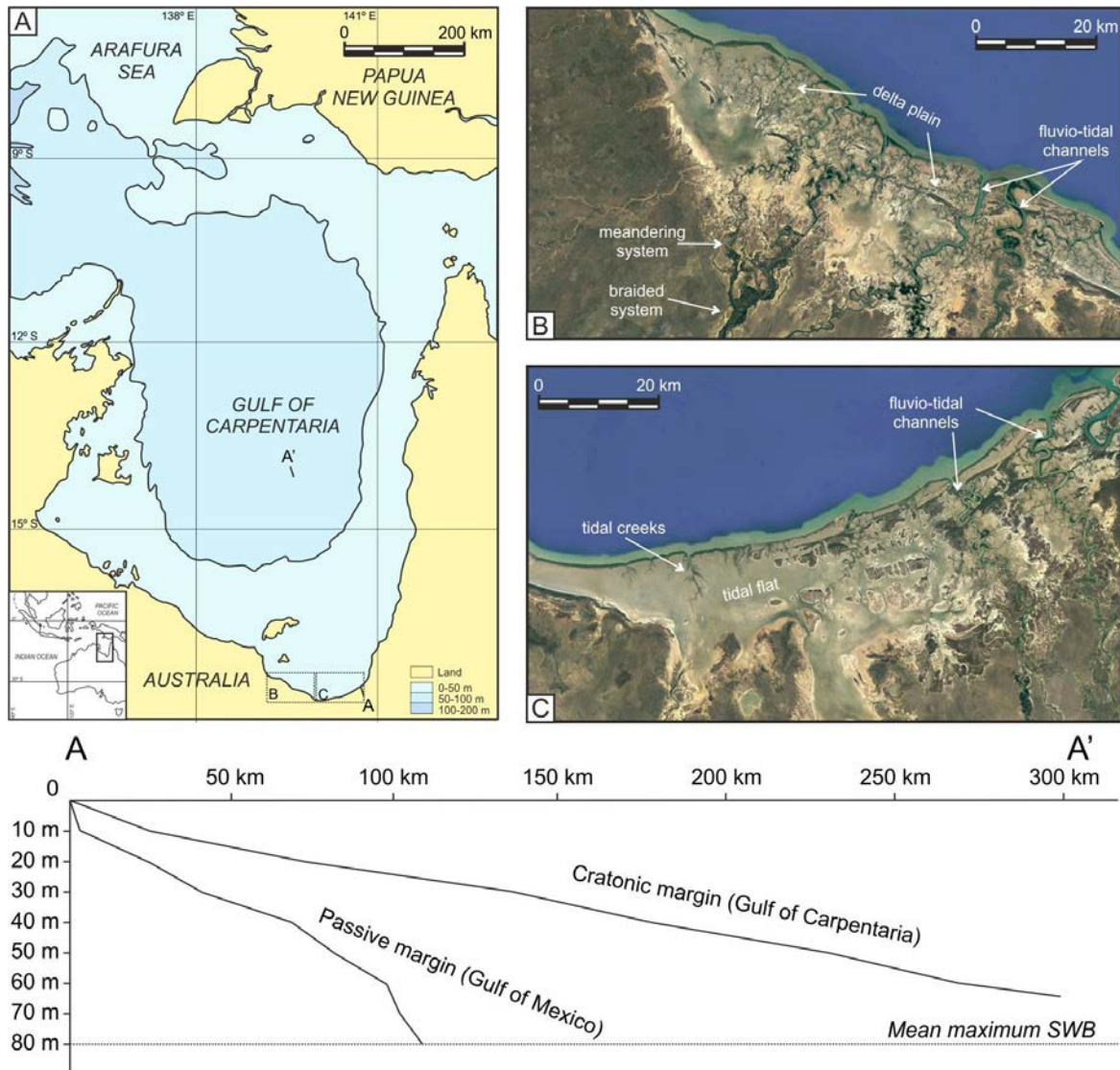


Figure 5.4. A) Map of the Gulf of Carpentaria and Arafura Sea between Australia and Papua New Guinea as a partial analogue of the Hawaz Formation depositional setting as a marginal to shallow marine cratonic margin. See also in the right part of the figure two close-up views images from Google Earth (© 2021 Google) showing along-strike variability of sub-environments; B) in the upper right image it can be seen braided rivers which rapidly evolve to meandering fluvial channels on a small delta plain, highly modelled by tides, whereas in C) tidal flat deposits domain the area, cross-cut by ephemeral tidal creeks and high sinuosity fluvio-tidal channels. Note in the lower part of the figure, a comparative scheme between the shoreface dip profile from the Gulf of Carpentaria, represented by line A-A', and the bathymetric profile off Bay City, Texas (Gulf of Mexico). The x-axis represents distance from shoreline and the y-axis, bathymetry. Note also the distance from shore at which the mean maximum Storm Wave Base (SWB) is reached in both types of basins (~80 m water depth). Location of shoreface profile A-A' and satellite close-up view images, B and C, are represented in map A (southern part of the map).

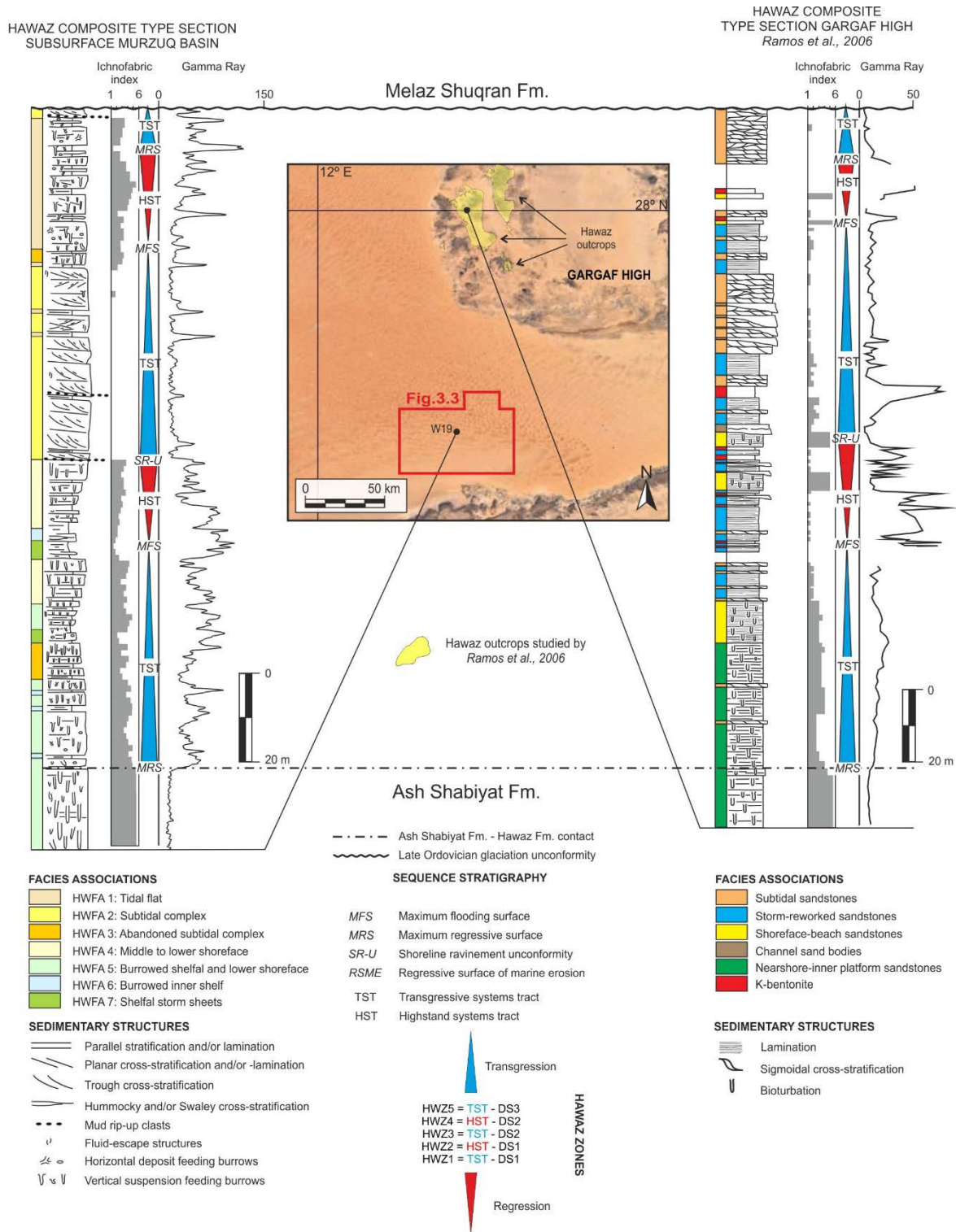


Figure 5.5. Hawaz Formation in the subsurface vs in the outcrop. Comparative summary of Hawaz type sections, in the studied area of the subsurface of the Murzuq Basin and their laterally equivalent deposits located 150 km to the N-NNE in the neighbouring Gargaf High, studied by Ramos et al. (2006). A synthetic stratigraphic column is shown both, for the subsurface as represented by well W19 (See Fig. 3.3 for location), and in outcrop, each with their corresponding facies associations. Ichnofabric index is also shown together with the corresponding gamma ray profiles. See also the sequence stratigraphic framework discussed in this paper, which is also displayed for both locations, in order to compare in terms of genetic-based sedimentary packages or Hawaz zones. DS = Depositional sequence; HST = Highstand systems tract; HWFA = Hawaz facies association; HWZ = Hawaz zone; TST = Transgressive systems tract.





CHAPTER 6. CONCLUSIONS

6.1. The sedimentology of the Hawaz Formation

6.2. The sedimentary architecture of the Hawaz Formation

6.3. General conclusions

6.4. Potential for future work

The cover photo of the Chapter 6 shows the incision of a subtidal channel on top of vertically stacked subtidal complex deposits of the Hawaz Formation. The picture was taken in the outcrops of the Gargaf High (Murzuq Basin, SW Libya).

Photograph courtesy of Emilio Ramos.

6.1. The sedimentology of the Hawaz Formation

Where encountered in the subsurface of the northern Murzuq, the Hawaz Formation is represented by a clastic succession mainly comprising fine- to locally medium-grained quartz arenites and subarkosic arenites, with subordinate sublithic arenites, up to 210 m thick. After a sedimentological and sequence stratigraphic analysis of this succession in the area of study it can be determined that:

- The Hawaz Formation can be described as a detrital succession of fifteen major lithofacies, comprising sandstones, muddy sandstones and heterolithics, based on grain size, sorting, sedimentary structures, type and degree of bioturbation and accessory elements.
- After this purely descriptive analysis, the fifteen lithofacies have been grouped into seven facies associations including: (1) tidal flat (HWFA1); (2) subtidal complex (HWFA2); (3) abandoned subtidal complex (HWFA3); (4) middle to lower shoreface (HWFA4); (5) burrowed shelfal and lower shoreface (HWFA5); (6) burrowed inner shelf (HWFA6); and (7) shelfal storm sheets (HWFA7). The interpretation of these facies associations suggest deposition of the Hawaz within the framework of an intertidal to subtidal setting.
- A clear relationship exists between facies and reservoir quality for the Hawaz Formation, the best reservoir quality sandstones being those comprising facies association HWFA2 (subtidal complex) with an average measured porosity of 11% and horizontal permeability of 125 mD associated with a general absence of thick mud drapes and interlayered claystone laminae.
- The Hawaz Formation can be divided into three main depositional sequences (DS1–DS3), each with characteristic systems tracts bounded by key surfaces: maximum regressive surface, maximum flooding surface, and unconformable shoreline ravinement surface. Based upon this systems tract architecture, a genetic zonation composed of five zones has been proposed (HWZ1 to HWZ5) in order to help to improve the management of the subsurface reserves and resources contained into the Hawaz reservoir in this highly productive basin.

6.2. The sedimentary architecture of the Hawaz Formation

The results obtained from the facies analysis of the Hawaz Formation, provided a framework for a reconstruction of the sedimentary architecture of this succession. This was based on eight high resolution correlation panels and four Gross Depositional Environment (GDE) maps, which contributed to a better understanding of the depositional model giving new insight in these yet poorly studied deposits, leading us to the following conclusions:

- It has been demonstrated that the seven facies associations (HWFA) form laterally extensive, correlatable facies belts extending for tens to hundreds of kilometres across the area of study. Their extent and distribution can be linked to the proposed genetic stratigraphic framework of three main low order depositional sequences and their respective systems tracts, which form the basis for a sequence-stratigraphic zonation supported by both petrophysical and reservoir quality properties.
- The depositional model for the Hawaz Formation was updated based on the interpretation of correlation panels and the construction of four Gross Depositional Environment (GDE) maps, showing the Hawaz to be an areally extensive and continuous reservoir across the study area, deposited in a subtidal to intertidal paralic environment, with few if any modern analogues, a reflection of the controlling factors and depositional processes associated with the northern margin of Gondwana during Early Paleozoic times. The Gulf of Carpentaria – Arafura Sea is perhaps a partial modern analogue for the Hawaz Formation despite the obvious differences with the north-western Gondwana cratonic margin during the Middle Ordovician.
- The results of this study suggest that the Hawaz Formation was deposited in a non-linear, relatively protected or embayed shoreline with multiple bays/estuaries most likely influenced by the subtle effects of pre-existing north-northwest to south-southeast Pan-African structures controlling accommodation space and reactivated during Ordovician times. These structures were probably active from the onset of Hawaz Depositional Sequence 1, most notably since the start of deposition of reservoir zone HWZ2. Faults are likely to have locally controlled the bathymetry on this very low gradient platform. Subsequently, both fault activity and intraformational paleorelief determined the deposition and lateral distribution of facies within zone HWZ3 during the transgressive stage of Depositional Sequence 2 in relatively shallower areas.
- The area of study appears to have been aligned with a preferential sediment entry point into the basin, mainly comprising subtidal complex deposits during early transgressive stages.

These developed with a SSE to NNW direction, whereas interbay sub-environments appear to be represented by extensive lower energy sand-prone tidal flats, identified in the south-western and north-eastern margins of the concession NC186. In contrast, burrowed shelf to shoreface deposits prevailed during periods of relative high sea level offshore, together with common intercalated storm deposits, whilst prograding tidal flats dominated the most proximal zones of the system, covering a significant part of the study area.

6.3. General conclusions

The previous conclusions together with the discussions presented in this thesis highlight a series of processes and factors controlling the deposition of detrital deposits, together with the fabric and geometry of reservoir units, in Lower Paleozoic, specifically Middle Ordovician, marginal to shallow marine settings. Accordingly, deposition of the Hawaz Formation in the Murzuq Basin was constrained by:

- A limited amount of clay in the environment, this resulted in a sand-prone succession. Despite deposition in a paralic environment, where some tide-dominated settings tend to deposit fine-grained sediments during slack water periods, the presence of shale intervals is relatively scarce, even in the most heterolithic units. The reason behind the lack of available clay-size material in the source area is interpreted to be associated with the absence of land flora promoting chemical weathering and, consequently, generating soils which are the main source of clays in non-marine settings. Hence, the presence of clays in erodible rocks coming from the source area was also very limited before the “greening” of the continents. Potential clay-size particles would be possibly associated with volcanic ashes from distant eruptions or diagenetic authigenic clays from older successions.
- Tide-dominated environments tend to be associated with a favourable shoreline geometry such as an incised valley, where the power of tides can prevail over waves as in open linear barred or unbarred coastlines. However, the global greenhouse climatic conditions and associated high sea levels, during the Middle Ordovician, were not favourable for the formation of major incised valleys during sea level falls. In addition, the very low gradient bathymetry and tectonic stability of the Saharan Platform diminished even more the possibility of generating major unconformities related to eustatic changes and true lowstand systems tract deposits. From both the strike-oriented correlation panels and observations made in seismic, we can conclude that the Hawaz Formation was not deposited in a conventional incised estuary but more in an un-incised, low relief set of shallow, broad

estuaries or bays. Instead of pure eustatic control, the deposition of the Hawaz was notably sensitive to minor local tectonic influence in terms of sedimentary architecture (i.e. lateral facies changes and local variations in accommodation space to sediment supply ratios) and geographical control of sediment entry points.

- Following on from the previous point and considering that the Hawaz Formation was deposited on a very low gradient cratonic margin, the higher tidal ranges calculated for Middle Ordovician times presumably had a significant impact on the lateral extension of facies belts, specially in the depositional dip direction, extending for hundreds to thousands of square kilometres, whilst maintaining the same or very similar character and internal fabric.

6.4. Potential for future work

Upon completion of this research, it would also be of significant interest to focus attention on some aspects which are recommended for a future work and deeper analysis, such as:

- Given the broad area covered by our dataset and the numerous gaps produced by cross-cutting Late Ordovician glacial paleovalleys, the interpretation of the sedimentary architecture of the Hawaz in this PhD was largely based on a series of two-dimensional correlation panels. In this respect, it is recommended to carry out a three-dimensional modelling of this succession, limited by the key sequence stratigraphic surfaces bounding reservoir Hawaz zones. This study would allow us to better determine the lateral extension of facies belts and mapping of geobodies with assigned petrophysical properties, which might considerably improve the subsurface management at production scale.
- As highlighted in the discussion, one of the key factors limiting the interpretation of some results was the extension of the area of study. It would thus be of considerable value to attempt an extrapolation of the current interpretation further to the more proximal (south) and distal (north) domains in order to generate more extensive paleogeographic reconstructions. The acquisition of outcrop data from the southwestern Ghat area, in the Tihemboka High, and some limited well data from the neighbour NC115 license would be highly valuable. In addition, an attempt to get conventional well log data from more closely spaced production wells within NC186 fields would improve several 3D key aspects of the correlation and architecture of the Hawaz Formation in the area of study.

- This thesis has carried out a qualitative identification of the key factors controlling sedimentation in ancient marginal to shallow marine deposits that should be considered in any sedimentological description and interpretation. Hence, a quantitative analysis of these factors and processes with measurable outputs is key for the understanding of significant differences in sedimentology and sedimentary architecture of Lower Paleozoic and older deposits and highly recommended in future works. Comparison of this case of study with other age-equivalent analogues in the world would be also both necessary and recommended.
- The integration of techniques such as outcrop data comparison, core description, image logs, conventional wireline logs, sequence stratigraphy and statistical facies analysis, proved to be an effective method of interpretation in this study. Application of similar workflow in other projects of similar characteristics would benefit from the experience obtained during this study, specially considering the limited information that seismic data provided us for the pre-glacial succession in our area of study.

REFERENCES

- A**bouessa, A. (2012). Diagenetic properties of Hawaz Formation, Murzuq Basin, Libya, in Salem, M. J., Elbakai, M. T. and Abutarruma, Y. (Eds.), *The geology of southern Libya: Tripoli, Libya. Earth Science Society of Libya, 1*, 47–82.
- Abouessa, A. and Morad, S. (2009). An integrated study of diagenesis and depositional facies in tidal sandstones: Hawaz Formation (Middle Ordovician), Murzuq Basin, Libya. *Journal of Petroleum Geology, 32 (1)*, 39–65. doi: 10.1111/j.1747-5457.2009.00434.x.
- Abuhmida, F. H. and Wellman, C. H. (2017). Palynology of the Middle Ordovician Hawaz Formation in the Murzuq Basin, south-west Libya. *Palynology, 41*, 31-56. doi: 10.1080/01916122.2017.1356393.
- Ambrose, W. A., Ferrer, E. R., Dutton, S. P., Wang, F. P., Padron, A., Carrasquel, W., Yeh, J. S. and Tyler, N. (1995). Production optimization of tide-dominated deltaic reservoirs of the lower Misoa Formation (lower Eocene), LL-652 Area, Lagunillas field, Lake Maracaibo, Venezuela. The University of Texas at Austin, Bureau of Economic Geology Report of Investigations, n° 226, 46 p.
- Anfray, R. and Rubino, J. -L. (2003). Shelf depositional systems of the ordovician Hawaz Formation in the central Al qarqaf high. In: Salem, M.J., Oun, K.M. and Seddiq, H.M. (Eds.), *The Geology of Northwest Libya II: Second Symposium on the Sedimentary Basin of Libya*, Tripoli, Libya, vol. 3, pp. 123–134.
- Astini, R. A., Mángano, M. G. and Thomas, W. A. (2000). El icnogénero *Cruziana* en el Cámbrico Temprano de la Precordillera Argentina: El registro más antiguo de Sudamérica. *Revista de la Asociación Geológica Argentina, 55*, 111–120.
- Aziz, A. (2000). Stratigraphy and hydrocarbon potential of the lower paleozoic succession of license NC-115, Murzuq Basin, SW Libya. In: Sola, M.A. and Worsley, D. (Eds.), *Geological Exploration in Murzuq Basin*: Amsterdam. Elsevier Science, pp. 349–368.
- B**aldwin, C.T., Strother, P.K., Beck, J.H., and Rose, E. (2004). Palaeoecology of the Bright Angel Shale in the eastern Grand Canyon, Arizona, USA, incorporating sedimentological, ichnological and palynological data. In: McIlroy, D. (Eds.), *The Application of Ichnology to Palaeoenvironmental and Stratigraphic Analysis. Geological Society of London Special Publication 228*, 213–236.
- Bataller, J. B., McDougall, N. and Moscariello, A. (2019). Ordovician glacial paleogeography: Integration of seismic spectral decomposition, well sedimentological data, and glacial modern analogs in the Murzuq Basin, Libya. *Interpretation, 7*, 383-408.

- Bataller, F. J., McDougall, N. D., Moscariello, A., Gil-Ortiz, M., and de Paula, B. C. (2021). Late Ordovician deglaciation of the Murzuq Basin (SW Libya): a core to seismic-scale characterization of the depositional environments and sedimentary architecture. *Marine and Petroleum Geology*, 134, 105335.
- Bataller, F. J., McDougall, N. D., and Moscariello, A. (2022). Reviewing the correlation potential of spectral gamma ray: A case study in Ordovician glacial environments in the Murzuq basin, SW Libya. *Journal of African Earth Sciences*, 104475.
- Belaid, A., Krooss, B.M. and Littke, R. (2010). Thermal history and source rock characterization of a Paleozoic section in the Awbari Trough, Murzuq Basin, SW Libya. *Marine and Petroleum Geology*, 27, 612-632.
- Bellini, E. and Massa, D. (1980). A stratigraphic contribution to the Paleozoic of the Southern basins of Libya. In: Salem, M.J. and Buswelly, M.T. (Eds.), *The Geology of Libya*. 2nd Symposium on the Geology of Libya. Academic Press, London, p. 84.
- Bhattacharya, J. P. (2006). Deltas. In: Posamentier, H. W. and Walker, R. G. (Eds.), *Facies Models Revisited, SEPM, Special Publication, 84*. SEPM, Tulsa, pp 237–292.
- Blanpied, C., Deynoux, M., Ghienne, J. -F., Rubino, J. -L. (2000). Late Ordovician glacially related depositional systems of the Gargaf uplift (Libya) and comparisons with correlative deposits in the Taoudeni basin (Mauritania). In: Sola, M.A. and Worsley, D. (Eds.), *Symposium on Geological Exploration in Murzuq Basin*. Elsevier, pp. 485–507.
- Boote, D.R.D., Clark-Lowes, D.D. and Traut, M.W. (1998). Paleozoic petroleum systems of north Africa. In: MacGregor, D.S., Moody, R.T.J. and Clark-Lowes, D.D. (Eds.), *Petroleum Geology of North Africa. Geological Society (London), Special Publication, 132*, 7–68.
- Boote, D.R.D., Dardour, A., Green, P.F., Smewing, J.D. and Van Hoeflaken, F. (2008). Burial and unroofing history of the base Tanezzuft 'hot' Shale source rock, Murzuq Basin, SW Libya: new AFTA constraints from basin margin outcrops (abstract). In: Salem, M.J., Elbakai, M.T. and Abutarruma, Y. (Eds.), *The Geology of Southern Libya: Fourth Sedimentary Basins of Libya Symposium*, Tripoli, Libya, November 17–20, 2012, pp. 21–36.
- Bottjer, D. J. and Droser, M. L. (1991). Ichnofabric and basin analysis. *Palaios*, 6, 199– 205.
- Boyd, R., Dalrymple, R. and Zaitlin, B. A. (1992). Classification of clastic coastal depositional environments: *Sedimentary Geology*, 80 (3–4), 139–150. doi:10.1016/0037-0738(92)90037-R.

- Bradley, G., Redfern, J., Hodgetts, D., George, A. D. and Wach, G. D. (2018). The applicability of modern tidal analogues to pre-vegetation paralic depositional models: *Sedimentology*, 65 (6), 2171–2201. doi: 10.1111/sed.12461.
- Bridges, P. H. and Leeder, M. R. (1976). Sedimentary model for intertidal mudflat channels, with examples from the Solway Firth, Scotland. *Sedimentology*, 23, 533–552.
- British Petroleum (2021). BP *Statistical Review of World Energy*, 2021, 70th edition.
- Buatois, L., Gingras, M., Maceachern, J., Mangano, M., Zonneveld, J., Pemberton, S., Netto, R. and Martin, A. (2005). Colonization of brackish-water systems through time: evidence from the trace-fossil record. *Palaios* 20, 321–347.
- Burrollet, P. F. (1960). Lexique stratigraphique international: Paris, Congress Geologique International–Commission de Stratigraphie, v. IV, fasc. IVa, p. 62.
- Carneiro de Castro, J. (1983). Facies, reservoirs and stratigraphic framework of the Mossoro Member (latest Cenomanian–earliest Turonian) in Potiguar Basin, NE Brazil: An example of a tide and wave dominated delta. In: Rhodes, E. G. and Moslow, T. F. (Eds.), *Marine clastic reservoirs: Examples and analogues*. London, Springer-Verlag, p. 161–182.
- Cattaneo, A. and Steel, R. J. (2003). Transgressive deposits: A review of their variability: *Earth-Science Reviews*, 62, 187–228.
- Clifton, H. E. (2006). A reexamination of facies models for clastic shorelines. *Facies Models Revisited. SEPM Special Publication*, 84, 293-337.
- Cohen, K. M., Finney, S. C., Gibbard, P.L. and Fan, J. -X. (2021). *The ICS International Chronostratigraphic Chart, Episodes* 36, 199-204. www.stratigraphy.org (visited: 2021/04/07).
- Collomb, G. R. (1962). Etude geologique du Jebel Fezzan et de sabordure Paleozoique. *Notes et Mémoires Compagnie Française du Pétrole*, 1, 735.
- Cocks, L. R. M. and Torsvik, T. M. (2002). Earth geography from 500 to 400 million years ago: A faunal and palaeomagnetic review. *Journal of the Geological Society (London)*, 159, 631– 644.
- Cocks, L. R. M. and Torsvik, T. M. (2021). Ordovician palaeogeography and climate change. *Gondwana Research*, 100, 53–72. <https://doi.org/10.1016/j.gr.2020.09.008>.

- Craig, J., Rizzi, C., Said, F., Thusu, B., Luning, S., Asbali, A.I., Keeley, M.L., Bell, J.F., Durham, M.J., Eales, M.H., Beswetherick, S. and Hamblett, C. (2008). Structural styles and prospectivity in the Precambrian and Paleozoic Hydrocarbon systems of North Africa. In: Salem, M.J., Oun, K.M. and Essed, A.S. (Eds.), *The Geology of East Libya 4. Earth Science Society of Libya*, Tripoli, 51–122.
- Craik, D., Quesada, S., Lemaire, R., Odriozola, A. and Bolatti, N. D. (2001). Sistema petrolero Tanezzuf-Mamuniyat. Cuenca de Murzuq, Libia. *Boletín de Informaciones Petroleras*, 68, 97–108.
- D**abard, M. P., Loi, A., Ghienne, J. -F., Pistis, M. and Vidal, M. (2015). Sea-level curve for the Middle to early Late Ordovician in the Armorican Massif (western France): Icehouse third-order glacio-eustatic cycles. *Palaeogeography, Palaeoclimatology, Palaeoecology*, 436, 96-111.
- Dalrymple, R.W. (1992). Tidal depositional systems. In: Walker, R.G. and James, N.P. (Eds.), *Facies Models: Response to Sea Level Change*. Waterloo, Canada. Geological Association of Canada, pp. 195–218.
- Dalrymple, R. W., Makino, Y. and Zaitlin, B. A. (1991). Temporal and spatial patterns of rhythmite deposition on mud flats in the macrotidal Cobequid Bay-Salmon River estuary, Bay of Fundy, Canada. Clastic tidal sedimentology. *Canadian Society of Petroleum Geology, Memoir 16*, 137–160.
- Dalrymple, R. W., Zaitlin, B. A. and Boyd, R. (1992). Estuarine facies models; conceptual basis and stratigraphic implications. *Journal of Sedimentary Research*, 62 (6), 1130–1146. doi: 10.1306/D4267A69-2B26-11D7-8648000102C1865D.
- Dalrymple, R. W. and Choi, K. (2007). Morphologic and facies trends through the fluvial–marine transition in tide-dominated depositional systems: A schematic framework for environmental and sequence-stratigraphic interpretation. *Earth-Science Reviews*, 81 (3–4), 135–174. doi: 10.1016/j.earscirev.2006.10.002.
- Dalrymple, R. W, Mackay, D. A., Ichaso, A. A. and Choi, K. (2012). Processes, Morphodynamics, and Facies of Tide-Dominated Estuaries. In: Davis, R. A., Jr. and Dalrymple, R. W. (Eds.), *Principles of Tidal Sedimentology*. Springer, Dordrecht, 79–107. doi: 10.1007/978-94-007-0123-6_5.
- Dalrymple, E. W., Kurcinka, C. E., Jablonski, B.V.J., Ichaso, A. A. and Mackay, D. A. (2015). Deciphering the relative importance of fluvial and tidal processes in the fluvial–marine transition. *Developments in sedimentology*, 68, 1-45.

- Dardour, A. M., Boote, D. R. D. and Baird, A. W. (2004). Stratigraphic controls on Paleozoic petroleum systems, Ghadames basin, Libya. *Journal of Petroleum Geology*, 27, 141-162.
- Davidson, L., Beswetherick, S., Craig, J., Eales, M., Fisher, A., Himmali, A., Jho, J., Mejrab, B. and Smart, J. (2000). The structure, stratigraphy and petroleum geology of the Murzuq Basin, Southwest Libya. In Sola, M. A. and Worsley, D. (Eds.), *Geological exploration in Murzuq Basin*. Amsterdam, Elsevier Science, Geological Conference on Exploration in the Murzuq Basin, Sabha, Libya, September 20–22, 1998, 295–320. doi: 10.1016/B978-044450611-5/50016-7.
- Davies, N. S. and Gibling, M. R. (2010). Cambrian to Devonian evolution of alluvial systems: The sedimentological impact of the earliest land plants. *Earth-Science Reviews*, 98 (3–4), 171–200. doi:10.1016/j.earscirev.2009.11.002.
- Davies, N. S., Gibling, M. R. and Rygel, M. C. (2011). Alluvial facies evolution during the Paleozoic greening of the continents: Case studies, conceptual models and modern analogues. *Sedimentology*, 58 (1), 220–258. doi: 10.1111/j.1365-3091.2010.01215.x.
- Davis (2012). Tidal signatures and their preservation potential in stratigraphic sequences. In: Davis, R. A., Jr. and Dalrymple, R. W. (Eds.), *Principles of Tidal Sedimentology*. Springer, Dordrecht, 35–55.
- Desjardins, P. R., Buatois, L. A. and Mángano, M. G. (2012a). Tidal flats and subtidal sand bodies. *Developments in sedimentology*, 64, 529-561. doi: 10.1016/B978-0-444-53813-0.00018-6.
- Desjardins, P. R., Buatois, L. A., Pratt, B. R. and Mángano, M. G. (2012b). Forced regressive tidal flats: Response to falling sea level in tide-dominated settings. *Journal of Sedimentary Research*, 82 (3), 149–162. doi: 10.2110/jsr.2012.18.
- Droser, M. L. (1991). Ichnofabric of the Paleozoic *Skolithos* ichnofacies and the nature and distribution of *Skolithos* piperock. *Palaios*, 6, 316– 325.
- Droser, M. L. and Bottjer, D. J. (1986). A semiquantitative field classification of ichnofabric. *Journal of Sedimentary Research*, 56, 558–559.
- E**chikh, K. and Sola, M. A. (2000). Geology and hydrocarbon occurrences in the Murzuq Basin, SW Libya. In Sola, M. A. and Worsley, D. (Eds.), *Geological exploration in Murzuq Basin*. Amsterdam, Elsevier Science, p. 175– 222.

- Edgar, N. T., Cecil, C. B., Mattick, R. E., Chivas, A. R., De Deckker, P. and Djajadihardjaa, Y. S. (2003). A modern analogue for tectonic, eustatic, and climatic processes in cratonic basins: Gulf of Carpentaria, Northern Australia. *Climate Controls on Stratigraphy*, 77, 193-205. doi: 10.2110/pec.03.77.0193.
- Eriksson, P. G., Condie, K. C., Tirsgaardc, H., Mueller, W. U., Altermanne, W., Miall, A. D., Aspler, L. B., Catuneanu, O. and Chiarenzell, J. R. (1998). Precambrian clastic depositional systems. *Sedimentary Geology*, 120, 5-53.
- Eriksson, K. A. and Simpson, E. (2012). Precambrian Tidal Facies. In: Davis, R.A., Jr. and Dalrymple, R.W. (Eds.), *Principles of Tidal Sedimentology*. Springer, Dordrecht, 397–419. doi: 10.1007/978-94-007-0123-6_15.
- Embry, A. (2009). *Practical sequence stratigraphy*. Calgary, Alberta, Canada, Canadian Society of Petroleum Geologists, 79 p.
- F**ello, N., Lüning, S., Storch, P. and Redfern, J. (2006). Identification of early Llandovery (Silurian) anoxic palaeodepressions at the western margin of the Murzuq Basin (southwest Libya), based on gamma-ray spectrometry in surface exposures. *GeoArabia*, 11, 101–118.
- Franco, A., Perona, R., Dwyianti, R., Yu, F., Helal, S., Suarez, J. and Ali, A. (2012). NC186 Block, Murzuq Basin: Lessons learned from exploration, in M. J. Salem, I. Y. Mriheel, and A. S. Essed. (Eds.), *The geology of southern Libya*. Tripoli, Libya, Earth Science Society of Libya, p. 37–50.
- G**hienne, J.-F., Deynoux, M., Manatschal, G. and Rubino, J. -L. (2003). Palaeovalleys and fault-controlled depocentres in the Late-Ordovician glacial record of the Murzuq Basin (central Libya). *Comptes Rendus Geoscience*, 335 (15), 1091–1100. doi: 10.1016/j.crte.2003.09.010.
- Ghienne, J. -F., Girard, F., Moreau, J., Rubino, J. -L. (2010). Late Ordovician climbing-dune cross-stratification: a signature of outburst floods in proglacial outwash environments? *Sedimentology*, 57, 1175–1198. <https://doi.org/10.1111/j.1365-3091.2009.01142.x>.
- Ghienne, J. -F., Moreau, J., Degermann, L. and Rubino, J. -L. (2012). Lower Paleozoic unconformities in an intracratonic platform setting: glacial erosion versus tectonics in the eastern Murzuq Basin (southern Libya). *International Journal of Earth Sciences*, 102, 455–482.
- Gibert, J. M. de, Ramos, E. and Marzo, M. (2011). Trace fossils and depositional environments in the Hawaz Formation, Middle Ordovician, western Libya. *Journal of African Earth Sciences*, 60 (1–2), 28–37. doi: 10.1016/j.jafrearsci.2011.01.010.

- Gibling, M. R. and Davies, N. S. (2012). Paleozoic landscapes shaped by plant evolution. *Nature Geoscience*, 5 (2), 99–105. doi: 10.1038/ngeo1376.
- Gil-Ortiz, M., McDougall, N. D., Cabello, P., Marzo, M. and Ramos, E. (2019). Sedimentology of a “nonactualistic” Middle Ordovician tidal-influenced reservoir in the Murzuq Basin (Libya). *AAPG Bulletin*, 103 (9), 2219–2246. doi: 10.1306/02151918138.
- Gil-Ortiz, M., McDougall, N. D., Cabello, P., Marzo, M. and Ramos, E. (2022). Sedimentary architecture of a Middle Ordovician embayment in the Murzuq Basin (Libya). *Marine and Petroleum Geology*, 135, 105339. <https://doi.org/10.1016/j.marpetgeo.2021.105339>.
- Gingras, M.K., Pemberton, S.G., Saunders, T. and Clifton, H.E. (1999). The ichnology of modern and Pleistocene brackish-water deposits at Willapa Bay, Washington; variability in estuarine settings. *Palaios*, 14, 352–374.
- Gingras, M. K. and MacEachern, J. A. (2012). Tidal ichnology of shallow water clastic settings. In: Davis, R. A., Jr. and Dalrymple, R. W. (Eds), *Principles of Tidal Sedimentology*. Springer, Dordrecht, 57–77. doi:10.1007/978-94-007-0123-6_4.
- Gingras, M. K., MacEachern, J. A. and Dashtgard, S. E. (2012). The potential of trace fossils as tidal indicators in bays and estuaries. *Sedimentary Geology*, 279, 97–106. doi: 10.1016/j.sedgeo.2011.05.007.
- Girard, F., Ghienne, J. -F. and Rubino, J. -L. (2012). Occurrence of hypercylindrical flows and hybrid event beds related to glacial outburst events in a Late Ordovician proglacial delta (Murzuq Basin, SW Libya). *Journal of Sedimentary Research*, 82, 688–708. doi: 10.2110/jsr.2012.61.
- Girard, F., Ghienne, J. -F., Du-Bernard, X., Rubino, J. -L. (2015). Sedimentary imprints of former ice-sheet margins: insights from an end-Ordovician archive (SW Libya). *Earth-Science Reviews*, 148, 259–289. <https://doi.org/10.1016/j.earscirev.2015.06.006>.
- Gubanov, A. P. and Mooney, W. D. (2009). New global geological maps of crustal basement age. Eos transactions, AGU, 90, Fall Meet. Suppl, (abstract) T53B-1583.
- H**all, P. B., Bjorøy, M., Ferriday, I. L. and Ismail, Y. (2012). Murzuq Basin source rocks. In Salem, M. J., Mriheel, I. Y. and Essed, A. S. (Eds.), *The geology of southern Libya*. Tripoli, Libya, *Earth Science Society of Libya*, 2, 63–84.

- Hallet, D. (2002). *Petroleum geology of Libya*. Amsterdam, Elsevier, 503 p. doi: 10.1016/B978-0-444-50525-5.X5000-8.
- Hallet, D. and Clark-Lowes, D. (2016). *Petroleum geology of Libya*. Second edition. Elsevier, 404 p.
- Haq, B. U. and Al-Qahtani, A. M. (2005). Phanerozoic cycles of sea-level change on the Arabian Platform. *GeoArabia*, 10(2), 127-160.
- Harris, P. T. and Heap, A. D. (2003). Environmental management of clastic coastal depositional environments: Inferences from an Australian geomorphic database. *Ocean and Coastal Management*, 46 (5), 457–478. doi: 10.1016/S0964-5691(03)00018-8.
- Harris, P. T., Heap, A. D., Bryce, S. M., Porter-Smith, R., Ryan, D. A. and Heggie, D. T. (2002). Classification of Australian clastic coastal depositional environments based upon a quantitative analysis of wave, tidal, and river power. *Journal of Sedimentary Research*, 72 (6), 858–870. doi: 10.1306/040902720858.
- Havlicek, V., and D. Massa (1973). Brachiopodes de l'Ordovicien Supérieur de Libye occidentale. Implications stratigraphiques regionales. *Geobios*, 6, 267– 290.
- Havord, P.J. (1993). Mereenie Field—Australia Amadeus Basin, Northern Territory. In: TR: Structural Traps. (Eds.), Foster, N.H. and Beaumont, E.A. AAPG Treatise of Petroleum Geology Atlas of Oil & Gas Fields Series; N° 8, 1–27.
- Higley, D. K. (1994). 3-D Fluid-flow model of the House Creekfield, Powder River Basin, Wyoming. *AAPG Bulletin*, 78 (13), 171.
- Ielpi, A., Fralick, P., Ventra, D., Ghinassi, M., Lebeau, L. E., Marconato, A., Meek, R., Rainbird, R. H. (2018). Fluvial floodplains prior to greening of the continents: Stratigraphic record, geodynamic setting, and modern analogues. *Sedimentary Geology*, 372, 140-172.
- James, N. P. and Dalrymple, R.W. (2010). *Facies models 4*. GEOtext 6, Geological Association of Canada. St. John's, Newfoundland, 586 p.
- Jabir, A., Cerepi, A., Loisy, C. and Rubino, J. -L. (2021). Evaluation of reservoir systems in Paleozoic sedimentary formations of Ghadames and Jefarah basins. *Journal of African Earth Sciences*, 183. doi: <https://doi.org/10.1016/j.jafrearsci.2021.104324>.

Johnson, H. D. and Baldwin, C. T. (1996). Shallow siliciclastic seas. In: Reading, H. G. (Eds.), *Sedimentary environments: Processes, facies and stratigraphy*. Oxford, Blackwell Science, p. 232–280.

Kenrick, P., Strullu-Derrien, C. and Mitchell, R. L. (2015). The origins of land plants communities (abstract). In: *The rise and fall of photosynthate: Evolution of plant/fungus interactions from paleobotanical and phylogenomic perspectives*. Botony Symposium, Edmonton, Alberta, Canada, July 28, 2015.

Kenrick, P., Strullu-Derrien, C. and Mitchell, R. L. (2016). The early fossil record of land plants and their environment (abstract). In: *Colonization of the Terrestrial Environment*. 38th New Phytologist Symposium, Bristol, United Kingdom, July 25–27, 2016.

Khoja, A., Gashgash, T., Swedan, M., Garea, B. and Ghnia, S. (2000). Paleorreliieves fósiles del Ordovícico en la Cuenca de Murzuq, Sudoeste de Libia. *Boletín de Informaciones Petroleras*, 64, 14–31.

Klein, G. D. (1970). Depositional and dispersal dynamics of tidal sand bars. *Journal of Sedimentary Petrology*, 33, 844–854.

Kuhn, T. S. and Barnes, C. R. (2005). Ordovician conodonts from the Mithaka Formation (Georgina Basin, Australia). Regional and paleobiogeographical implications. *Geologica Acta*, 3, 317– 337.

Kvale, E. P. (2003). Tides and tidal rhythmites. *Encyclopedia of Sediments and Sedimentary Rocks*. Kluwer Academic, 741-744.

Kvale, E. P. (2012). Tidal constituents of modern and ancient tidal rhythmites: criteria for recognition and analyses. In: Davis, R. A., Jr. and Dalrymple, R. W. (Eds.), *Principles of Tidal Sedimentology*. Springer, Dordrecht, 1–17.

Le Heron, D.P., Craig, J., Sutcliffe, O.E. and Whittington, R.J. (2003). Ice sheets during the Late Ordovician in Libya and their impact on the quality of a major hydrocarbon reservoir. Petroleum Group of the Geological Society of London: New Insights into Petroleum Geoscience Research through collaboration between academia and industry. 2003.

Le Heron, D.P., Sutcliffe, O., Bourgig, K., Craig, J., Visentin, C. and Whittington, R. (2004). Sedimentary architecture of Upper Ordovician tunnel valleys, Gargaf Arch, Libya: implications for the genesis of a hydrocarbon reservoir. *GeoArabia*, 9, 137–160.

- Le Heron, D. P., Craig, J., Sutcliffe, O. E. and Whittington, R. (2006). Late Ordovician glaciogenic reservoir heterogeneity: An example from the Murzuq Basin, Libya. *Marine and Petroleum Geology*, 23, 655-677.
- Le Heron, D. P., Armstrong, H. A., Wilson, C., Howard, J. P. and Gindre, L. (2010). Glaciation and deglaciation of the Libyan Desert: The Late Ordovician record. *Sedimentary Geology*, 223, 100-125.
- Lüning, S., Craig, J., Loydell, D.K., Storch, P. and Fitches, B. (2000). Lower Silurian "hot shales" in North Africa and Arabia: regional distribution and depositional model. *Earth-Science Reviews*, 49, 121-200.
- Lüning, S., Adamson, K. and Craig, J. (2003). Frasnian organic-rich shales in North Africa: regional distribution and depositional model. In: Arthur, T., MacGregor, D.S. and Cameron, N.R. (Eds.), *Petroleum Geology of Africa: New Themes and Developing Technologies*. Geological Society (London), *Special Publication*, 207, 165-184.
- Lyell, C. (1832). *Principles of geology*. London, John Murray, 2, 586 p.
- M**ángano, M. G., and Astini, R. A. (2000). El icnogénero *Cruziana* en ambientes intermareales del Cámbrico inferior, Formación Los Sombreros, Precordillera sanjuanina, Argentina. Segundo Congreso Latinoamericano de Sedimentología. Resúmenes, Mar del Plata, p. 106–107.
- Mángano, M. G. and Buatois, L. A. (2003). *Rusophycus Leiferikssoni* en la Formación Campanario: Implicancias paleobiológicas, paleoecológicas y paleoambientales. In: Buatois, L.A. and Mángano, M. G. (Eds.), *Iconología: Hacia una Convergencia Entre Geología y Biología: Publicación Especial de la Asociación Paleontológica Argentina*, 9, 65–84.
- Mángano, M. G. and Buatois, L. A. (2004). Reconstructing early Phanerozoic intertidal ecosystems: Ichnology of the Cambrian Campanario Formation in northwest Argentina. In Webby, B. D., et al. (Eds.), *Trace fossils in evolutionary palaeoecology: Fossils and Strata*, 51, 17–38.
- Mángano, M. G., Buatois, L. A. and Aceñolaza, G. F. (1996). Trace fossils and sedimentary facies from a Late Cambrian –Early Ordovician tide-dominated shelf (Santa Rosita Formation, northwest Argentina): Implications for ichnofacies models of shallow marine successions. *Ichnos*, 5, 53– 88.

- Mángano, M.G., Buatois, L. A., Astini, R. and Rindsberg, A. K. (2014). Trilobites in early Cambrian tidal flats and landward expansion of the Cambrian explosion. *Geology*, 42 (2), 143–146. doi: 10.1130/G34980.1.
- Marjanac, T. and Steel, R. J. (1997). Dunlin Group sequence stratigraphy in the northern North Sea: A model for Cook Sandstone deposition. *AAPG Bulletin*, 81 (2), 276–292.
- Martinius, A. W., Ringrose, P. S., Ness, A. and Wen, R. (2000). Multi-scale characterization and modelling of heterolithic tidal systems, offshore mid-Norway. In: Weimer, P., Slatt, R. M., Coleman, J., Rosen, N. C., Nelson, H., Bouma, A. H., Spyzen, M. J. and Lawrence, D. T. (Eds.), *Deep-water reservoirs of the world: Gulf Coast Section*. SEPM 20th Annual Bob F. Perkins Research Conference, CD publication.
- Marzo, M. and Ramos, E. (2003). Stratigraphy and sedimentology of the Hawaz Formation and its relationships with the Mamuniyat Formation. Ordovician, Gargaf Arch, Libya. Confidential Remsa report. 108 p.
- Massa, D. and Collomb, G. R. (1960). Observations nouvelles sur la region d'Aouinet Ouenine et du Djebel Fezzan (Libye). Copenhagen, 21st International Geological Congress Proceedings, 12, 65– 73.
- Matte, P. (2001). The Variscan collage and orogeny (480–290 Ma) and the tectonic definition of the Armorica microplate: A review. *Terra Nova*, 13, p. 122– 128.
- McDougall, N. and Martin, M. (2000). Facies models and sequence stratigraphy of Upper Ordovician outcrops in the Murzuq Basin, SW Libya. In: Sola, M. A. and Worsley, D. (Eds.), *Geological exploration in Murzuq Basin*. Elsevier, Amsterdam, p. 223–236, doi: 10.1016/B978-044450611-5/50012-X.
- McDougall, N. D., Figari, E. and Jauregui, J. M. (2008a). Estratigrafía secuencial y sedimentología del Cambro-Ordovícico de la Plataforma del Sahara en el Norte de Africa (abstract). Abstract volumen 12th Congress Argentine Association of Sedimentologists.
- McDougall, N. D., Gerard, J., Wloszczowski, D. and Sharky, K. (2008b). Ordovician plays on the Arabian and Saharan platforms: A comparison (poster and abstract). AAPG International Conference and Exhibition, Cape Town, South Africa October 26–29, 2008.
- McDougall, N. D., Bellik, M. and Jauregui, J. M. (2011). Sedimentology and sequence stratigraphy of the Ordovician section in the Gassi-Touil-Gassi Chergui-In Amedjane area (poster and abstract). 5th Algerian Oil and Gas Energy Week, Oran, Algeria, May 21–25, 2011.

- Meinhold, G., Howard, J. P., Strogon, D., Kaye, M. D., Abutarruma, Y., Elgadry, M., Thusu, B. and Whitham, A. G. (2013). Hydrocarbon source rock potential and elemental composition of lower Silurian subsurface shales of the eastern Murzuq Basin, southern Libya. *Marine and Petroleum Geology*, 48, 224-246.
- Miles, N. H. (2001). A Palynological Correlation of the Palaeozoic. Repsol Exploration Murzuq SA NC186, NC187 and NC190 Concessions, Libya. Robertson Research International Limited. Confidential report No. 6204/Ib.
- Miles, N. H. (2003). A Palynological Correlation of the Mesozoic and Palaeozoic. Repsol Exploration Murzuq SA NC186, NC187 and NC190 Concessions, Libya. Robertson Research International Limited. Confidential report No. 6481/Ib.
- Middleton, G. V. (1991). A short historical review of clastic tidal sedimentology. In: Smith, D. G., Reinson, G. E., Zaitlin, B. A. and Rahmani, R. A. (Eds.), *Clastic tidal sedimentology: Canadian Society of Petroleum Geologists, Memoir 16*, 4–15.
- Milliman, J. D. and Meade, R. H. (1983). World-wide delivery of river sediments to the oceans. *Journal of Geology*, 91, 1–21.
- Millson, J.A., Quin, J.G., Idiz, E., Turner, P. and Al-Harthy, A. (2008). The Khazzan gas accumulation, a giant combination trap in the Cambrian Barik Sandstone Member, Sultanate of Oman: implications for Cambrian petroleum systems and reservoirs. *AAPG Bulletin*, 92, 885–917.
- Molyneux, S.G., Le Hérisse, A. and Wicander, R. (1996). Chapter 16: Paleozoic phytoplankton. In: Jansonius, J. and McGregor, D.C. (Eds.), *Palynology: principles and applications. AASP Foundation*, 2, 493-529.
- Morad, S., Al-Ramadan, K., Ketzer, J. M. and De Ros, L. F. (2010). The impact of diagenesis on the heterogeneity of sandstone reservoirs: A review of the role of depositional facies and sequence stratigraphy. *AAPG Bulletin*, 94 (8), 1267-1309. doi: 10.1306/04211009178.
- N**ichols, G. (2017). Challenging orthodoxy: Is the present the key to the past?. *The Sedimentary Record*, 15 (3), 4–9. doi: 10.2110/sedred.2017.3.4.
- Nio, S. D., and Yang, C. (1991). Diagnostic attributes of clastic tidal deposits: a review. In: Smith, D.G., Reinson, G.E., Zaitlin, B.A., and Rahmani, R.A. (Eds.), *Clastic Tidal Sedimentology. Canadian Society of Petroleum Geologists, Memoir 16*, 3–28.

- Odenwald, S. (2018). SpaceMath@NASA, accessed April 4, 2022, [jhhttps://spacemath.gsfc.nasa.gov/](https://spacemath.gsfc.nasa.gov/).
- Paris, F. (1990). The Ordovician chitinozoan biozones of the northern Gondwana Domain. *Review of Palaeobotany and Palynology*, 66, 181-289.
- Paris, F. (1996). Chapter 17: Chitinozoan biostratigraphy and palaeoecology. In: Jansonius, J. and McGregor, D.C. (Eds.), *Palynology: principles and applications*. AASP Foundation, 2, 531-552.
- Pemberton, S. G., Spila, M., Pulham, A. J., Saunders, T., MacEachern, J. A., Robin, D. and Sinclair, I. K. (2001). Ichnology and sedimentology of shallow to marginal marine systems: St. John's, vol. 15. Geological Association of Canada, Short Course, 343 p.
- Pemberton, S. G., MacEachern, J. A., Dashtgard, S. E., Bann, K. L., Gingras, M. K. and Zonneveld, J. P. (2012). Shorefaces. *Developments in Sedimentology*, 64, 563-603.
- Petters, S. W. (1991). *Regional Geology of Africa*. Lecture Notes in Earth Sciences, 40. Springer-Verlag, Berlin. 722 p.
- Ramos, E., Marzo, M., Gibert, J. M. de, Tawengi, K. S., Khoja, A. A. and Bolatti, N. D. (2006). Stratigraphy and sedimentology of the Middle Ordovician Hawaz Formation (Murzuq Basin, Libya). *AAPG Bulletin*, 90 (9), 1309–1336. doi: 10.1306/03090605075.
- Ramos, E., Willmott, V., Cabello, P., Marzo, M., Casamor, J., Tawengi, K., Khoja, A. and Bolatti, N. (2012). A Holocene analogue for the Late Ordovician 3-D glacial topography of the Murzuq Basin. In: Salem, A. M. J., Mriheel, I.Y., Essed, A.S. (Eds.), *The Geology of Southern Libya*. Earth Science Society of Libya, 2, 261–270.
- Reineck, H. E. (1967). Layered sediments of tidal flats, beaches and shelf bottom of the North Sea. In: Lauff, G. H. (Eds.), *Estuaries*. American Association for the advancement of science, publication 83. American Association for the Advancement of Science, Washington, DC, pp 191–206.
- Reineck, H. E. and Wunderlich, F. (1968). Classification and origin of flaser and lenticular bedding. *Sedimentology*, 11, 99-104.
- Rider, M. (2004). *The geological interpretation of well logs*. Second edition (revised). Sutherland, United Kingdom, Rider-French Consulting, 280 p.

- Ron Martín, M., Buitrago, J., Erquiaga, M., Sarkawi, I. and Gonzalez Muñoz, J. M. (2016). Mature Exploration Challenges in Murzuq Basin (Libya) – Chasing Stratigraphic Traps (abstract). 78th EAGE Conference & Exhibition, Vienna, Austria, 30 May – 2 June.
- S**eilacher, A. (1970). *Cruziana* stratigraphy of non-fossiliferous Paleozoic sandstones. In: Crimes T.P. and Harper J.W. (Eds.), Trace Fossils. *Geological Journal Special Issue*, 3, 447–476.
- Seilacher, A. (2000). Ordovician and Silurian arthropycid ichnostratigraphy. In: Sola, M.A. and Worsley, D. (Eds.), *Geological Exploration in Murzuq Basin*. Elsevier Science, Amsterdam, pp. 237–258.
- Seilacher, A. (2007). *Trace Fossil Analysis*. Springer, Berlin. 226 p.
- Seilacher, A., Lüning, S., Martin, M. A., Klitzsch, E., Khoja, A. and Craig, J. (2002). Ichnostratigraphic correlation of lower Paleozoic clastics in the Kufra Basin (SE Lybia). *Lethaia*, 35, 257– 262.
- Senalp, M. and Al-Duaiji, A. A. (2001). Qasim Formation: Ordovician storm-and tide-dominated shallow-marine siliciclastic sequences, Central Saudi Arabia. *GeoArabia*, 6(2), 233-268.
- Shalbak, F. (2015). Paleozoic Petroleum Systems of the Murzuq Basin, Libya. Universitat de Barcelona, Barcelona, Spain, p. 203. PhD thesis.
- Sola, M. A. and Worsley, D. (2000). *Geological exploration in Murzuq Basin*. Amsterdam, Elsevier Science, 519 p.
- T**amar-Agha, M. Y. (2009). The influence of cementation on the reservoir quality of the Risha Sandstone Member (Upper Ordovician), Risha gasfield, NE Jordan. *Journal of Petroleum Geology*, 32, 193-208. <https://doi.org/10.1111/j.1747-5457.2009.00443.x>.
- Thomas, R. G., Smith, D. G., Wood, J. M., Visser, J., Calverley-Range, E. A. and Koster, E. H. (1987). Inclined heterolithic stratification – terminology, description, interpretation and significance. *Sedimentary Geology*, 53, 123–179.
- Turner, B. R., Armstrong, H. A., Wilson, C. R. and Makhlof, I. M. (2012). High frequency eustatic sea-level changes during the Middle to early Late Ordovician of southern Jordan: Indirect evidence for a Darriwilian Ice Age in Gondwana. *Sedimentary geology*, 251-252, 34-48.

- Tyler, N. and Finley, R. J. (1991). Architectural controls on the recovery of hydrocarbons from sandstone reservoirs. In: Miall, A.D. and Tyler, N. (Eds.), *The three-dimensional facies architecture of terrigenous clastic sediments and its implications for hydrocarbon discovery and recovery. SEPM Concept in Sedimentology and Paleontology*, 3, 1–5.
- Van Hinsbergen, D. J. J., Buitter, S. J. H., Torsvik, T. H., Gaina, C. and Webb, S. J. (2011). The Formation and Evolution of Africa: A Synopsis of 3.8 Ga of Earth History. Geological Society, London, Special Publications, 357, 1–8. <https://doi.org/10.1144/SP357.1>.
- Vecoli, M. (1999). Cambro-Ordovician palynostratigraphy (acritarchs and prasiniphytes) of the Hassi-R'Mel area and northern Rhadames Basin, North Africa. *Palaeonographia Italica*, 86, 1–112.
- Verdier, A. C., Oki, T. and Suardy, A. (1980). Geology of the Handil field (East Kalimantan—Indonesia), in M 30: Giant oil and gas fields of the decade 1968–1978. *AAPG Special Publication*, 399–421.
- Videt, B., Paris, F., Rubino, J. -L., Boumendjel, K., Dabard, M. P., Loi, A., Ghienne, J. -F. and Gorini, A. (2010). Biostratigraphical calibration of third order Ordovician sequences on the northern Gondwana platform. *Palaeogeography, Palaeoclimatology, Palaeoecology*, 296(3–4), 359–375.
- Vos, R. G. (1981). Sedimentology of an Ordovician fan delta complex, Western Libya. *Sedimentary Geology*, 29 (2–3), 153–170. doi: 10.1016/0037-0738(81)90005-1.
- Walker, R. G. and Plint, A. G. (1992). Wave- and storm dominated shallow marine systems. In: Walker, R. G. and James, N. P. (Eds.), *Facies models: Response to sea level change*. Waterloo, Ontario, Canada, Geological Association of Canada, p. 219–238.
- White, H. J., Skopec, R. A., Ramirez, F. A., Rodas, J. A. and Bonilla, G. (1995). Reservoir characterization of the Hollin and Napo formations, Western Oriente Basin, Ecuador. In: Tankard, A. J., Suarez S., R. and Welsink, H. J. (Eds.), *Petroleum basins of South America. AAPG Memoir*, 62, 573–596.
- White, C. D. and Barton, M. D. (1997). Comparison of the recovery behavior of contrasting units in the Ferron sandstone using outcrop studies and numerical simulation. The University of Texas at Austin, Bureau of Economic Geology, topical report prepared for the Gas Research Institute, GRI-97/0095.

- Williams, G. E. (1991). Upper Proterozoic tidal rhythmites, South Australia: sedimentary features, deposition, and implications for the earth's paleorotation. In Smith, D.G., Reinson, G.E., Zaitlin, B.A. and Rahmani, R.A. (Eds.), *Clastic Tidal Sedimentology*. *Canadian Society of Petroleum Geologists, Memoir, 16*, 161-177.
- Williams, G. E. (2000). Geological constraints on the Precambrian history of Earth's rotation and the Moon's orbit. *Reviews of Geophysics, 38 (1)*, 37–59. doi: 10.1029/1999RG900016.
- Wood, L. J. (2004). Predicting tidal sand reservoir architecture using data from modern and ancient depositional systems. In: *Integration of outcrop and modern analogs in reservoir modelling*. *AAPG Memoir 80*, 45– 66.

ANNEXES

Annex 1. Publications in Science Citation Index Journals

Annex 2. Abstracts presented in international congresses

Annex 3. Other publications

Annex 4. Hawaz thickness summary table

Annex 5. Well composites

Annex 1. Publications in Science Citation Index Journals

Sedimentology of a “nonactualistic” Middle Ordovician tidal-influenced reservoir in the Murzuq Basin (Libya)

**Marc Gil-Ortiz, Neil David McDougall, Patricia Cabello,
Mariano Marzo, and Emilio Ramos**

ABSTRACT

The subsurface of the highly productive Murzuq Basin in southwest Libya remains poorly understood. As a consequence, a need exists for detailed sedimentological studies of both the oil-prone Mamuniyat Formation and Hawaz Formation reservoirs in this area. Of particular interest in this case is the Middle Ordovician Hawaz Formation, interpreted as an excellent example of a “nonactualistic,” tidally influenced clastic reservoir that appears to extend hundreds of kilometers across much of the North African or Saharan craton. The Hawaz Formation comprises 15 characteristic lithofacies grouped into 7 correlatable facies associations distributed in broad and laterally extensive facies belts deposited in a shallow marine, intertidal to subtidal environment. Three main depositional sequences and their respective systems tracts have also been identified. On this basis, a genetic-based stratigraphic zonation scheme has been proposed as a tool to improve subsurface management of this reservoir unit. A nonactualistic sedimentary model is proposed in this work with new ideas presented for marginal to shallow marine depositional environments during the Middle Ordovician in the northern margin of Gondwana.

INTRODUCTION

For many years, the main Libyan petroleum province was the prolific Sirte Basin with a limited contribution from the Ghadames Basin (Berkine Basin in Algeria) (Hallet, 2002; Figure 1). However,

AUTHORS

MARC GIL-ORTIZ ~ *Repsol Exploración, Madrid, Spain; Institut de Recerca Geomodels, Universitat de Barcelona, Barcelona, Spain; marc.gil@repsol.com*

Marc Gil Ortiz is currently working as a clastic sedimentologist in the Stratigraphy and Sedimentology Team of Repsol Exploración. He is a member of the Geomodels Research Institute and researcher of the Universitat de Barcelona, where he is currently also doing his Ph.D. His research is mainly focused on clastic sedimentology, sequence stratigraphy, and the relationships between tectonics and sedimentation.

NEIL DAVID MCDUGALL ~ *Consultant, Madrid, Spain; neil85mcdougall@gmail.com*

Neil McDougall was awarded his Ph.D. in geology at the University of Liverpool in 1988. Since then, he has worked as a senior sedimentologist for Robertson Research and as a clastic sedimentologist advisor and consultant for Repsol Exploración. He has studied clastic reservoirs in various basins worldwide with a special focus on the lower Paleozoic of Libya and Algeria.

PATRICIA CABELLO ~ *Departament de Dinàmica de la Terra i de l'Oceà, Facultat de Ciències de la Terra, Universitat de Barcelona, Barcelona, Spain; Institut de Recerca Geomodels, Universitat de Barcelona, Barcelona, Spain; pcabello@ub.edu*

Patricia Cabello is a lecturer at the Universitat de Barcelona and is a member of the Geomodels Research Institute and the Research Group of Geodynamics and Basin Analysis. She received her Ph.D. from the Universitat de Barcelona in 2010. Her research is mainly focused on the characterization of reservoirs and outcrop analogs.

MARIANO MARZO ~ *Departament de Dinàmica de la Terra i de l'Oceà, Facultat de Ciències de la Terra, Universitat de Barcelona, Barcelona, Spain; Institut de Recerca Geomodels, Universitat de Barcelona, Barcelona, Spain; mariano.marzo@ub.edu*

Copyright ©2019. The American Association of Petroleum Geologists. All rights reserved.

Manuscript received June 19, 2018; Revised manuscript provisional acceptance October 10, 2018; revised manuscript received November 30, 2018; final acceptance February 15, 2019.

DOI:10.1306/02151918138

Mariano Marzo is a professor of stratigraphy at the Universitat de Barcelona. His research interest focuses on the application of clastic sedimentology, sequence stratigraphy, reservoir modeling, and basin analysis to the exploration and production of hydrocarbons. He has been involved in several research projects funded by oil companies in southern Europe, the North Sea, South America, and northern Africa.

EMILIO RAMOS ~ *Departament de Dinàmica de la Terra i de l'Oceà, Facultat de Ciències de la Terra, Universitat de Barcelona, Barcelona, Spain; Institut de Recerca Geomodels, Universitat de Barcelona, Barcelona, Spain; emilio.ramos@ub.edu*

Emilio Ramos was awarded his Ph.D. in geology at the Universitat de Barcelona in 1988. Since then, he has held a post as a lecturer in basin analysis and petroleum geology at the same university. He has worked on several research projects on sedimentology and basin analysis in Spain, North Africa, Antarctica, and South America.

ACKNOWLEDGMENTS

Special thanks are due to the Libyan National Oil Corporation, notably Bashir Garea and Khaeri Tawengi, and partners Total, Equinor, and OMV both for the technical support in this project and permission to publish the results. Special thanks are also due to Edward Jarvis of CGG Robertson for discussions concerning the key core descriptions. Thanks are also due to colleagues Manuel Ron, Javier Buitrago, Mikel Erquiaga, Lamin Amh Abushaala, and Mourad Bellik for introduction to the project and their continuous help throughout the study. Special thanks to Eduard Remacha and Francisco Pángaro for constructive discussions in the field and in the office. Support from the Ministerio de Economía y Competitividad (Project Sedimentary Sediment Routing Systems: Stratigraphic Analysis and Models CGL2014-55900-P) and Generalitat de Catalunya (2014SGR467) is gratefully acknowledged. Thanks to reviewers David Boote and Jonathan Redfern and also to the editors of the

since the mid-1990s, the Murzuq Basin has developed into a major oil- and gas-producing province. The Hawaz Formation constitutes one of the most important reservoirs in several producing fields in the central and northern part of the basin. The generally high reservoir quality (average 5%–15% porosity and 0.1–150 md permeability) and lateral continuity, characteristic of the Hawaz, are key factors in the development and production of these accumulations. However, despite the well-documented potential of the Hawaz Formation, its subsurface character remains poorly understood.

To date, only a few sedimentological studies of this formation have been carried out, and all are exclusively based on surface geology (Vos, 1981; Anfray and Rubino, 2003; M. Marzo and E. Ramos, 2003, personal communication; Ramos et al., 2006; Gibert et al., 2011). Other published works have focused on diagenesis (Abouessa and Morad, 2009; Abouessa, 2012) and trapping mechanisms (Franco et al., 2012). In addition, subsurface interpretations of the formation are based on inconsistent lithostratigraphic correlations unconstrained by a consistent sequence stratigraphic framework. As such, no genetic or sequence stratigraphy-based zonation exists. This limited database highlights the necessity of providing a sequence stratigraphic framework based on a robust sedimentological model of the transitional to shallow marine Hawaz Formation.

As Dalrymple and Choi (2007) have highlighted, transitional tide-dominated and deltaic facies reflect the interaction of numerous terrestrial and marine processes in a very complex depositional environment. Any paleoenvironmental or stratigraphic interpretation of such transition zone successions requires a comprehensive understanding of the facies and facies associations. Hence, a comprehensive understanding of the facies changes through this transition zone is necessary to make proper paleoenvironmental and sequence-stratigraphic interpretations of the sedimentary successions. However, is it actually possible to compare these paleoenvironments with any “actualistic” sedimentary model?

The limitations of the approach become apparent when the uniformitarian principle is extended to depositional environments in the most ancient geological record. In particular, the assumption that modern environments can provide analogs for all geological successions must be questioned (Nichols, 2017). It is broadly accepted that Earth's dynamics have changed considerably throughout geological history, and accordingly, factors controlling sedimentation have changed also, such as a lack of flora stabilizing river banks, greenhouse versus icehouse periods defining coastal geomorphology, tidal ranges controlling facies belts or characteristic ichnofacies during a particular period of geological time. The analysis of some of these factors suggests that the facies succession of the Hawaz Formation

reflects different depositional processes from those observed in modern environments. From this point forward, we will use the term “nonactualistic” to describe those processes affecting the geological signature of the Hawaz Formation that are difficult to compare with any modern depositional environment analog.

Consequently, the main aim of this paper is to present a sedimentological characterization of the Hawaz Formation based on a detailed lithofacies description and interpretation together with the development of a facies association classification. This forms the basis for an appropriate depositional model in accordance with plausible physical and chemical processes during the Middle Ordovician. In addition, the overall analysis aims to build a genetically based zonation through sequence stratigraphy that will improve reservoir management and provide tools for maximizing hydrocarbon recovery efficiency. Finally, it is intended that these sedimentological and stratigraphic models should be a well-documented subsurface analog for clastic reservoirs in similar settings.

GEOLOGICAL SETTING

The Structure and Stratigraphy of the Murzuq Basin

The Paleozoic succession of the Murzuq Basin is an erosional remnant of a much more extensive regional succession extending along the northern margin of the Gondwana supercontinent (Davidson et al., 2000; Shalbak, 2015). Its present extent reflects several periods of uplift and unroofing during the late Paleozoic, Mesozoic, and Cenozoic, which, together, are responsible for its modern architecture. As a consequence, the present-day basin geometry bears little relation to the broader and larger preexisting sedimentary basin. The current basin is composed of a central Cretaceous depression bounded to the northwest by the Atshan arch, the Gargaf high to the north, and the Tibesti and Tihemboka highs on the southeast and southwest, respectively (Figure 1). These structural highs were formed by multiphase tectonic uplifts from the middle Paleozoic to Cenozoic, although the main periods of uplift and erosion occurred during the Pennsylvanian (late Carboniferous; Hercynian) and early Cenozoic (Alpine) orogenic cycles.

A series of geological events can be recognized in the stratigraphic record of the Murzuq Basin, some represented by basin-scale unconformities within the sedimentary infill reflecting the Pan-African, Caledonian, and Hercynian orogenesis and the short Late Ordovician glacial event responsible for the Taconic or basal glacial erosional surface (Figure 2). Other unconformities

AAPG Bulletin for their constructive comments that have improved the content of this paper.

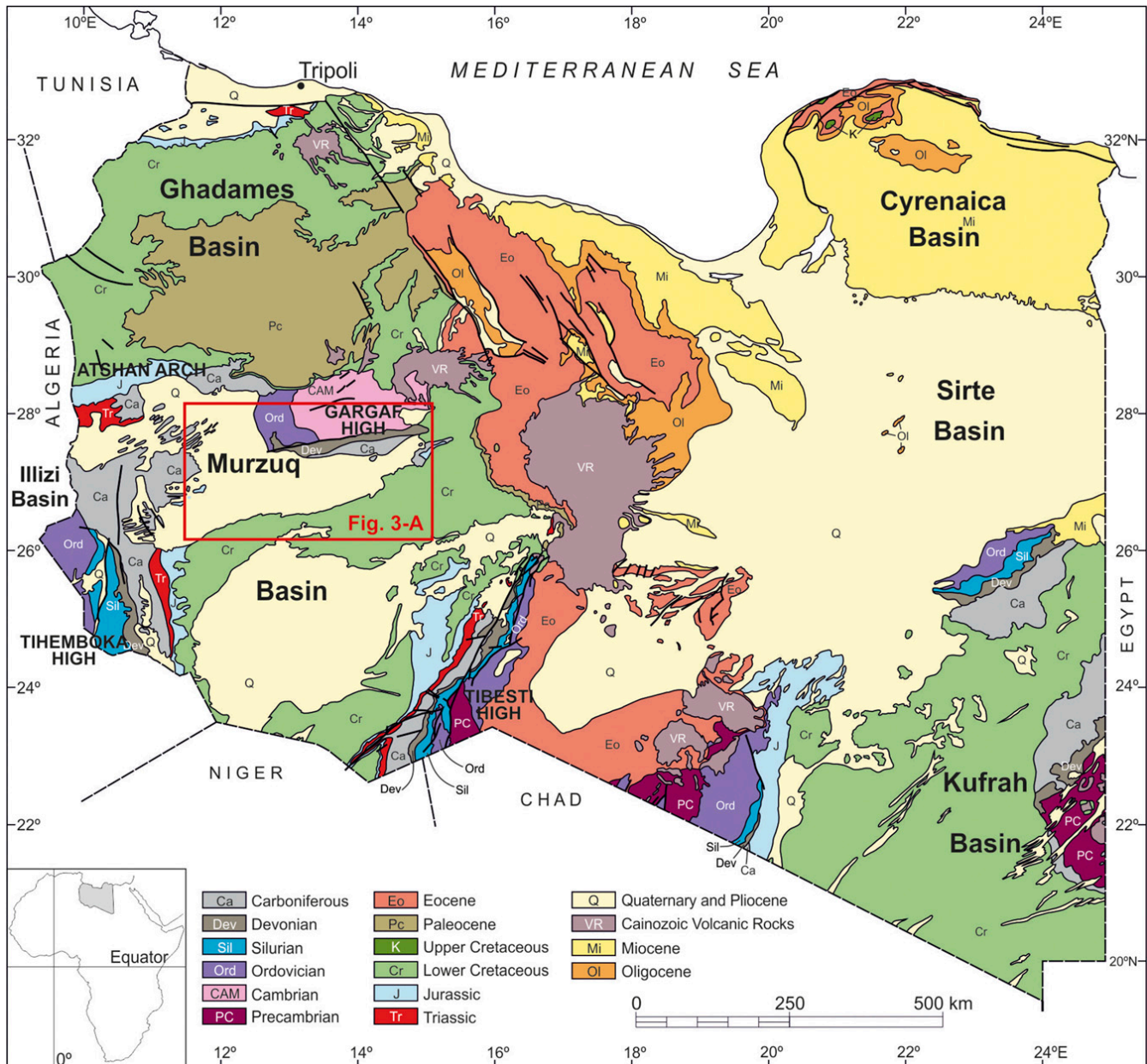


Figure 1. Geological map of Libya showing the main sedimentary basins. The Murzuq Basin is bounded by the Atshan arch to the northwest, the Gargaf high to the north, the Tiheimboka high to the southwest and the Tibesti high to the southeast. The area of interest represented in Figure 3A is highlighted in the red box. Modified from M. Marzo and E. Ramos (2003, personal communication).

that may be recognized within the sedimentary record are minor or belong to the younger Austrian or Alpine cycles, and consequently, they do not strongly affect the Paleozoic section directly in the central Murzuq Basin; although, they may have had strong implications in terms of overburden removal, source rock maturity, and reservoir quality because of uplift and unroofing of Mesozoic series on the Paleozoic section (Boote et al., 2008).

The maximum sedimentary thickness in the present-day Murzuq Basin is approximately 4000 m (~13,000 ft). Despite successive erosive episodes during several phases of uplift throughout the history of the basin, the maximum sedimentary thickness most probably never exceeded 5000 m (16,400 ft) (Davidson et al., 2000). The age of the infill ranges from Cambrian to Cretaceous, commonly covered by large Quaternary sand dunes in the central part of the basin. The sedimentary infill can be subdivided

into four main units: (1) Cambrian–Ordovician, (2) Silurian, (3) Devonian–Carboniferous, and (4) Mesozoic (Figure 2).

The lower Paleozoic succession comprises the terrigenous Cambrian–Ordovician Gargaf Group consisting of at least five formations; from bottom to top, they are the following: Hasawnah, Ash Shabiyat, Hawaz, Melaz Shuqran, and Mamuniyat Formations (Figure 2). The lowermost Hasawnah Formation rests unconformably on the Precambrian basement and is composed of Cambrian to Lower Ordovician conglomeratic to sandy continental and shallow marine littoral deposits. The Hasawnah Formation is overlain, above a transgressive surface of erosion, by the shallow marine and preglacial Ash Shabiyat and Hawaz Formations, attributed respectively to the Lower and Middle Ordovician (Tremadocian–Sandbian). The Upper Ordovician

succession, associated with a major glaciation, principally comprises the Melaz Shuqran and Mamuniyat Formations, locally overlain by a thin and somewhat enigmatic package known as the Bir Tlacin. The former is most probably lower Hirnantian and predominantly mud-prone, representing the period of the highest relative sea level during the Late Ordovician (McDougall and Martin, 2000), whereas the Mamuniyat Formation is a major Hirnantian sand-prone package.

The Petroleum Systems and the Hydrocarbon Production History of the Murzuq Basin

Early exploration in the Murzuq Basin focused upon surface structures. The first exploratory well

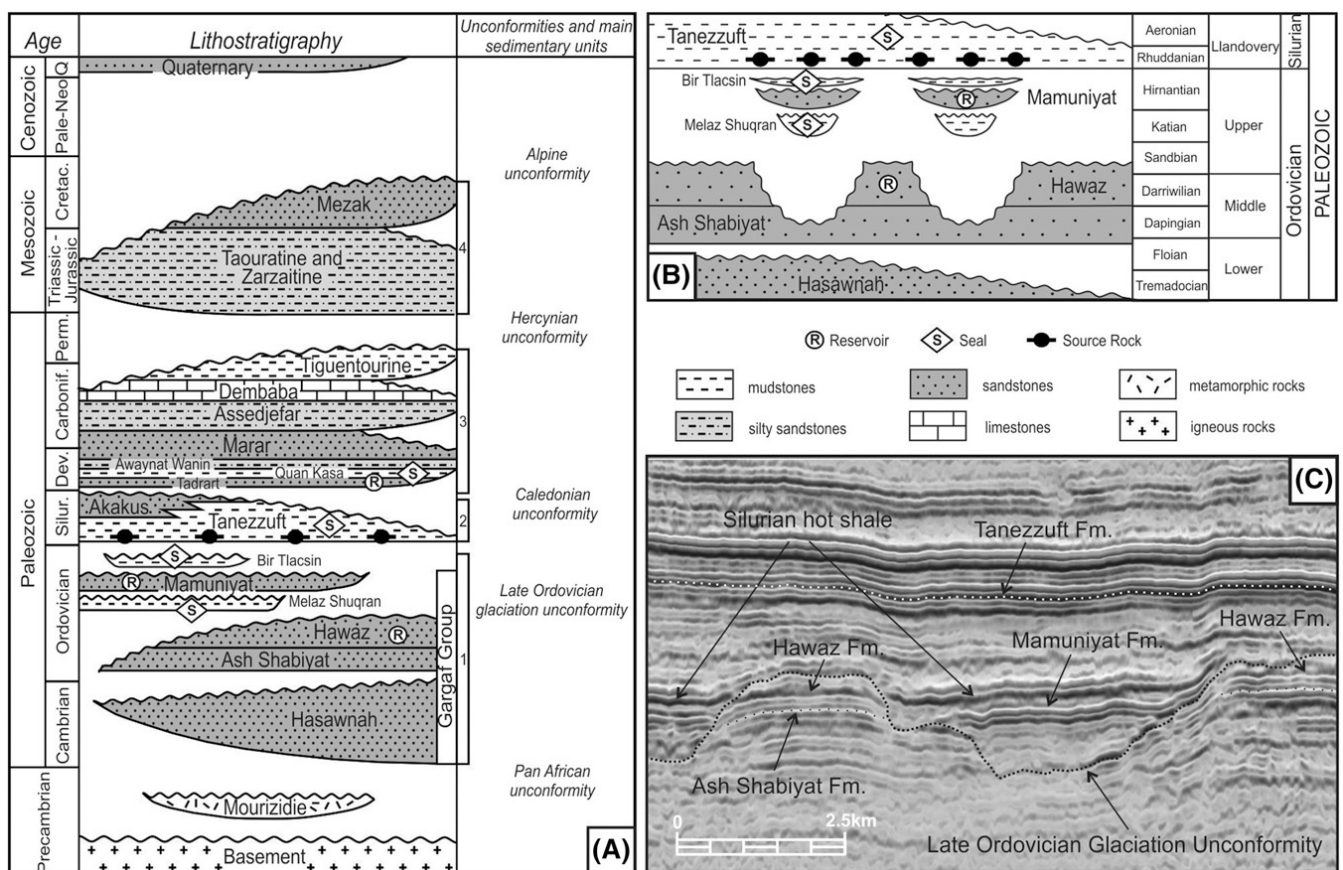


Figure 2. (A) Stratigraphic chart summarizing the stratigraphic column for the Murzuq Basin highlighting the main stratigraphic units and major basin-scale unconformities. 1 = Cambrian–Ordovician; 2 = Silurian (Silur.); 3 = Devonian (Dev.)–Carboniferous (Carbonif.); 4 = Mesozoic. (B) Wheeler diagram showing lithostratigraphic to chronostratigraphic relationships of the Ordovician and Lower Silurian succession in the area of study. (C) Seismic line showing the typical geomorphological signature of the Ordovician succession in form of paleo-highs (“buried hills”) and paleovalleys. The main petroleum systems elements are also represented in Figure 2A, B. Cretac. = Cretaceous; Dev. = Devonian; Fm. = Formation; Pale-Neo = Paleogene–Neogene; Perm. = Permian; Q = Quaternary.

was drilled in the northern Murzuq in 1955–1956. Subsequently, several successful discoveries in the neighboring Illizi Basin (southeastern Algeria) encouraged further exploration across the border. Three years later, Exxon discovered gas at the Atshan region and Gulf tested oil at low rates from Ordovician sandstones. However, in 1958, industry attention shifted east with the discovery of a major oil accumulation in the Sirte Rift province, and there was little further exploration of the Murzuq Basin for the next 20 yr. During the late 1980s to 1990s, Rompetrol, and later Repsol, drilled up to 57 exploratory wells in the basin, all of which targeted Ordovician prospects. This exploratory activity resulted in many significant oil discoveries, highlighting the rapidly growing potential of the basin.

The most recent hydrocarbons-in-place estimation for the Murzuq Basin is approximately 6 billion bbl ($\sim 9.5 \times 10^8 \text{ m}^3$) of oil and approximately 35 tcf (~ 1 trillion m^3) of gas, which represent approximately 6.5% of Libya's resources and 30% of Libya's current oil production (Shalbak, 2015).

The main petroleum system in the Murzuq Basin comprises a basal Silurian (Tanezzuft) hot-shale source rock, Ordovician sandstone reservoirs, and a thick Tanezzuft shale seal (Figure 2). A secondary petroleum system in the basin (noncommercial to date) is composed of the basal Devonian sandstones as reservoirs and the intra-Devonian shales as the seal (Hallet, 2002; Shalbak, 2015), which also involves the basal Silurian hot-shale source rock (Fello et al., 2006; Hall et al., 2012).

The Ordovician sandstone reservoirs, associated with the primary petroleum system, are the Middle Ordovician Hawaz Formation and the Upper Ordovician Mamuniyat Formation, separated by a deeply incised unconformity related to the Late Ordovician glaciation. This succession was cut by north-northwest- to west-flowing Hirnantian glaciers (Ghienne et al., 2003; Le Heron et al., 2004), eroding down into the Hawaz Formation to create a rugged landscape of paleovalleys and highs ("buried hills"). The valleys were partially infilled by the periglacial to subglacial Melaz Shuqran, Mamuniyat and Bir Tlacin clastics, and the residual topography subsequently buried by Tanezzuft shales. This sometimes sealed the Hawaz erosional highs to form paleotopographic traps with now reservoir-significant volume of hydrocarbons (Figure 2).

The Hawaz Formation

In the subsurface of the northern Murzuq Basin, the Hawaz Formation is represented by a detrital succession slightly more than 200 m (>650 ft) thick, composed of fine-grained quartz arenites and subarkosic arenites with subordinate sublithic arenites similar to the equivalent succession exposed on the Gargaf high (Ramos et al., 2006).

Trace fossils are frequent and locally abundant enough to overprint most primary sedimentary structures (Ramos et al., 2006). Gibert et al. (2011) identify 11 ichnogenera that exhibit a close relationship with both lithofacies and depositional paleoenvironments (facies associations). In broad terms, nearshore to shoreface facies are dominated by dense "pipe rock" fabric formed by *Skolithos* and *Siphonichnus*. In contrast, storm-dominated heterolithic facies are characterized by horizontal deposit-feeding *Cruziana* bioturbation.

Two main paleocurrent trends have been identified by Ramos et al. (2006): (1) small-scale sedimentary structures including ripples and small sigmoidal cross-bedded sets, indicative of widely dispersed flow directions; and (2) large-scale sedimentary structures suggesting a dominant flow toward the northeast and northwest but locally with bidirectional currents.

Several sedimentary models have been proposed for the Hawaz Formation, but all within transitional to shallow marine setting. Vos (1981) suggested the outcrop succession represented a fan-delta complex. Other authors (i.e., Anfray and Rubino, 2003; Ramos et al., 2006) identified sedimentary structures indicative of strong tidal influence, and the latter proposed a tide-dominated model with deposition in a megaestuary or gulf where the morphology of the paleocoastline enhanced tidal action, especially during transgressive episodes, when the coastal embayment was flooded.

Measured porosity can reach up to 25.7%, although values approximately 15% to 16% are the most frequent. Pore connectivity is good, with pore-throat diameters ranging from 0.1 to 64 μm (average 14.6 μm). Measured horizontal permeability values from core plugs may reach 900–1000 md (Shalbak, 2015), although most commonly average values in wells are approximately 0.2–150 md. However, diagenetic alterations have also had an

impact on reservoir quality, as noted by Abouessa and Morad (2009). Specifically, the presence of higher amounts of feldspar, illite, a higher dickite to kaolinite ratio, and more abundant quartz cement, compared with those sampled in outcrops, is possibly because of the longer residence time under deep burial conditions.

DATABASE AND METHODOLOGY

The present study was based on data from 36 wells located across the northcentral sector of the Murzuq Basin (Figure 3). These data included core descriptions, high-resolution image logs (formation microimager [FMI]), gamma-ray (GR), sonic, neutron porosity, and density wire-line logs. The methodology that followed consisted of the following.

1. Well data synthesis and standardization from the 36 wells by means of building well composite charts with the wire-line logs available for each well.
2. Description and interpretation of the sedimentary facies based on 14 cored wells and FMI data. Conventional wire-line logs were not used to define lithofacies at this stage because the typical

thickness of most lithofacies units is below the vertical resolution of these tools. The resultant facies analysis was compared with previous outcrop descriptions from the northern Gargaf high by M. Marzo and E. Ramos (2003, personal communication), Ramos et al. (2006), and Gibert et al. (2011), and was used as an analog for subsurface correlations.

3. Grouping the resultant lithofacies into facies associations, defined by cores and FMI logs, each with distinct wire-line log profiles and stacking patterns. These log profiles were then used to identify facies associations in wells lacking core or FMI data.
4. Construction of a comprehensive depositional model defined by the lithofacies and facies associations identified in cores, FMI logs, and conventional wire-line log profiles.
5. Sequence stratigraphic analysis of the Hawaz Formation. Vertical changes in facies associations and their stacking patterns were used to identify correlatable stratigraphic genetic units. These units were then preliminary traced throughout the study area and used to define the sedimentary architecture of the Hawaz succession (M. Gil-Ortiz et al., personal communication).

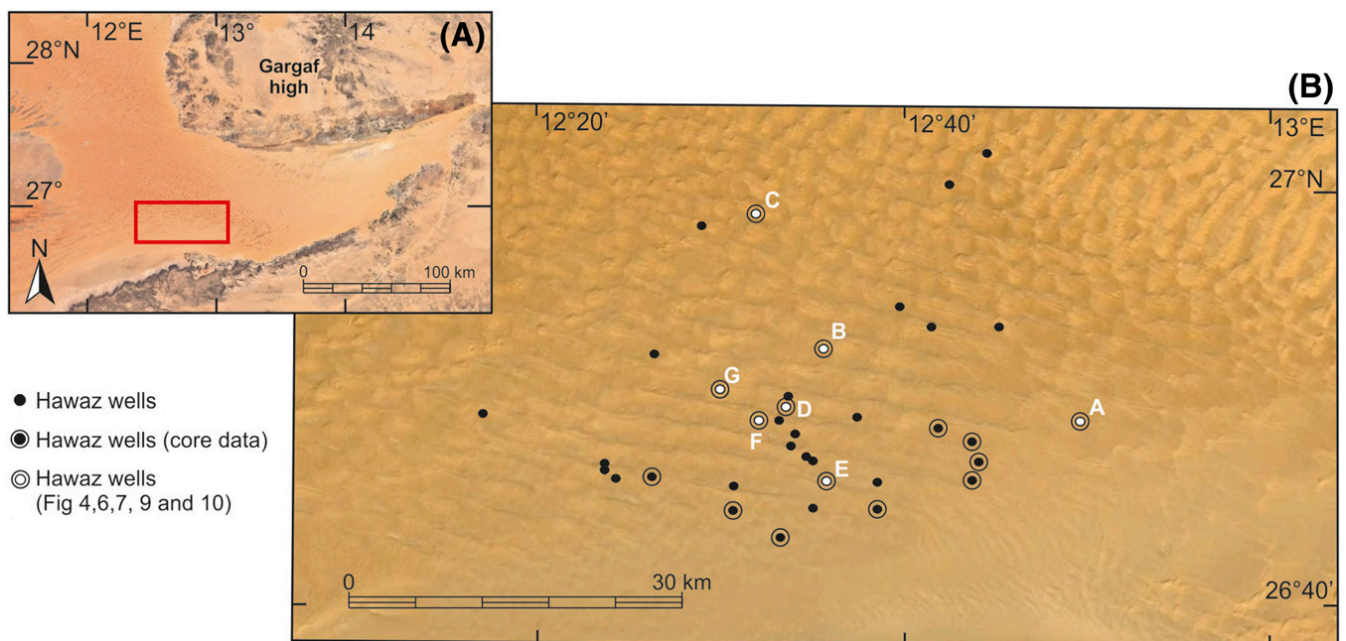


Figure 3. (A) Satellite image of the northern Murzuq Basin highlighting the study area (red box). (B) Study area showing the position of the wells. Find highlighted the wells with core data available and, in white, the wells from Figures 4, 6, 7, 9, and 10. Note the distance between the studied area in the subsurface and the western Gargaf high where the outcrops studied by Ramos et al. (2006), referred to in this paper, are located.

SEDIMENTOLOGY OF THE HAWAZ FORMATION

Lithofacies

Fifteen Hawaz lithofacies were defined in the sub-surface of the central Murzuq Basin based upon their lithology and internal fabric, including sedimentary structures and bioturbation (Table 1). These include sandstones (S), muddy sandstones (MS), heterolithic sandstones (HS), and heterolithic mudstones (HM). These lithofacies have been compared with those outcropping in the Gargaf high, as described by M. Marzo and E. Ramos (2003, personal communication) and Ramos et al. (2006), and complemented with valuable ichnofacies observations from outcrops described by Gibert et al. (2011). Each of the lithofacies is described and interpreted as follows.

Large-Scale Cross-Bedded Sandstones

Lithofacies Sx1 are fine-grained, well-sorted, and cross-bedded sandstones with high-angle foresets ($>15^\circ$) (Figure 4) characterized by a north-northwest-directed paleoflow derived from image log dip picking. Locally, mud drapes, and rare mudstone intraclasts line set bases and foresets. No evidence of bioturbation exists. Typically, these sandstones form sets more than 50 cm (>20 in.) thick and cosets up to 10 m (33 ft) thick. The cross-bedding is interpreted as a response to the migration of dune bedforms under conditions of net sedimentation. The mud-draped foresets reflect alternating periods of slack water in a tidal regime. The lack of detrital clays and bioturbation suggests moderate- to high-energy conditions, under which the fines were carried off in suspension. Equivalent lithofacies have been described by Ramos et al. (2006) in outcrops as large-scale, sigmoidal cross-bedded sandstones with occasional horizontal trace fossils (*Cruziana* ichnofacies).

Small- to Medium-Scale Cross-Bedded Sandstones

Lithofacies Sx2 are fine- to medium-grained, well-sorted, and cross-bedded sandstones characterized by low-angle (5° – 15°) foresets (Figure 4) again characterized by a north-northwest-directed paleoflow as suggested by image log interpretation.

Table 1. Lithofacies Scheme for the Hawaz Formation

Lithology	Lithofacies
Sandstones	
Nonburrowed	Sx1: large-scale cross-bedded sandstones Sx2: small- to medium-scale cross-bedded sandstones Sl: parallel-laminated sandstones Sxl: cross-laminated sandstones Sr: ripple cross-laminated sandstones Sv: massive sandstones
Burrowed	Sxb: burrowed cross-bedded sandstones Sxlb: burrowed cross-laminated sandstones Srb: burrowed ripple cross-laminated sandstones Sb: burrowed sandstones with <i>Siphonichnus</i> MSb: burrowed sandstones with feeding ichnofauna
Sandy heterolithic	HS: sandy heterolithic HSb: burrowed sandy heterolithic
Muddy heterolithic	HM: muddy heterolithic HMb: burrowed muddy heterolithic

Planar lamination, current ripple cross-lamination, mud drapes, and mudstone intraclasts also occur locally. The degree of bioturbation ranges from absent to weak with rare *Planolites*. It forms sets up to 50 cm (20 in.) thick. The cross stratification and cross-lamination record the migration of medium-scale dunes and ripples and megaripples, respectively, under the influence of unidirectional current flow. This lithofacies could also be interpreted as corresponding to toesets of the previously described large-scale cross-bedded sandstones (i.e., lithofacies Sx1). Most probably, deposition occurred within a high-energy, tidally influenced environment. Equivalent lithofacies have been described by Ramos et al. (2006) outcropping as medium-scale, sigmoidal cross-bedded sandstones with occasional horizontal trace fossils (*Cruziana* ichnofacies).

Parallel-Laminated Sandstones

Lithofacies Sl are fine-grained sandstones with parallel lamination ($<5^\circ$) (Figure 4). Bioturbation was not recognized (Figure 4). The lithofacies is organized in sets 10–100 cm (4–39 in.) thick. It is interpreted to record sand deposition from nearshore

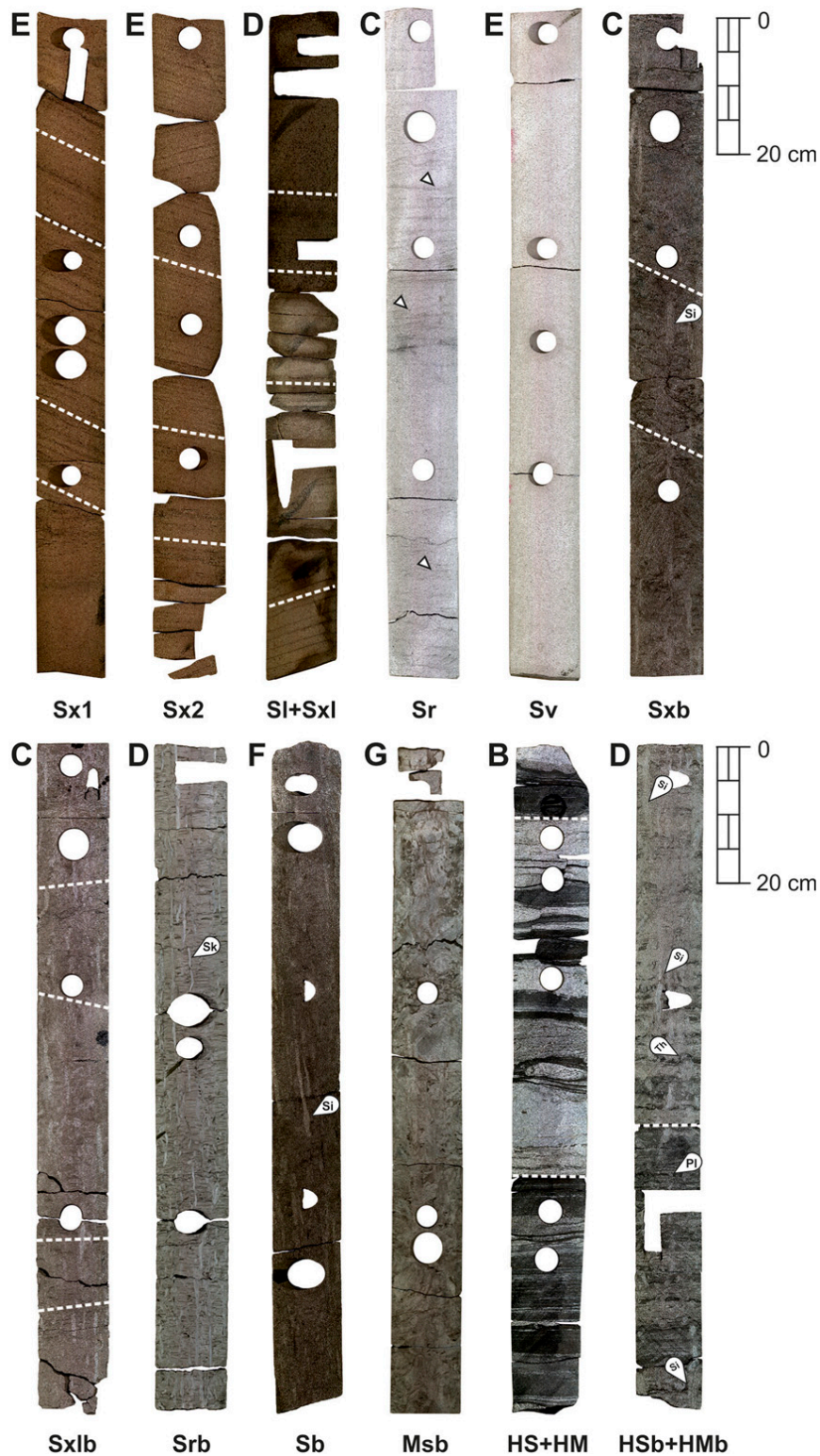


Figure 4. Core sections (~90-cm [~35-in.] length) of the main lithofacies identified in this study. See the location of the corresponding wells (B–G) in Figure 3B. HM = muddy heterolithic; HMB = burrowed muddy heterolithic; HS = sandy heterolithic; HSb = burrowed sandy heterolithic; MSb = burrowed sandstone with feeding ichnofauna; Pl = *Planolites*; Sb = burrowed sandstone with *Siphonichnus*; Si = *Siphonichnus*; Sk = *Skolithos*; Sl = parallel-laminated sandstone; Sr = ripple cross-laminated sandstone; Srb = burrowed ripple cross-laminated sandstone; Sv = massive sandstone; Sx1 = large-scale cross-bedded sandstone; Sx2 = small- to medium-scale cross-bedded sandstone; Sxb = burrowed cross-bedded sandstone; Sxl = cross-laminated sandstone; Sxlb = burrowed cross-laminated sandstone; Th = *Thalassionides*.

currents under a moderate- to high-energy, upper-flow regime. A similar lithofacies has been described by Ramos et al. (2006) in outcrops as parallel-laminated sandstones with occasional parting lineation and very scarce bioturbation.

Cross-Laminated Sandstones

Lithofacies Sx1 are fine-grained sandstones with low-angle cross-lamination (Figure 4). Climbing ripple lamination and mud drapes are also occasionally present. In general, it is a nonbioturbated lithofacies, although sparse *Skolithos* were occasionally observed. The set thicknesses range from 10 to 140 cm (4 to 55 in.). This lithofacies is interpreted as the deposits of storm events in a nearshore environment. When climbing ripples are present, a high rate of sedimentation under unidirectional flows is inferred. Similar lithofacies are described by Ramos et al. (2006) outcropping in the Gargaf high as low-angle, swaley to hummocky cross-stratified sandstones.

Ripple Cross-Laminated Sandstones

Lithofacies Sr are fine-grained, very well-sorted sandstones with ripple cross-lamination and locally intraclasts. Locally, the current ripples display bimodal foreset directions. Bedset or coset thickness does not exceed 50 cm (20 in.), whereas individual sets are up to 3 cm (1 in.) thick, typically associated with very thin clay drapes (Figure 4). This is an unbioturbated lithofacies. The cross-lamination records the migration of current ripples under low to moderate velocity currents. The presence of clay drapes and the bimodal foreset directions, observed in some sets, would suggest deposition in a subtidal setting. Equivalent ripple cross-laminated sandstones with occasional horizontal trace fossils (*Cruziana* ichnofacies) have also been identified in outcrop by Ramos et al. (2006) characterized by a dominantly north-northwest paleoflow direction, locally bimodal toward south-southeast.

Massive Sandstones

Lithofacies Sv are fine-grained, clean, generally well-sorted sandstones with poorly defined planar lamination and cross-bedding (Figure 4). Locally, mud intraclasts and basal erosive surfaces were identified. This lithofacies is characterized by the absence

of bioturbation. It is organized, forming sets of 30–100 cm (10–39 in.) thick. The massive appearance of this facies could be interpreted as the result of early postdepositional processes involving dewatering and partial fluidization suggestive of a high sedimentation rate in the depositional system. This lithofacies can be easily misinterpreted as Sx1 in cores when the clean nature of the sandstones, reflecting the lack of micaceous and fine-grained sedimentary layers obscures the limits between cross-bed sets. The lack of detrital clays and micaceous in these sandstones suggests deposition in a relatively high-energy environment where fines were carried off in suspension. Equivalent lithofacies have been observed by Ramos et al. (2006) outcropping in the northern margin of the basin as apparently massive sandstones.

Burrowed Cross-Bedded Sandstones

Lithofacies Sxb are clean, fine-grained sandstones displaying small- to medium-scale cross-bedding with local mudstone intraclasts. Moderate degree of bioturbation with *Skolithos* and *Siphonichnus* burrows (Figure 4). It is typically organized in 30- to 200-cm (10- to 79-in.)-thick beds. The clean nature of the sandstones and the presence of mudstone intraclasts suggest moderate- to high-energy conditions in which fines were carried off in suspension. The cross-bedding records the migration of dune and bar bedforms, whereas the vertical to oblique burrows suggest a shallow, high-energy marine environment.

Burrowed Cross-Laminated Sandstones

Lithofacies Sxlb are fine-grained, variably argillaceous, and micaceous sandstones with low-angle cross-lamination and local mud laminae and mudstone intraclasts. This lithofacies is moderately bioturbated with an ichnofabric dominated by *Skolithos* and *Siphonichnus*, indeterminate burrows and meniscate-backfilled burrows (Figure 4). The minimum thickness observed of this lithofacies is 70 cm (28 in.). The moderately intense bioturbation, dominated by mainly vertical, suspension-feeding burrows suggests a shallow, high-energy subtidal environment. However, the mud laminae also reflect low-energy conditions. Thus, depending on the context, this lithofacies may have different

interpretations ranging from a lower shoreface to an intertidal environment. The low-angle cross-lamination is interpreted as reflecting deposition from subtidal sand sheets or low relief sand bars.

Burrowed Ripple Cross-Laminated Sandstones

Lithofacies Srb are very fine- to fine-grained sandstones, locally argillaceous, and micaceous characterized by current ripple cross-lamination and planar lamination. A moderate degree of bioturbation characterizes this lithofacies (Figure 4), with an ichnofabric dominated by *Skolithos* (6–8-mm [0.24–0.31-in.] diameter and maximum length of 30 cm [12 in.]), *Siphonichnus*, and local indeterminate burrows. This lithofacies forms packages 15–170 cm (6–67 in.) thick. The fine grain size and the locally argillaceous composition of this lithofacies imply deposition in a relatively low-energy environment. The cross-lamination records the migration of current ripples under conditions of net sedimentation and implies that the sand was transported by a unidirectional current of low to moderate velocity. The ichnofauna (mostly represented by vertical burrows) suggests a shallow marine environment dominated by suspension-feeding benthonic fauna.

Burrowed Sandstones with *Siphonichnus*

Lithofacies Sb are fine-grained, well-sorted sandstones locally with mud laminae. This lithofacies is highly bioturbated, with an ichnofauna dominated by *Siphonichnus* burrows, locally up to 100 cm (39 in.) in length, giving rise to a distinctive pipe rock fabric. The minimum bed thickness appears to be approximately 20 cm (~8 in.), although bed boundaries are typically obscured by bioturbation (Figure 4). This lithofacies is volumetrically very abundant, and continuous sections of up to 20 m (66 ft) have been identified in some wells. The occurrence of vertical burrows (*Skolithos* ichnofacies) suggests a moderate- to low-energy restricted to shallow marine environment, and the presence of mud laminae (mud drapes) implies fluctuating energy levels. Equivalent lithofacies have been described by Ramos et al. (2006) in outcrops as thick-bedded, massive, bioturbated sandstones.

Burrowed Sandstones with Feeding Ichnofauna

Lithofacies MSb are argillaceous fine-grained sandstones characterized by moderately intense bioturbation dominated by horizontal, deposit-feeding burrows (Figure 4), notably *Teichichnus* and *Thalassinoides*. Individual beds range in thickness from 10 to 270 cm (4 to 106 in.). The moderately high detrital clay content of these sandstones and the characteristic low-energy ichnofauna suggests a relatively protected depositional setting or open-marine conditions.

Sandy Heterolithic

Lithofacies HS are interbedded very fine- to fine-grained sandstones and argillaceous siltstones (>50% sand content). This lithofacies displays flaser structures together with combined current and wave ripple cross-lamination and also planar lamination (Figure 4). Only a limited amount of bioturbation with rare *Chondrites* and *Planolites* burrows exists. The thickness of this lithofacies ranges between 1 cm (0.4 in.) sets up to an accumulated bedset thickness of 5 m (16 ft). The interbedding of sandstone and argillaceous siltstone implies fluctuating energy levels. Sands were transported and deposited by both unidirectional and oscillatory (wave-generated) flows. Unidirectional current flow was mostly of low to moderate velocity, resulting in the formation of current ripples. By contrast, the presence of cross-bedding (because of the migration of dune and bar bedforms) and mudstone intraclasts indicates higher current velocities. The presence of *Chondrites* indicates that burrowing took place under marine conditions; the remaining burrows, *Planolites* and indeterminate horizontal tubes, also suggest a marine environment. The low bioturbation index together with the local occurrence of *Chondrites* (generally considered to be characteristic of low oxygen conditions), suggests that oxygenation levels were low. Wave, current, and combined flow cross-lamination suggests sands were deposited during storm events below fair-weather wave base (FWWB).

Burrowed Sandy Heterolithic

Lithofacies HSb are thinly interbedded, very fine-grained, micaceous, argillaceous sandstone and micaceous, argillaceous siltstone (>50% sand content).

Locally, the argillaceous siltstones display planar lamination and the sandstones' current and wave ripple cross-lamination. Bioturbation is moderately intense characterized by overprinted *Skolithos* and *Cruziana* ichnofacies (*Siphonichnus* burrows, with subordinate *Planolites* and indeterminate burrows) (Figure 4). Minimum bed thickness is 1 cm (0.4 in.), whereas accumulated bedset thickness can reach 4 m (13 ft). The interbedding of sandstone and siltstone suggests fluctuating energy conditions, with the sandstones representing higher energy levels. The cross-lamination within the sandstones records the migration of combined current and wave ripples under conditions of net sedimentation and low to moderate current velocities. The mixed assemblage of ichnofauna suggests the transition from a high-energy to a low-energy setting, from an open-marine inner shelf up to a lower shoreface setting. A variation of this lithofacies in the upper part of the Hawaz Formation exists, in which the base of the sandy intervals locally displays rip-up mudstone clasts and a rhythmic alternation of thin, inclined mud drapes and sandstones. In this case, the interpretation given to this lithofacies corresponds to inclined heterolithic stratification (IHS) associated with minor channels or tidal creeks in a restricted, sandy to mixed intertidal subenvironment.

Muddy Heterolithics

Lithofacies HM are mudstones interbedded with micaceous argillaceous siltstone and very fine-grained sandstone (>50% clay content). The mudstone and argillaceous siltstone display planar lamination and lenticular bedding (current and wave-rippled sand lenses). The sandstone contains current ripples and rare wave ripples (Figure 4). Individual lithofacies packages have a minimum thickness of 5 cm (2 in.) but may reach an accumulated bedset thickness up to 3.5 m (11.5 ft). The sandstone beds and lenses represent energetic pulses in an overall low-energy setting where mud settled out of suspension. During the higher-energy pulses, sand was moved by both unidirectional and oscillatory (wave-generated) flows. The lack of burrows indicates anoxic conditions in a fairly distal marine setting or a restricted and stressed subenvironment, such as a tidal mudflat or lagoon.

Burrowed Muddy Heterolithics

Lithofacies HMB are argillaceous siltstone interbedded with minor fine-grained sandstone layers and sandstone laminae (>50% clay content). It is characterized by a variable degree of bioturbation with *Siphonichnus*, *Skolithos*, *Planolites*, and indeterminate vertical burrows (Figure 4). Shrinkage cracks may occur locally. The minimum thickness of individual facies units is 7 cm (3 in.), whereas the accumulated bedset thickness is up to 3.8 m (12.5 ft). The interbedding of argillaceous siltstone and very fine- to fine-grained sandstone suggests fluctuating energy conditions in an overall low-energy setting. The shrinkage cracks are probably related to variations in salinity and temperature when present. The depositional setting of this lithofacies ranges from a relatively distal, inner shelf subenvironment to a restricted intertidal flat subenvironment.

Facies Associations

The proposed scheme based on the previously described lithofacies establishes seven facies associations designated as Hawaz facies association 1 (HWFA1) to HWFA7 assigned to proximal and increasingly distal environments (Figure 5).

Hawaz Facies Association 1: Tidal Flat

Facies association HWFA1 mainly consists of lithofacies Sxlb, MSb, Sb, HMB, and HSb with subordinate Srb and Sv (Figure 5). The thickness of individual packages of this facies association is very variable, ranging from 30 to 60 m (100 to 200 ft) as a direct consequence of the downcutting associated with the Upper Ordovician glaciogenic unconformities. The GR log response ranges significantly from 30 to 140 API units in a characteristic fining-upward succession. The intensity of bioturbation is moderate to very high, characterized by a mixed low diversity *Skolithos* and *Cruziana* ichnofacies assemblage indicative of a relatively high-energy environment grading toward a more protected and restricted low-energy setting. It is also characterized by an upward-increasing detrital clay content typical of tidal flat environments. Furthermore, the low diversity of acritarch assemblages and the strong predominance of leiospheres, characteristic of a marginal marine setting, identified in palynological studies of

some wells, suggests a relatively protected tidal sand to mixed flat environment grading normally from the underlying HWFA3 or HWFA2 (see below). Some ichnogenera identified as *Planolites*, *Siphonichnus*, and *Thalassinoides* strongly associated with tidal flat deposits (Gingras et al., 2012) also support this hypothesis together with the common occurrence of clay drapes and flaser lenticular bedding (Figure 6A). The sporadic occurrences of individual massive to rippled sandstone levels (Sv and Srb) and the presence of rip-up mudstone clasts at the base of these units in the heterolithic intervals (locally associated with small syndimentary faults) are interpreted in terms of bank collapse in tidal creeks on the sand flat. The same package in the Gargaf high was described as an upper shoreface wave dominated facies assemblage by Ramos et al. (2006), which probably would represent a beach to barrier island setting laterally equivalent to this facies association HWFA1.

Hawaz Facies Association 2: Subtidal Complex

Facies association HWFA2 is mainly composed of lithofacies Sx2, Sx1, Sxl, Sr, Sl, and Sv with subordinate HM (Figure 5). It is organized into stacked packages 0.3–40 m (1–131 ft) thick. The basal contact of these packages is typically erosive, locally marked by the presence of mud clasts (Figure 6B), and the GR response is both clean and blocky (GR values ~25 API units) locally marked by peaks (up to 65 API units) related to the presence of thin mud drapes or concentrations of mica. These values are within the established range for micaceous sandstones, which could have values of up to 80 API units (Rider, 2004). Bioturbation is scarce to absent, probably related to a very high sediment supply in a relatively short period of time. Paleocurrents, measured in this facies association from image log data, indicate a dominant trend toward the north-northwest with some bidirectionality, probably related to tidal effects as indicated by the mud drapes in lithofacies Sx1, Sx2, and Sr (Figure 6C). However, an additional secondary trend has also been identified, indicating flow toward the northeast. The reservoir quality of this facies association is the best of the entire Hawaz Formation, with an average porosity of 11% and an average horizontal permeability of 125 md.

Facies association HWFA2 is interpreted as an amalgamated complex of sand bars and dunes (slightly coarsening-upward profile with Sx1, Sx2, and Sr lithofacies) and channel deposits (slightly fining-upward profile with Sv, Sl, and Sr lithofacies) influenced by the action of the tides. The interpretation is a laterally extensive fluviotidal to subtidal complex. Subordinate heterolithic intervals are also found intercalated with the cross-stratified sand bars, possibly related to periods of slack water and deposition in relatively protected lagoonal or interbar subenvironments. The features of this facies association are very similar to those described by Ramos et al. (2006) from the Gargaf high 100 km (62 mi) to the north. They are almost equivalent in depositional environment; although in the subsurface of the northern Murzuq Basin, HWFA2 would represent a shallower lateral equivalent with higher fluvial influence because of the general absence of bioturbation reflecting higher energy and sedimentation rates.

Hawaz Facies Association 3: Abandoned Subtidal Complex

Facies association HWFA3 is primarily characterized by lithofacies Sxlb, Sxb, Srb, Sxl, Sv, and Sx2 (Figure 5). It forms packages ranging in thickness from 0.6 to 12 m (2 to 40 ft). Facies packages are distinguished by a fining-upward succession of fine-grained sandstones represented by a distinctive upward increase in the GR characterized by API values between 25 and 70. Bioturbation is moderate, typically becoming more abundant toward the upper part of these successions with common *Skolithos* and *Siphonichnus* burrows.

This facies association is interpreted to represent the abandonment of the associated subtidal complex (HWFA2) after a general rise in relative sea level and a cessation or major decrease in sediment supply, promoting colonization in a subtidal setting. It is quite common to find this facies association gradationally intercalated with the subtidal complex, reflecting a transgressive trend in a relatively protected environment.

Hawaz Facies Association 4: Middle to Lower Shoreface

Facies association HWFA4 is mainly composed of lithofacies Sr, Srb, Sxlb, Sxb, Sv, and HSb (Figure 5).

Depositional setting	Facies association	Description (Typical section with lithofacies & thickness ranges)	Interpretation	CCA average Ø / K Gamma Ray	Systems Tracts in Figure 8
FORESHORE Intertidal zone	HWFA1 Tidal flat		Tidal sand to mixed flat deposited during high relative sea levels in an embayed tidal-influenced setting	13% / 30.4md 30 - 140 API	HST (Figure 8-C)
	HWFA2 Subtidal complex		Amalgamated complex of sand bars, dunes and channel deposits deposited in a fluvio-tidal to subtidal setting	11% / 125md 25 - 65 API	Early and late TST (Figure 8-A & B)
MIDDLE SHOREFACE Subtidal zone	HWFA3 Abandoned subtidal complex		Distal equivalent of the subtidal complex product of the abandonment of previously active subtidal channels	14% / 152md 25 - 70 API	Early and late TST (Figure 8-A & B)
	HWFA4 Middle to lower shoreface		Prograding middle to lower shoreface related to regressive sand belts during highstand sea level conditions	14% / 56md 30 - 80 API	HST (Figure 8-C)
LOWER SHOREFACE below MFWB	HWFA5 Burrowed shelfal and lower shoreface		Deposition in a relatively protected to more open lower shoreface to inner shelf setting	14% / 3.5md 30 - 80 API	Early TST, late TST and HST (Figure 8-A, B & C)
	HWFA6 Burrowed inner shelf		Deposition in an open-marine inner shelf setting	9% / 0.2md 60 - 120 API	Late TST and HST (Figure 8-B & C)
INNER SHELF above MSWB	HWFA7 Shelfal storm sheets		Distal mixed sand to mud rich deposits product of waning storm events in an open-marine shelf setting	5% / 0.2md 80 - 160 API	Early TST, late TST and HST (Figure 8-A, B & C)

Parallel stratification/lamination
 Through cross-stratification
 Mud rip-up clasts
 Current ripples
 Horizontal deposit feeding burrows
 Planar cross-stratification/lamination
 Hummocky/Swaley cross-stratification
 Fluid scape structures
 Combined current and wave ripples
 Vertical suspension feeding burrows

The thickness of individual packages ranges between 0.6 and 14 m (2 and 46 ft). The GR response is typically a serrate, coarsening-upward succession with values ranging between 30 and 80 API units (Figure 9). Bioturbation ranges from scarce to moderate. Overall packages of this facies association form clear, coarsening-upward successions with a characteristic *Skolithos* ichnofacies related to regressive sand belts prograding during highstand sea-level conditions (Gibert et al., 2011). On this basis, the interpretation proposed is of a low- to moderate-energy, middle to lower shoreface setting prograding in a relatively high-energy subtidal environment.

Hawaz Facies Association 5: Burrowed Shelfal and Lower Shoreface

Facies association HWFA5 mainly consists of lithofacies Sb, MSb, and Sxlb (Figure 5). Thickness of individual packages ranges between 0.6 and 33 m (2 and 108 ft). The typical GR log response of this facies association is irregularly serrate, with values between 30 and 80 API units, reflecting a relative increase in the detrital clay content. Bioturbation is moderate to very abundant, tending to overprint and obscure all primary sedimentary structures (Figure 6D).

This facies association is interpreted to have been deposited in a lower shoreface to shelf environment as suggested by the variably clean to argillaceous nature of the sandstones and ubiquitous bioturbation with a well-developed *Skolithos* ichnofacies.

Hawaz Facies Association 6: Burrowed Inner Shelf

Facies association HWFA6 comprises lithofacies Hmb and HSb (Figure 5). The minimum thickness of individual packages is approximately 30 cm

(~1 ft), whereas the maximum value is 15.8 m (52 ft). It may be considered as the distal equivalent of HWFA5 characterized by a spiky GR response characterized by notably higher values ranging from 60 to 120 API units. Bioturbation intensity is moderate, with an ichnofaunal assemblage dominated by the *Cruziana* ichnofacies.

This facies association is interpreted as having been deposited in a distal burrowed lower shoreface to inner shelf setting based on its heterolithic lithology, *Cruziana* ichnofacies (Figure 6E), and the occurrence of combined current and wave ripples. This suggests a low-energy, open-marine environment in moderate water depths above storm wave base (SWB).

Hawaz Facies Association 7: Shelfal Storm Sheets

Facies association HWFA7 is mostly composed of lithofacies HS and HM (Figure 5). The thickness of these facies packages ranges from 0.3 to 18 m (1 to 59 ft). It is characterized by a continuously high GR response with values of up to 150 API units or even higher. Where notably high GR peaks occur, these may represent local flooding events interrupting a shallower depositional sequence. This facies association has the lowest reservoir quality in the formation with an average porosity of approximately 5% and an average horizontal permeability of 0.2 md.

It is interpreted to have been deposited in a distal shelf environment on the basis of a high detrital clay content and the occurrence of combined wave and current ripples (Figure 6F). These suggest fluctuating energy levels in broadly very low-energy environment between the FWWB and SWB. This is supported by the generally very low intensity of bioturbation, the occasional occurrence of *Chondrites*

Figure 5. Summary of facies associations and interpreted depositional settings. Description includes typical core sections and thickness ranges. See also the main lithofacies composing each facies association and the location of detailed features shown in Figure 6. Interpretation in terms of depositional environment is also included. In addition, summary conventional core analysis (CCA), porosity (\emptyset), and permeability (K) and data for every facies association and average gamma ray values are also shown. The last column shows the sequence stratigraphic interpretation plus the location of each association within the depositional model of the Figure 8. Cl = clay; fs = fine sandstone; HM = muddy heterolithic; Hmb = burrowed muddy heterolithic; HS = sandy heterolithic; HSb = burrowed sandy heterolithic; HST = highstand systems tract; HWFA = Hawaz facies association; MFWB = mean fairweather wave base; ms = medium sandstone; MSb = burrowed sandstone with feeding ichnofauna; MSWB = mean stormweather wave base; Sb = burrowed sandstone with *Siphonichnus*; si = silt; Sl = parallel-laminated sandstone; Sr = ripple cross-laminated sandstone; Srb = burrowed ripple cross-laminated sandstone; Sv = massive sandstone; Sx1 = large-scale cross-bedded sandstone; Sx2 = small- to medium-scale cross-bedded sandstone; Sxb = burrowed cross-bedded sandstone; Sxl = cross-laminated sandstones; Sxlb = burrowed cross-laminated sandstone; TST = transgressive systems tract; vfs = very fine sandstone.

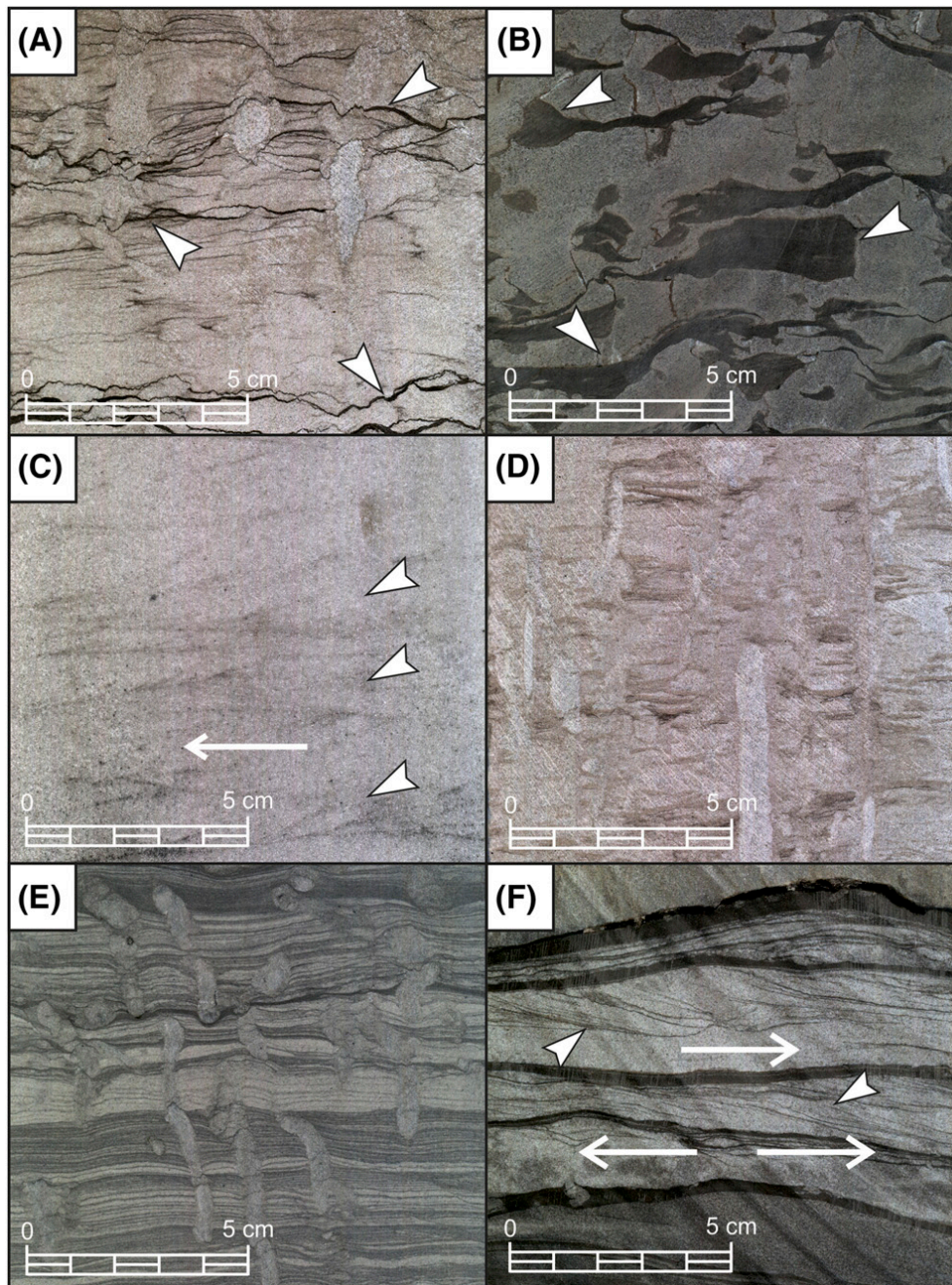


Figure 6. Detailed close-up views of some characteristic sedimentary structures and fabrics of the Hawaz Formation in core. (A) Mud-draped (flaser) lamination (arrows) in Hawaz facies association (HWFA1) tidal flat facies association from well E. (B) Mudstone rip-up clasts (arrows) from fluviotidal to subtidal channels of HWFA2 subtidal complex in well F. (C) Clay-draped current ripples (small arrows) from HWFA2 subtidal complex from well C. Notice the direction of the paleocurrent flow leftward (horizontal arrow). (D) Burrowed sandstones with characteristic *Skolithos* ichnofacies of the HWFA5 burrowed shelfal and lower shoreface facies association in well E. (E) Characteristic view of the HWFA6 burrowed inner shelf deposits from well D. (F) Clay-draped combined flow ripples (small arrows) from Hawaz facies association 7 shelfal storm sheets in well D. Notice the direction of the paleocurrent flow rightward in the upper part and bidirectional in the lower part of the image (horizontal arrows). See the location of the corresponding wells (C, D, E, and F) in Figure 3B.

burrows, and shrinkage cracks indicating deposition in a fairly distal, poorly oxygenated setting, perhaps associated with distal waning storm events capable of transporting sand to the open-marine shelf.

When core data were not available for several sections in the studied wells, image log data were key to characterize the seven facies associations previously mentioned (Figure 7).

NONACTUALISTIC SEDIMENTARY MODEL

Ever since James Hutton's key observations in the late eighteenth century (modified by the work of John Playfair) and, critically, Lyell's (1832) development of the concept of uniformitarianism in his *Principles of Geology*, geologists have sought to explain ancient processes by reference to actualistic

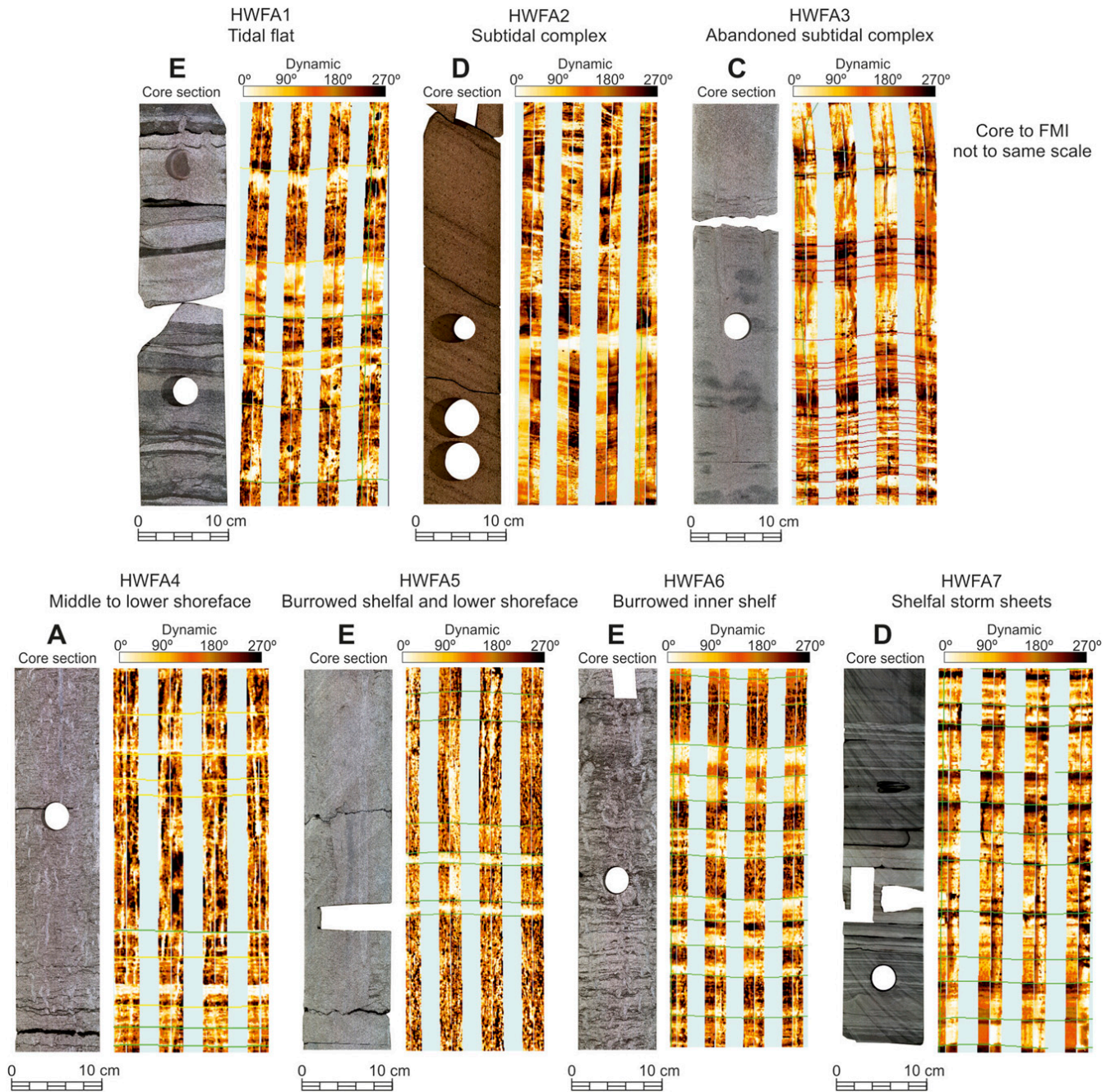


Figure 7. Representative sections of slabbed cores (40 cm [16 in.]) for each facies association and a typical high-resolution formation microimager (FMI) image (3 m [10 ft] long) showing their main characteristics. From top left to bottom right: Hawaz facies association 1 (HWFA1) tidal flat, HWFA2 subtidal complex, HWFA3 abandoned subtidal complex, HWFA4 middle to lower shoreface, HWFA5 burrowed shelfal and lower shoreface, HWFA6 burrowed inner shelf, and HWFA7 shelfal storm sheets corresponding wells (A, C, D, and E) in Figure 3B.

processes to better understand the sedimentary record.

However, Earth has changed significantly through geological history. Indeed, even from the early Paleozoic until present day, some processes and depositional environments simply cannot be directly compared, because conditions were significantly different. As Nichols (2017, p. 4) certainly points out, if choosing a “present” to be the “key of the past,” probably choosing the most recent present is not the best idea.

After careful study of the Hawaz Formation and the sedimentary processes involved in its deposition, several significant concepts have been developed which require further discussion in this respect (Table 2). First, the lack of fauna and, specifically,

flora in subaerial conditions during the Middle Ordovician and more ancient times must have constituted a key controlling factor on depositional processes operating in marginal marine and coastal environments (Kenrick et al., 2015, 2016; Bradley et al., 2018). First, vegetation constitutes a fixing element within the substrate, allowing the stabilization of floodplains and the control of lateral river channel migration (Davies and Gibling, 2010; Davies et al., 2011; Gibling and Davies, 2012), generally lowering the energy and net sediment throughput of the environment. Whereas fluvial meandering systems can be considered a general pattern in continental to marine transitional zones for most present-day cases (with the notable exception of glacial-influenced settings or proximity to high-relief

Table 2. Comparative Table between Key Actualistic (Present) and Nonactualistic (Early Paleozoic and Older) Main Processes or Controlling Factors Affecting the Geological Signature of Tidal-Influenced Successions in the Geological Record

Processes/Controlling Factors	Actualistic (Present)	Nonactualistic (Early Paleozoic and Older)
Land flora	Vegetation in continental to transitional environments helps to stabilize river banks, limiting channel shifting and changing river style from braided to meandering in low-gradient systems. Chemical weathering and related clay generation	The lack of vegetation in subaerial conditions led to the development of high-energy fluvial systems (mainly braided style) characterized by rapid channel shifting of rivers, even in very low-gradient systems. Lack of clay generation by induced chemical weathering because of the absence of vegetation in subaerial environments; clay-size particles alternatively sourced from volcanic ash, hydrothermalism, diagenesis, etc.
Greenhouse versus icehouse	Incision of valleys during sea level fall in recent icehouse periods and subsequent development of estuarine environments with marine transgressions. Fluvial sediments are common in proximal parts of the systems and related hyperpycnal deposits in more distal settings during lowstand stages.	Epeiric seas in large cratonic basins during greenhouse periods developing really extensive paralic environments; very difficult to identify lowstand deposits because of very limited incision in proximal environments; very low gradients imply major paleoshoreline shifts with only limited relative sea-level rises.
Tidal range	Lower tidal range caused by tidal energy dissipation because of larger distance between Earth and the moon with time. Maximum known current tidal range is approximately 12 m (~40 ft).	Higher tidal range because of the reduced distance between Earth and the moon (unknown maximum tidal range in the early Paleozoic)
Ichnofacies	Broader and more diversified ichnofacies at present times. Characteristic <i>Skolithos</i> and <i>Cruziana</i> ichnofacies found in Hawaz Formation have a different signature because of the presence of different fauna in present depositional environments.	Characteristic, commonly low diversity, mix of <i>Skolithos</i> and <i>Cruziana</i> ichnofacies is largely confined to the early Paleozoic, commonly occurring in the form of ichnofabrics characterized by a distinctive pipe rock texture and trilobite traces.

source areas), the lack of vegetation in the Middle Ordovician would have almost certainly contributed to maintaining high-energy levels in the sedimentary system as far as the coastal plain, characterized by laterally extensive braided floodplains (Table 2).

The other remarkable aspect worthy of note is the effect of vegetation on the generation of clay minerals (Table 2). Many Precambrian to Ordovician clastic deposits are characterized by their low claystone or detrital clay content. One of the reasons for this may be the absence of vegetation and the resultant enhanced chemical weathering on land surfaces. The generation of clays by weathering was significantly less than at the present time, and therefore, the availability of clays in the source areas, including potentially erodible rocks, was also less for the same reason. Other mechanisms for inputting a clay fraction into the depositional environment may be associated with hydrothermal processes, diagenesis, or volcanic ash deposits; the latter has been identified by M. Marzo and E. Ramos (2003, personal communication) and Ramos et al. (2006).

This is indeed what we see in the upper part of the Hawaz Formation, typically comprising a package of sand-prone tidal flat deposits with very few clear claystone intervals, accumulating in a restricted low-energy environment where, in a modern system, vegetation would fix finer sediments at the very top of this kind of depositional succession. Furthermore, the possibility of a clay input of volcanoclastic origin should not be ruled out, because Ramos et al. (2006) highlight the presence of K-bentonite layers within the Hawaz Formation as observed in outcrops.

Second, in line with Nichols (2017), the climate factor related to periods of greenhouse and icehouse is also key in understanding how coastal environments have evolved. Given that the last few million years of geological history are considered as an icehouse period, some processes related to the characteristic low relative sea levels are clearly not equivalent to those produced during greenhouse periods, because much of the Cambrian–Ordovician actually was. The relative sea level, during much of the Ordovician (at least until the onset of the Hirnantian glaciation), was probably tens of meters higher than at present time, which, in the case study,

would represent a very extensive area of land flooded across a very low relief cratonic margin (Table 2). Thus, confined estuary systems produced by incised valleys during sea-level drop are not expected in this setting. This discussion can be applied to the depositional model of the Hawaz Formation. As such, classical estuarine environments are inherently unlikely. Indeed, conventional lowstand systems tracts would be, in any case, extremely difficult to identify, because major erosive features related to sea-level drop would not be produced in this low-gradient, cratonic transitional setting.

Third, it is also relevant to our study that tidal range has not been constant through the whole of Earth's history. Tides are largely controlled by differential gravitational forces exerted between Earth and the moon, but the distance between both bodies has changed through time at a currently calculated rate of 3.8 cm/yr (1.5 in./yr) (Odenwald, 2018), entailing an average Earth–moon distance of 367,000 km (228,000 mi) as opposed to 384,000 km (238,000 mi) today. Tidal-energy dissipation over time is thus a well-established process reflected in the increasing length of the day and thus number of days per year. This appears to be a purely linear process reflecting the progressive slowing of Earth's rotation and the associated outward spiraling of the moon. Thus, a day in the Ordovician is calculated to have been 21 hr long and the year 414 days long. For our purposes, it is also true that the potential sediment load of nearshore tidal currents together with their depositional effectiveness are related directly to the tidal range or maximum tidal height (Williams, 2000), itself, controlled by global tidal forces, water depths, and local topography. In general, therefore, we can assume notably higher tidal ranges and more powerful tidal currents during the deposition of the Hawaz Formation. Going further, we may also assume that, in the case of the upper Hawaz Formation, for example, even very small variations in tidal range in such low-gradient depositional environment would result in a significant increase in the areal extension of marginal or paralic, tidally influenced environments (Table 2).

Fourth, ichnofacies are commonly related to sedimentary environments and, particularly in tidal settings, specific parameters exist such as salinity, depositional energy, sediment grain size, and sedimentation rates that control fauna colonization

(Gingras, et al., 2012). However, some ichnological assemblages exist that may also have a chronostratigraphic value when looked at on the basis of bioturbation intensity and lateral extent. A very good example is the lower part of the Hawaz Formation and the underlying Lower Ordovician Ash Shabiyat Formation, which are characterized by their distinctive “pipe rock” or high-density burrowed *Skolithos* ichnofabric. Similarly, the association of this suspension-feeding fabric, commonly overprinting a deposit feeding burrowing characterized by common trilobite traces, and thus a “true” *Cruziana* ichnofacies is distinctive. Some, if not many or even all, of the organisms responsible for these ichnofabrics are already extinct (Table 2). Thus, the occurrence of these ichnofacies in such a very low gradient, cratonic platform is highly unlikely in the present day.

After these comments, it is also worthwhile considering that the geomorphology of clastic coastal depositional environments is closely linked to the relative influence of waves and tides along the coastline (Harris and Heap, 2003); their evolution is controlled by three main factors: sediment supply, physical processes (river currents, tidal currents, and waves), and relative sea-level variation (Boyd et al., 1992; Dalrymple, 1992, Dalrymple et al., 1992; Harris et al., 2002).

Thus, taking all of this into account with and applying it to the study data set in the area, a nonactualistic depositional model is proposed for the Hawaz Formation based upon modern sedimentological criteria but constrained and adapted to Middle Ordovician environmental conditions (Figure 8).

It was a constantly evolving tide-dominated environment, evolving from a relatively open-marine setting characterized by mixed storm tide-dominated deposition toward a more protected subtidal to intertidal setting on an embayed coastline. This promoted tides as the dominant controlling factor on sedimentation process, supported by the vertical arrangement or stacking of facies associations. It shows a lower shoreface to shelf environment with sandy storm sheet deposits present across much of the basin. Above this lower interval, a laterally extensive and fluviotidal to subtidal complex comprising of tidal channels and bars developed across the study area (Figure 8A). The distal part of this subtidal

complex eventually became abandoned as sea level rose, creating a system of lagoons and barrier islands (not clearly identified in the subsurface) (Figure 8B). Finally, prograding tidal flats developed during a relative high-sea-level stage (Figure 8C).

From subsurface paleocurrent data, it is apparent that the depositional system evolved from a coastal environment in the south-southeast to fully marine environments toward the north-northwest. The data show only limited dispersion defining a clear depositional trend from southeast to northwest with strong ebb current indicators. These data are in accordance with those of Ramos et al. (2006) from outcrops in the Gargaf high. Evidence of bidirectional current indicators in primary sedimentary structures is, however, hard to observe. Although the presence of this kind of feature would strongly support an important tidal influence, it is not always present in many tidal deposits. However, no evidence for a seasonally controlled river have so far been found in the succession, which would help to preserve this type of reverse flow structure during periods of low fluvial regime (Dalrymple and Choi, 2007). However, the presence of clay drapes in most of the lithofacies described does strongly support an important tidal effect throughout the depositional system.

SEQUENCE STRATIGRAPHY AND ZONATION OF THE HAWAZ FORMATION

The purpose of this section is to recognize and correlate stratigraphic surfaces representing changes in depositional trends and to interpret the resulting stratigraphic units bounded by these surfaces.

The key bounding surfaces splitting genetic sedimentary packages were recognized using a material-based sequence stratigraphic approach (Embry, 2009). The defined surfaces are the following.

- Maximum regressive surface, in which a conformable horizon marks a change from coarsening and shallowing upward to fining and deepening upward.
- Maximum flooding surface, in which a conformable horizon marks a change from fining and deepening upward to coarsening and shallowing

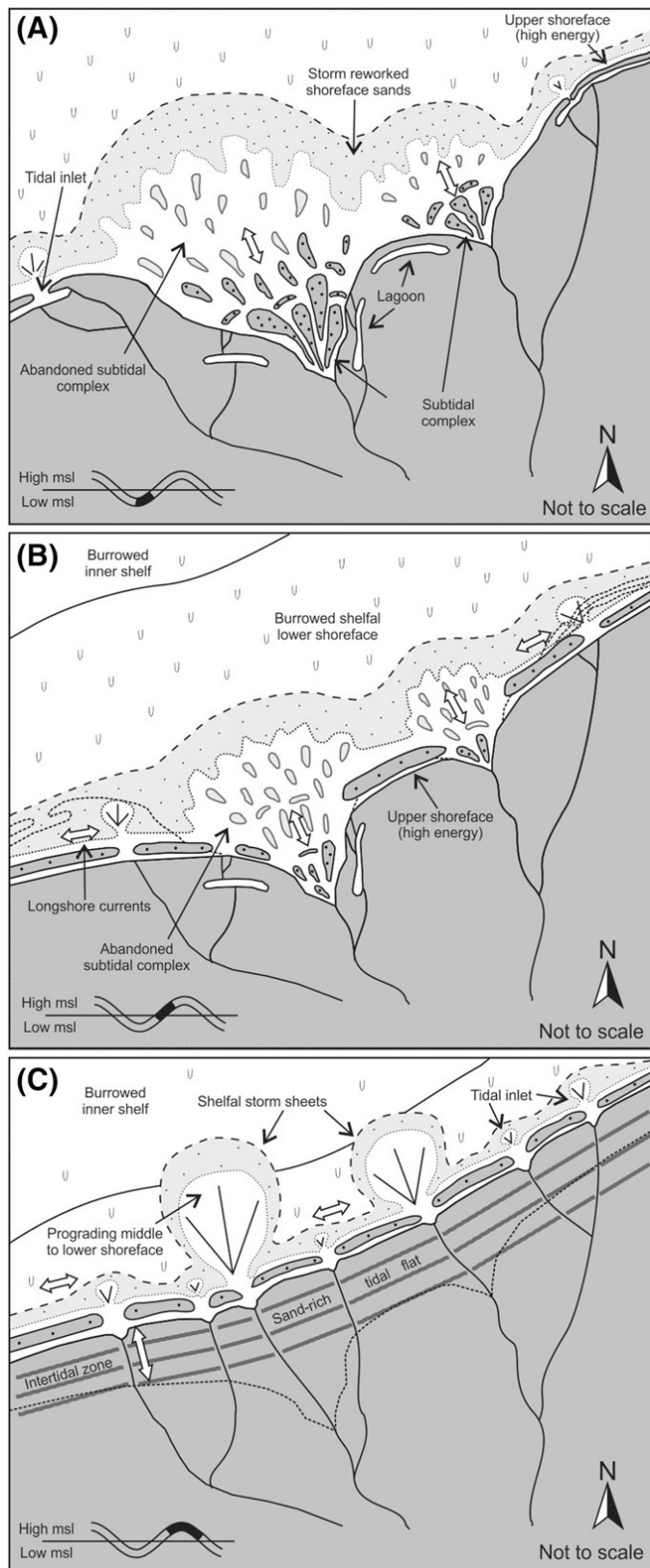


Figure 8. Evolutionary sedimentological model for the deposition of the Hawaz Formation. (A) Early transgressive systems tract highlighting embayments. (B) Late transgressive systems tract. (C) Highstand systems tract. The main facies associations are represented in the sketches. The sketches are purely conceptual but consistent with observed trends in the study area, but not geographically tied to well data. msl = mean sea level.

upward and is normally represented by the highest clay content in the succession.

- Shoreline ravinement unconformity, in which a clear erosive surface is overlain by brackish marine deposits and which represents erosion in the stratigraphic unit produced by wave and tidal currents during an early transgressive stage just after a base level fall.
- Regressive surface of marine erosion, in which, in an overall regressive succession, a clear change exists in depositional trend with shelfal deposits abruptly overlain by prograding shoreface deposits. As suggested by Embry (2009), this last surface is not a suitable surface for correlation because of its highly diachronous nature, so it has not been used as a main bounding surface for our sequence stratigraphic framework. However, locally, it may be of use in explaining trend changes in the facies succession observed in some wells.

Several low-order and numerous high-order sequences can be recognized in the stratigraphic record of the Hawaz Formation (Figure 9); but, after analyzing the evolution or stacking of the facies associations in each well, it is possible to erect a simplified scheme with three major depositional sequences (DS1–DS3) and five Hawaz reservoir zones (HWZ1–HWZ5), each defined by key, correlatable, genetic, material-based surfaces (Figure 9).

The top of the Ash Shabiyat Formation is marked by a sharp or slightly more gradational shift from the blocky, low GR response, characteristic of this formation, to a notably more spiky or serrate GR response typical of much of the lower Hawaz. This shift is interpreted not only as a maximum regressive surface, but also as a sequence boundary. As such, it is a compound surface and might be considered in terms of marine erosion as a ravinement, which marks the base of DS1 (Figure 9).

The overlying HWZ1 is broadly transgressive in character, comprising stacked fining-upward parasequences (including a regionally distinctive and extensive abandoned subtidal complex) capped by a regional flooding surface (Figure 9), and, finally, a cleaning-upward, progradational parasequence or parasequence set.

The boundary between HWZ1 and HWZ2 is marked in all the wells by an abrupt change in lithology to more argillaceous facies, recording a marked deepening in the basin. This is an excellent and consistent correlatable surface but is not fully genetic, because the maximum flooding surface of the DS1 only rarely coincides with the lithological change and is, instead, typically picked a short distance above the shift at the highest GR peak in the well (Figure 9).

The maximum flooding surface defines the onset of the highstand systems tract (HST) of DS1, which coincides completely with the zone HWZ2. This can commonly be divided into two subzones (HWZ2a and HWZ2b) separated by a regressive surface of marine erosion (Figure 9), created by the cut of waves and tides in the lower shoreface during the regression of the shoreline. This surface separates a dirty sandy package from a cleaner sandy package within a coarsening-upward parasequence or parasequence set, as suggested by the GR response and facies analysis. However, this surface is not easily recognizable in all wells and has not been used as a regional correlative surface because of its probable diachronous nature.

The HST of DS1 is truncated by an erosive surface interpreted as a shoreline ravinement unconformity (Figure 9) generated by the action of wave and tidal currents during an early transgressive stage just after a base level fall and probably enhanced by an allocyclic trigger mechanism, perhaps tectonics related. This surface would also be a sequence boundary and would correspond with the onset of the DS2 and the base of zone HWZ3, the main reservoir section of the Hawaz Formation. The facies association immediately overlying this key boundary is commonly HWFA2 (subtidal complex), considered to represent an early transgressive systems tract (TST) equivalent to zone HWZ3. Locally, this zone shows minor higher-frequency flooding surfaces mostly composed of heterolithics (Figure 9). These flooding surfaces could be interpreted as condensed lagoonal deposits, but the lack of biostratigraphic data in this sand-prone package suggests we should treat this hypothesis with caution, although the presence of these subenvironments should not be rejected. Tidal inlet storm deposits or IHS could also be a plausible option, considering the broad general subtidal setting of this zone.

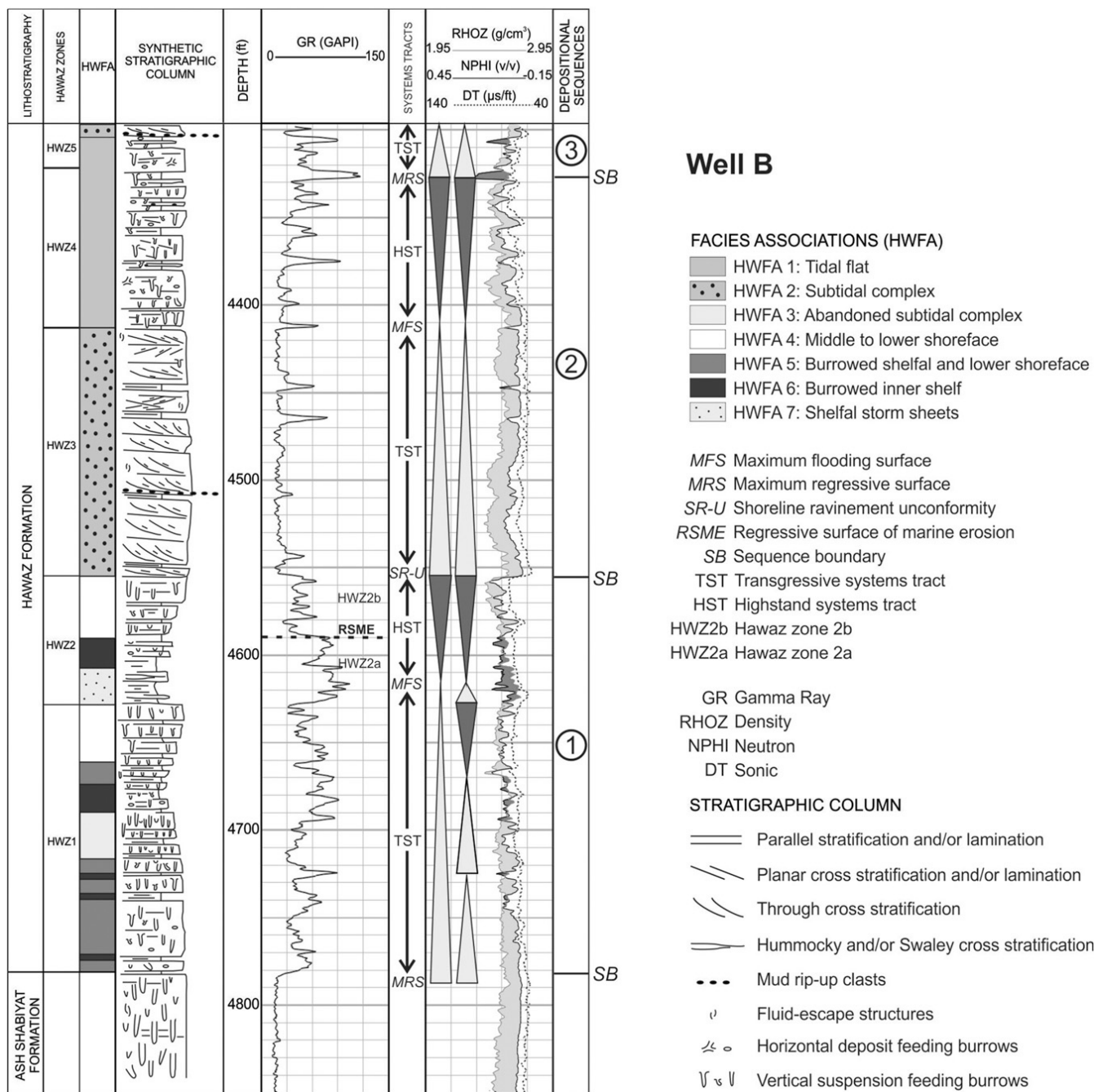


Figure 9. Composite section of a well showing a synthetic stratigraphic column of the Hawaz Formation, the wire-line log responses, the suggested zonation for the reservoir based on the facies associations, and sequence stratigraphic framework. The transgressive and regressive stacking patterns are represented on the figure together with the three main depositional sequences. See the location of the corresponding well (well B) in Figure 3B.

The boundary between zones HWZ3 and HWZ4 is marked by a change in depositional environment from a subtidal to intertidal setting. This boundary would be close to the maximum flooding surface; after which, the tidal flat would prograde infilling the available space (bay infilling) under a forced regression pattern, whereas farther

to the north barrier island deposits (observed in Gargaf outcrops by Ramos et al. [2006]) would most likely have limited the connection to the open sea.

Zone HWZ4 comprises stacked fining-upward parasequences mainly formed by tidal sand to mixed flat deposits cut by tidal creeks (Figure 9). Similar processes have been highlighted by Desjardins et al.

(2012) in the lower Cambrian Gog Group of the Canadian Rocky Mountains where tidal flats are forced to regress in response to falling sea level in tide-dominated settings.

Above zone HWZ4, the depositional trend changes again, and GR values begin to decrease in response to increasingly abundant, cleaner sand deposits. No evidence of sharp changes exists either in lithology or in conventional log responses, suggesting no major unconformity exists. However, some subtidal packages are preserved sometimes at the very top of the Hawaz Formation, which would denote a new transgression. Thus, the boundary between HWZ4 and HWZ5 is considered to be a compound maximum regressive surface and sequence boundary that would constitute the beginning of a rarely preserved DS3 (Figure 9). Zone HWZ5 is commonly eroded and overlain by the Upper Ordovician formations or the base of the Silurian.

DISCUSSION

Following Boyd et al. (1992) and Dalrymple et al. (1992), clastic coastal depositional environments are classified on a ternary diagram, summarizing the main factors (rivers, waves, and tides) controlling the geomorphology of linear shorelines, deltas, or estuaries. This is a very useful and powerful tool in actualistic or near-actualistic systems; but in many cases, it might be hard to apply to very ancient coastal to shallow marine depositional systems, notably those of the Precambrian to lower Paleozoic because of major differences in Earth surface dynamics. Nevertheless, whereas some of these ancient depositional systems lack obvious modern analogs, some features remain comparable with modern environments. A detailed interpretation from subsurface cores and logs highlights the major depositional and paleogeographic factors responsible for the Middle Ordovician Hawaz Formation of the northern Murzuq Basin. The resultant seven correlatable facies associations (HWFA1–HWFA7) and the robust sequence stratigraphic framework suggest that the Hawaz Formation was deposited in an intertidal to subtidal environment prograding from south to north. The facies associations and their linked ichnogenes suggest that

water depths are unlikely to have exceeded several tens of meters, with the sea floor above SWB at most locations.

Considering the significant areal extent, not only of the Hawaz Formation across the Murzuq Basin, but also its lateral equivalents in both Kufra and Illizi Basins, which lack the key unburrowed cross-bedded sandstones (McDougall et al., 2008, 2011) typical of the subtidal complex described in this work, it is clear that deposition occurred in and on the margins of an epeiric sea characterized by a very low bathymetric relief and very broad facies belts tracts. Dalrymple and Choi (2007) suggest fluviotidal transition zones may range in width up to hundreds of kilometers (hundreds of miles) in low-gradient settings, as would indeed be the case for the northern margin of Gondwana during the Middle Ordovician. In such environments, small changes in relative sea level would be sufficient to cause major lateral shifts in facies belts. These small changes occurred during a greenhouse period with relatively high global sea levels. No evidence exists of incised valley systems within the Hawaz succession, suggesting global sea level remained relatively high through its deposition. As such, lowstand systems tract facies could not be observed either in the Gargaf high outcrops (Anfray and Rubino, 2003) or in the subsurface of the Murzuq Basin.

During the initial stages of sea-level rise (TST), coastal areas were slowly flooded, producing subtidal sedimentation associated with fluvial discharge along embayed coastlines, presumably because of flooding of braided fluviotidal systems, whereas during stages of high sea levels (HST), the shoreline migrated seaward, resulting in the progradation of tidal-wave influenced strand plains, beaches, or deltas associated with gentle lobate to linear coasts. The embayed morphology of coastal areas was probably enhanced by tectonism, which controlled the size and subsidence of the basin, generating a large-scale depressed area elongated in an approximately north-south direction (Klitzsch, 2000). Such a large-scale embayment characterized by a very low gradient probably increased tidal power (Ramos et al., 2006).

The vertical stacking of the facies association packages was principally controlled by eustasy, as suggested by the presented zonation. However, other secondary factors exist that almost certainly acted to control the evolution of sedimentation in

these coastal and shallow marine environments, notably subsidence and sediment supply (Dalrymple, 1992; Dalrymple et al., 1992; Walker and Plint, 1992; Johnson and Baldwin, 1996).

Given that this environment was characterized by a very low gradient, it is possible that sedimentation was controlled by a preexisting paleorelief expressed as complex lobate to linear shoreline. The low gradient of this depositional system impeded the development and identification of well-defined clinofolds both in outcrops and in seismic images. What is evident is the significant influence of tidal processes in these deposits with a preferential paleocurrent direction toward the north-northwest according to both outcrop (Ramos et al., 2006) and FMI data from wells showing some bidirectional current indicators in some cases. In addition, strong evidence also exists for a secondary paleocurrent dispersal system flowing toward the northeast which requires further study.

Several depositional models have been proposed for the Hawaz Formation. Vos (1981) suggested a fan delta complex as the more likely setting, whereas other scientists, including Ramos et al. (2006), have argued for deposition within a megaestuary or tidal gulf setting. The current study strongly suggests that the Hawaz Formation cannot be compared with any present-day coastal environment. The clear tidal influence observed in the system and the vertical stacking of facies associations highlight the evolution of a shallow marine environment from a subtidal to an intertidal setting accompanied by parallel evolution of ichnofacies and fossil content (Figure 10).

The presence of some ichnogenera, such as *Chondrites*, in heterolithics from the most distal facies associations HWFA6 and HWFA7, compared with those deposited in the most proximal association HWFA1, suggests that a different setting for the lower (DS1; HWZ1 and HWZ2) and upper (DS2 and DS3; HWZ3–HWZ5) parts of the Hawaz Formation should be considered. Gibert et al. (2011) concluded that the restricted and uncommon ichnofacies assemblage in the upper part of the Hawaz was not clear. A mixed *Cruziana* and *Skolithos* ichnofacies has been observed both in the subsurface and in outcrops; the latter showing many excellent examples of trilobite traces (Ramos et al., 2006; Gibert et al., 2011). Some scientists have realized that, although trilobite tracks typical of the *Cruziana* ichnofacies are commonly regarded as

indicators of open-marine offshore to nearshore settings, their presence in heterolithic facies can no longer be taken as an absolute indicator of deposition in subtidal settings in the early Paleozoic, and indeed, they may have been notably more common within intertidal deposits than currently envisioned (Mángano et al., 2014). The nonactualistic sedimentary model presented in this study incorporates this observation so that the *Cruziana* ichnofacies is also considered a common characteristic element of shallow tidal flat settings (Figure 10).

CONCLUSIONS

Where encountered in the subsurface of the northern Murzuq, the Hawaz Formation is represented by a clastic succession mainly comprising fine- to locally medium-grained quartzarenites and subarkosic arenites, with subordinate sublithic arenites, up to 210 m (690 ft) thick. Fifteen major lithofacies, comprising sandstones and heterolithics, have been recognized and grouped into seven correlatable facies associations. These include the following: (1) tidal flat (HWFA1); (2) subtidal complex (HWFA2); (3) abandoned subtidal complex (HWFA3); (4) middle to lower shoreface (HWFA4); (5) burrowed shelfal and lower shoreface (HWFA5); (6) burrowed inner shelf (HWFA6); and (7) shelfal storm sheets (HWFA7), all deposited within the framework of an intertidal to subtidal setting.

A clear relationship exists between facies and reservoir quality for the Hawaz Formation. The best reservoir quality sandstones are those comprising facies association HWFA2 (subtidal complex) with an average porosity of 11% and horizontal permeability of 125 md and general absence of thick mud drapes and interlayered claystones.

The depositional model for the Hawaz Formation cannot be compared with an actualistic sedimentary analog because of the major differences stemming from the following: (1) the absence of fauna and especially flora in subaerial environments, which directly determines coastal dynamics; (2) the difference in relative sea level and its control on erosion in shallow marine settings together with the low-gradient depositional setting, which promoted very wide facies belts compared with most present-day moderate- to high-gradient

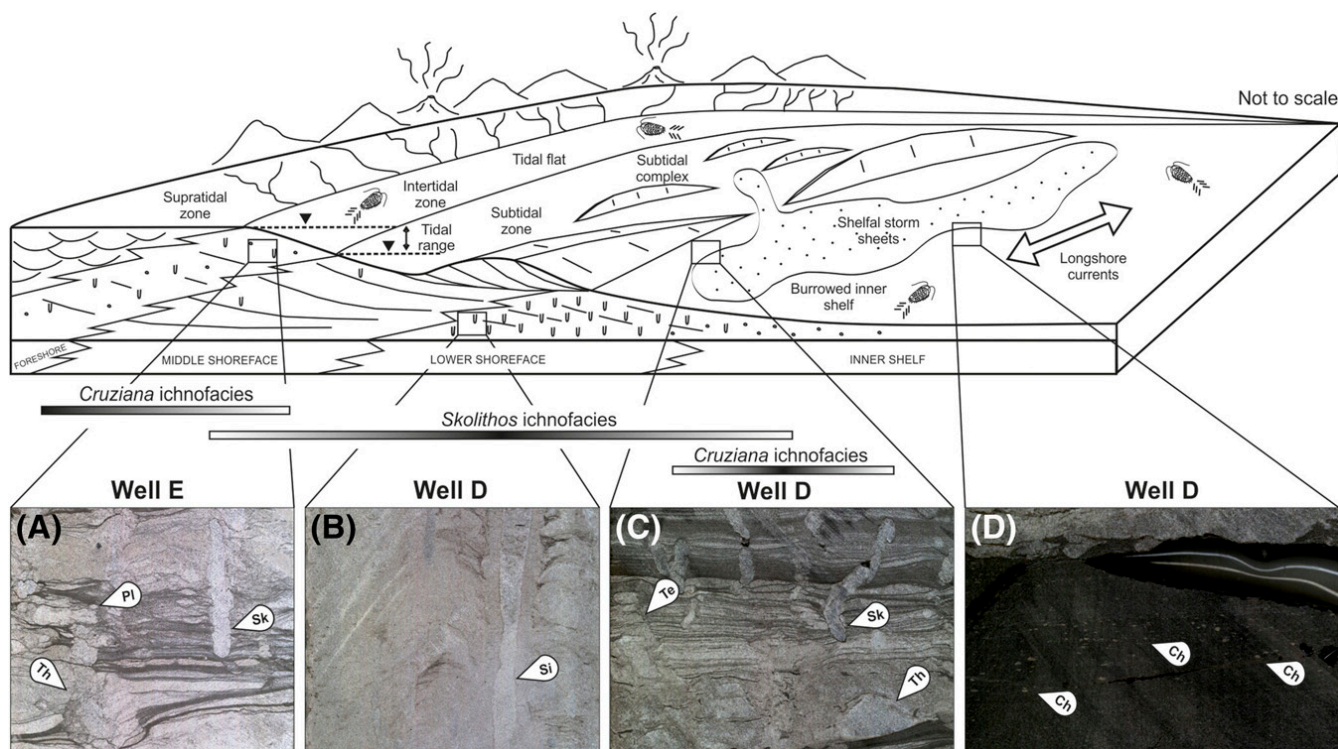


Figure 10. Three-dimensional conceptual sketch of a coastal, tidal-influenced environment analog to the Hawaz Formation deposition during a highstand systems tract stage, grading from a braided coastal plain environment in the most proximal part of the sedimentary system to intertidal and subtidal environments and lower shoreface to inner shelf settings. Note the clear relationship between the ichnofacies assemblage and the energy of the depositional environment. From left to right: (A) mixed *Cruziana* and *Skolithos* (Sk) ichnofacies assemblage with characteristic vertical suspension feeder burrows of Sk overprinting an ichnofabric comprising horizontal deposit feeders and miners such as *Thalassionides* (Th) and *Planolites* (Pl) associated with tidal flat deposits. (B) Characteristic Sk pipe rock ichnofacies with typical *Siphonichnus* (Si) burrows from lower shoreface to burrowed shelfal deposits. (C) Mixed *Cruziana* and Sk ichnofacies assemblage, from burrowed inner shelf sediments with characteristic *Teichichnus* (Te), Th, and Sk burrows. (D) Heterolithic mudstones belonging to the most distal storm deposits with *Chondrites* (Ch) burrows characteristic of the distal *Cruziana* ichnofacies. See the location of the corresponding well (wells E and D) in Figure 3B.

depositional systems; (3) the difference in tidal ranges reflecting the progressive change in the distance between Earth and the moon, and finally; (4) the characteristic ichnofacies observed in the Hawaz are not present in modern environments.

The Hawaz Formation can be divided into three main depositional sequences (DS1–DS3), each with characteristic systems tracts bounded by key surfaces: maximum regressive surface, maximum flooding surface, and unconformable shoreline ravinement surface.

Based upon this systems tracts architecture, a genetic zonation composed of five zones has been proposed (HWZ1 to HWZ5). This new stratigraphic zonation should serve as a useful tool to improve the management in oil production from the Hawaz Formation. The Hawaz Formation extends laterally hundreds of kilometers away from the study area,

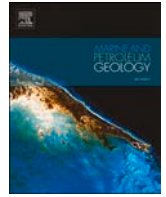
forming an excellent regional reservoir across the Murzuq and southern Ghadames (Berkiné) Basins and, to a lesser extent, as the laterally equivalent unit III in the Illizi Basin. The facies schemes, depositional model, and zonation framework proposed here should also be applicable to existing or potential Hawaz reservoirs elsewhere within this larger region.

REFERENCES CITED

- Abouessa, A., 2012, Diagenetic properties of Hawaz Formation, Murzuq Basin, Libya, in M. J. Salem, M. T. Elbakai, and Y. Abutarruma, eds., *The geology of southern Libya: Tripoli, Libya*, Earth Science Society of Libya, v. 1, p. 47–82.
- Abouessa, A., and S. Morad, 2009, An integrated study of diagenesis and depositional facies in tidal sandstones: Hawaz Formation (Middle Ordovician), Murzuq Basin,

- Libya: *Journal of Petroleum Geology*, v. 32, no. 1, p. 39–65, doi:10.1111/j.1747-5457.2009.00434.x.
- Anfray, R., and J.-L. Rubino, 2003, Shelf depositional systems of the Ordovician Hawaz Formation in the Central Al Qarqaf high, *in* M. J. Salem, K. M. Oun, and H. M. Seddiq, eds., *The geology of northwest Libya II: Second Symposium on the Sedimentary Basin of Libya*, Tripoli, Libya, v. 3, p. 123–134.
- Boote, D. R. D., A. Dardour, P. F. Green, J. D. Smewing, and F. Van Hoeflaken, 2008, Burial and unroofing history of the base Tanezzuft 'hot' Shale source rock, Murzuq Basin, SW Libya: New AFTA constraints from basin margin outcrops (abs.), *in* M. J. Salem, M. T. Elbakai, and Y. Abutarruma, eds., *The geology of southern Libya: Fourth Sedimentary Basins of Libya Symposium*, Tripoli, Libya, November 17–20, 2012, p. 21–36.
- Boyd, R., R. Dalrymple, and B. A. Zaitlin, 1992, Classification of clastic coastal depositional environments: *Sedimentary Geology*, v. 80, no. 3–4, p. 139–150, doi:10.1016/0037-0738(92)90037-R.
- Bradley, G., J. Redfern, D. Hodgetts, A. D. George, and G. D. Wach, 2018, The applicability of modern tidal analogues to pre-vegetation paralic depositional models: *Sedimentology*, v. 65, no. 6, p. 2171–2201, doi:10.1111/sed.12461.
- Dalrymple, R. W., 1992, Tidal depositional systems, *in* R. G. Walker and N. P. James, eds., *Facies models: Response to sea level change*: Waterloo, Canada, Geological Association of Canada, p. 195–218.
- Dalrymple, R. W., and K. Choi, 2007, Morphologic and facies trends through the fluvial–marine transition in tide-dominated depositional systems: A schematic framework for environmental and sequence-stratigraphic interpretation: *Earth-Science Reviews*, v. 81, no. 3–4, p. 135–174, doi:10.1016/j.earscirev.2006.10.002.
- Dalrymple, R. W., B. A. Zaitlin, and R. Boyd, 1992, Estuarine facies models; conceptual basis and stratigraphic implications: *Journal of Sedimentary Petrology*, v. 62, no. 6, p. 1130–1146, doi:10.1306/D4267A69-2B26-11D7-8648000102C1865D.
- Davidson, L., S. Beswetherick, J. Craig, M. Eales, A. Fisher, A. Himmali, J. Jho, B. Mejrab, and J. Smart, 2000, The structure, stratigraphy and petroleum geology of the Murzuq Basin, Southwest Libya, *in* M. A. Sola and D. Worsley, eds., *Geological exploration in Murzuq Basin*: Amsterdam, Elsevier Science, Geological Conference on Exploration in the Murzuq Basin, Sabha, Libya, September 20–22, 1998, p. 295–320, doi:10.1016/B978-044450611-5/50016-7.
- Davies, N. S., and M. R. Gibling, 2010, Cambrian to Devonian evolution of alluvial systems: The sedimentological impact of the earliest land plants: *Earth-Science Reviews*, v. 98, no. 3–4, p. 171–200, doi:10.1016/j.earscirev.2009.11.002.
- Davies, N. S., M. R. Gibling, and M. C. Rygel, 2011, Alluvial facies evolution during the Palaeozoic greening of the continents: Case studies, conceptual models and modern analogues: *Sedimentology*, v. 58, no. 1, p. 220–258, doi:10.1111/j.1365-3091.2010.01215.x.
- Desjardins, P. R., L. A. Buatois, B. R. Pratt, and M. G. Mángano, 2012, Forced regressive tidal flats: Response to falling sea level in tide-dominated settings: *Journal of Sedimentary Research*, v. 82, no. 3, p. 149–162, doi:10.2110/jsr.2012.18.
- Embry, A., 2009, *Practical sequence stratigraphy*: Calgary, Alberta, Canada, Canadian Society of Petroleum Geologists, 79 p.
- Fello, N., S. Lüning, P. Storch, and J. Redfern, 2006, Identification of early Llandovery (Silurian) anoxic palaeodepressions at the western margin of the Murzuq Basin (southwest Libya), based on gamma-ray spectrometry in surface exposures: *GeoArabia*, v. 11, p. 101–118.
- Franco, A., R. Perona, R. Dwyianti, F. Yu, S. Helal, J. Suarez, and A. Ali, 2012, NC186 Block, Murzuq Basin: Lessons learned from exploration, *in* M. J. Salem, I. Y. Mriheel, and A. S. Essed, eds., *The geology of southern Libya: Tripoli, Libya*, Earth Science Society of Libya, p. 37–50.
- Ghienne, J.-F., M. Deynoux, G. Manatschal, and J.-L. Rubino, 2003, Palaeovalleys and fault-controlled depocentres in the Late-Ordovician glacial record of the Murzuq Basin (central Libya): *Comptes Rendus Geoscience*, v. 335, no. 15, p. 1091–1100, doi:10.1016/j.crte.2003.09.010.
- Gibert, J. M. de, E. Ramos, and M. Marzo, 2011, Trace fossils and depositional environments in the Hawaz Formation, Middle Ordovician, western Libya: *Journal of African Earth Sciences*, v. 60, no. 1–2, p. 28–37, doi:10.1016/j.jafrearsci.2011.01.010.
- Gibling, M. R., and N. S. Davies, 2012, Palaeozoic landscapes shaped by plant evolution: *Nature Geoscience*, v. 5, no. 2, p. 99–105, doi:10.1038/ngeo1376.
- Gingras, M. K., J. A. MacEachern, and S. E. Dashtgard, 2012, The potential of trace fossils as tidal indicators in bays and estuaries: *Sedimentary Geology*, v. 279, p. 97–106, doi:10.1016/j.sedgeo.2011.05.007.
- Hall, P. B., M. BJORØY, I. L. Ferriday, and Y. Ismail, 2012, Murzuq Basin source rocks, *in* M. J. Salem, I. Y. Mriheel, and A. S. Essed, eds., *The geology of southern Libya: Tripoli, Libya*, Earth Science Society of Libya, v. 2, p. 63–84.
- Hallet, D., 2002, *Petroleum geology of Libya*: Amsterdam, Elsevier, 503 p., doi:10.1016/B978-0-444-50525-5.X5000-8.
- Harris, P. T., and A. D. Heap, 2003, Environmental management of clastic coastal depositional environments: Inferences from an Australian geomorphic database: *Ocean and Coastal Management*, v. 46, no. 5, p. 457–478, doi:10.1016/S0964-5691(03)00018-8.
- Harris, P. T., A. D. Heap, S. M. Bryce, R. Porter-Smith, D. A. Ryan, and D. T. Heggie, 2002, Classification of Australian clastic coastal depositional environments based upon a quantitative analysis of wave, tidal, and river power: *Journal of Sedimentary Research*, v. 72, no. 6, p. 858–870, doi:10.1306/040902720858.
- Johnson, H. D., and C. T. Baldwin, 1996, Shallow siliciclastic seas, *in* H. G. Reading, ed., *Sedimentary environments: Processes, facies and stratigraphy*: Oxford, Blackwell Science, p. 232–280.
- Kenrick, P., C. Strullu-Derrien, and R. L. Mitchell, 2015, The origins of land plants communities (abs.): The rise and

- fall of photosynthate: Evolution of plant/fungus interactions from paleobotanical and phylogenomic perspectives: Botony Symposium, Edmonton, Alberta, Canada, July 28, 2015.
- Kenrick, P., C. Strullu-Derrien, and R. L. Mitchell, 2016, The early fossil record of land plants and their environment (abs.): Colonization of the Terrestrial Environment: 38th New Phytologist Symposium, Bristol, United Kingdom, July 25–27, 2016.
- Klitzsch, E. H., 2000, The structural development of the Murzuq and Kufra basins—Significance for oil and mineral exploration, *in* M. A. Sola and D. Worsley, eds., Geological exploration in Murzuq Basin: Geological Conference on Exploration in the Muzuq Basin, Sabha, Libya, September 20–22, 1998, p. 143–150, doi:10.1016/B978-044450611-5/50009-X.
- Le Heron, D. P., O. Sutcliffe, K. Bourgie, J. Craig, C. Visentin, and R. Whittington, 2004, Sedimentary architecture of Upper Ordovician tunnel valleys, Gargaf Arch, Libya: Implications for the genesis of a hydrocarbon reservoir: *GeoArabia*, v. 9, p. 137–160.
- Lyell, C., 1832, Principles of geology: London, John Murray, v. 2, 586 p.
- Mángano, M. G., L. A. Buatois, R. Astini, and A. K. Rindsberg, 2014, Trilobites in early Cambrian tidal flats and landward expansion of the Cambrian explosion: *Geology*, v. 42, no. 2, p. 143–146, doi:10.1130/G34980.1.
- McDougall, N., and M. Martin, 2000, Facies models and sequence stratigraphy of Upper Ordovician outcrops in the Murzuq Basin, SW Libya, *in* M. A. Sola and D. Worsley, eds., Geological exploration in Murzuq Basin: Amsterdam, Elsevier, p. 223–236, doi:10.1016/B978-044450611-5/50012-X.
- McDougall, N. D., M. Bellik, and J. M. Jauregui, 2011, Sedimentology and sequence stratigraphy of the Ordovician section in the Gassi-Touil-Gassi Chergui-In Amedjane area (abs.): 5th Algerian Oil and Gas Energy Week, Oran, Algeria, May 21–25, 2011.
- McDougall, N. D., D. Wloszczowski, and K. Sharky, 2008, Ordovician plays on the Arabian and Saharan platforms: A comparison (abs.): AAPG International Conference and Exhibition, Cape Town, South Africa October 26–29, 2008, accessed July 19, 2019, http://www.searchanddiscovery.com/abstracts/html/2008/intl_capetown/abstracts/472196.htm?q=%2BtextStrip%3Awloszczowski.
- Nichols, G., 2017, Challenging orthodoxy: Is the present the key to the past?: *The Sedimentary Record*, v. 15, no. 3, p. 4–9, doi:10.2110/sedred.2017.3.4.
- Odenwald, S., 2018, SpaceMath@NASA, accessed February 2, 2018, <https://spacemath.gsfc.nasa.gov/>.
- Ramos, E., M. Marzo, J. M. de Gilbert, K. S. Tawengi, A. A. Khoja, and N. D. Bolatti, 2006, Stratigraphy and sedimentology of the Middle Ordovician Hawaz Formation (Murzuq Basin, Libya): *AAPG Bulletin*, v. 90, no. 9, p. 1309–1336, doi:10.1306/03090605075.
- Rider, M., 2004, The geological interpretation of well logs, 2nd ed. (revised): Sutherland, United Kingdom, Rider-French Consulting, 280 p.
- Shalbak, F., 2015, Paleozoic petroleum systems of the Murzuq Basin, Libya, Ph.D. thesis, Universitat de Barcelona, Barcelona, Spain, 203 p.
- Vos, R. G., 1981, Sedimentology of an Ordovician fan delta complex, Western Libya: *Sedimentary Geology*, v. 29, no. 2–3, p. 153–170, doi:10.1016/0037-0738(81)90005-1.
- Walker, R. G., and A. G. Plint, 1992, Wave- and storm-dominated shallow marine systems, *in* R. G. Walker and N. P. James, eds., Facies models: Response to sea level change: Waterloo, Ontario, Canada, Geological Association of Canada, p. 219–238.
- Williams, G. E., 2000, Geological constraints on the Precambrian history of Earth's rotation and the Moon's orbit: *Reviews of Geophysics*, v. 38, no. 1, p. 37–59, doi:10.1029/1999RG900016.



Sedimentary architecture of a Middle Ordovician embayment in the Murzuq Basin (Libya)

Marc Gil-Ortiz^{a,*}, Neil David McDougall^b, Patricia Cabello^{a,c}, Mariano Marzo^{a,c}, Emilio Ramos^{a,c}

^a Institut de Recerca Geomodels, Universitat de Barcelona, c/Martí i Franquès s/n, 08028, Barcelona, Spain

^b Consultant clàstic sedimentològic, Madrid, Spain

^c Departament de Dinàmica de la Terra i de l'Oceà, Facultat de Ciències de la Terra, Universitat de Barcelona, c/Martí i Franquès s/n, 08028, Barcelona, Spain

ARTICLE INFO

Keywords:

Gondwana
Middle Ordovician
Nonactualism
Basin architecture
Shallow marine
Marginal marine

ABSTRACT

The Hawaz Formation comprises a siliciclastic, shallow to transitional marginal marine succession, deposited on the north-western cratonic margin of Gondwana during the Middle Ordovician. This unit is well documented in the north central part of the Murzuq Basin, where it is often dramatically truncated by Late Ordovician glaciation unconformities, generating a major discontinuity, not only in the studied area but also across the whole Saharan Platform of North Africa. The Hawaz Formation is particularly relevant as one of the two major oil-bearing reservoirs in the Murzuq Basin. However, Late Ordovician erosion ensures that its present configuration bears very little relation to the original sedimentary architecture and, consequently, there is a need for a detailed large-scale correlation and sedimentary reconstruction of the Hawaz in order to improve subsurface management of this reservoir unit. The present study was developed from a previous sedimentological characterization of the Hawaz Formation, based on subsurface data provided by 35 wells. This sedimentological background provided the basis for the reconstruction of the sedimentary architecture of this unit by means of eight correlation panels oriented along both sedimentological dip (NNW-SSE) and strike (WSW to ENE). In addition, a series of Gross Depositional Environment (GDE) maps were also generated with the aim of providing insight into the lateral distribution of facies belts within the framework of a sequence stratigraphic-based reservoir zonation. The results of this study suggest that the Hawaz Formation was deposited in a relatively protected or embayed shoreline with multiple bays/estuaries as the main entry points for sediment into the basin, most likely influenced by the effects of pre-existing north-northwest to south-southeast Pan-African structures controlling local accommodation space and reactivated during Ordovician times. Correlation panels and GDE maps also show the Hawaz Formation to be an extensive and continuous reservoir across the studied area, deposited in a broadly extensive subtidal to intertidal paralic environment, with very few or possibly no modern sedimentary analogues.

1. Introduction

Exploration in the Murzuq Basin began in 1950's with the first hydrocarbon discovery made by Exxon in 1957. However, it was not until some 25 years later that the basin became an emerging hydrocarbon province after attention shifted to the Sirte Basin following a number of big discoveries before returning in response to political changes. This was especially so from the late 1980's to 1990's when many significant discoveries were made such as the El Sharara fields in the mid 1980's by Rompetrol and the Elephant Field (El Feel Field) in 1997 by LASMO (Fig. 1). Repsol and partners took over the operatorship of Rompetrol's

licenses in 1997 and subsequently undertook an intensive exploratory program, mainly over the central Murzuq exploratory licenses (NC115 and NC186; Fig. 1) focused on the most obvious and distinctive closures, making several significant discoveries, both in Upper and Middle Ordovician sandstones, between 1998 and 2006 (Ron Martín et al., 2016). The high exploration success rate encouraged a period of near-continuous exploration activity for Ordovician targets. However, despite the increasing maturity of the basin several key geological issues remain unresolved in both the Upper Ordovician Mamuniyat and Middle Ordovician Hawaz Formations. This is highlighted by the observation that, despite significant exploratory success, more than 20 dry holes

* Corresponding author.

E-mail address: mgilorti7@alumnes.ub.edu (M. Gil-Ortiz).

have been drilled in the last 10 years (Ron Martín et al., 2016).

An extensive collection of papers was reviewed by Sola and Worsley (2000) with the aim of summarizing the state of knowledge in the Murzuq Basin. These were followed by a series of more recent publications, encouraged by the growing interest in this basin (i.e. Anfray and Rubino, 2003; Ghienne et al., 2003; Le Heron et al., 2004; Le Heron et al., 2006; Ramos et al., 2006; Boote et al., 2008; Abouessa and Morad, 2009; Gibert et al., 2011; Abouessa, 2012; Franco et al., 2012; Ghienne et al., 2012; Ron Martín, 2016; Shalbak, 2015; Bataller et al., 2019; Gil-Ortiz et al., 2019).

The current study area lies within the north central part of the Murzuq Basin (SW Libya), mostly covered by Quaternary aeolian deposits associated with two major ergs or sand seas and only at the margins, or along the central Messak Escarpment, are the Paleozoic and Mesozoic deposits observed outcropping (Fig. 1).

Much effort has been devoted to better understanding the reservoir architecture of the oil-prone glaciogenic Upper Ordovician Mamuniyat Formation (McDougall and Martin, 2000; Le Heron et al., 2004, 2006, 2010; Ghienne et al., 2003, 2012; Girard et al., 2012; Bataller et al., 2019), whilst the underlying and also oil-bearing Middle Ordovician Hawaz Formation has not received comparable attention and is still, in a number of key aspects, poorly understood. The limited continuity of this formation, a reflection of the often-spectacular end-Ordovician glacial paleorelief, presents a challenge to the interpretation of this reservoir in terms of large-scale sedimentary architecture and the lateral connectivity of facies belts. The few studies that have been carried-out to date are based mainly on outcrop data from the neighbouring area of the Gargaf High and/or very limited subsurface data (Vos, 1981; Anfray and

Rubino, 2003; Abouessa and Morad, 2009; Ramos et al., 2006; Gibert et al., 2011; Abouessa, 2012; Franco et al., 2012). This limited database and the challenging subsurface expression of the Hawaz Formation, in the form of isolated paleohighs or “buried hills” (Khoja et al., 2000) highlights the necessity of generating large-scale, regional correlations based on a robust sedimentological model.

The Middle Ordovician Hawaz Formation is mainly represented by tidal-influenced transitional to shallow marine deposits (Ramos et al., 2006; Gibert et al., 2011; Gil-Ortiz et al., 2019). Shallow marine tide-dominated environments are typically represented by mixed sand- and mud-prone systems restricted to estuaries, tidal flats, or tide-dominated deltas (Boyd et al., 1992; Dalrymple, 1992; Dalrymple et al., 1992, 2012, 2015; Dalrymple and Choi, 2007; Desjardins et al., 2012a; Harris et al., 2002; Harris and Heap, 2003). The combined effect of fluvial currents, waves and tides provide an effective system of sediment sorting and accumulation of sand-prone deposits in nearshore settings. These depositional environments offer notable reservoir potential for the oil and gas industry, which has devoted significant exploration effort in the search for incised valley fill and deltas in the subsurface, given the excellent reservoir quality properties and areal extension of the related delta front, subtidal and fluvio-tidal deposits.

The dominant facies present characteristic and ubiquitous tidal sedimentary structures, suggesting a protected to semi-protected, marginal to shallow marine environment, rather than an exposed wave-dominated coast, or a fluvial-dominated environment. A paleo-embayment or paleo-estuary are also possible depositional settings for the Hawaz Formation, despite the lack of such coastal features as major incisions or valleys apparent on seismic or outcrops (Ramos et al., 2006;

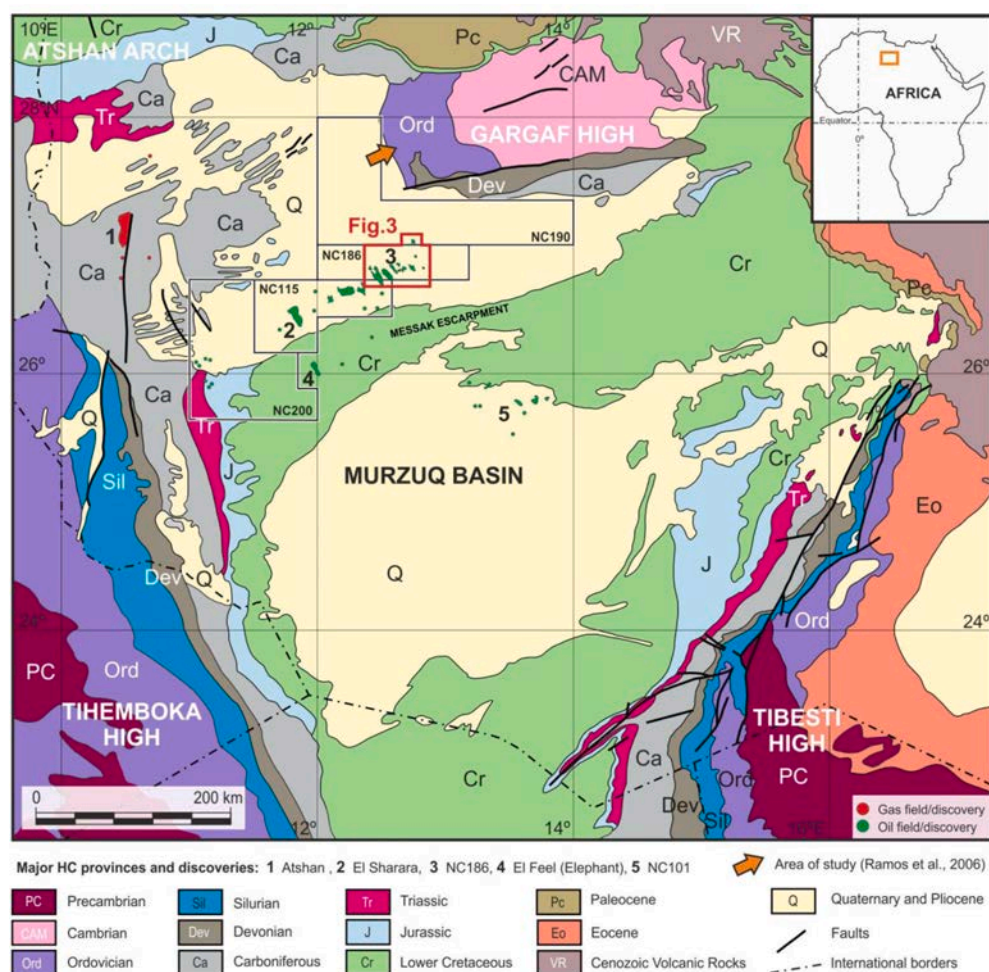


Fig. 1. – Geological map of the Murzuq Basin. Note the main structures forming the boundaries of this basin, the Atshan Arch to the northwest, the Gargaf High to the north and the Tihemboka and Tibesti highs to the southwest and southeast respectively. Note also the main exploration concessions and the major hydrocarbon provinces in the Murzuq Basin after Hallet and Clark-Lowes (2016). The area of interest represented in Fig. 3 is highlighted by the red polygon. The outcrop area studied by Ramos et al. (2006), referred to in this paper is also highlighted with an orange arrow in the Gargaf High area. After Marzo and Ramos (2003, personal communication) and Shalbak (2015). (For interpretation of the references to colour in this figure legend, the reader is referred to the Web version of this article.)

Gil-Ortiz et al., 2019). However, by combining different data sources, we have suggested that the factors controlling sedimentation of the Hawaz Formation could differ significantly from those associated with modern marginal marine to shallow marine depositional environments (Gil-Ortiz et al., 2019). These sediments were deposited before vascular land plants were established, so the lack of vegetation providing river bank stabilization, the extensive shallow cratonic seas present on the northern margin of Gondwana during the Middle Ordovician, higher tidal ranges associated with a shorter distance between the Earth and the Moon and a characteristic ichnofacies assemblage not found in present day ecosystems, are most likely the key factors suggesting a rather different depositional system to its closest modern equivalents (Gil-Ortiz et al., 2019).

The main goal of this project is the reconstruction of the detailed sedimentary architecture of the Hawaz Formation in the north central Murzuq Basin (SW Libya), based on the spatial distribution and vertical stacking of facies associations and a genetic or sequence stratigraphic-based zonation, capable of providing a robust tool for stratigraphic correlations. An updated non-actualistic depositional model, supported by large-scale, regional well correlations and Gross Depositional Environment (GDE) maps are also presented in order to justify the presence, stacking and spatial distribution of facies belts in this area. The results of this study will hopefully prove useful in exploration and improve management of the subsurface Hawaz reservoir in this highly productive basin, together with potential strategic CO₂ storage portfolios.

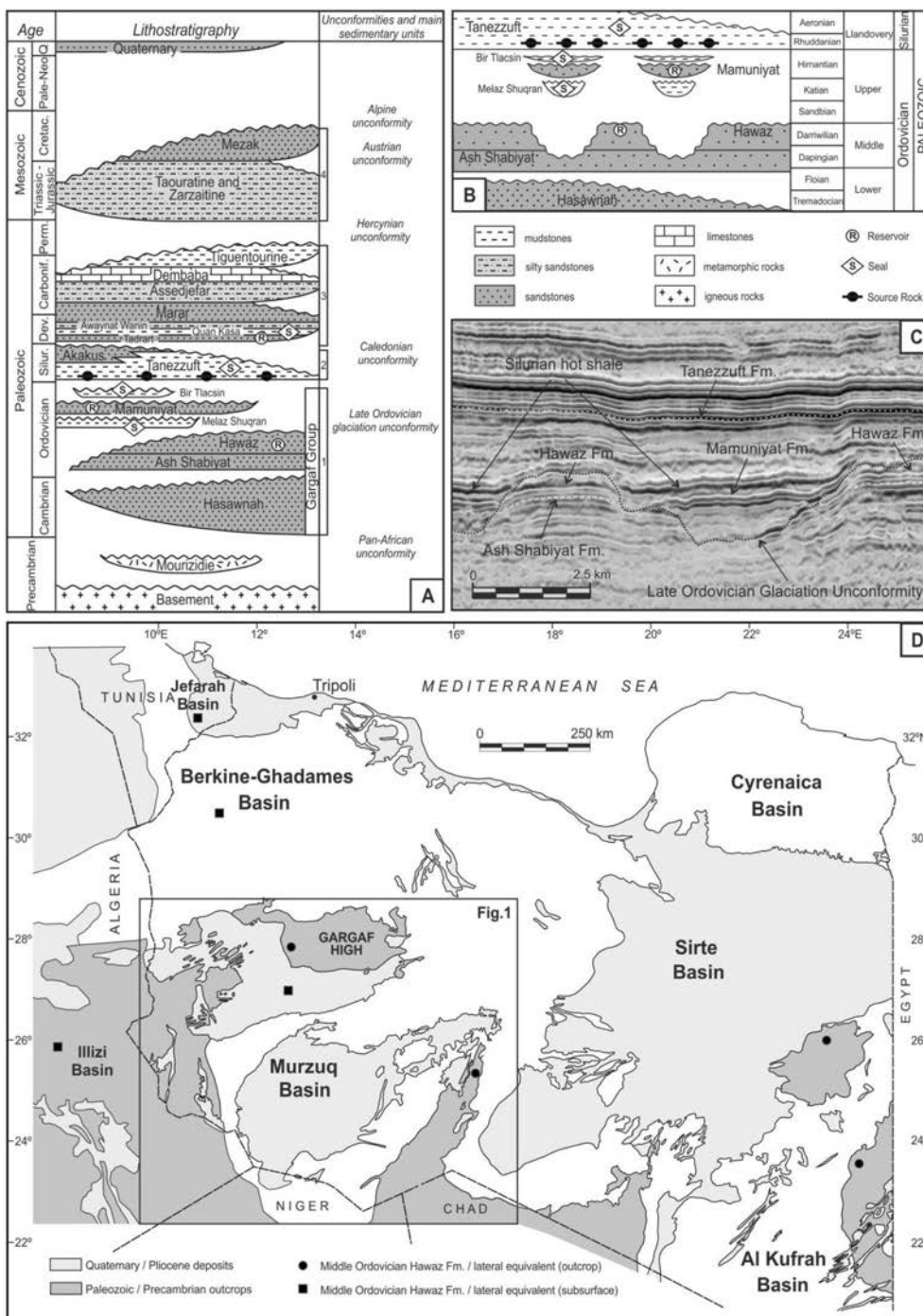


Fig. 2. – Murzuq Basin stratigraphy and architecture. A) Stratigraphic chart summarizing the lithostratigraphy of the Murzuq Basin highlighting the main stratigraphic units and major basin-scale unconformities. 1 = Cambrian–Ordovician; 2 = Silurian (Silur.); 3 = Devonian (Dev.)–Carboniferous (Carbonif.); 4 = Mesozoic. B) Wheeler diagram showing the lithostratigraphic to chronostratigraphic relationships of the Ordovician and Lower Silurian succession in the area of study. C) Seismic line showing the typical geomorphological profile of the Ordovician succession in the form of paleo-highs and paleovalleys. D) Regional map showing the inferred areal extension of the Hawaz Fm. and its Middle Ordovician lateral equivalents based on locations in the surface (outcrops) and subsurface of the neighbouring basins/areas where this succession has been identified beyond the Murzuq Basin. The location corresponding to Fig. 1 is also highlighted. The main petroleum systems elements are also represented in Fig. 2-A, -B. Cretac. = Cretaceous; Dev. = Devonian; Fm. = Formation; Pale-Neo = Paleogene–Neogene; Perm. = Permian; Q = Quaternary. Modified from Gil-Ortiz et al. (2019).

2. Geological setting

2.1. The Murzuq Basin

During early Paleozoic times, the African craton was part of the Gondwana supercontinent. Paleogeographic reconstructions (cf. Matte, 2001; Cocks and Torsvik, 2002; Kuhn and Barnes, 2005), suggest northwest Africa was located on the western-northwestern margin of Gondwana supercontinent during the Ordovician. The region appears to have been a very low gradient shallow marine shelf located south of the Iapetus Ocean, where a semi-continuous facies tract can be observed across the larger North African cratonic margin (Boote et al., 1998). According to Klitzsch (2000), sedimentation in the eastern sector (Libya) of the Sahara was controlled by the development of a north-south to north-northwest–south-southeast-oriented extensional system of horsts and grabens, forming wide elongate troughs and basinal areas during the Cambrian and the Early–Middle Ordovician times.

One of these areas was the Murzuq Basin, whose present-day geometry bears little relation to the broader and larger pre-existing sedimentary basin that existed during the Paleozoic. The Paleozoic succession of this basin is an erosional remnant of a large continental margin (Saharan Platform) which originally extended along the north-western margin of the Gondwana supercontinent (Davidson et al., 2000). Its present extent reflects several periods of uplift and unroofing during the late Paleozoic, Mesozoic, and Cenozoic, which, together, are responsible for its modern architecture and present basin geometry, which according to Boote et al. (1998) was formed mostly by mid-Cretaceous Austrian tectonism followed by intra-Cenozoic uplift/exhumation that exposed the pre-existing basin. The current basin is composed of a central Cretaceous depression bounded to the northwest by the Atshan Arch, the Gargaf High to the north, and the Tihemboka and Tibesti (Mourizidie-Dor el Gussa) highs to the southwest and southeast, respectively (Fig. 1). These structural highs were formed by multiphase tectonic uplifts ranging from the middle Paleozoic to Cenozoic, although the main periods of uplift and erosion occurred during the

late Carboniferous (Hercynian), mid-Cretaceous (Austrian), early Cenozoic (Alpine) orogenic cycles (Fig. 2-A) and subsequent intra-Cenozoic exhumation.

Several geological events are imprinted on the stratigraphic record of the Murzuq Basin and some of them can be recognized as basin-scale unconformities within the sedimentary infill. Most of these were tectonically-controlled (Craig et al., 2008) and correspond to the Pan-African, Caledonian, Austrian and Hercynian tectonic phases (Fig. 2-A). The Taconic unconformity is also widely recognized and corresponds to the remarkable basal glacial erosional surface marking the base of the Late Ordovician glaciation (Fig. 2-A). Other unconformities can also be recognized within the sedimentary record and mainly correspond to younger Alpine cycle, with minor impact on the Paleozoic section in the central Murzuq Basin. Within this framework, Boote et al. (2008), comment on the implications for the Paleozoic petroleum system elements, such as overburden removal, source rock maturity and reservoir quality due to diagenesis triggered by successive uplift events and unroofing of Mesozoic series and should be considered in future opportunities in hydrocarbon exploration. This combination of major tectonic events, key regional unconformities and the lithostratigraphic sub-division of the Murzuq Basin succession is reflected in Fig. 2-A, which is a data synthesis derived from Bellini and Massa (1980); Aziz (2000), Davidson et al. (2000), Echikh and Sola (2000), Craik et al. (2001) and Ramos et al. (2006).

The basement is composed of high-grade metamorphic and plutonic rocks, as well as low-grade metamorphic rocks of Precambrian age (Mourizidie Formation). The top of the basement is typically recognized and bounded by the Pan-African unconformity, which is overlain by the first main sedimentary unit of the lower Paleozoic (Fig. 2-A).

Above the Pan-African unconformity, the sedimentary infill of the Murzuq Basin can be subdivided into four main units: (1) Cambrian–Ordovician, (2) Silurian, (3) Devonian–Carboniferous and (4) Mesozoic (Fig. 2-A), which commonly are covered by large Quaternary aeolian deposits in the central part of the basin. The Cambrian–Ordovician succession or main sedimentary unit 1, also known as the

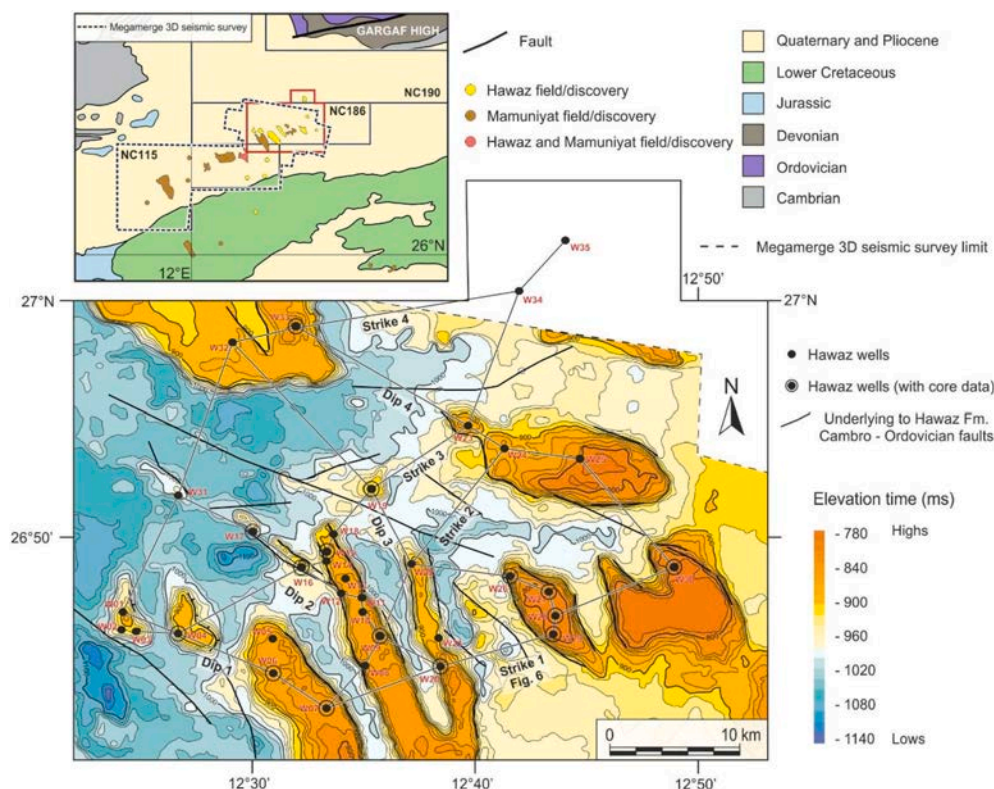


Fig. 3. – Area of study and dataset location. See in the upper left corner of this figure a close-up view from Fig. 1 showing the main study area (NC186 concession) and two adjacent exploration concessions, NC115 and NC190, as well as the main discoveries made in this area classified by their main reservoir, Hawaz or Mamuniyat. Note the limit of the 3D seismic survey (“Megamerge 3D seismic survey”) available in both the area of study and surrounding concessions. The red polygon highlighted here corresponds to our area of study whilst the map below is a two-way time contour map representing an interpreted top Hawaz surface from Bataller et al. (2019), flattened on an intra-Silurian horizon in the area of study. Note also the superposition of the underlying basement-linked, apparently non-displacing, Cambro-Ordovician faults on this map and their relationship with paleovalley boundaries, interpreted from seismic data. Also see the location of the 35 wells used in this study differentiated by the presence or absence of core data, together with the location of the correlation panels presented in this paper as well as the location of the seismic section shown in Fig. 6. (For interpretation of the references to colour in this figure legend, the reader is referred to the Web version of this article.)

Gargaf Group (after Burolet, 1960), comprises, from bottom to top, the Hasawnah, Ash Shabiyat, Hawaz, Melaz Shuqran, Mamuniyat and Bir Tlacin Formations (Fig. 2-A), including the two most important oil-bearing reservoirs in the Murzuq Basin.

There are two petroleum systems in the Murzuq Basin (Boote et al., 1998; Davidson et al., 2000; Shalbak, 2015) both involving the basal Silurian hot-shale source rock of the Tanezzuft Formation (Lüning et al., 2000, 2003; Fello et al., 2006; Belaid et al., 2010; Hall et al., 2012; Meinhold et al., 2013). The main petroleum system is associated with the Middle and Upper Ordovician sandstones of the Hawaz and Mamuniyat reservoirs respectively, bounded by a deeply incised unconformity related to the Late Ordovician glaciation (Fig. 2-C); both sealed by a thick succession of the Tanezzuft Formation shales (Fig. 2). The other petroleum system, considered as secondary, due to the non-commercial discoveries made to date, is composed of the basal Devonian sandstones as reservoirs and the intra-Devonian shales as the seal (Hallet, 2002; Shalbak, 2015).

2.2. The Hawaz Formation

The Hawaz Formation was originally defined by Massa and Collomb (1960) as the entire sandy Ordovician succession outcropping in the Gargaf area, bounded by two unconformities on top of the Hasawnah Formation and below the Melaz Shuqran or the Mamuniyat Formations. Later, Collomb (1962) subdivided the Hawaz Formation into three members: a) "Tigillites inferieurs", b) "Gres intermediaries" and c) "Tigillites superieurs", referring to basal and upper successions highly bioturbated with *Skolithos* traces (Droser, 1991) separated by a cross-bedded sandstone member. Subsequently, Havlicek and Massa (1973) introduced the term Ash Shabiyat Formation for the lower and part of the middle member from the former subdivision by Collomb (1962) creating the current lithostratigraphic sub-division for the Middle Ordovician succession (Fig. 2-A).

The age of the Hawaz Formation is defined by reference to the acritarch and chitonozoan data of Molyneux et al. (1996) and Paris (1990, 1996), complemented by data from Tunisia and Algeria (Vecoli, 1999). An internal study by Robertson Research International Limited from wells W04, W28, W29, W27, W32 and W35 of the present area of study (Fig. 3), Miles (2001, 2003, unpublished results) confirms the best evidence for the age of the Hawaz Formation comes from the lower part of the unit where top *Stelliferidium striatulum* and *S. cortinulum* indicate an age no younger than the Llandeilo stage. Other acritarch datums within the Hawaz Formation suggest a Llanvirnian or older age, justified by the tops of *Dicrodiacrodium ancoriforme* and *Franke longiuscula*. The bases of *Villosacapsula irrorata* and *V. setosapellicula* indicate an age no older than upper Arenig, Fenn stage, on the basis of extensive data from the neighbouring Algerian basins. This is supported by the bases of *Frankea breviscula* and *Frankea saribernardensis*. Thus, we can assume an Upper Arenig to Upper Llanvirn range (according to the traditional Ordovician British series), for the Hawaz Formation, which correlates with the Late Dapingian to Late Darriwilian stages (Fig. 2-B) of the current International Chronostratigraphic Chart.

The Hawaz Formation is recorded in the subsurface of the Murzuq Basin as a siliciclastic dominated succession, slightly more than 200 m in thickness (Table A.1), mainly composed of fine-grained quartz arenites and arkosic arenites with subordinate sub-lithic arenites (Gil-Ortiz et al., 2019). It is considered as an excellent reservoir, with mean measured porosities of up to 25.7% and modal values of 15–16% into the best reservoir sections of the middle Hawaz. Horizontal permeabilities can reach 900–1000 mD, although values are most commonly between 0.2 and 150 mD (Shalbak, 2015). Depositional facies, together with diagenesis, have an important impact on reservoir quality as documented by Abouessa and Morad (2009). Some of these diagenetic processes are related to near-surface eogenetic alterations, mediated by meteoric pore waters resulting in kaolinization of framework silicates and formation of small amounts of pyrite by marine pore waters.

Table 1

– Lithofacies scheme for the Hawaz Formation.

Sandstones (S)	Non burrowed	Sx1: Large scale cross-bedded sandstones Sx2: Small to medium scale cross-bedded sandstones Sl: Parallel-laminated sandstones Sxl: Cross-laminated sandstones Sr: Ripple cross-laminated sandstones Sv: Massive sandstones
	Burrowed (b)	Sxb: Burrowed cross-bedded sandstones Sxlb: Burrowed cross-laminated sandstones Srb: Burrowed ripple cross-laminated sandstones Sb: Burrowed sandstones with Siphonichnus MSb: Burrowed sandstones with feeding ichnofauna HS: Sandy heterolithics HSb: Burrowed sandy heterolithics HM: Muddy heterolithics HMB: Burrowed muddy heterolithics
Sandy Heterolithics (HS)		
Muddy Heterolithics (HM)		

Subsequently, sandstones were also affected by deeper diagenetic processes related to the presence of feldspar, illite and high dickite/kaolinite ratios, which are considerably higher in the subsurface than in outcrops probably due to a longer residence time and/or deeper burial conditions before final exhumation. In addition, there was also a significant phase of quartz overgrowth cementation in response to pressure dissolution of quartz grains, mechanical and chemical compaction (mesogenetic conditions). Finally, sandstones were affected by telogenetic alterations related to calcitization of mesogenetic siderite, oxidation of pyrite and formation of goethite, only identified in outcrop samples by Abouessa and Morad (2009) in this last case.

Several depositional models have been proposed for the Hawaz Formation (Vos, 1981; Anfray and Rubino, 2003; Ramos et al., 2006; Abouessa and Morad, 2009; Gil-Ortiz et al., 2019) all framed in a transitional to shallow marine setting. Gibert et al. (2011) identified up to 11 ichnogenera in the outcropping series of the Hawaz Formation on the Gargaf High, which are closely linked with both lithofacies and depositional environments. In broad terms, nearshore to shoreface facies are characterized by a dense 'Pipe rock' fabric dominated by *Skolithos* and *Siphonichnus* fossil traces, whereas storm-dominated heterolithics are characterized by horizontal deposit-feeding *Cruziana* ichnofossils.

Paleocurrents interpreted from image log tools suggest that there is a dominant flow direction toward the north-northwest with certain subordinate paleocurrents in the opposite direction related to tidal-flood currents effect. This trend would be mostly in accordance with large-scale sedimentary structures measured by Ramos et al. (2006) from outcrops of the Gargaf High (Fig. 1).

The architecture of the Hawaz Formation now observed in the subsurface and outcrop reflects deep Late Ordovician erosional incision by north-northwest-to west-flowing glaciers during the Hirnantian (Ghinne et al., 2003; Le Heron et al., 2004; Ramos et al., 2012), eroding deeply down into the Hawaz and even the underlying Ash Shabiyat Formation. This event generated a distinctive stratal geometries architecture comprising a series of paleovalleys and paleohighs (Fig. 2-C, 6). This paleorelief makes any correlation between the remnant Hawaz paleohighs a challenging task.

The Middle Ordovician Hawaz succession is well represented in the Murzuq Basin although its lateral equivalents extend for hundreds of kilometres along North Africa and can most definitely be recognized in the neighbouring areas of the Al Kufrah Basin to the east (Seilacher et al., 2002; Le Heron et al., 2010), in the Jefarah and Berkine-Ghadames basins to the north (Dardour et al., 2004; Jabir et al., 2021) and in the Illizi Basin to the west (McDougall et al., 2008a, 2008b, 2011bib_McDougall_et_al_2008a, 2008bbbib_McDougall_et_al_2011), where the equivalent is known as the In Tahouite Formation (or Unit III-3 in the subsurface), on the basis of published data (Fig. 2-D).

This study is therefore focussed on only a small part of a broader and widespread facies complex deposited during the Middle Ordovician in

the north-western part of the Gondwana cratonic margin.

3. Database and methods

The present study is based on a previous sedimentological characterization of the Hawaz Formation (Gil-Ortiz et al., 2019) using sub-surface data from 35 wells located across the north central sector of the Murzuq Basin (Fig. 3). This previous study was carried out with a broad spectrum of data types including conventional wire-line logs (gamma ray, density, neutron and sonic), slabbed core descriptions and high resolution core images, a fullbore formation microimager image logs

(FMI) for most of the wells, palynological data from a limited number of wells (Miles, 2001, 2003, unpublished results) and comparisons to outcropping equivalents studied by Ramos et al. (2006) on the Gargaf High (Fig. 1). After well data synthesis, description and interpretation, fifteen lithofacies (Table 1) were identified and grouped into seven facies associations interpreted as deposits of a nearshore intertidal to subtidal environment. On the basis of this interpretation, it was then possible to create a genetic sequence stratigraphic-based framework and zonation for the Hawaz Formation (Gil-Ortiz et al., 2019).

This previous work provided the framework for reconstructing the sedimentary architecture of the Hawaz Formation in the study area by

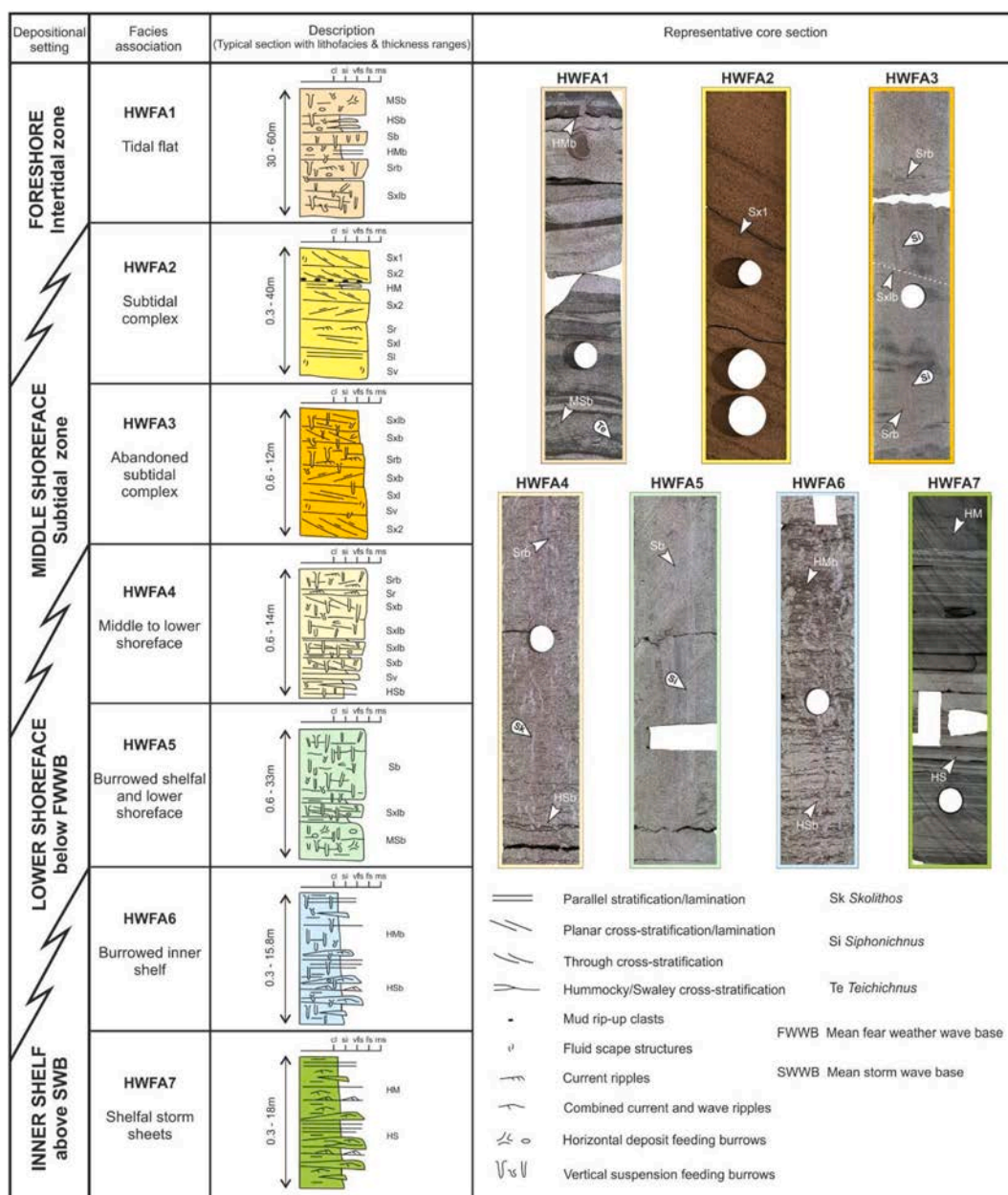


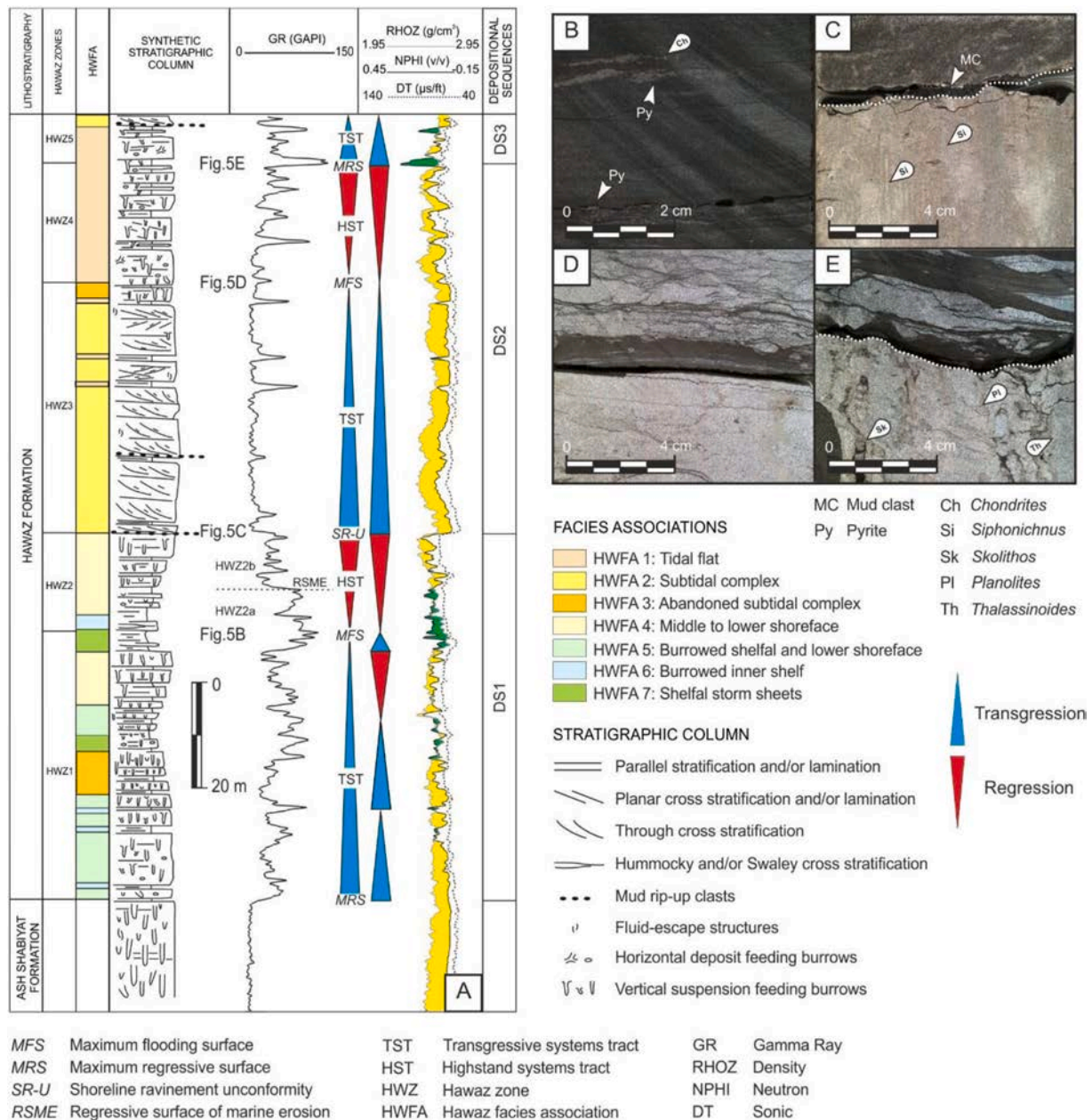
Fig. 4. – Summary of facies associations and interpreted depositional settings. Description includes typical sections and thickness ranges (in metres) with the main lithofacies composing each facies association. See also representative core sections extracted from wells W09 (HWFA1, HWFA2, HWFA4, HWFA6), W15 (HWFA5, HWFA7) and W33 (HWFA3). Interpretation in terms of depositional environment is also included. Cl = clay; fs = fine sandstone; HM = muddy heterolithic; HMB = burrowed muddy heterolithic; HS = sandy heterolithic; HSb = burrowed sandy heterolithic; HWFA = Hawaz facies association; ms = medium sandstone; MSb = burrowed sandstone with feeding ichnofauna; Sb = burrowed sandstone with Siphonichnus; si = silt; Sl = parallel-laminated sandstone; Sr = ripple cross-laminated sandstone; Srb = burrowed ripple cross-laminated sandstone; Sv = massive sandstone; Sx1 = large-scale cross-bedded sandstone; Sx2 = small-to medium-scale cross-bedded sandstone; Sxb = burrowed cross-bedded sandstone; Sxl = cross-laminated sandstones; Sxlb = burrowed cross-laminated sandstone; vfs = very fine sandstone. Modified from Gil-Ortiz et al. (2019).

means of eight correlation panels (Fig. 3) following both depositional strike (west-southwest to east-northeast) and dip (north-northwest to south-southeast), as inferred from paleocurrent data and the depositional model for the Hawaz Formation (Gil-Ortiz et al., 2019). Given the deeply incised character of top Hawaz, we chose the base of the Silurian Tanezzuft Fm. as a regional stratigraphic datum, when constructing the stratigraphic correlation sections. The Tanezzuft is, however, diachronous in character, onlapping the incised Hawaz paleotopography. As such, the age of this horizon may be Rhuddanian, Aeronian or even younger, so that at least two stages may be missing locally, constituting a hiatus of up to 7 ma. However, despite this limitation, the base of Tanezzuft Fm. is a distinctive, commonly well-preserved surface

represented by a bright negative reflector in seismic (Fig. 2-C) covering the entire underlying Ordovician succession (Fig. 6).

This datum was flattened across all wells in order to obtain a detailed, consistent picture of Hawaz Formation architecture at the time of deposition and to correlate facies belts more easily across the study area. Only the more complete Hawaz sections preserved on the paleotopographic highs were correlated, whereas the erosional gaps caused by subsequent Late Ordovician glaciation, filled with the Upper Ordovician lithostratigraphic units (Melaz Shuqran, Mamuniyat and Bir Tlacin Formations), were deliberately ignored in order to avoid Hawaz interpretation gaps between wells in the correlation panels.

In addition, a series of Gross Depositional Environment (GDE) maps



were also created (Figs. 15–18) to illustrate the lateral extent of facies belts within the framework of sequence stratigraphic-based zones. These maps merge data from the isolated control points to predict the pre-erosional distribution of facies associations, depositional environments, and the presence of reservoir facies by describing the sedimentological evolution of the studied area, extrapolating the facies associations between wells, on the basis of their relative proportions within genetic sequences. Thus, following the sequence stratigraphic framework presented in Gil-Ortiz et al. (2019), a GDE map was created for each systems tract and its corresponding Hawaz zone (Fig. 5) except for the last transgressive systems tract (TST-DS3), which was excluded, through being partially or totally eroded by the Late Ordovician glacial unconformities in the studied area.

Some of the limits between depositional environments represented in these maps, may well be out of the scale of these representations considering that our area of study forms only a little part of a much larger and widespread regional facies complex deposited in a Middle Ordovician age, very low gradient cratonic margin. Nevertheless, we have opted to represent some of these changes in depositional environment on the margins of these maps, despite the lack of well data, provided that we had a regional insight from the variations in the proportions of facies associations in wells, suggesting a change in the trend of dominant facies belts, and/or complementary information from neighbouring areas. These maps are not a representation of a specific time but a synthesis of depositional trends during the period of time comprising each systems tract, with the aim of summarizing the main paleogeographic relationships found in each sequence stratigraphic package.

In summary, the methodology followed was 1) characterize lithofacies and facies associations in each control point mainly from both cores and image logs (FMI), 2) build a sequence stratigraphic framework for each well identifying potential correlatable systems tracts/stratigraphic zones, 3) correlate these sedimentary packages throughout the study area with a set of 8 correlation panels along sedimentary dip and strike direction, 4) calculate the relative proportions of facies associations for every well and systems tract and 5) extrapolate these data from wells to surrounding areas together with paleocurrents, insights from the conceptual sedimentary model and correlation panels interpretation for each systems tract or zone, within 4 different GDE maps.

4. Previous work

4.1. Facies associations and sedimentary model

The Hawaz Formation in the subsurface of the north central Murzuq Basin comprises fifteen lithofacies defined on the basis of lithologies and internal fabric (Table A.1), as observed in 35 wells (Fig. 3). This lithofacies scheme contains sandstones (S), muddy sandstones (MS),

heterolithic sandstones (HS) and heterolithic mudstones (HM), with a high density and diverse assemblage of sedimentary structures and variation in the degree and types of bioturbation (Gil-Ortiz et al., 2019). This scheme was compared with equivalent deposits in outcrop studied by Ramos et al. (2006) complemented with valuable observations on ichnofacies made by Gibert et al. (2011), both in the same area of the Gargaf High (Fig. 1), approximately 120 km distant from our area of study.

Based on the lithofacies scheme introduced by Gil-Ortiz et al. (2019), seven Hawaz facies associations (HWFA) were interpreted (Fig. 4), ranging from proximal to distal, tidal flat (HWFA1), subtidal complex (HWFA2), abandoned subtidal complex (HWFA3), middle to lower shoreface (HWFA4), burrowed shelfal and lower shoreface (HWFA5), burrowed inner shelf (HWFA6) and shelfal storm sheets (HWFA7).

HWFA1 was interpreted as tidal sand to mixed flat deposits, representing periods of high relative sea level in embayed coastal settings, although also present in interbay sub-environments during transgressive stages.

HWFA2 mainly composed of an amalgamated complex of sand bars, dunes and channels deposited in subtidal nearshore settings mainly during transgressions, it is the principal reservoir in the Hawaz (mean measured porosity of 11% and mean horizontal permeability of 125 mD from conventional core analysis).

HWFA3 was interpreted as the distal and/or low energy lateral equivalent of the subtidal complex, the product of the abandonment of the previous active subtidal channels and partially overlapping with tidal inlets and rip channels in nearshore settings.

HWFA4 was considered to be the deposits of a prograding middle to lower shoreface linked to regressive sand belts during sea level highstands.

HWFA5 represents deposition of sands and muddy sands in a lower shoreface to inner shelf environment.

HWFA6 was interpreted as the deposits of a low energy open marine inner shelf setting.

HWFA7 was interpreted as distal mixed sand to mud rich deposits related to storm events in a shelf environment.

The interpretation of these facies associations was based mainly on high resolution image logs calibrated with available core data and supported with complementary conventional wireline logs, including gamma ray, sonic, density and neutron, which provided valuable data on stacking patterns and clay content, which was especially helpful on those sections without core and, less commonly, without image log data.

On the basis of this work, the Hawaz Formation was interpreted as a broadly shallowing-upward succession, from nearshore marine inner shelf to marginal marine tidal flat deposits (Gil-Ortiz et al., 2019). This interpretation is also supported by palynological data, which distinguish different assemblages in the lower and upper part of the succession, grading from distal to proximal from bottom to top of this

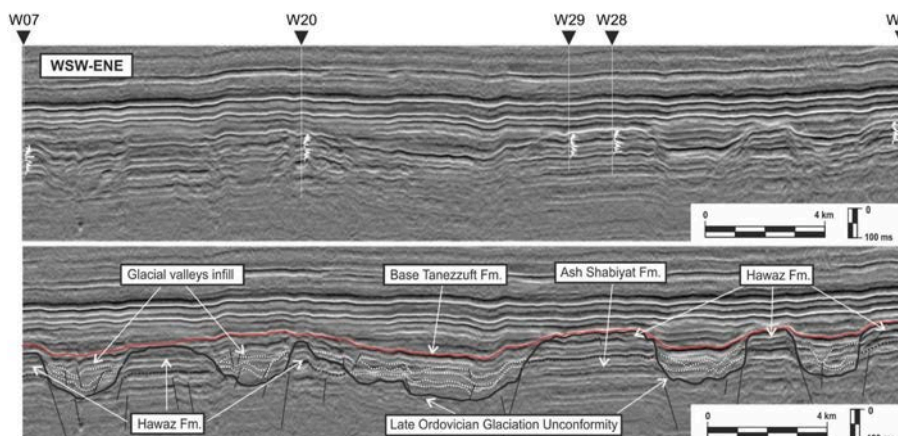


Fig. 6. – Hawaz Formation subsurface architecture. This seismic section across the area of study illustrates the subsurface Hawaz paleotopography and infill geometries incised by multiple erosional events during the Late Ordovician glaciation. Note the interpreted base Tanezzuft Fm., which was the datum selected for the construction of the correlation panels presented in this paper. The gamma ray signature of the Hawaz Formation is shown aligned with wells intersecting this seismic line. See also the normal faults bounding many of the paleohighs and the paleovalleys, presumably active during the Cambro-Ordovician. Both the location of the wells and the position of this seismic line are shown in Fig. 3.

lithostratigraphic unit. The lower section is characterized by moderate and diverse acritarch assemblages, including a number of complex acanthomorph taxa (Miles, 2001, 2003, unpublished results), sphaeromorph acritarchs and rare chitinozoans and cryptospores (Abuhmida and Wellman, 2017), typical of shallow inner shelf marine environments. In marked contrast, the upper section of the Hawaz is distinguished by a low diversity assemblage of acanthomorphic and sphaeromorph acritarchs (rare to absent), absence of chitinozoans and high recovery of leiospheres and cryptospores, a characteristic palynoflora of marginal marine settings (Miles, 2001, 2003, unpublished results; Abuhmida and Wellman, 2017).

Observations by Gil-Ortiz et al. (2019) suggests the Hawaz Formation was deposited in a tide-dominated environment evolving from a shallow open-marine setting, characterized by both storm- and tide-influenced facies, to a relatively protected subtidal to intertidal setting on an embayed shoreline. Based on paleocurrent data interpreted from image logs in the study area, the depositional system appears to have shifted from proximal coastal environments in the south-southeast to open marine settings toward the north-northwest. This trend was also in agreement with observations made by Ramos et al. (2006) in the outcrops of the Gargaf High.

In the building of a depositional model (Gil-Ortiz et al., 2019), we encountered significant difficulty in identifying a comparable modern analogue because of major differences in the factors controlling sedimentation, such as: 1) the absence of fauna and especially flora in subaerial environments during the Middle Ordovician, which directly impacts on coastal dynamics; 2) changes in relative sea level on a low gradient cratonic shelf during a global greenhouse period, which promoted very wide facies belts compared with most present-day moderate-to high-gradient depositional systems in a current global icehouse period; 3) the difference in tidal ranges triggered by the distance between Earth and the Moon, which 460 Ma ago were 13,000 to 18,000 km closer to each other with respect to the present day, with respectively higher tidal ranges and extent of flooded areas during high tide periods; and 4) the characteristic ichnofacies observed in the Hawaz Formation, not present in modern environments due to the extinction of the originating paleofauna. In view of this, an updated non-actualistic sedimentary model was developed to better explain the depositional patterns observed in the Hawaz Formation as a result of the current work and discussed in a later section (Fig. 19).

4.2. Sequence stratigraphy of the Hawaz Formation

Based on the vertical changes observed in facies associations and their stacking patterns, some depositional trends and genetic stratigraphic units can be clearly identified in the Hawaz Formation. These patterns, defined correlatable system tracts bounded by high frequency sequence boundaries and flooding surfaces, which in turn reflect changes in sediment supply, relative sea level and accommodation. Following an adapted sequence stratigraphic approach from Embry (2009) a series of genetic-based sedimentary packages can be identified in the Hawaz Formation (Gil-Ortiz et al., 2019).

Although a number of high-frequency sequences can be identified, a simplified scheme of three major, possibly 3rd order, depositional sequences (DS1-DS3) is presented (Fig. 5-A). Each sequence is composed of their respective systems tracts bounded by key surfaces, which were then used to create a five-fold reservoir zonation scheme (HWZ1 to HWZ5), each zone equivalent to an individual systems tract (Fig. 5-A), in order to provide a more robust genetic correlation avoiding a tempting purely lithostratigraphic correlation in an apparent Hawaz "layer cake" succession.

The first and oldest depositional sequence (DS1) is widely preserved across the study area and corresponds to a transgressive systems tract (TST) defined as reservoir zone 1 (HWZ1). It comprises several stacked fining-upward parasequences overlying the contact with the underlying Ash Shabiyat Formation, which is interpreted as a maximum regressive

surface (MRS) and sequence boundary (Fig. 5-A). This sedimentary package is dominated by retrogradational shelfal and lower shoreface deposits commonly interlayered with a higher order progradational package, but culminating with an abrupt lithological change to argillaceous facies representing a regionally extensive flooding surface associated with shelfal storm deposits (Fig. 5-A). This flooding surface is commonly represented by the highest GR peak in the entire Hawaz succession and is interpreted as a maximum flooding surface (MFS), normally represented by black shales, moderately rich in organic matter, and with evidence of anoxic conditions as represented by pyritic nodules and ichnofossils such as *Chondrites*, characteristic of low-oxygen environments (Fig. 5-B). This MFS represents a major shift in stacking patterns and the beginning of a regressive package dominated by inner shelf to middle shoreface deposits, interpreted as the highstand systems tract (HST) of DS1 and reservoir zone 2 (HWZ2). This package can commonly be divided into two sub-zones (HWZ2a and HWZ2b) separated by a regressive surface of marine erosion (RSME) representing a sharp shift in relative sea level and shallowing of facies associations, interpreted as a response to a forced regression and consequently a lower wave base (Fig. 5-A).

The base of the second depositional sequence (DS2) is marked by a sharp erosive surface interpreted as a shoreline ravinement unconformity and sequence boundary (Fig. 5-A, -C), generated during early transgressive stages by the action of tides and waves just after relative sea level fall. This surface also constitutes the base of the TST (Fig. 5-A) and reservoir zone 3 (HWZ3). This package is commonly dominated by subtidal complex deposits and constitutes the main reservoir of the Hawaz Formation. The DS2 package continues with a marked change in depositional environment, from subtidal complex or abandoned subtidal complex, to tidal flat deposits (Fig. 5-A). This change is interpreted in terms of a MFS in a nearshore environment and is commonly represented by thin, condensed, argillaceous deposits (Fig. 5-D). Above, the remainder of the package is dominated by tidal flat deposits with common intercalated ephemeral distributary channels and constitutes the HST of this DS2, and reservoir zone 4 (HWZ4) (Fig. 5-A). This HST is interpreted to represent a bay infilling with prograding sand to mixed tidal flat deposits during a period of falling relative sea level. The upwards increase in shale content is typical for the low energy conditions associated with these tide-dominated environments together with a parallel decrease in the diversity of ichnofossils and the increased abundance of marginal marine palynofossils (Miles, 2001, 2003, unpublished results; Abuhmida and Wellman, 2017), both suggesting a more proximal domain.

The third depositional sequence (DS3) is rarely preserved after being typically stripped away during the Late Ordovician glaciation, and only the basal part is sometimes preserved locally (Table A.1). The onset of DS3 is marked by a change in depositional trend, from the underlying low energy mixed-argillaceous tidal flat deposits of the HST-DS2, to slightly higher energy and cleaner deposits of the same facies association (Fig. 5-A). No major unconformities are preserved although the contact between the underlying clay-rich tidal flat deposits and the subsequent cleaner sandstones tends to be erosive in character (Fig. 5-E) and is interpreted in terms of maximum regressive surface (MRS) and sequence boundary (Fig. 5-A). Commonly, subtidal complex deposits can be recognized in the uppermost section of some wells suggesting a slight deepening, and a new TST and reservoir zone 5 (HWZ5) (Fig. 5-A).

5. Results

5.1. Sedimentary architecture of the Hawaz Formation

The sedimentary architecture of the present day Hawaz Formation bears little relation to its configuration and depositional profile at the time of deposition. Its current architecture is characterized by a number of paleohighs separated by a set of northwest to southeast or west-east aligned paleovalleys in the area of study, generated by multiple

erosive episodes associated with the Late Ordovician Hirnantian glaciation (Figs. 3 and 6). This remnant subglacial paleorelief was subsequently infilled with Late Ordovician deposits, through multiple erosive and deposition events related to the advance and retreat of ice sheets, which might have accumulated more than 500 m of sediment at some locations (Fig. 6). The resultant paleotopography has remained largely unchanged since the late Ordovician, with only slight modifications during subsequent major tectonic events (Fig. 2-A).

Many of the paleohighs in this “buried” paleorelief are notably bounded by faults (Fig. 6), which follow a north-northwest to south-southeast trend, linked to Pan-African basement structures, apparently connected to lower intervals within the Cambro-Ordovician succession. It is suggested by some authors that the structural weaknesses and/or distribution of Pan-African fault-bounded basins in the zone might have acted as guides for the glacial erosion and also local glacio-isostatic fault reactivation during the Late Ordovician (Ghienne et al., 2003).

Although the separation between some paleohighs is barely a few kilometres (Figs. 3 and 6), others are ten or more kilometres apart, which makes any stratigraphic correlation a challenging task in this particular area of study.

After Gil-Ortiz et al. (2019) and supported by paleocurrent data obtained from image logs, the sedimentological model suggested for the Hawaz is a depositional system evolving from the south-southeast (proximal) to north-northwest (distal). With this as framework, we generated a series of eight correlation panels (Fig. 3), four along the direction of depositional dip (Figs. 7–10) to capture the main depositional changes across the study area as the system evolved, and four along the depositional strike (Figs. 11–14) to better capture lateral, alongshore variations within systems tracts.

The results of this work show that, in most wells, at least four sedimentary packages can be recognized across the study area. Although an

initial impression might suggest a “layer-cake” architecture, the correlations reveal that the Hawaz does in fact show a significant degree of internal heterogeneity. These four packages are related to several transgressive and regressive systems tracts, grouped into three depositional sequences (DS1-3) introduced in the previous section, which correspond to well-defined reservoir zones (HWZ1-4) (Fig. 5). In addition, the remnants of a fifth package corresponding to the last transgression into the Hawaz Formation (HWZ5) in DS3, are hardly preserved due to the Late Ordovician glaciation unconformities.

Based on key observations from correlations, we outline here the principal interpretations derived from first, dip correlation panels and second, strike-oriented correlation panels.

5.1.1. Dip-oriented correlations

From dip-oriented correlations, several key observations can be made. Firstly, from the lowermost HWZ1 reservoir zone (Fig. 5) it is apparent that there was a subtle deepening of the basin towards the NW inferred from the occurrence and increase in thickness of the most distal burrowed shelfal and lower shoreface (HWFA5), burrowed inner shelf (HWFA6) and shelfal storm sheets (HWFA7) facies associations in this direction. This is best developed in correlation panel Dip 3 between wells W32 and W19 (Fig. 9) and in correlation panel Dip 4 between wells W24 and W25 (Fig. 10), where a lateral facies change is observed, from shallower middle to lower shoreface (HWFA4) to burrowed shelfal and lower shoreface (HWFA5) deposits in a SE-NW trend, with an increased abundance of burrowed inner shelf (HWFA6) and also shelfal storm sheet deposits (HWFA7) towards the northwest. Also worthy of note is the presence of a distinctive and extensive (more than 15 km down dip) abandoned subtidal complex (HWFA3) towards the central and south-eastern part of the study area as seen in correlation panels Dip 2, 3 and 4 (Figs. 8–10) during the first main transgression of DS1. In

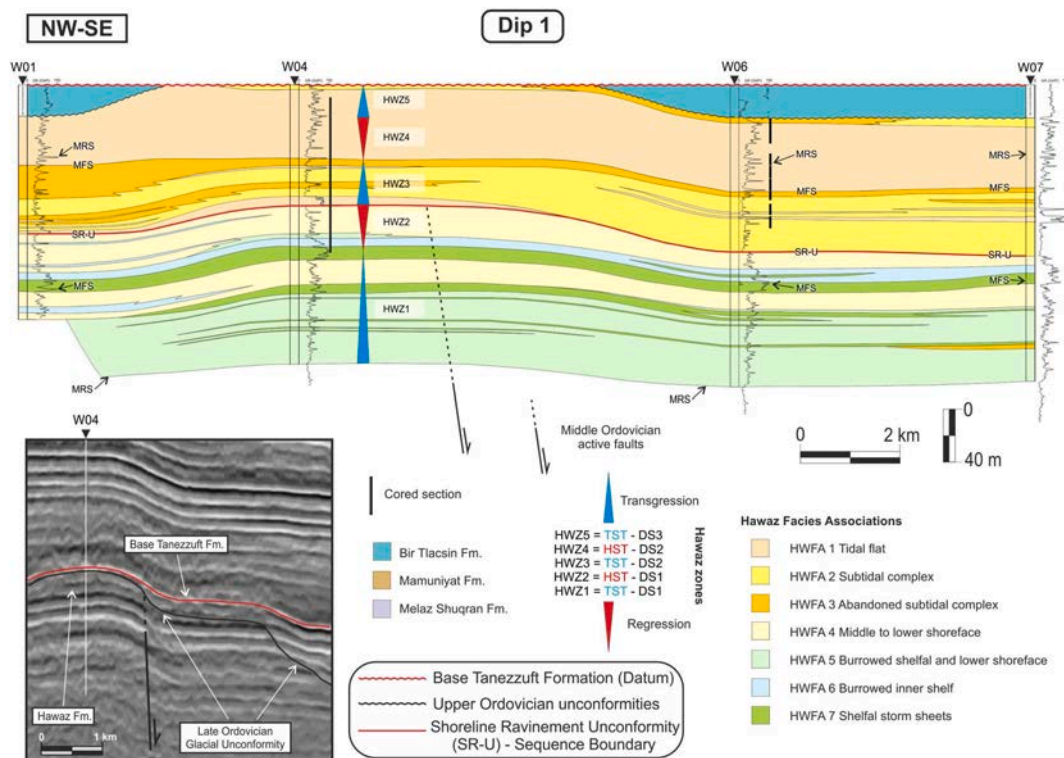


Fig. 7. – Correlation panel Dip 1. All the wells hang from the flattened base Tanezzuft Fm. datum. These are shown with their GR profile from 0 to 150 GAPI. Major transgressive and regressive cycles, systems tracts and Hawaz reservoir zones are also shown. A seismic section, oriented NW-SE around well W04, is also shown in the bottom left corner, highlighting the relationship of the paleohigh flank with respect to the bounding paleovalley normal fault and the Late Ordovician Glacial Unconformity. Also note the link between fault position and facies associations variations and slight variation in thickness represented above. DS = Depositional sequence; HST = Highstand systems tract; HWFA = Hawaz facies association; HWZ = Hawaz zone; MFS = Maximum Flooding Surface; MRS = Maximum Regressive Surface; TST = Transgressive systems tract.

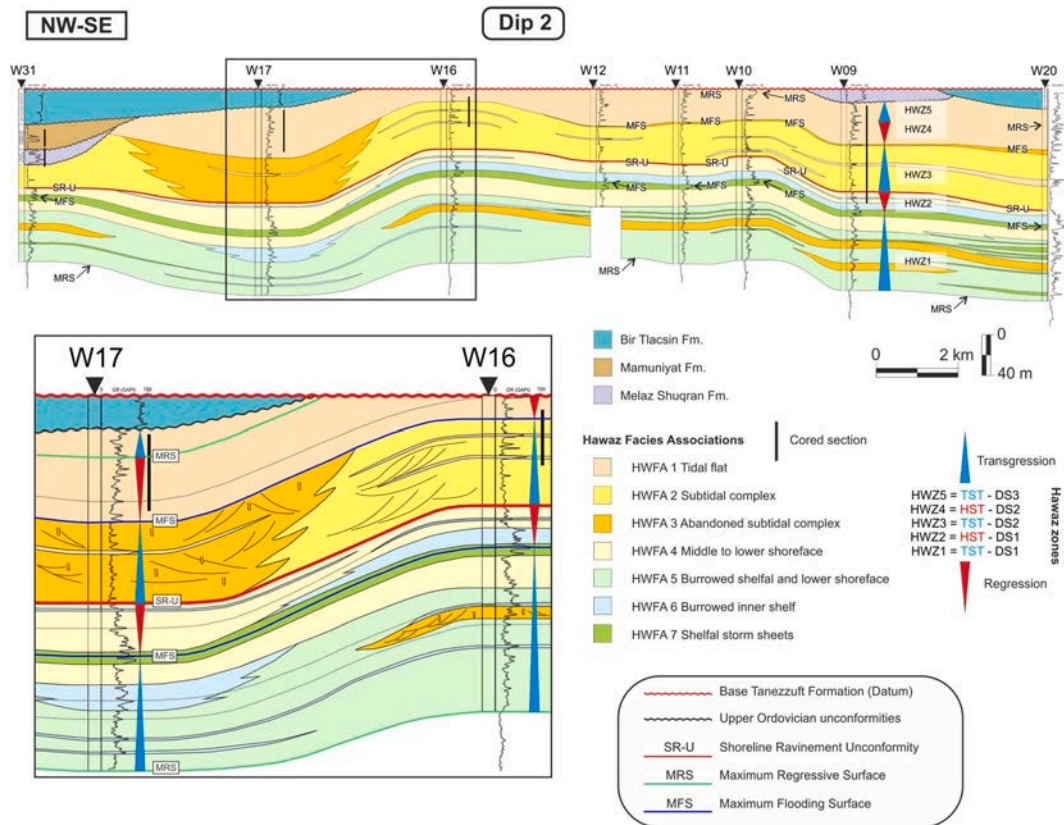


Fig. 8. – Correlation panel Dip 2. All the wells hang from the flattened base Tanezzuft Fm. datum. These are shown with their GR profile from 0 to 150 GAPI. Transgressive and regressive cycles corresponding to systems tracts and Hawaz reservoir zones are displayed. Note the enlargement of the stratigraphic correlation around wells W17 and W16 in the bottom left corner, showing an abrupt lateral facies change, especially for the middle section of the Hawaz Formation. DS = Depositional sequence; HST = Highstand systems tract; HWFA = Hawaz facies association; HWZ = Hawaz zone; TST = Transgressive systems tract.

addition, shelfal storm sheet deposits are present across the area, intercalated with shallower, burrowed shelfal and lower shoreface deposits, some of them forming relatively thick packages (around 15–20 m) in the lowermost part of the succession in the south-eastern sector and pinching-out towards the NW, likely representing tempestite lobes connected to shallower shoreface areas (Figs. 8 and 10).

The overlying package, corresponding to zone HWZ2 (Fig. 5), comprises three main facies belts; shelfal storm sheets (HWFA7), burrowed inner shelf (HWFA6) and middle to lower shoreface (HWFA4), respectively. Despite the significant areal extent of this package and its apparent high continuity over the entire area, internal differences are observed, which demonstrate deepening towards the NW with a progradational trend from SSE to NNW as can be seen in the north-western part of panels Dip 3 and 4 (Figs. 9 and 10), where burrowed inner shelf (HWFA6) and shelfal storm sheets (HWFA7) become more common and relatively thicker towards the NW.

Depositional Sequence 2 begins above a major shoreline ravinement surface with a relative sea level rise and deposition of the main reservoir of the Hawaz Formation in zone HWZ3 (Fig. 5), mainly comprising subtidal complex deposits (HWFA2). Firstly, correlation panel Dip 1 (Fig. 7) shows an abrupt decrease in depositional energy toward the western part of the studied area represented by wells W01 and W04, where a characteristic high energy, subtidal environment evolved to a lower energy abandoned subtidal setting. This trend is also apparent in the area of wells W17 (Fig. 8), W26 (Fig. 9) and, quite notably, W25 (Fig. 10). These lateral facies changes might be explained within the framework of distal, but active subtidal complexes, and/or their abandonment due to seasonal fluctuations in sediment supply and/or changes in accommodation space by oscillations in relative sea level (Dalrymple et al., 1992; Cattaneo and Steel, 2003; Dalrymple and Choi,

2007). Even major storms might play an important role in triggering subtidal channel switching and consequent abandonment (Dalrymple et al., 2012).

Depositional Sequence 2 culminates with a regressive section of tidal flat deposits (HWFA1) widely present across the entire study area. This section corresponds to reservoir zone HWZ4 (Fig. 5) and is extremely uniform in character, interrupted only by some ephemeral distributary channels and tidal creeks cutting the tidal flat deposits and embedded within this major facies association HWFA1.

Depositional Sequence 3 and reservoir zone HWZ5 (Fig. 5), which is often partially or totally eroded by the Late Ordovician unconformities, has not been evaluated here due to the limited preserved thickness and restricted lateral extent.

5.1.2. Strike-oriented correlations

Along strike, correlations show lateral facies changes within time-equivalent deposits. Some of the most remarkable observations are the significant variations in thickness and facies associations, presumably related to alongshore differences in accommodation space and sediment supply ratios. Many of these variations may well be related to the presence of a series of normal faults, the traces of which often coincide with the erosional limits of Late Ordovician paleovalleys as identified in seismic (Fig. 6). Whether these faults were active during deposition of the Hawaz is difficult to confirm but along strike changes in thickness and facies patterns are certainly suggestive.

These changes mainly occur in reservoir zones HWZ2 and HWZ3, corresponding to the HST-DS1 and TST-DS2 (Fig. 5), although the most significant variations appear in the main reservoir or zone HWZ3, characterized, not only by lateral facies changes but also thickness variations presumably linked to the above-mentioned faults.

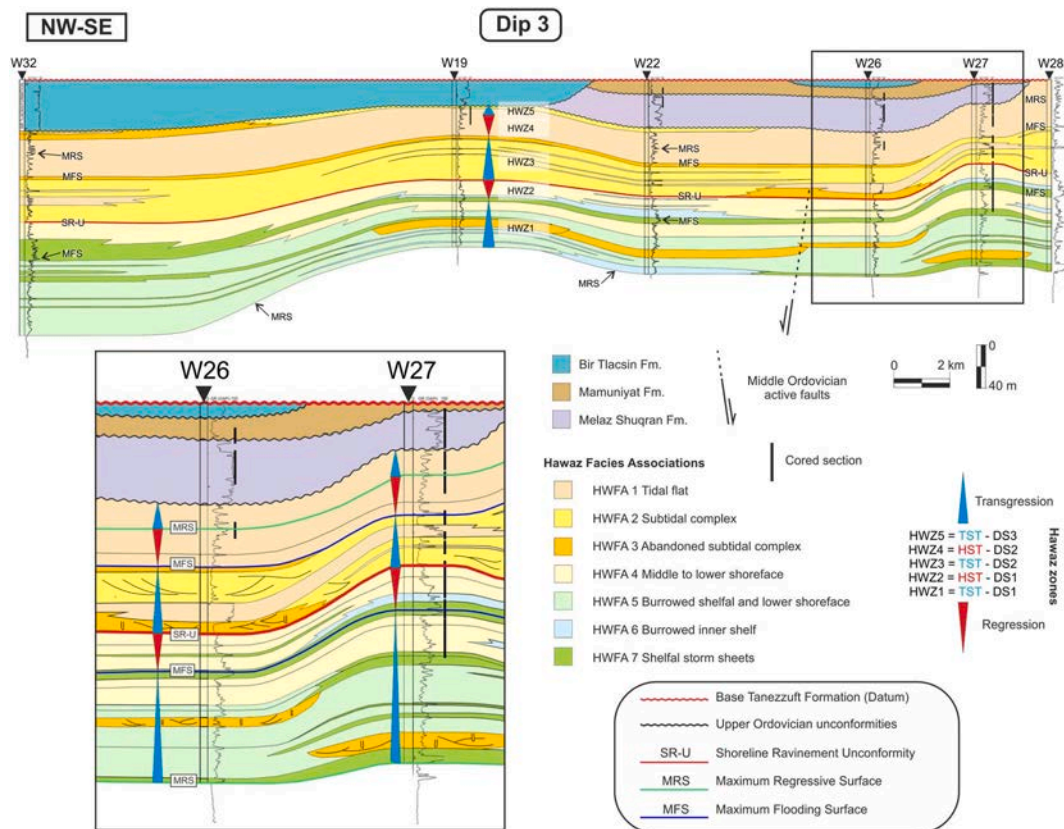


Fig. 9. – Correlation panel Dip 3. All the wells hang from the flattened base Tanezzuft Fm. datum. These are shown with their GR profile from 0 to 150 GAPI. Transgressive and regressive cycles corresponding to systems tracts and Hawaz reservoir zones are shown. See a close-up view of the stratigraphic correlation between wells W26 and W27 in the bottom left corner, showing a facies change, especially for the middle section of the Hawaz Formation, from subtidal complex deposits to the SE to abandoned subtidal complex deposits and thicker tidal flat deposits to the NW. DS = Depositional sequence; HST = Highstand systems tract; HWFA = Hawaz facies association; HWZ = Hawaz zone; TST = Transgressive systems tract.

Specifically, in the hanging wall of these potentially active faults, the HWZ3 succession is dominated by high energy, thicker subtidal complex deposits (HWFA2), whereas, in the footwall of these faults the equivalent succession tend to be more frequently represented by less energetic and thinner abandoned subtidal complex (HWFA3) and tidal flat (HWFA1) deposits. These variations in thickness and/or lateral facies changes can be seen in correlation panels Dip 1, between wells W04 and W06 (Fig. 7); Dip 3, between wells W22 and W26 (Fig. 9); Dip 4, between wells W25 and W30 (Fig. 10); in Strike 1 between wells W07 and W29, and between W29 and W30 (Fig. 11); in panel Strike 2, between wells W22 and W24, and especially between W07 and W22 (Fig. 12); in the central part of Strike 3, between wells W04 and W23 (Fig. 13); and finally, between W01 and W33 in correlation panel Strike 4 (Fig. 14). It is also possible that these faults were active during earlier periods of Hawaz deposition, at least since reservoir zone HWZ2. This is suggested by the relationship between deposition of more distal and thicker burrowed inner shelf (HWFA6) deposits in the hanging wall of these faults, compared to shallower and thicker middle to lower shoreface (HWFA4) deposits present in the footwall. This relationship can be seen in correlation panels Strike 1 between wells W20 and W29, and between wells W28 and W30 (Fig. 11), Strike 2 between wells W22 and W24 (Fig. 12) and Strike 3 between wells W19 and W23 (Fig. 13).

Several additional key observations from strike correlations are outlined as follows. Reservoir zone HWZ1 (Fig. 5) is dominated by burrowed shelfal to lower shoreface deposits (HWFA5) with a characteristic interlayered abandoned subtidal complex (HWFA3) present in the central and south-eastern part of the area of study, most probably related to distal subtidal complex deposits sourced from the SE, most notably in correlation panels Strike 2 and 3 (Figs. 12 and 13). Also, a

characteristic interval of storm sheet deposits, in the lowermost Hawaz, immediately overlying the Ash Shabiyat Fm., can be observed in the most eastern part of the study area (Figs. 11 and 12) as previously inferred from Dip correlation panels 3 and 4 (Figs. 9 and 10).

Reservoir zone HWZ2 (Fig. 5) shows important differences in thickness as observed in Strike panels 1, 2 and 3 (Figs. 11–13), presumably related to the activity of normal faults. In contrast, whilst the thickness and occurrence of middle to lower shoreface (HWFA4) deposits is notably higher in the west-southwest and central-eastern part of the study area, in the central to north-western areas the succession is dominated by distal burrowed inner shelf deposits (HWFA6) and shelfal storm sheets (HWFA7). Hence, active faulting may have controlled the spatial distribution of facies associations locally and perhaps slightly determine the shoreface profile.

As an alternative explanation to these alongshore variations, local differences in accommodation and/or energy in a broad exposed low gradient tidal shelf could have provided these lateral facies associations changes as well. The trigger for these variations in accommodation space and energy of the sedimentary system could be attributed to thermal subsidence and/or alongshore lateral migration of entry points of sediment into the basin.

Additional key observations of reservoir zone HWZ3 in strike correlation panels 3 and 4 (Figs. 13 and 14) show, not only variations in thickness, possibly linked to fault-generated accommodation space, but also a transition from subtidal complex deposits to lower energy abandoned subtidal complex and tidal flat deposits in footwall positions, as shown in panel Strike 3 in the area of wells W03, W04 and W34 (Fig. 13) and in panel Strike 4 around wells W01 and W34 (Fig. 14). A subtle increase in the abundance of abandoned subtidal complex deposits from

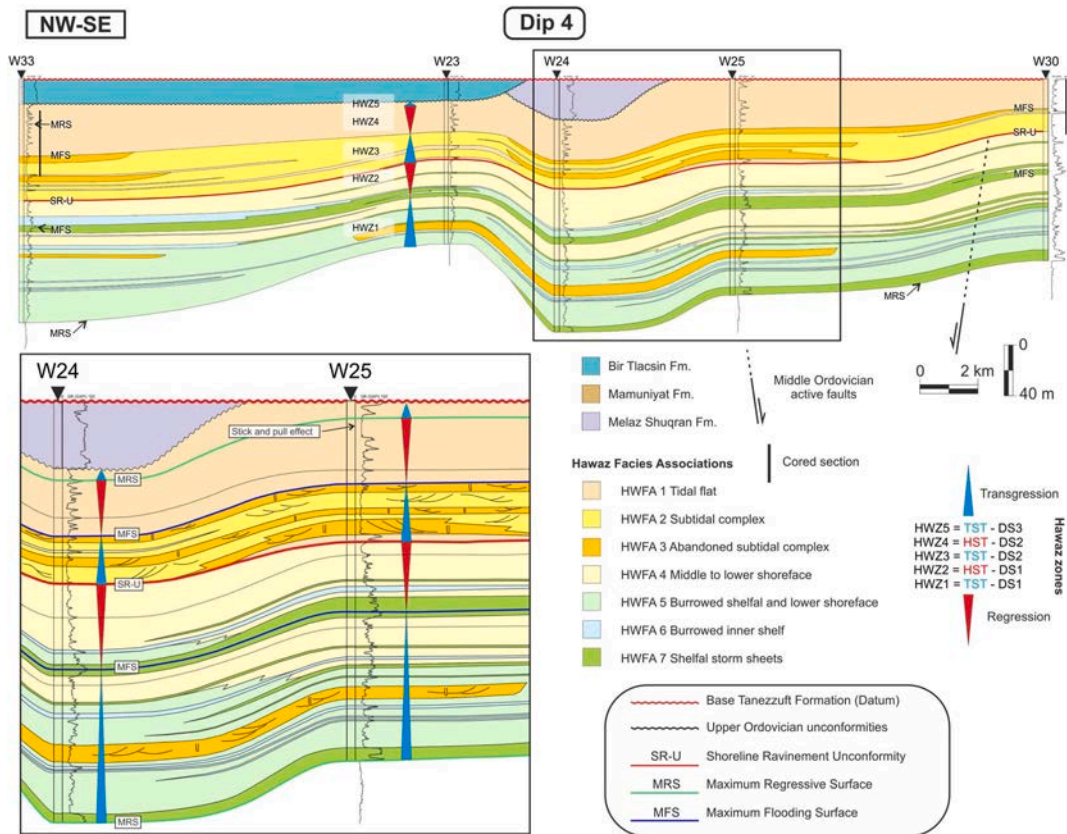


Fig. 10. Correlation panel Dip 4. All the wells hang from the flattened base Tanezzuft Fm. datum. These are shown with their GR profile from 0 to 150 GAPI. Principle transgressive and regressive cycles, corresponding to systems tracts and Hawaz reservoir zones are also displayed. An enlarged view of the correlation between wells W24 and W25 is presented in the bottom left corner, showing a distinctive lateral facies change from middle to lower shoreface deposits to the SE to burrowed shelfal and lower shoreface deposits to the NW in the lower section of the Hawaz Formation. Note also the significant accumulation of abandoned subtidal complex deposits in the middle Hawaz in well W25. DS = Depositional sequence; HST = Highstand systems tract; HWFA = Hawaz facies association; HWZ = Hawaz zone; TST = Transgressive systems tract.

south to north within HWZ3 zone may also suggest a slight deepening trend towards the north.

5.2. Paleogeographic reconstruction of the Hawaz Formation

5.2.1. Reservoir zone HWZ1 (TST-DS1; Fig. 15)

The HWZ1 reservoir unit comprises a 3rd order transgressive sequence, including two higher order transgressive cycles capped by a regressive sequence and culminating with a new transgressive cycle (Fig. 5). The proportion of facies associations calculated for this zone in each well, as well as the lateral distribution of these facies associations proved by the correlation panels, shows that there is a deepening trend from southeast to northwest based on the occurrence of shallower abandoned subtidal complex deposits (av. 7%) in the central to southeast areas evolving to distal burrowed inner shelf deposits (av. 5%) to the northwest, within a dominant background of a burrowed shelfal and lower shoreface environment (av. 53%) mostly dominating the area of study (Fig. 15). In addition, tempestites or storm sheets are generally widely present across the study area (av. 11%) as shown by most of the wells. Most of these storm deposits were most probably supplied to the shelf through subtidal channels as suggested by Fig. 15, although the exact location and geometries of such bodies are speculative as none have been drilled by any of the wells used in this study. Another explanation for some of these tempestites are sands ripped in mass by waves action in shallower waters and re-deposited further seaward during storm events; the combination of both processes is also possible. The wells W01, W12 and W21 (Fig. 15) did not penetrate the full interval and so are not representative.

5.2.2. Reservoir zone HWZ2 (HST-DS1; Fig. 16)

The overlying zone is characterized by an overall regressive sequence (Fig. 5) and dominated by middle to lower shoreface deposits grading upwards from areally extensive shelfal storm sheets and burrowed inner shelf packages. In fact, in terms of facies abundance, the middle to lower shoreface deposits are predominant (av. 59%) and significantly thicker prevailing over the shelfal storm sheets (av. 15%) and burrowed inner shelf (av. 23%) in the area of study. The lateral distribution of facies associations again suggests a deepening trend from the southeast toward the northwest. However, the presence of possible active normal faults, inferred from correlation panels and seismic data, might have played a significant role in the control of the lateral distribution of facies as shown in the lower central part of the map (Fig. 16), and in correlation panels strike 1, 2 and 3 (Figs. 11–13). These faults may have also influenced the paleobathymetric profile of the area, by creating accommodation space and allowing deeper water facies associations to dominate in the lows created by these structures. In marked contrast, shallower water locations in the west-southwest and central-eastern areas accumulated thicker successions of prograding middle to lower shoreface deposits (Fig. 16). As before, storm sheets are present across much of the studied area for this zone although they become more important towards the distal north-western areas. For example, in well W32 storm sheets form a 60 m thick package (Fig. 16). As in the case of zone HWZ1, it is assumed that the storm sands accumulated in lobes, were fed by subtidal channels connected to the middle and upper shoreface, although the exact location of these geobodies can only be speculatively represented in this map.

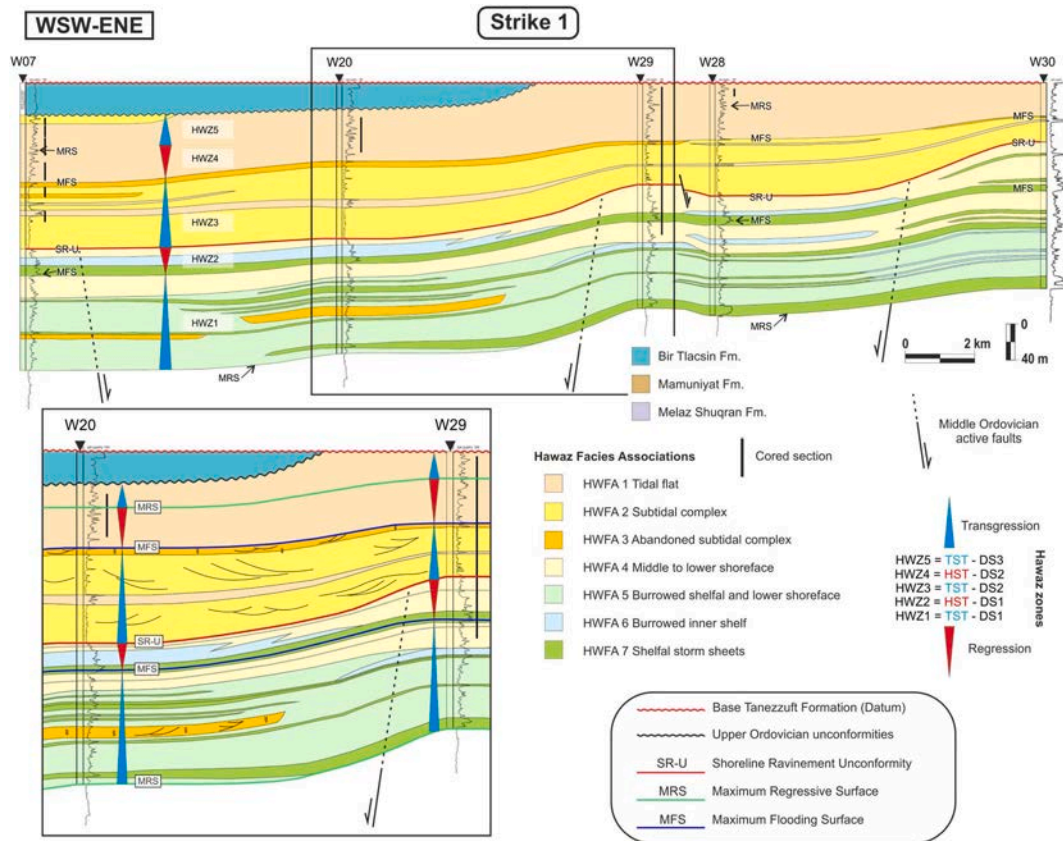


Fig. 11. – Correlation panel Strike 1. All the wells hang from the flattened base Tanezzuft Fm. datum. These are shown with their GR profile from 0 to 150 GAPI. The main transgressive and regressive cycles, systems tracts and Hawaz reservoir zones are shown. A close-up view of the stratigraphic correlation between wells W20 and W29 is included in the bottom left corner, showing the relationship between an inferred fault and its possible control on paleobathymetry. Note the lateral evolution from proximal HFWA4 to distal HFWA6 deposits in the HST of Depositional Sequence 1 and the growth in thickness of HFWA2 in the TST of Depositional Sequence 2 in the hanging wall of a Middle Ordovician active normal fault. DS = Depositional sequence; HST = Highstand systems tract; HFWA = Hawaz facies association; HWZ = Hawaz zone; TST = Transgressive systems tract.

5.2.3. Reservoir zone HWZ3 (TST-DS2; Fig. 17)

The succeeding zone was deposited during a transgressive stage dominated by subtidal complex deposits (Fig. 5) in a protected to semi-protected nearshore environment. From the proportions of facies associations and the interpretation of correlation panels, it is apparent that the zone comprises three main facies associations; the dominant subtidal complex (av. 71%), and the subordinate abandoned subtidal complex (av. 17%) and tidal flat deposits (av. 12%). Within this broad framework, the boundary between the subtidal and the intertidal zones may well have been conditioned by the presence and activity of NNW to SSE-trending normal faults as interpreted in Fig. 17. The thickness of the main reservoir facies may also have been controlled by both syndepositional activity on these faults and compensation associated with the pre-existing paleorelief left after deposition of underlying HST-DS1. This is demonstrated in correlation panels Strike 1, 2 and 3 (Figs. 11–13) where thicker sections of HWZ2 are sometimes associated with a notably thinner HWZ3 above. Another key observation is the apparent existence of two areas dominated by the lower energy abandoned subtidal complex and tidal flat deposits, respectively towards the SW and the NE (Fig. 17). These deposits may represent the margins of a bay or estuary, although neither major scours or incised valleys were observed in seismic nor more obviously proximal, fluvial deposits were identified in the studied area, although the presence of such features further to the SE is entirely possible. From paleocurrent data we infer a mean dominant flow towards the NNW, across most of the wells, most likely associated with the main sediment input and ebb tidal direction. Paleocurrent data also shows that wells in the north-western half of the map show an increase in bidirectionality of sedimentary structures, which suggests an

increase in the power of the subordinate flow, considered here as the effect of flood tides. Finally, it should be emphasized that the interpretation proposed for the north-western corner of this GDE map is purely speculative and driven, in the absence of any well data, by our sedimentary model (Fig. 19). Accordingly, it is entirely possible that the suggested shoreface deposits may occur much further towards the NW given that none of the wells found evidence of such distal facies associations within this unit in the studied area.

5.2.4. Reservoir zone HWZ4 (HST-DS2; Fig. 18)

This reservoir zone is mainly characterized by sandy to mixed tidal flat deposits across the whole area of study. It corresponds to the HST of the second 3rd order depositional sequence and shows a marked prograding trend from distal sandy tidal flat deposits to proximal mixed sandy and shaly tidal flat deposits (Fig. 5). The very low gradient of the Middle Ordovician cratonic margin allowed the progradation of these deposits for hundreds of kilometres across the studied area and very likely also further to south-eastern, more proximal areas. This facies association was drilled by all the wells in the study area, only interrupted by thin ephemeral distributary channels and tidal creeks embedded in an overall intertidal setting (Fig. 18). Some of these ephemeral distributary channels were identified in wells as 1–2 m thick, erosively-based, fining-upwards bodies comprising clean, cross-laminated to heterolithic sandstones. From image log data (FMI), paleocurrent directions were obtained for these channels and plotted in this GDE map (Fig. 18). The interpretation suggested for the north-western corner of this map, it should be emphasized, largely speculative, driven by the depositional model, but also by the evidence for barrier

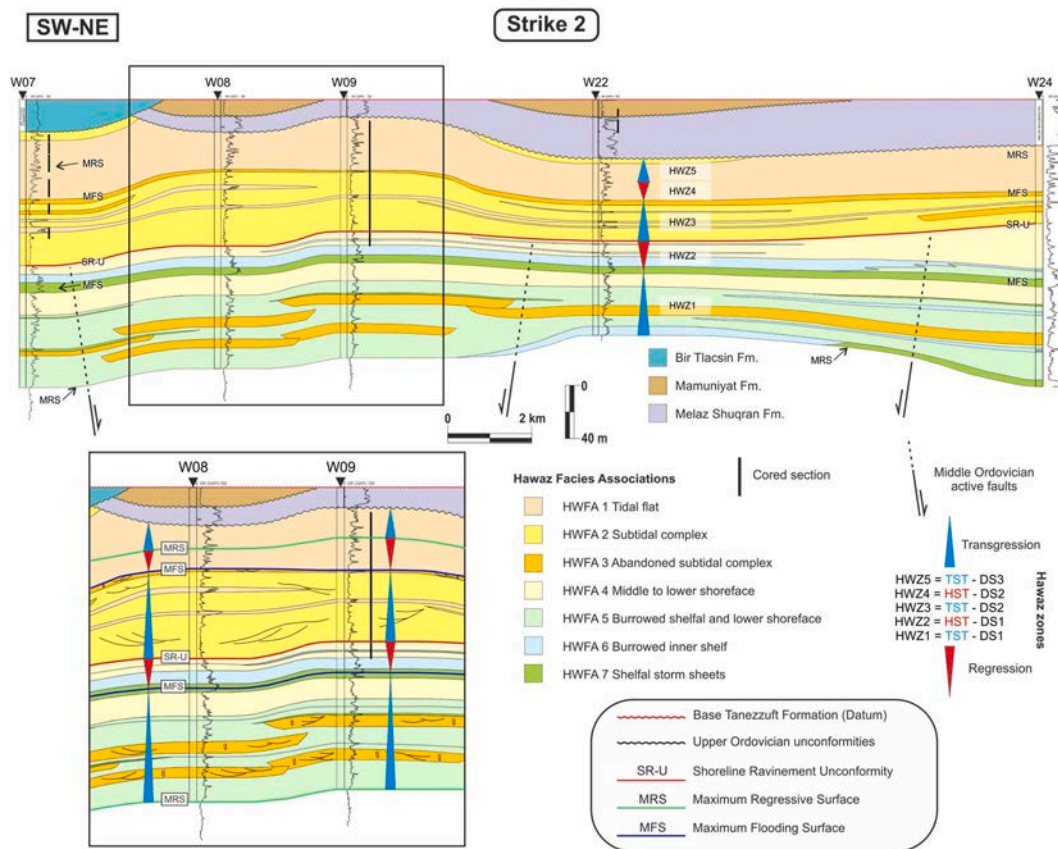


Fig. 12. – Correlation panel Strike 2. All the wells hang from the flattened base Tanezzuft Fm. datum. These are shown with their GR profile from 0 to 150 GAPI. Transgressive and regressive systems tracts and Hawaz reservoir zones are shown. An extension of the stratigraphic correlation between wells W08 and W09 is presented in the bottom left corner, showing the characteristic extensive abandoned subtidal complex deposits appearing in the TST of DS1. DS = Depositional sequence; HST = Highstand systems tract; HWFA = Hawaz facies association; HWZ = Hawaz zone; TST = Transgressive systems tract.

island and tidal inlets, based on sedimentological and ichnofacies assemblages, found by Ramos et al. (2006) and Gibert et al. (2011) for laterally equivalent deposits in the neighbouring Gargaf High (Fig. 1).

6. Discussion

The Hawaz Formation could be classified as a lithostratigraphic unit deposited in a clastic coastal depositional environment mainly controlled by tidal processes. From classification of major coastal depositional environments, developed by both Boyd et al. (1992) and Dalrymple et al. (1992) and based upon a comparison with modern coastal environments, the Hawaz Formation could be considered a composite sequence of transgressive tide dominated bay/estuarine facies and regressive tidal flats. However, this comparison assumes that modern fluvial, wave and tidal processes were similar to those in the past. Thus, there may be some limitations in the application of this approach when comparing Cambro-Ordovician or older systems with most present day nearshore depositional environments (Eriksson et al., 1998; Eriksson and Simpson, 2012).

These limitations and differences derive from observations made in this study, where factors controlling the sedimentation and the architecture of the Hawaz Formation might have been significantly influenced by at least four processes (Gil-Ortiz et al., 2019); most notably, 1) the absence of vegetation, responsible for stabilizing river banks and lateral migration of fluvial systems in modern coastal plain environments, and chemical weathering leading to clay generation before the “greening” of the continents (Davies and Gibling, 2010; Davies et al., 2011; Gibling and Davies, 2012; Kenrick et al., 2015, 2016; Kenrick et al., 2015; Bradley et al., 2018), 2) a much

warmer Greenhouse climate in the past and its control on relative sea level and shoreface dynamics (Nichols, 2017) together with a vast, low gradient cratonic shelf responsible for exceptionally broad facies tracts over wide paralic environments, and limited incision of valleys during lower base levels, 3) higher tidal ranges during early Paleozoic times due to a closer distance between the Earth and the Moon and the related potential sediment load of nearshore tidal currents (Williams, 2000), and 4) a characteristic, low diversity “Pipe rock” *Skolithos* (Droser, 1991) and *Cruziana* ichnofacies (Seilacher, 1970; Mángano et al., 1996, 2014; Mángano et al., 1996; Seilacher et al., 2002; Gibert et al., 2011; Mángano et al., 2014) unknown from any modern analogue, result of an already extinct marine paleofauna.

Several key observations made from the correlation panels and gross depositional environment maps presented in this paper, allowed us to improve the conceptual depositional models suggested for the Hawaz Fm. in previous works (Vos, 1981; Anfray and Rubino, 2003; Ramos et al., 2006; Abouessa and Morad, 2009; Gibert et al., 2011; Gil-Ortiz et al., 2019) and also to define the relationships between the facies associations and paleogeographic implications of their lateral distribution patterns in the north central part of the Murzuq Basin.

Given the significant differences between the factors controlling modern and ancient Ordovician environments, the Hawaz Formation is best described by an updated conceptual depositional model discussed below (Fig. 19). This model is based on both the sedimentological study presented by Gil-Ortiz et al. (2019) and the results obtained from correlations and GDE maps presented in this paper.

The Hawaz Formation comprises two, well-distinguished, sedimentary domains; an open shallow marine setting represented by DS1 (HWZ1 and HWZ2 reservoir zones) and a transitional marginal marine

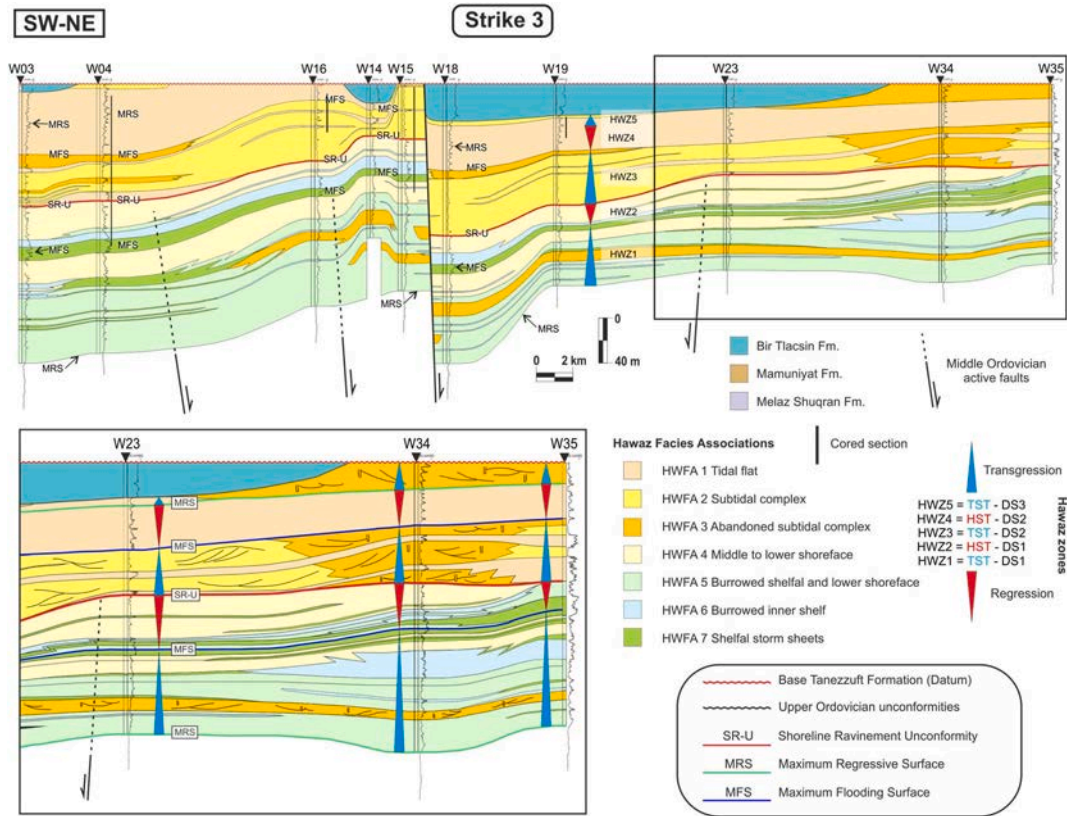


Fig. 13. – Correlation panel Strike 3. All the wells hang from the flattened base Tanezzuft Fm. datum. These are shown with their GR profile from 0 to 150 GAPI. The main transgressive and regressive cycles, corresponding to systems tracts and Hawaz reservoir zones are shown. An enlarged view of the stratigraphic correlation between wells W23, W34 and W35 is included in the bottom left corner. Note the generally distal position of wells W35 and especially W34 with respect to W23 for the whole Hawaz section as shown by the presence of deeper facies associations in these wells. Note also the control on thickness associated with an apparently active normal fault to the SW of well W23 in the middle Hawaz. DS = Depositional sequence; HST = Highstand systems tract; HWFA = Hawaz facies association; HWZ = Hawaz zone; TST = Transgressive systems tract.

unit represented by DS2 (HWZ3 and HWZ4 reservoir zones) and DS3 (HWZ5 reservoir zone) (Fig. 5). Our conceptual depositional model reflects variations in the presence and abundance of the facies associations and dominant ichnofacies across both depositional dip and strike with changing relative sea level, during transgressive (Fig. 19-A) and highstand regressive stages (Fig. 19-B).

The early stages of transgression (Fig. 19-A) are dominated by shallow water, open marine facies represented by a transition from inner shelf to burrowed shelfal to lower shoreface deposits with common interlayered storm deposits. In shallower, marginal marine subtidal to intertidal environments, subtidal complex deposits developed in relatively protected nearshore areas associated with dominant ebb tides and further fluvial discharge directed from SSE to NNW, along an embayed coastline surrounded by bounding lower energy tidal flats (Fig. 19-A). The ichnofacies associated with these environments show a characteristic lateral evolution down depositional dip within a dominant low energy *Cruziana* ichnofacies, represented here with a high diversity and degree of horizontal deposit-feeding traces, very characteristic of low energy open marine settings (Seilacher, 1970, 2000, 2007bib_Seilacher_1970; Droser and Bottjer, 1986; Bottjer and Droser, 1991; Mángano et al., 1996bib_Seilacher_2000; Pemberton et al., 2001, 2012bib_Pemberton_et_al_2001; Seilacher et al., 2002bib_Seilacher_2007; Gingras et al., 2012; Gingras and MacEachern, 2012bib_Pemberton_et_al_2012). In some areas there is overlap with a mixed *Cruziana* and *Skolithos* ichnofabric (Gingras et al., 1999; Buatois et al., 2005), which coexisted, both in the deeper open marine lower shoreface but also in shallower marginal marine settings under mixed marine and brackish water conditions (Fig. 19-A).

In contrast, as sea level rose deeper water shelfal storm sheets and

burrowed inner shelf facies became more common passing up into regressive middle to lower shoreface deposits. In this context, the shoreline migrated seaward under tidal-wave influence possibly developing barrier island systems protecting extensive backshore intertidal flat areas favoured by the embayed morphology of the shoreline but also by the very low gradient (possibly less than 1°) of the Middle Ordovician cratonic margin (Fig. 19-B). Similar processes have been presented by Desjardins et al. (2012b) for the lower Cambrian Gog Group of the Canadian Rocky Mountains where tidal flats were forced to prograde in response to falling sea level in tide-dominated settings. In addition, a transition is again observed from a dominant *Cruziana* ichnofacies, in low energy shelfal deposits, to a predominant *Skolithos* ichnofacies, in higher energy middle to lower shoreface deposits with common *Skolithos* and *Siphonichnus* suspension-feeding trace fossils. In contrast, a lower diversity but still high bioturbation index *Cruziana* ichnofacies is present in the shallowest section of the Hawaz Formation (Fig. 19-B). Despite the typical linkage of *Cruziana* trilobite traces with open-marine and near-shore settings, some authors have proved the presence of traces of this paleofauna as very common in intertidal environments too during the early Paleozoic (Mángano et al., 2014).

The deposition of the Hawaz Formation occurred on the margins of an epeiric sea characterized by very shallow water that is unlikely to have exceeded some tens of meters in depth, with the sea floor above storm wave-base at most locations.

The controlling factors influencing the vertical stacking of facies associations were mainly changes in relative sea level (Dalrymple, 1992; Dalrymple et al., 1992; Walker and Plint, 1992; Johnson and Baldwin, 1996), possibly also affected by local tectonic subsidence as inferred from lateral changes in both facies associations and relative thickness,

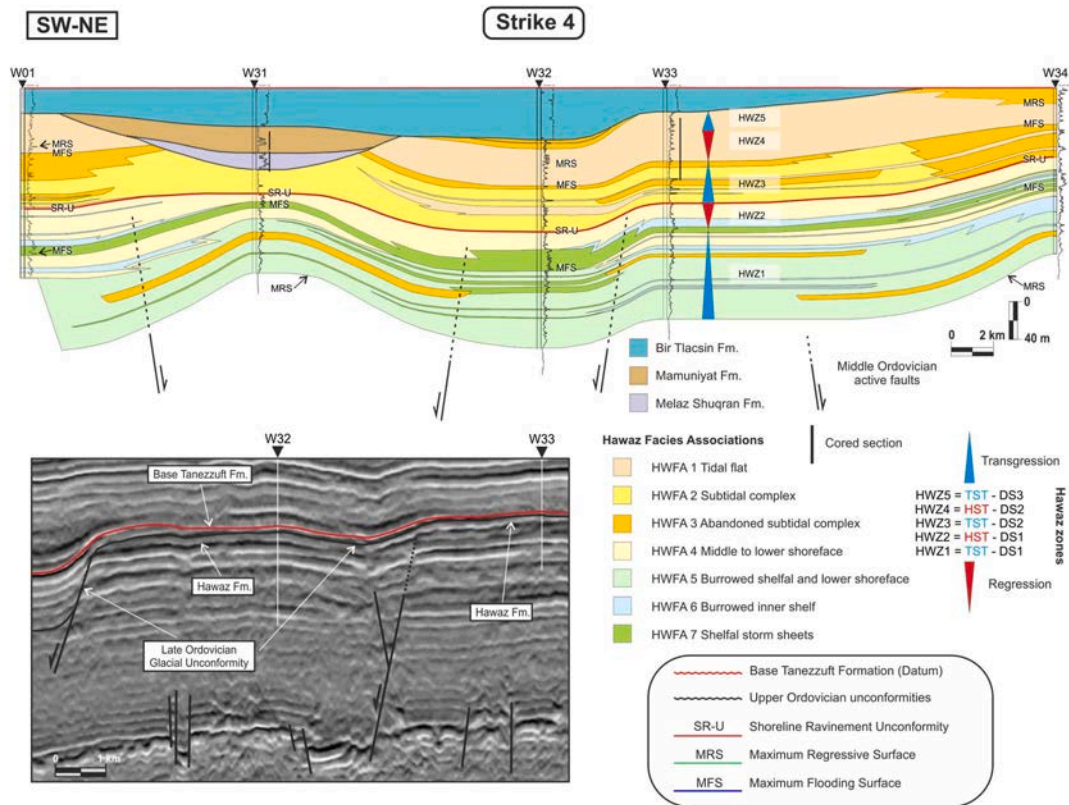


Fig. 14. Correlation panel Strike 4. All the wells hang from the flattened base Tanezzuft Fm. datum. These are shown with their GR profile from 0 to 150 GAPI. Transgressive and regressive cycles, corresponding to systems tracts and Hawaz reservoir zones are also displayed. Also included is a seismic section, oriented SW-NE around wells W32 and W33 in the bottom left corner, showing the relationship of the paleohigh flank with respect to the normal fault bounding the paleovalley and the Late Ordovician Glacial Unconformity to the SW. Note how some of these faults appear to be connected to pre-existing basement structures. Also note the link between fault location and variations in character and thickness of facies associations. DS = Depositional sequence; HST = Highstand systems tract; HWFA = Hawaz facies association; HWZ = Hawaz zone; TST = Transgressive systems tract.

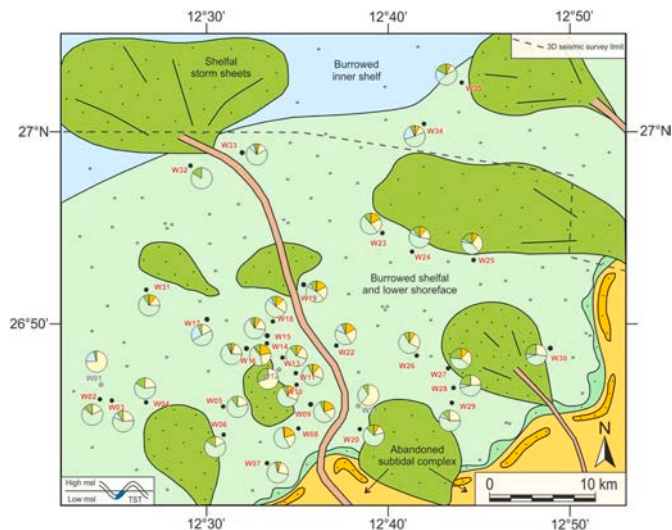


Fig. 15. – Gross Depositional Environment map corresponding to the transgressive systems tract (TST) of Depositional Sequence 1. Facies association proportions are posted next to their corresponding wells. W01, W12 and W21 are anomalies reflecting a reduced section associated with a shallower than normal Total Depth (TD).

which controlled the accommodation and sediment supply in the study area.

The Hawaz Formation and its lateral equivalents occur over

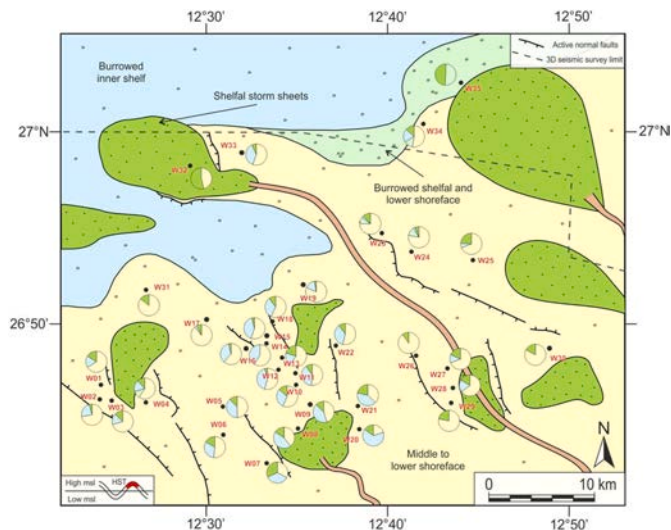


Fig. 16. – Gross Depositional Environment map corresponding to the highstand systems tract (HST) of Depositional Sequence 1. Facies association proportions are posted next to their corresponding wells. Note also the presence of apparently active normal faults, inferred from seismic and correlation panels, which correspond with some of the faults picked in underlying Cambro-Ordovician sections from seismic data and shown in Fig. 3.

hundreds to thousands of kilometres across the Saharan Platform in both Libya and Algeria and certainly extend across the Murzuq and southern

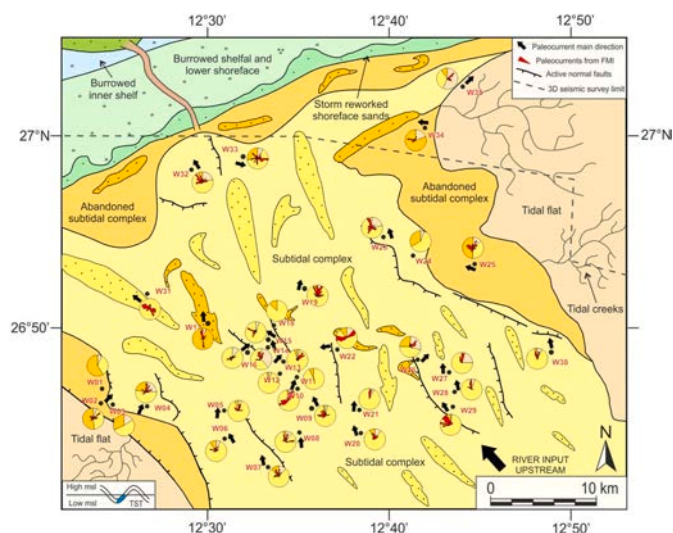


Fig. 17. – Gross Depositional Environment map corresponding to the transgressive systems tract (TST) of Depositional Sequence 2. Facies association proportions are posted next to their corresponding wells. Note also the presence of apparently active normal faults during the Middle Ordovician, which correspond with some of the faults picked in underlying Cambro-Ordovician sections from seismic data and shown in Fig. 3. Note also the paleocurrent directions inferred from image log data (FMI) and their main direction expressed by black arrows. The interpretation in the north-western corner is purely speculative and driven by our depositional model, possibly out of the scale of this map.

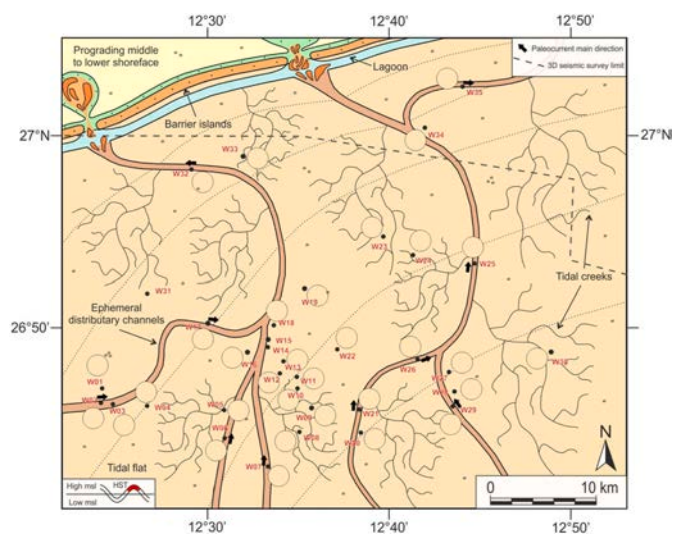


Fig. 18. – Gross Depositional Environment map corresponding to the highstand systems tract (HST) of Depositional Sequence 2. Facies association proportions are posted next to their respective wells. Note also paleocurrent data associated with those wells intercepting ephemeral distributary channels in the tidal flat. The interpretation in the north-western corner is largely speculative and driven by our depositional model and outcrop data from the neighbouring Gargaf High zone, where Ramos et al. (2006) and Gibert et al. (2011) identified evidence of barrier island and tidal inlet facies and associated ichnofacies assemblages.

Berkine-Ghadames basins (Dardour et al., 2004; Jabir et al., 2021). However, there are certain significant differences when comparing this lithostratigraphic unit in the Murzuq Basin with equivalent lateral deposits in the neighbouring Illizi Basin (Middle Ordovician Unit III-3 or In Tahouite Formation). Most notably, the middle Hawaz reservoir zone HWZ3 (Fig. 5) mainly comprising characteristic high energy subtidal complex deposits, present in our study area, is apparently missing from

the Illizi succession (McDougall et al., 2008a, 2008b, 2011bib_McDougall_et_al_2008a, 2008bbib_McDougall_et_al_2011), implying non-deposition or significant condensation in laterally equivalent lower energy deposits. From this observation, we may infer that the subtidal complex deposits of our study area, represent the distal expression of a main entry point of sediment into the basin, located further to the SE, compared to contiguous areas, such as the SE Illizi Basin. This inferred sediment entry point is characteristic of our area of study but most definitely is not unique, as similar features can be observed in the middle Hawaz in nearby areas of Block NC115 or in outcrops of the Gargaf High (Fig. 20) and also possibly further to the east in the Al Kufrah Basin (Seilacher et al., 2002; Le Heron et al., 2010). In this respect, active faulting may have contributed to the deposition of the Hawaz Formation, in the study area, by controlling local accommodation space, but also the location and width of the main entry points for sediment into the basin, defining a non-linear shoreline with multiple estuaries or bays during Middle Ordovician times (Fig. 19).

Although some faults clearly affect the overlying Upper Ordovician, it is difficult to confirm whether most of the described faults created significant offset in the displacement of syn-tectonic deposits during the Hawaz deposition. It is also possible that faults only created local accommodation related to deeper basement-linked structures, during Hawaz succession sedimentation.

A key limitation in the interpretation of both the correlation panels and GDE maps was the difficulty encountered in representing lateral facies variations, particularly in a down dip direction, within a single picture for the studied area as well as interpreting the exact location of the contacts bounding facies belts. We suggest that, in large measure, this may be related to the very low gradient, typical of the cratonic margin across which the Hawaz was deposited, and which considerably affected the width of facies belts (very likely more than 100 km from subtidal middle shoreface to open marine shelfal settings) and enlarged the transitional zones between depositional environments. In such circumstances, it would be appropriate to appeal to modern analogues but, as it is often the case in lower Paleozoic and Precambrian successions, the Hawaz Formation may have very few present day analogues. Some possibilities could be the Gulf of Carpentaria – Arafura Sea, which may be a partial modern analogue (Edgar et al., 2003), together with the Kara, Laptev and East Siberian Seas, or the Hudson Bay, in Canada, as remnants of cratonic margins, broadly comparable in some key respects to the Middle Ordovician transitional marginal to shallow marine environments. Also significant in understanding the limitations of the conclusions drawn from the correlation panels and maps is the distance between many of the wells, which in many cases, might be several kilometres apart and thus too distant to precisely locate lateral facies changes. Accordingly, we believe that the area of study considered here, despite of covering an approximate area of 1600 km², might be too small to capture the whole set of heterogeneities associated with the depositional environments of the Hawaz Formation. In this respect, we should consider the similarities and differences within the Hawaz Formation of this study area when compared with the laterally equivalent outcrop sections in the Gargaf High (Fig. 20) described by Ramos et al. (2006).

Although, the outcrops of the Gargaf High are approximately at 100–150 km distant from the current area of study and may constitute a slightly distal lateral equivalent to the section found in the subsurface, they nonetheless show similar and/or identical sedimentological and ichnological assemblages. Only in the HST-DS2, there are significant differences, high energy shoreface-beach barrier island and tidal inlet deposits in Gargaf outcrops, compared to more proximal, protected inter-bay tidal flat deposits further to the south. We should also consider that the present day Hawaz architecture, in form of paleohighs often separated by large continuous paleovalleys filled with Upper Ordovician deposits, will inevitably introduce uncertainties into the correlations and maps. Despite these inherent difficulties it has nevertheless proved possible to demonstrate important lateral sedimentological heterogeneities within the Hawaz Formation and to infer paleogeographies

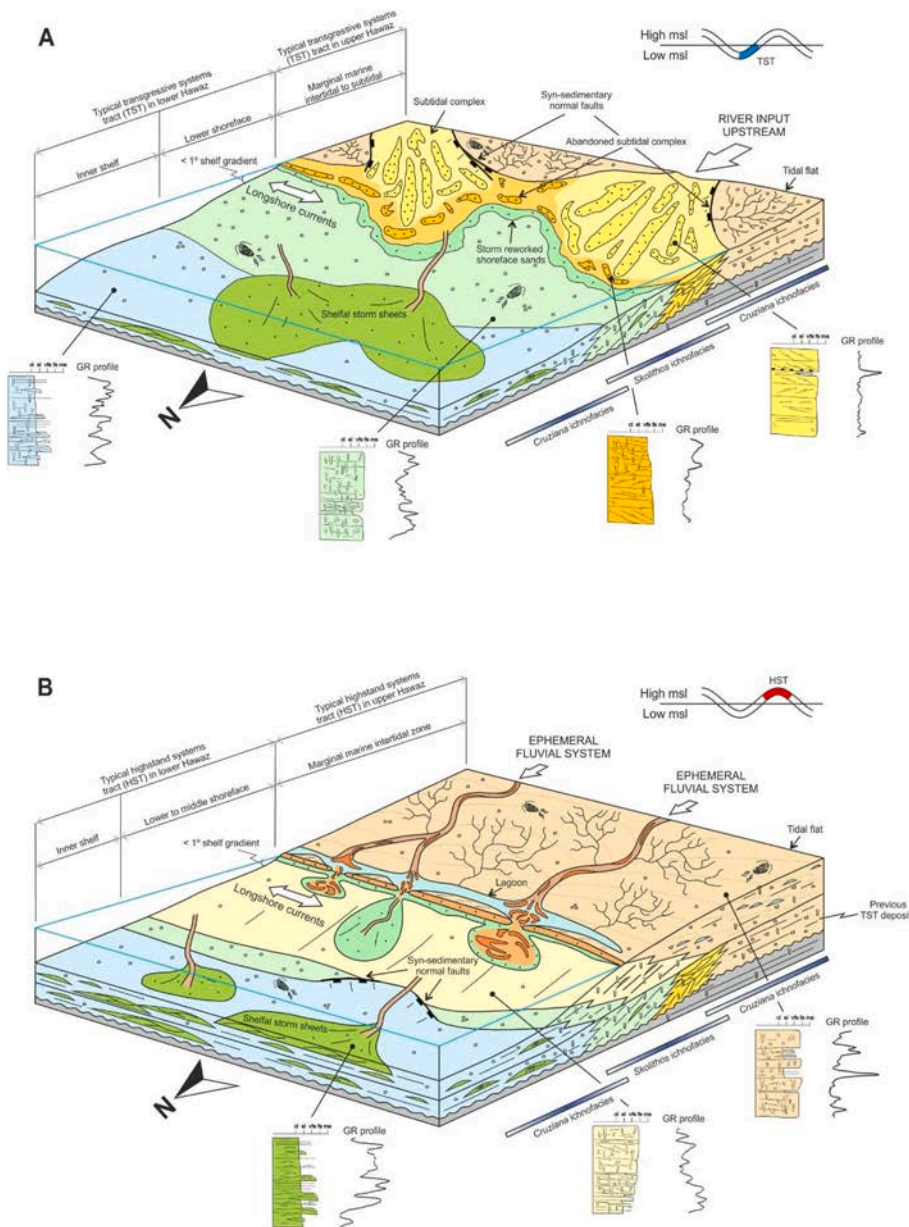


Fig. 19. Conceptual depositional model for the Hawaz Formation in the Murzuq Basin. A) The interpretation of the depositional model corresponding to a typical early transgressive systems tract of the Hawaz Formation. B) The interpretation corresponding to a typical highstand or regressive systems tract of this same lithostratigraphic unit. A synthetic stratigraphic column for each Hawaz facies associations, identified in the subsurface of the Murzuq Basin, together with their typical gamma ray response (left, low GR; right, high GR) and stacking pattern are also shown. Note the approximate limits and overlap of the main ichnofacies identified in this project are also included. Not to scale. Cl = clay, fs = fine sandstone, GR = gamma ray, ms = medium sandstone, si = silt, vfs = very fine sandstone.

across the area of study.

7. Conclusions

Based on eight, high resolution correlation panels, aligned both across depositional dip and strike, the proposed seven facies associations, including tidal flat (HWFA1), subtidal complex (HWFA2), abandoned subtidal complex (HWFA3), middle to lower shoreface (HWFA4), burrowed shelfal and lower shoreface (HWFA5), burrowed inner shelf (HWFA6) and shelfal storm sheets (HWFA7), have been proven to form laterally extensive, correlatable facies belts extending for tens to hundreds of kilometres across the area of study. Their extent and distribution can be linked to a genetic stratigraphic framework of three main low order depositional sequences and their respective systems tracts, which form the basis for a sequence-stratigraphic zonation supported by both petrophysical and reservoir quality properties.

The depositional model for the Hawaz Formation was updated based on the interpretation of correlation panels and the construction of four Gross Depositional Environment (GDE) maps. This showed the Hawaz to

be an extensive and continuous reservoir across the study area, deposited in a broadly extensive subtidal to intertidal paralic environment, with few if any modern analogues due to the controlling factors and depositional processes associated with the northern margin of Gondwana during early Paleozoic times. The Gulf of Carpentaria – Arafura Sea is perhaps a partial modern analogue (Edgar et al., 2003) for the Hawaz Formation despite the obvious differences with the north-western Gondwana cratonic margin during the Middle Ordovician.

The results of this study suggest that the Hawaz Formation was deposited in a non-linear, relatively protected or embayed shoreline with multiple bays/estuaries most likely influenced by the subtle effects of pre-existing north-northwest to south-southeast Pan-African structures controlling accommodation space and reactivated during Ordovician times. These structures were probably active from the onset of Hawaz Depositional Sequence 1, most notably since the start of deposition of reservoir zone HWZ2. Faults are likely to have locally controlled the bathymetry of a very low gradient cratonic margin. Subsequently, both fault activity and intraformational paleorelief

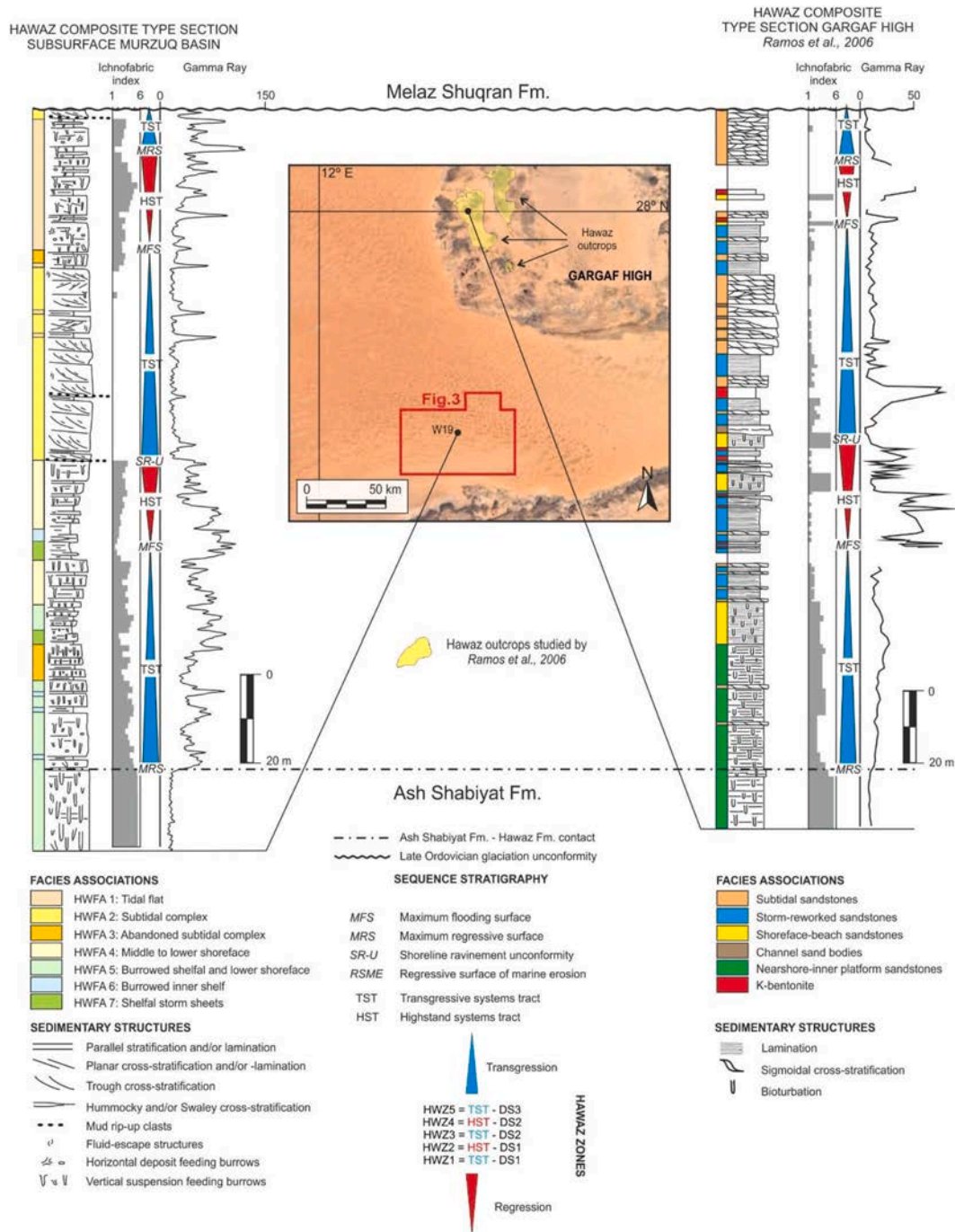


Fig. 20. – Hawaz Formation in the subsurface vs in the outcrop. Comparative summary of Hawaz type sections, in the studied area of the subsurface of the Murzuq Basin and their laterally equivalent deposits located 150 km to the N-NNE in the neighbouring Gargaf High, studied by Ramos et al. (2006). A synthetic stratigraphic column is shown both, for the subsurface as represented by well W19 (See Fig. 3 for location), and in outcrop, each with their corresponding facies associations. Ichnofabric index is also shown together with the corresponding gamma ray profiles. See also the sequence stratigraphic framework discussed in this paper, which is also displayed for both locations, in order to compare in terms of genetic-based sedimentary packages or Hawaz zones. DS = Depositional sequence; HST = Highstand systems tract; HWFA = Hawaz facies association; HWZ = Hawaz zone; TST = Transgressive systems tract.

determined the deposition and lateral distribution of facies within zone HWZ3 during the transgressive stage of Depositional Sequence 2 in relatively shallower areas.

The area of study was characterized by a preferential sediment entry point into the basin mainly comprising subtidal complex deposits during early transgressive stages. These developed from SSE to NNW direction, whereas interbay sub-environments appear to be represented by extensive lower energy sand-prone tidal flats. In contrast, burrowed shelf to shoreface deposits prevailed during periods of relative high sea

level offshore, together with common intercalated storm deposits, whilst prograding tidal flats dominated the most proximal zones of the system, covering a significant part of the study area.

Declaration of competing interest

The authors declare that they have no known competing financial interests or personal relationships that could have appeared to influence the work reported in this paper.

Acknowledgements

Special thanks are due to Repsol Exploración Murzuq SA (REMSA) for technical support and data sharing. Special thanks are also due to the Libyan National Oil Corporation and partners TotalEnergies, Equinor and OMV both for the review of the manuscript and permission to publish the results. Thanks are also due to Francisco J. Bataller for sharing his top Hawaz seismic interpretation and constructive technical discussions in the office. Thanks are also due to Advanced Logic

Technology (ALT) for providing us with a WellCAD 5.4 software license, used in the elaboration of some figures of this paper and especially to Mariano Rodríguez Andrino for his continuous support. Support by the project 3D-MODGHASY (RTI 2018-097312-A-I00) (MCI/AEI/FEDER, UE) and by the Generalitat de Catalunya (2017SGR596) is gratefully acknowledged. Thanks to reviewers David Boote and Jonathan Redfern and also to the editors of the *Marine and Petroleum Geology*, especially to Claudio Nicola Di Celma, for their constructive comments that have improved the content of this paper.

Appendix

Table A.1

Thickness of the Hawaz zones by well and total accumulated thickness.

	HWZ1	HWZ2	HWZ3	HWZ4	HWZ5	Thickness Hawaz
	(m)	(m)	(m)	(m)	(m)	(m)
W01	20,9	40,6	49,8	5,8	29,7	146,8
W02	85,6	36,0	56,0	26,7	6,4	210,7
W03	85,4	34,8	39,1	23,8	22,3	205,3
W04	82,1	33,9	34,4	30,9	23,2	204,4
W05	76,5	20,4	45,4	21,8	30,0	194,1
W06	75,2	23,4	44,7	23,1	30,0	196,3
W07	72,5	19,0	50,0	23,4	27,4	192,3
W08	73,2	18,8	58,2	12,5	15,0	177,7
W09	74,9	20,2	45,1	20,9	19,7	180,9
W10	75,1	25,8	35,2	25,2	4,6	166,0
W11	76,0	20,0	41,8	27,0	4,2	169,0
W12	22,6	20,3	34,4	20,6	14,5	112,4
W13	79,6	23,1	34,9	20,9	3,4	161,9
W14	51,9	25,5	24,0	0,0	0,0	101,4
W15	78,3	24,7	38,1	0,0	0,0	141,1
W16	79,5	27,6	33,4	11,8	0,0	152,3
W17	54,2	23,6	41,5	31,1	14,0	164,4
W18	67,7	21,2	44,7	16,8	18,1	168,5
W19	50,6	18,8	47,1	22,5	9,4	148,5
W20	89,4	14,9	64,8	19,0	15,1	203,2
W21	18,3	15,9	37,0	24,5	10,9	106,6
W22	57,7	25,7	34,5	15,1	22,1	155,1
W23	50,7	32,4	27,8	26,3	4,1	141,2
W24	71,3	39,6	21,3	26,4	5,4	164,0
W25	68,4	32,5	26,5	30,4	8,3	166,1
W26	60,5	20,3	37,4	20,9	13,4	152,4
W27	71,8	21,6	23,5	18,5	11,6	147,0
W28	72,0	19,2	41,4	25,5	17,4	175,5
W29	64,8	27,2	32,4	26,8	15,7	166,9
W30	69,1	26,7	21,8	22,5	0,0	140,2
W31	63,2	6,6	23,0	0,0	0,0	92,8
W32	70,5	33,5	41,2	23,8	17,9	186,9
W33	79,6	21,5	39,2	33,0	11,2	184,5
W34	74,1	26,7	36,0	21,5	16,0	174,3
W35	71,1	16,8	37,3	21,0	13,0	159,3

References

- Abouessa, A., 2012. Diagenetic properties of Hawaz Formation, Murzuq Basin, Libya. In: Salem, M.J., Elbakai, M.T., Abutarruma, Y. (Eds.), *The Geology of Southern Libya: Tripoli, Libya*, vol. 1. Earth Science Society of Libya, pp. 47–82.
- Abouessa, A., Morad, S., 2009. An integrated study of diagenesis and depositional facies in tidal sandstones: Hawaz Formation (Middle Ordovician), Murzuq Basin, Libya. *J. Petrol. Geol.* 32 (1), 39–65. <https://doi.org/10.1111/j.1747-5457.2009.00434.x>.
- Abuhmida, F.H., Wellman, C.H., 2017. Palynology of the middle ordovician Hawaz Formation in the Murzuq Basin, south-west Libya. *Palynology* 41, 31–56. <https://doi.org/10.1080/01916122.2017.1356393>.
- Anfray, R., Rubino, J.-L., 2003. Shelf depositional systems of the ordovician Hawaz Formation in the central Al qarqaf high. In: Salem, M.J., Oun, K.M., Seddiq, H.M. (Eds.), *The Geology of Northwest Libya II: Second Symposium on the Sedimentary Basin of Libya, Tripoli, Libya*, vol. 3, pp. 123–134.
- Aziz, A., 2000. Stratigraphy and hydrocarbon potential of the lower paleozoic succession of license NC-115, Murzuq Basin, SW Libya. In: Sola, M.A., Worsley, D. (Eds.), *Geological Exploration in Murzuq Basin: Amsterdam. Elsevier Science*, pp. 349–368.
- Bataller, J.B., McDougall, N., Moscardiello, A., 2019. Ordovician glacial paleogeography: integration of seismic spectral decomposition, well sedimentological data, and glacial modern analogs in the Murzuq Basin, Libya. *Interpretation* 7, 383–408.
- Belaid, A., Krooss, B.M., Littke, R., 2010. Thermal history and source rock characterization of a paleozoic section in the awbari trough, Murzuq Basin, SW Libya. *Mar. Petrol. Geol.* 27, 612–632.
- Bellini, E., Massa, D., 1980. A stratigraphic contribution to the Paleozoic of the Southern basins of Libya. In: Salem, M.J., Busrewill, M.T. (Eds.), *The Geology of Libya. 2nd Symposium on the Geology of Libya*. Academic Press, London, p. 84.
- Boote, D.R.D., Clark-Lowes, D.D., Traut, M.W., 1998. Paleozoic petroleum systems of north Africa. In: MacGregor, D.S., Moody, R.T.J., Clark-Lowes, D.D. (Eds.), *Petroleum Geology of North Africa*, vol. 132. Geological Society (London) Special Publication, pp. 7–68.
- Boote, D.R.D., Dardour, A., Green, P.F., Smewing, J.D., Van Hoeflaken, F., 2008. Burial and unroofing history of the base Tanezzuft 'hot' Shale source rock, Murzuq Basin, SW Libya: new AFTA constraints from basin margin outcrops (abs.). In: Salem, M.J., Elbakai, M.T., Abutarruma, Y. (Eds.), *The Geology of Southern Libya: Fourth Sedimentary Basins of Libya Symposium, Tripoli, Libya, November 17–20, 2012*, pp. 21–36.
- Botter, D.J., Droser, M.L., 1991. Ichnofabric and basin analysis. *Palaios* 6, 199–205.

- Boyd, R., Dalrymple, R., Zaitlin, B.A., 1992. Classification of clastic coastal depositional environments. *Sediment. Geol.* 80 (3–4), 139–150. [https://doi.org/10.1016/0037-0738\(92\)90037-R](https://doi.org/10.1016/0037-0738(92)90037-R).
- Bradley, G., Redfern, J., Hodgetts, D., George, A.D., Wach, G.D., 2018. The applicability of modern tidal analogues to pre-vegetation paralic depositional models. *Sedimentology* 65 (6), 2171–2201. <https://doi.org/10.1111/sed.12461>.
- Buatois, L., Gingras, M., Maceachern, J., Mangano, M., Zonneveld, J., Pemberton, S., Netto, R., Martin, A., 2005. Colonization of brackish-water systems through time: evidence from the trace-fossil record. *Palaios* 20, 321–347.
- Burrollet, P.F., 1960. *Lexique stratigraphique international*: Paris, Congress Geologique International-Commission de Stratigraphie, v. IV, fasc. IVa, p. 62.
- Cattaneo, A., Steel, R.J., 2003. Transgressive deposits: a review of their variability. *Earth Sci. Rev.* 62, 187–228.
- Collomb, G.R., 1962. Etude géologique du Jebel Fezzan et de sabordure Paléozoïque. Notes et Mémoires Compagnie Française du Pétrole 1, 735.
- Cocks, L.R.M., Torsvik, T.M., 2002. Earth geography from 500 to 400 million years ago: a faunal and palaeomagnetic review. *J. Geol. Soc. (Lond.)* 159, 631–644.
- Craig, J., Rizzi, C., Said, F., Thusu, B., Luning, S., Asbali, A.I., Keeley, M.L., Bell, J.F., Durham, M.J., Eales, M.H., Beswetherick, S., Hamblett, C., 2008. Structural styles and prospectivity in the Precambrian and Paleozoic hydrocarbon systems of north Africa. In: Salem, M.J., Oun, K.M., Essed, A.S. (Eds.), *The Geology of East Libya 4*. Earth Science Society of Libya, Tripoli, pp. 51–122.
- Craik, D., Quesada, S., Lemaire, R., Odriozola, A., Bolatti, N.D., 2001. Sistema petrolero tanezzuf-mamuniyat. *Cuenca de Murzuq, Libia: Bol. Inf. Pet.* (1924) 68, 97–108.
- Dalrymple, R.W., 1992. Tidal depositional systems. In: Walker, R.G., James, N.P. (Eds.), *Facies Models: Response to Sea Level Change*: Waterloo, Canada. Geological Association of Canada, pp. 195–218.
- Dalrymple, R.W., Zaitlin, B.A., Boyd, R., 1992. Estuarine facies models; conceptual basis and stratigraphic implications. *J. Sediment. Res.* 62 (6), 1130–1146. <https://doi.org/10.1306/D4267A69-2B26-11D7-8648000102C1865D>.
- Dalrymple, R.W., Choi, K., 2007. Morphologic and facies trends through the fluvial-marine transition in tide-dominated depositional systems: a schematic framework for environmental and sequence-stratigraphic interpretation. *Earth Sci. Rev.* 81 (3–4), 135–174. <https://doi.org/10.1016/j.earscirev.2006.10.002>.
- Dalrymple, R.W., Mackay, D.A., Ichaso, A.A., Choi, K., 2012. Processes, morphodynamics, and facies of tide-dominated estuaries. *Principles of Tidal Sedimentology*. https://doi.org/10.1007/978-94-007-0123-6_5.
- Dalrymple, E.W., Kurcinka, C.E., Jablonski, B.V.J., Ichaso, A.A., Mackay, D.A., 2015. Deciphering the relative importance of fluvial and tidal processes in the fluvial-marine transition. *Dev. Sedimentol.* 68, 1–45.
- Dardour, A.M., Boote, D.R.D., Baird, A.W., 2004. Stratigraphic controls on Paleozoic petroleum systems, Ghadames basin, Libya. *J. Petrol. Geol.* 27, 141–162.
- Davidson, L., Beswetherick, S., Craig, J., Eales, M., Fisher, A., Himmali, A., Jho, J., Mejrab, B., Smart, J., 2000. The structure, stratigraphy and petroleum geology of the Murzuq Basin, Southwest Libya. In: Sola, M.A., Worsley, D. (Eds.), *Geological Exploration in Murzuq Basin*: Amsterdam, Elsevier Science, Geological Conference on Exploration in the Murzuq Basin, Sabha, Libya, September 20–22, 1998, pp. 295–320. <https://doi.org/10.1016/B978-0-44450611-5/50016-7>.
- Davies, N.S., Gibling, M.R., 2010. Cambrian to Devonian evolution of alluvial systems: the sedimentological impact of the earliest land plants. *Earth Sci. Rev.* 98 (3–4), 171–200. <https://doi.org/10.1016/j.earscirev.2009.11.002>.
- Davies, N.S., Gibling, M.R., Rygel, M.C., 2011. Alluvial facies evolution during the Paleozoic greening of the continents: case studies, conceptual models and modern analogues. *Sedimentology* 58 (1), 220–258. <https://doi.org/10.1111/j.1365-3091.2010.01215.x>.
- Desjardins, P.R., Buatois, L.A., Mángano, M.G., 2012a. Tidal flats and subtidal sand bodies. *Dev. Sedimentol.* 64, 529–561. <https://doi.org/10.1016/B978-0-444-53813-0.00018-6>.
- Desjardins, P.R., Buatois, L.A., Pratt, B.R., Mángano, M.G., 2012b. Forced regressive tidal flats: response to falling sea level in tide-dominated settings. *J. Sediment. Res.* 82 (3), 149–162. <https://doi.org/10.2110/jsr.2012.18>.
- Droser, M.L., 1991. Ichnofabric of the Paleozoic Skolithos ichnofacies and the nature and distribution of Skolithos piperock. *Palaios* 6, 316–325.
- Droser, M.L., Bottjer, D.J., 1986. A semiquantitative field classification of ichnofabric. *J. Sediment. Res.* 56, 558–559.
- Echikh, K., Sola, M.A., 2000. Geology and hydrocarbon occurrences in the Murzuq Basin, SW Libya. In: Sola, M.A., Worsley, D. (Eds.), *Geological Exploration in Murzuq Basin*: Amsterdam, Elsevier Science, pp. 175–222.
- Edgar, N.T., Cecil, C.B., Mattick, R.E., Chivas, A.R., De Deckker, P., Djajadihardja, Y.S., 2003. A modern analogue for tectonic, eustatic, and climatic processes in cratonic basins: Gulf of Carpentaria, Northern Australia. *Climate Controls on Stratigraphy* 77, 193–205. <https://doi.org/10.2110/pec.03.77.0193>.
- Eriksson, P.G., Condie, K.C., Tirsgaard, H., Mueller, W.U., Altermanne, W., Miall, A.D., Aspler, L.B., Catuneanu, O., Chiarenzelli, J.R., 1998. Precambrian clastic depositional systems. *Sediment. Geol.* 120, 5–53.
- Eriksson, K.A., Simpson, E., 2012. Precambrian tidal facies. In: Davis, R.A., Jr & Dalrymple, R.W. (eds). *Principles of Tidal Sedimentology*. Springer, Dordrecht, 397–419. https://doi.org/10.1007/978-94-007-0123-6_15.
- Embry, A., 2009. *Practical Sequence Stratigraphy*: Calgary, Alberta, Canada. Canadian Society of Petroleum Geologists, p. 79.
- Fello, N., Lüning, S., Storch, P., Redfern, J., 2006. Identification of early Llandovery (Silurian) anoxic palaeodepressions at the western margin of the Murzuq Basin (southwest Libya), based on gamma-ray spectrometry in surface exposures. *GeoArabia* 11, 101–118.
- Franco, A., Perona, R., Dwyanti, R., Yu, F., Helal, S., Suarez, J., Ali, A., 2012. NC186 Block, Murzuq Basin: lessons learned from exploration. In: Salem, M.J., Mriheel, I.Y., Essed, A.S. (Eds.), *The Geology of Southern Libya*: Tripoli, Libya. Earth Science Society of Libya, pp. 37–50.
- Ghienne, J.-F., Deynoux, M., Manatschal, G., Rubino, J.-L., 2003. Palaeovalleys and fault-controlled depocentres in the Late-Ordovician glacial record of the Murzuq Basin (central Libya). *Compt. Rendus Geosci.* 335 (15), 1091–1100. <https://doi.org/10.1016/j.crte.2003.09.010>.
- Ghienne, J.-F., Moreau, J., Degermann, L., Rubino, J.-L., 2012. Lower Paleozoic unconformities in an intracratonic platform setting: glacial erosion versus tectonics in the eastern Murzuq Basin (southern Libya). *Int. J. Earth Sci.* 102, 455–482.
- Gibert, J. M. de, Ramos, E., Marzo, M., 2011. Trace fossils and depositional environments in the Hawaz Formation, middle ordovician, western Libya. *J. Afr. Earth Sci.* 60 (1–2), 28–37. <https://doi.org/10.1016/j.jafrearsci.2011.01.010>.
- Gibling, M.R., Davies, N.S., 2012. Paleozoic landscapes shaped by plant evolution. *Nat. Geosci.* 5 (2), 99–105. <https://doi.org/10.1038/ngeo1376>.
- Gil-Ortiz, M., McDougall, N.D., Cabello, P., Marzo, M., Ramos, E., 2019. Sedimentology of a “nonactualistic” middle ordovician tidal-influenced reservoir in the Murzuq Basin (Libya). *AAPG (Am. Assoc. Pet. Geol.) Bull.* 103 (9), 2219–2246. <https://doi.org/10.1306/02151918138>.
- Gingras, M.K., Pemberton, S.G., Saunders, T., Clifton, H.E., 1999. The ichnology of modern and Pleistocene brackish-water deposits at Willapa Bay, Washington; variability in estuarine settings. *Palaios* 14, 352–374.
- Gingras, M. K., MacEachern, J. A., 2012. Tidal ichnology of shallow water clastic settings. In: Davis, R.A., Jr & Dalrymple, R.W. (eds). *Principles of Tidal Sedimentology*. Springer, Dordrecht, 57–77. [doi:10.1007/978-94-007-0123-6_4](https://doi.org/10.1007/978-94-007-0123-6_4).
- Gingras, M.K., MacEachern, J.A., Dastgird, S.E., 2012. The potential of trace fossils as tidal indicators in bays and estuaries. *Sediment. Geol.* 279, 97–106. <https://doi.org/10.1016/j.sedgeo.2011.05.007>.
- Girard, F., Ghienne, J.F., Rubino, J.L., 2012. Occurrence of hyperperical flows and hybrid event beds related to glacial outburst events in a Late Ordovician proglacial delta (Murzuq Basin, SW Libya). *J. Sediment. Res.* 82, 688–708. <https://doi.org/10.2110/jsr.2012.61>.
- Hall, P.B., Bjorøy, M., Ferriday, I.L., Ismail, Y., 2012. Murzuq Basin source rocks. In: Salem, M.J., Mriheel, I.Y., Essed, A.S. (Eds.), *The Geology of Southern Libya*: Tripoli, Libya, vol. 2. Earth Science Society of Libya, pp. 63–84.
- Hallet, D., 2002. *Petroleum Geology of Libya*. Elsevier, Amsterdam, p. 503. <https://doi.org/10.1016/B978-0-444-50525-5.X5000-8>.
- Hallet, D., Clark-Lowes, D., 2016. *Petroleum Geology of Libya*, second ed. Elsevier, p. 404.
- Harris, P.T., Heap, A.D., 2003. Environmental management of clastic coastal depositional environments: inferences from an Australian geomorphic database. *Ocean Coast Manag.* 46 (5), 457–478. [https://doi.org/10.1016/S0964-5691\(03\)00018-8](https://doi.org/10.1016/S0964-5691(03)00018-8).
- Harris, P.T., Heap, A.D., Bryce, S.M., Porter-Smith, R., Ryan, D.A., Heggie, D.T., 2002. Classification of Australian clastic coastal depositional environments based upon a quantitative analysis of wave, tidal, and river power. *J. Sediment. Res.* 72 (6), 858–870. <https://doi.org/10.1306/040902720858>.
- Havlicek, V., Massa, D., 1973. Brachiopodes de l'Ordovicien Supérieur de Libye occidentale. Implications stratigraphiques régionales: *Geobios* 6, 267–290.
- Jabir, A., Cerepi, A., Loisy, C., Rubino, J.L., 2021. Evaluation of reservoir systems in Paleozoic sedimentary formations of Ghadames and Jefarah basins. *J. Afr. Earth Sci.* <https://doi.org/10.1016/j.jafrearsci.2021.104324>.
- Johnson, H.D., Baldwin, C.T., 1996. *Shallow siliciclastic seas*. In: Reading, H.G. (Ed.), *Sedimentary Environments: Processes, Facies and Stratigraphy*. Blackwell Science, Oxford, pp. 232–280.
- Kenrick, P., Strullu-Derrien, C., Mitchell, R.L., 2015. The origins of land plants communities (abs.). In: *The Rise and Fall of Photosynthate: Evolution of Plant/fungus Interactions from Paleobotanical and Phylogenomic Perspectives*: Botany Symposium, Edmonton, Alberta, Canada, July 28, 2015.
- Kenrick, P., Strullu-Derrien, C., Mitchell, R.L., 2016. The early fossil record of land plants and their environment (abs.). In: *Colonization of the Terrestrial Environment: 38th New Phytologist Symposium*, Bristol, United Kingdom, July 25–27, 2016.
- Khoja, A., Gashghesh, T., Swedan, M., Garea, B., Ghnia, S., 2000. Paleorelieves fósiles del Ordovícico en la Cuenca de Murzuq. Sudoeste de Libia: *Boletín de Informaciones Petroleras* 64, 14–31.
- Klitzsch, E.H., 2000. The structural development of the Murzuq and Kufra basins—significance for oil and mineral exploration. In: Sola, M.A., Worsley, D. (Eds.), *Geological Exploration in Murzuq Basin*: Geological Conference on Exploration in the Muzuq Basin, Sabha, Libya, September 20–22, pp. 143–150. <https://doi.org/10.1016/B978-044450611-5/50009-X>, 1998.
- Kuhn, T.S., Barnes, C.R., 2005. Ordovician conodonts from the mithaka formation (georgina basin, Australia). Regional and paleobiogeographical implications: *Geol. Acta* 3, 317–337.
- Le Heron, D.P., Sutcliffe, O., Bourzig, K., Craig, J., Visentin, C., Whittington, R., 2004. Sedimentary architecture of Upper Ordovician tunnel valleys, Gargaf Arch, Libya: implications for the genesis of a hydrocarbon reservoir. *GeoArabia* 9, 137–160.
- Le Heron, D.P., Craig, J., Sutcliffe, O.E., Whittington, R., 2006. Late Ordovician glaciogenic reservoir heterogeneity: an example from the Murzuq Basin, Libya. *Mar. Petrol. Geol.* 23, 655–677.
- Le Heron, D.P., Armstrong, H.A., Wilson, C., Howard, J.P., Gindre, L., 2010. Glaciation and deglaciation of the Libyan desert: the late ordovician record. *Sediment. Geol.* 223, 100–125.
- Lüning, S., Craig, J., Loydell, D.K., Storch, P., Fitches, B., 2000. Lower Silurian “hot shales” in North Africa and Arabia: regional distribution and depositional model. *Earth Sci. Rev.* 49, 121–200.
- Lüning, S., Adamson, K., Craig, J., 2003. Frasnian organic-rich shales in North Africa: regional distribution and depositional model. In: Arthur, T., MacGregor, D.S.,

- Cameron, N.R. (Eds.), *Petroleum Geology of Africa: New Themes and Developing Technologies*, vol. 207. Spec. Publ., London, pp. 165–184. Geol. Soc.
- Mángano, M.G., Buatois, L.A., Aceñolaza, G.F., 1996. Trace fossils and sedimentary facies from a Late Cambrian–Early Ordovician tide-dominated shelf (Santa Rosita Formation, northwest Argentina): implications for ichnofacies models of shallow marine successions. *Ichnos* 5, 53–88.
- Mángano, M.G., Buatois, L.A., Astini, R., Rindsberg, A.K., 2014. Trilobites in early Cambrian tidal flats and landward expansion of the Cambrian explosion. *Geology* 42 (2), 143–146. <https://doi.org/10.1130/G34980.1>.
- Massa, D., Collomb, G.R., 1960. Observations nouvelles sur la region d'Aouinet Ouenine et du Djebel Fezzan (Libye): copenhagen, 21st. International Geological Congress Proceedings 12, 65–73.
- Matte, P., 2001. The Variscan Collage and Orogeny (480–290 Ma) and the Tectonic Definition of the Armorica Microplate: A Review, vol. 13. Terra Nova, pp. 122–128.
- McDougall, N., Martin, M., 2000. Facies models and sequence stratigraphy of upper ordovician outcrops in the Murzuq Basin, SW Libya. In: Sola, M.A., Worsley, D. (Eds.), *Geological Exploration in Murzuq Basin*. Elsevier, Amsterdam, pp. 223–236. <https://doi.org/10.1016/B978-044450611-5/50012-X>.
- McDougall, N.D., Figari, E., Jauregui, J.M., 2008a. Estratigrafía secuencial y sedimentología del Cambro-Ordovícico de la Plataforma del Sahara en el Norte de Africa. Abstract volumen 12th Congress Argentine Association of Sedimentologists.
- McDougall, N.D., Gerard, J., Włoszczowski, D., Sharky, K., 2008b. Ordovician plays on the Arabian and Saharan platforms: a comparison (Poster & abstract). In: AAPG International Conference and Exhibition, Cape Town, South Africa October 26–29, 2008.
- McDougall, N.D., Bellik, M., Jauregui, J.M., 2011. Sedimentology and sequence stratigraphy of the Ordovician section in the Gassi-Touil-Gassi Chergui-In Amedjane area (abs. In: 5th Algerian Oil and Gas Energy Week, Oran, Algeria, May 21–25, 2011).
- Meinhold, G., Howard, J.P., Strogen, D., Kaye, M.D., Abutarruma, Y., Elgadry, M., Thusu, B., Whitham, A.G., 2013. Hydrocarbon source rock potential and elemental composition of lower Silurian subsurface shales of the eastern Murzuq Basin, southern Libya. *Mar. Petrol. Geol.* 48, 224–246.
- Miles, N.H., Unpublished results. Repsol Exploration Murzuq SA NC186, NC187 and NC190 Concessions, Libya. A Palynological Correlation of the Mesozoic and Palaeozoic. Robertson Research International Limited.. Robertson Research International Limited.
- Molyneux, S.G., Le Hérisse, A., Wicander, R., 1996. Chapter 16: paleozoic phytoplankton. In: Jansonius, J., McGregor, D.C. (Eds.), *Palynology: Principles and Applications*, vol. 2. AASP Foundation, pp. 493–529.
- Nichols, G., 2017. Challenging orthodoxy: is the present the key to the past? *Sediment. Rec.* 15 (3), 4–9. <https://doi.org/10.2110/sedred.2017.3.4>.
- Paris, F., 1990. The Ordovician chitinozoan biozones of the northern Gondwana Domain. *Rev. Palaeobot. Palynol.* 66, 181–289.
- Paris, F., 1996. Chapter 17: chitinozoan biostratigraphy and palaeoecology. In: Jansonius, J., McGregor, D.C. (Eds.), *Palynology: Principles and Applications*, vol. 2. AASP Foundation, pp. 531–552.
- Pemberton, S.G., Spila, M., Pulham, A.J., Saunders, T., MacEachern, J.A., Robin, D., Sinclair, I.K., 2001. *Ichnology and Sedimentology of Shallow to Marginal Marine Systems*. St. John's, vol. 15. Geological Association of Canada, Short Course, p. 343.
- Pemberton, S.G., MacEachern, J.A., Dashtgard, S.E., Bann, K.L., Gingras, M.K., Zonneveld, J.P., 2012. Shorefaces. *Developments in Sedimentology* 64, 563–603.
- Ramos, E., Marzo, M., Gibert, J. M. de, Tawengi, K.S., Khoja, A.A., Bolatti, N.D., 2006. Stratigraphy and sedimentology of the middle ordovician Hawaz Formation (Murzuq Basin, Libya). *AAPG (Am. Assoc. Pet. Geol.) Bull.* 90 (9), 1309–1336. <https://doi.org/10.1306/03090605075>.
- Ramos, E., Willmott, V., Cabello, P., Marzo, M., Casamor, J., Tawengi, K., Khoja, A., Bolatti, N., 2012. A holocene analogue for the late ordovician 3-D glacial topography of the Murzuq Basin. In: Salem, A.M.J., Mriheel, I.Y., Essed, A.S. (Eds.), *The Geology of Southern Libya*, Vol II. Earth Science Society of Libya, pp. 261–270.
- Ron Martín, M., Buitrago, J., Erquiaga, M., Sarkawi, I., Gonzalez Muñoz, J.M., 2016. Mature exploration challenges in Murzuq Basin (Libya) – chasing stratigraphic traps (abs. In: 78th EAGE Conference & Exhibition, Vienna, Austria, 30 May – 2 June, 2016).
- Seilacher, A., 1970. Cruziana stratigraphy of non-fossiliferous Paleozoic sandstones. In: Crimes, T.P., Harper, J.W. (Eds.), *Trace Fossils*, vol. 3. Geological Journal Special Issue, pp. 447–476.
- Seilacher, A., 2000. Ordovician and Silurian arthropycid ichnostratigraphy. In: Sola, M. A., Worsley, D. (Eds.), *Geological Exploration in Murzuq Basin*. Elsevier Science, Amsterdam, pp. 237–258.
- Seilacher, A., Lüning, S., Martin, M.A., Klitzsch, E., Khoja, A., Craig, J., 2002. Ichnostratigraphic correlation of lower paleozoic clastics in the kufra basin (SE lybia). *Lethaia* 35, 257–262.
- Seilacher, A., 2007. *Trace Fossil Analysis*. Springer, Berlin, p. 226.
- Shalbak, F., 2015. *Paleozoic Petroleum Systems of the Murzuq Basin*. Universitat de Barcelona, Barcelona, Spain, p. 203. Libya, Ph.D. thesis.
- Sola, M.A., Worsley, D., 2000. *Geological Exploration in Murzuq Basin*: Amsterdam. Elsevier Science, p. 519.
- Vecoli, M., 1999. Cambro-ordovician palynostratigraphy (acritarchs and prasiniphytes) of the hassi-R'Mel area and northern rhadames basin, North Africa. *Palaeont. Italica* 86, 1–112.
- Vos, R.G., 1981. Sedimentology of an Ordovician fan delta complex, Western Libya. *Sediment. Geol.* 29 (2–3), 153–170. [https://doi.org/10.1016/0037-0738\(81\)90005-1](https://doi.org/10.1016/0037-0738(81)90005-1).
- Walker, R.G., Plint, A.G., 1992. Wave- and storm dominated shallow marine systems. In: Walker, R.G., James, N.P. (Eds.), *Facies Models: Response to Sea Level Change*: Waterloo, Ontario, Canada. Geological Association of Canada, pp. 219–238.
- Williams, G.E., 2000. Geological constraints on the Precambrian history of Earth's rotation and the Moon's orbit. *Rev. Geophys.* 38 (1), 37–59. <https://doi.org/10.1029/1999RG900016>.

Annex 2. Abstracts presented in international congresses



SAPIENZA
UNIVERSITÀ DI ROMA



34TH IAS

INTERNATIONAL
MEETING OF SEDIMENTOLOGY
ROME
10 - 13 SEPTEMBER 2019

*"SEDIMENTOLOGY TO FACE SOCIETAL CHALLENGES
ON RISK, RESOURCES AND RECORD OF THE PAST"*



ABSTRACT BOOK

ISBN 978-88-944576-2-9

Sedimentology of the 'nonactualistic' Middle Ordovician Hawaz Formation in the Murzuq Basin (Libya)

Marc Gil Ortiz (1), Neil McDougall (2), Patricia Cabello (3), Mariano Marzo (3), Emilio Ramos (3)

(1) Repsol Exploración & University of Barcelona, (2) Consultant Sedimentologist & Stratigrapher, (3) University of Barcelona (UB)

Geologists have traditionally sought to explain ancient processes by reference to 'actualistic' processes in order to better understand the sedimentary record. However, the Earth dynamics has changed significantly through geological history. Indeed, even from early Paleozoic times until the present, some processes and depositional environments simply cannot be directly compared, since conditions were significantly different. As a contribution to this debate, the Middle Ordovician Hawaz Formation in the Murzuq Basin (SW Libya) has been studied, identifying a set of features which makes a comparison with any modern analogue a difficult task.

After a sedimentological characterization of these clastic deposits, by means of an extensive database of core descriptions, image logs and conventional wireline log data, fifteen characteristic lithofacies have been identified. These have been grouped into seven correlatable facies associations, distributed into a series of broad and laterally extensive facies belts deposited in a shallow marine, inter-tidal to sub-tidal environment. A sequence stratigraphic framework is proposed on the basis of three main depositional sequences and their respective systems tracts to create a genetic-based stratigraphic zonation which in turn is linked to petrophysical and reservoir quality properties.

Several key factors and processes are discussed as critical in distinguishing between ancient 'nonactualistic' deposits and modern analogues from similar depositional environments. These principally include 1) the effect of vegetation-free substrates on river banks stabilization and thus fluvial styles and flow regimes in transitional continental to shallow marine environments together with clay generation by chemical weathering controlled by land flora, 2) greenhouse vs icehouse periods and related controls on the distribution of facies belts in coastal environments, 3) higher tidal ranges due to tidal spin-down in the Earth-Moon system, and also 4) characteristic early Paleozoic ichnofacies (such as "Pipe Rock") assemblages occurring across hundreds of kilometres.

The Hawaz Formation is therefore interpreted as an excellent example of a 'non-actualistic', tidally-influenced clastic reservoir which appears to extend for hundreds of kilometres across much of the North African or Saharan Craton. A sedimentary model is proposed with new ideas presented for marginal to shallow marine depositional environments during the Middle Ordovician, and particularly for the northern margin of Gondwana.

Keywords: nonactualism, Paleozoic, tidal-influenced, trace fossils, sequence stratigraphy

PRAGUE 2021



35th Meeting of Sedimentology:
Prague, Czech Republic
21–25 June 2021

BOOK OF ABSTRACTS



Sedimentary architecture of the Middle Ordovician Hawaz Formation in the Murzuq basin (Libya)

Marc Gil-Ortiz¹, Neil David McDougall², Patricia Cabello^{1,3}, Mariano Marzo^{1,3}, Emilio Ramos^{1,3}

¹Geomodels Research Institute, Barcelona, Spain

²Independent consultant sedimentologist, Madrid, Spain

³Departament de Dinàmica de la Terra i de l'Oceà, Facultat de Ciències de la Terra (Universitat de Barcelona), Barcelona, Spain

The Middle Ordovician Hawaz Formation is a siliciclastic lithostratigraphic unit well represented in the north-central part of the Murzuq basin (SW Libya), which appears to extend for hundreds of kilometres across the Saharan Platform. It constitutes a proven oil-bearing reservoir within the Ordovician-Silurian petroleum system in the Murzuq basin.

The present-day architecture and distribution of the Hawaz Formation bear little relation to its original configuration and depositional profile during the Middle Ordovician, when deposition occurred in a marginal to shallow marine environment over a continuous, areally extensive, very low gradient cratonic margin characterizing the northern margin of Gondwana. During the subsequent Upper Ordovician Hirnantian Glaciation, a series of icesheets often greatly truncated the Hawaz succession leaving a characteristic relief of paleohighs and paleovalleys which were partially infilled later by periglacial and subglacial clastic deposits, and then sealed by a thick succession of shales of the Silurian Tanezzuft Formation.

The Hawaz succession was deposited during Darriwilian to Sandbian Stages of the Middle Ordovician and facies distribution patterns were tightly linked to relative sea level fluctuations. Tidally-influenced facies belts dominated during transgressive stages whereas tide- and wave-dominated facies belts prevailed during high stand stages in an overall global greenhouse period. Seven facies associations were identified including, from proximal to distal, sandy tidal flat, subtidal bar and dune complexes, abandoned subtidal complexes, middle to lower shoreface, burrowed shelfal and lower shoreface, burrowed inner shelf and shelfal storm sheet deposits. These facies associations have been proven to form laterally extensive correlatable facies belts extending for tens to hundreds of kilometres over the area of study and probably further across the Saharan craton. Their extension and distribution can be linked to a genetic stratigraphic framework of three main depositional sequences and their respective systems tracts, which form the basis for a sequence-stratigraphic zonation supported by both petrophysical and reservoir quality properties.

By making use of an extensive and diverse subsurface dataset, a series of stratigraphic correlation panels were created to clarify possible facies lateral changes, together with paleogeographic gross depositional environment maps in order to infer the spatial distribution of facies across and down depositional dip within the study area in an apparently layer cake succession.

The results of this study suggest that the Hawaz Formation was deposited in a non-linear, relatively protected or embayed shoreline with multiple bays/estuaries most likely influenced by the subtle effects of pre-existing north-northwest to south-southeast Pan-African structures controlling accommodation space and reactivated during Ordovician times. The main sediment entry points are represented by fluvio-tidal to subtidal bar and dune complexes during transgressive stages (TST), whereas interbay sub-environments appear to be represented by extensive burrowed sand-prone tidal flats. In contrast, burrowed shelf to shoreface deposits prevailed during periods of relative high sea level (HST) offshore, whilst prograding tidal flat deposits dominated the most proximal zones of the system, covering a significant extension of the study area.

Annex 3. Other publications

Geo-Temas



Sociedad
Geológica
de
España

Volumen 18



5-7 julio 2021 Vitoria-Gasteiz

X Congreso Geológico de España

eman ta zabal zazu



Universidad
del País Vasco

Euskal Herriko
Unibersitatea

Sedimentología y arquitectura sedimentaria de la Formación Hawaz. El paradigma del uniformismo contra las cuerdas en un caso de estudio del Ordovícico Medio.

Sedimentology and sedimentary architecture of the Hawaz Formation. The uniformitarian paradigm on the ropes; a Middle Ordovician case study.

M. Gil-Ortiz^{1,3}, P. Cabello^{2,3}, N. D. McDougall⁴, M. Marzo^{2,3}, E. Ramos²

1 Repsol Exploración S. A. c/Méndez Álvaro, 44, 28045 (Madrid) amarquitus@gmail.com

2 Departament de Dinàmica de la Terra i de l'Oceà. Facultat de Ciències de la Terra. Universitat de Barcelona, c/Martí i Franquès s/n, 08028 (Barcelona) pcabello@ub.edu, mariano.marzo@ub.edu, emilio.ramos@ub.edu

3 Geomodels Research Institute, Universitat de Barcelona, c/Martí i Franquès s/n, 08028 (Barcelona)

4 Consultant Sedimentologist (Madrid) neil85mcdougall@gmail.com

Palabras clave: Actualismo, Paleozoico, marino somero, Cuenca de Murzuq, estratigrafía secuencial

Resumen

La Formación Hawaz constituye un excelente reservorio de hidrocarburos en la Cuenca de Murzuq (SO Libia). La morfología de las trampas en forma de paleoaltos aislados y rodeados por valles glaciares del Ordovícico Superior, hacen que un análisis sedimentológico detallado y una correlación estratigráfica secuencial entre dichos paleoaltos, sean necesarios para evaluar la continuidad lateral del reservorio.

En este estudio se ha llevado a cabo una caracterización sedimentológica de estos depósitos en el subsuelo de la Cuenca de Murzuq por mediación de datos de testigo, diagrfias convencionales y de imagen, de 35 pozos diferentes. Se han identificado hasta 15 litofacies en un primer estadio descriptivo, que han sido agrupadas posteriormente en siete asociaciones de facies correlacionables entre pozos, correspondientes a un ambiente marino somero y marginal. Tras la interpretación de estas asociaciones de facies, se ha llevado a cabo un análisis de estratigrafía secuencial con el objetivo de caracterizar cinturones de facies a lo largo del área de estudio por mediación de paneles de correlación de alta resolución entre pozos.

Después de realizar la descripción e interpretación sedimentológica y las correlaciones regionales de la Formación Hawaz, se propone un modelo sedimentario no actualístico donde se discute el efecto de los factores de control clave para justificar la complicada comparación de estos depósitos con ningún análogo actual.

Abstract

The Hawaz Formation is an excellent hydrocarbon reservoir in the Murzuq Basin (SW Libya). It typically occurs as isolated paleohighs or "buried hills", surrounded by Upper Ordovician glacial valley fill, and requires a detailed sedimentological analysis as well as a high resolution sequence stratigraphic correlation between paleohighs, in order to evaluate the lateral continuity and character of this reservoir.

To address these issues a sedimentological characterization of these deposits was carried out in the subsurface of the Murzuq Basin using core, wireline and image log data from 35 different wells. Up to 15 lithofacies were identified in a first purely descriptive stage. Subsequently, these were grouped into seven correlatable facies associations, corresponding to a marginal to shallow marine depositional environment. Following the interpretation of these facies associations, a sequence stratigraphic analysis was carried-out with the aim of distinguishing facies belts across the study area by means of high resolution correlation panels.

On the basis of both facies analysis and regional correlations a non-actualistic sedimentary model is proposed and the key factors distinguishing this model from any modern analogue highlighted and discussed.

Annex 4. Hawaz thickness summary table

	HWZ1	HWZ2	HWZ3	HWZ4	HWZ5	Thickness Hawaz
	(m)	(m)	(m)	(m)	(m)	(m)
W01	20,9	40,6	49,8	5,8	29,7	146,8
W02	85,6	36,0	56,0	26,7	6,4	210,7
W03	85,4	34,8	39,1	23,8	22,3	205,3
W04	82,1	33,9	34,4	30,9	23,2	204,4
W05	76,5	20,4	45,4	21,8	30,0	194,1
W06	75,2	23,4	44,7	23,1	30,0	196,3
W07	72,5	19,0	50,0	23,4	27,4	192,3
W08	73,2	18,8	58,2	12,5	15,0	177,7
W09	74,9	20,2	45,1	20,9	19,7	180,9
W10	75,1	25,8	35,2	25,2	4,6	166,0
W11	76,0	20,0	41,8	27,0	4,2	169,0
W12	22,6	20,3	34,4	20,6	14,5	112,4
W13	79,6	23,1	34,9	20,9	3,4	161,9
W14	51,9	25,5	24,0	0,0	0,0	101,4
W15	78,3	24,7	38,1	0,0	0,0	141,1
W16	79,5	27,6	33,4	11,8	0,0	152,3
W17	54,2	23,6	41,5	31,1	14,0	164,4
W18	67,7	21,2	44,7	16,8	18,1	168,5
W19	50,6	18,8	47,1	22,5	9,4	148,5
W20	89,4	14,9	64,8	19,0	15,1	203,2
W21	18,3	15,9	37,0	24,5	10,9	106,6
W22	57,7	25,7	34,5	15,1	22,1	155,1
W23	50,7	32,4	27,8	26,3	4,1	141,2
W24	71,3	39,6	21,3	26,4	5,4	164,0
W25	68,4	32,5	26,5	30,4	8,3	166,1
W26	60,5	20,3	37,4	20,9	13,4	152,4
W27	71,8	21,6	23,5	18,5	11,6	147,0
W28	72,0	19,2	41,4	25,5	17,4	175,5
W29	64,8	27,2	32,4	26,8	15,7	166,9
W30	69,1	26,7	21,8	22,5	0,0	140,2
W31	63,2	6,6	23,0	0,0	0,0	92,8
W32	70,5	33,5	41,2	23,8	17,9	186,9
W33	79,6	21,5	39,2	33,0	11,2	184,5
W34	74,1	26,7	36,0	21,5	16,0	174,3
W35	71,1	16,8	37,3	21,0	13,0	159,3

Annex 5. Well composites

TITLE:

WELL SUMMARY CHART

WELL:

W01

SCALE:

1:500

Hawaz Facies Associations



HWFA1 - Tidal flat



HWFA2 - Subtidal complex



HWFA3 - Abandoned subtidal complex



HWFA4 - Middle to lower shoreface



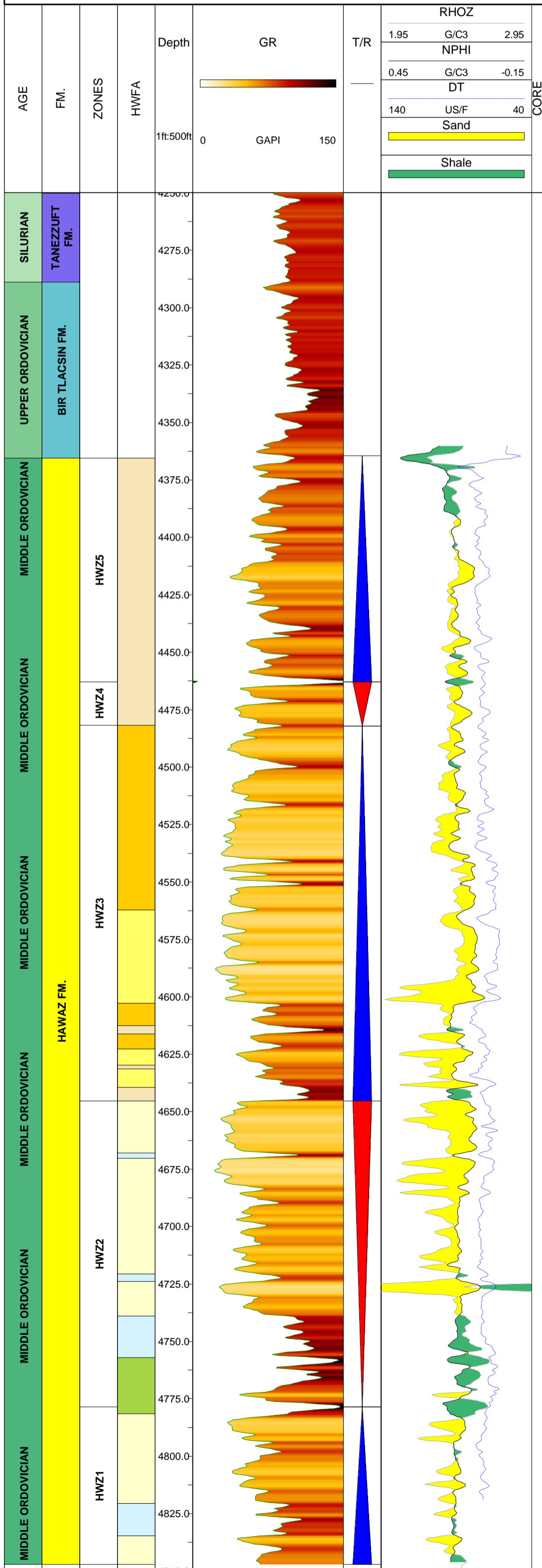
HWFA5 - Burrowed shelfal and lower shoreface



HWFA6 - Burrowed inner shelf



HWFA7 - Shelfal storm sheets



TITLE:

WELL SUMMARY CHART

WELL:

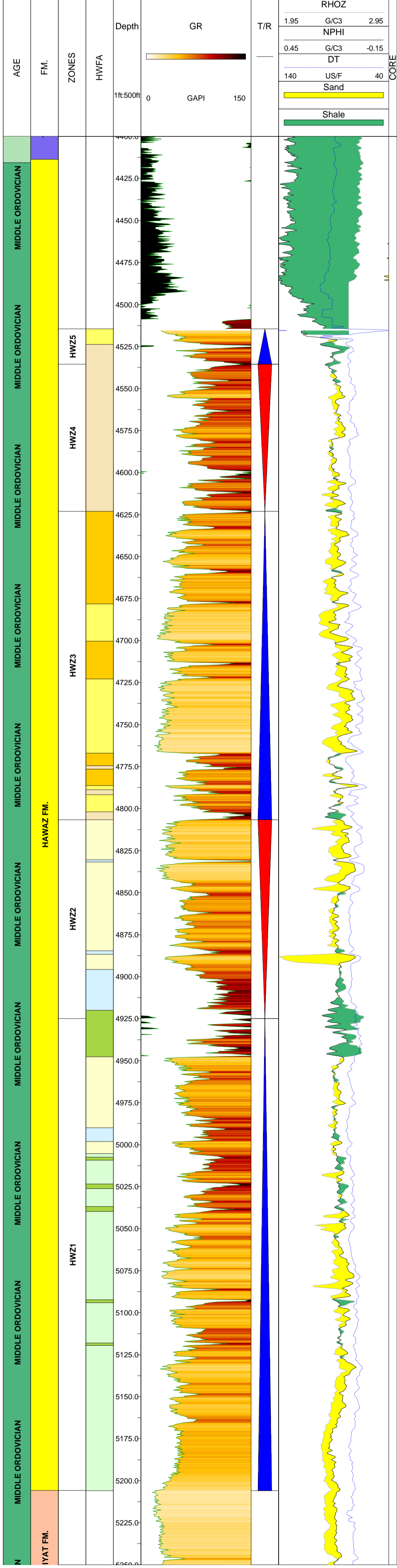
W02

SCALE:

1:500

Hawaz Facies Associations

- HWFA1 - Tidal flat
- HWFA2 - Subtidal complex
- HWFA3 - Abandoned subtidal complex
- HWFA4 - Middle to lower shoreface
- HWFA5 - Burrowed shelfal and lower shoreface
- HWFA6 - Burrowed inner shelf
- HWFA7 - Shelfal storm sheets



TITLE:

WELL SUMMARY CHART

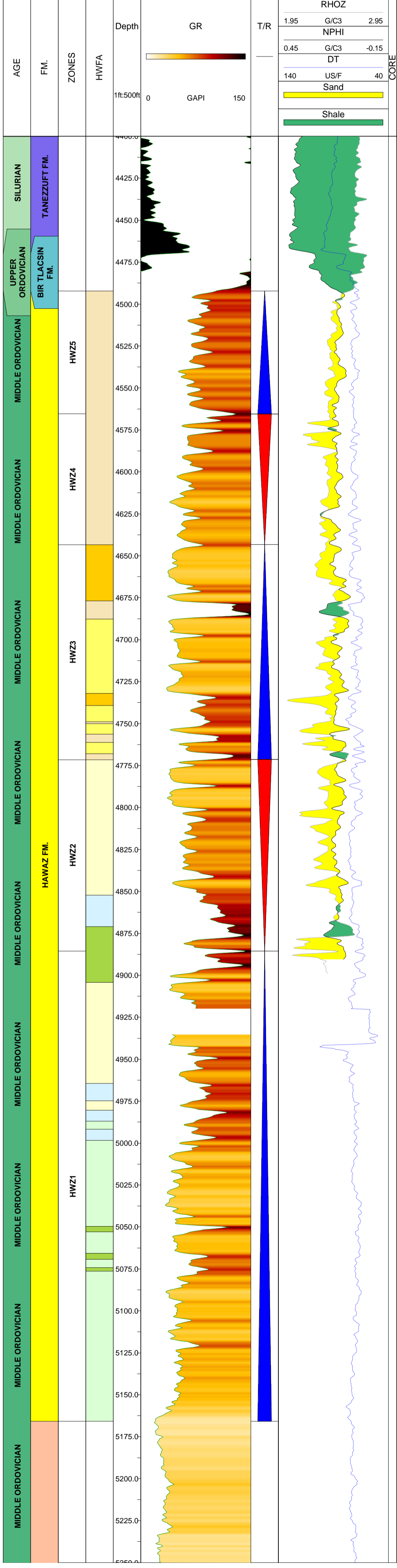
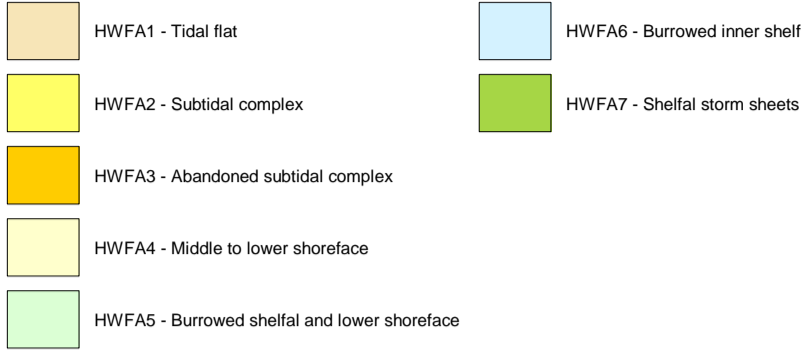
WELL:

W03

SCALE:

1:500

Hawaz Facies Associations



TITLE:

WELL SUMMARY CHART

WELL:

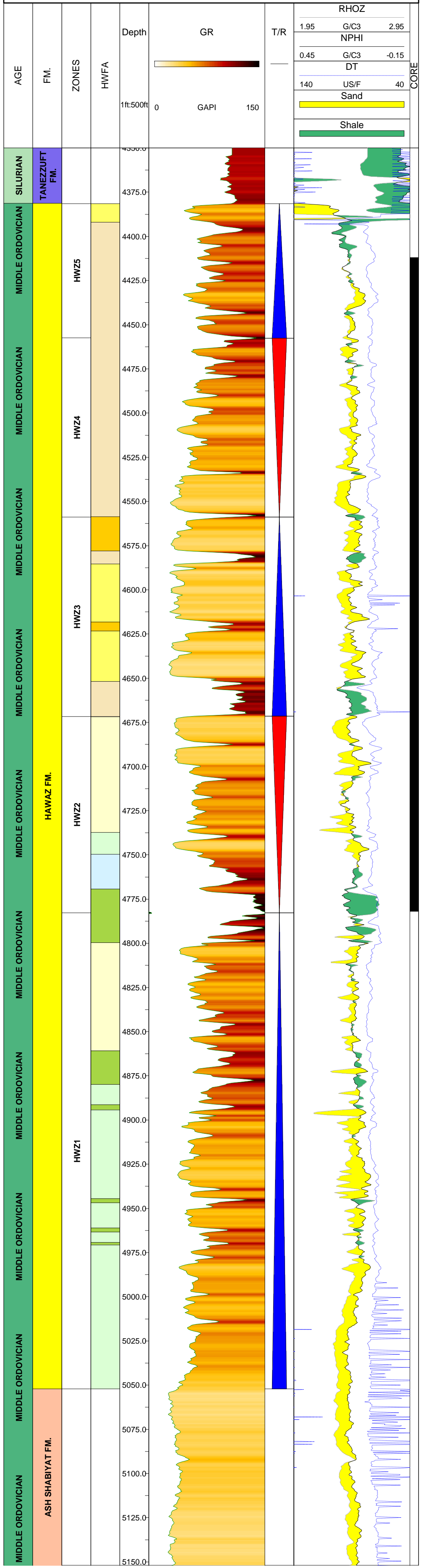
W04

SCALE:

1:500

Hawaz Facies Associations

- HWFA1 - Tidal flat
- HWFA6 - Burrowed inner shelf
- HWFA2 - Subtidal complex
- HWFA7 - Shelfal storm sheets
- HWFA3 - Abandoned subtidal complex
- HWFA4 - Middle to lower shoreface
- HWFA5 - Burrowed shelfal and lower shoreface



TITLE:

WELL SUMMARY CHART

WELL:

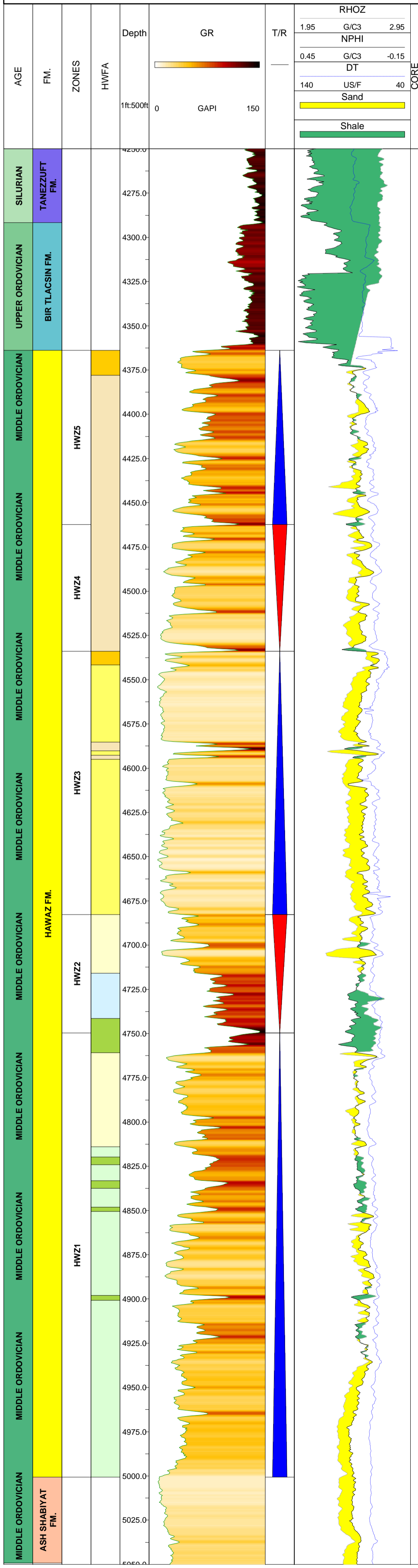
W05

SCALE:

1:500

Hawaz Facies Associations

- HWFA1 - Tidal flat
- HWFA6 - Burrowed inner shelf
- HWFA2 - Subtidal complex
- HWFA7 - Shelfal storm sheets
- HWFA3 - Abandoned subtidal complex
- HWFA4 - Middle to lower shoreface
- HWFA5 - Burrowed shelfal and lower shoreface



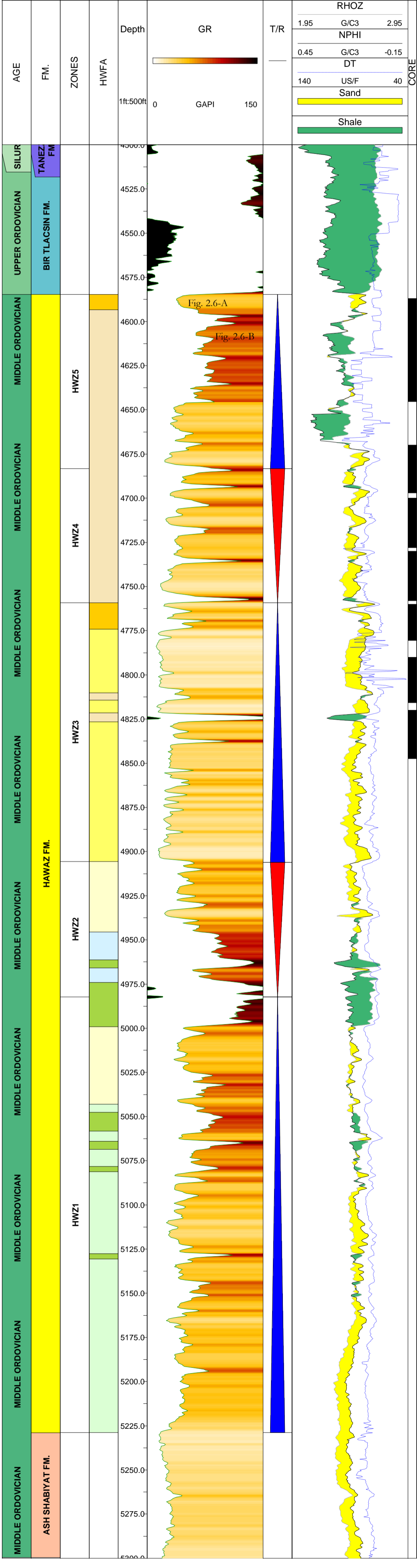
TITLE: **WELL SUMMARY CHART**

WELL: **W06**

SCALE: **1:500**

Hawaz Facies Associations

- HWFA1 - Tidal flat
- HWFA6 - Burrowed inner shelf
- HWFA2 - Subtidal complex
- HWFA7 - Shelfal storm sheets
- HWFA3 - Abandoned subtidal complex
- HWFA4 - Middle to lower shoreface
- HWFA5 - Burrowed shelfal and lower shoreface



TITLE:

WELL SUMMARY CHART

WELL:

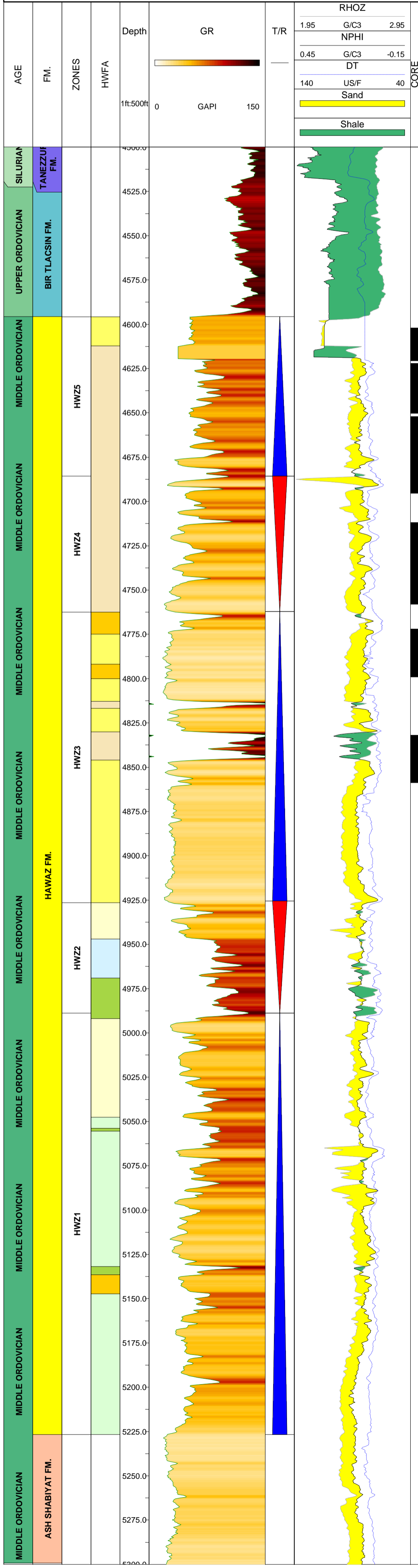
W07

SCALE:

1:500

Hawaz Facies Associations

- HWFA1 - Tidal flat
- HWFA2 - Subtidal complex
- HWFA3 - Abandoned subtidal complex
- HWFA4 - Middle to lower shoreface
- HWFA5 - Burrowed shelfal and lower shoreface
- HWFA6 - Burrowed inner shelf
- HWFA7 - Shelfal storm sheets



TITLE:

WELL SUMMARY CHART

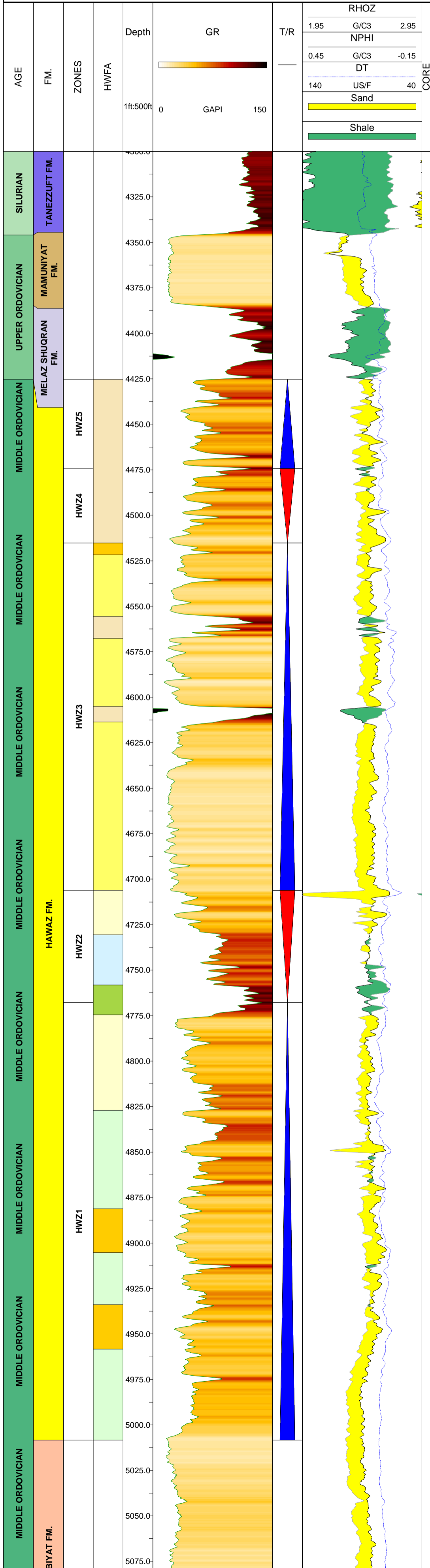
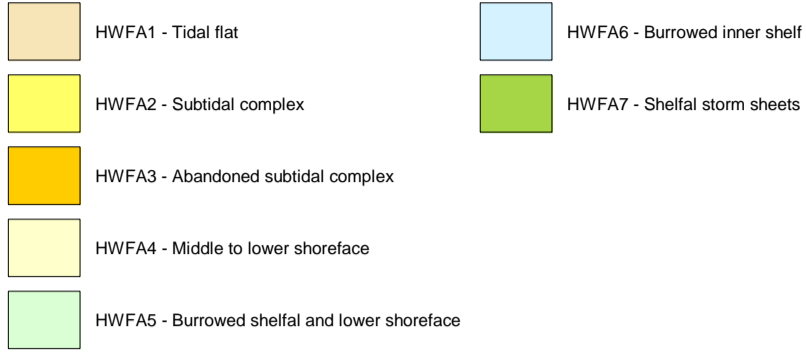
WELL:

W08

SCALE:

1:500

Hawaz Facies Associations



TITLE:

WELL SUMMARY CHART

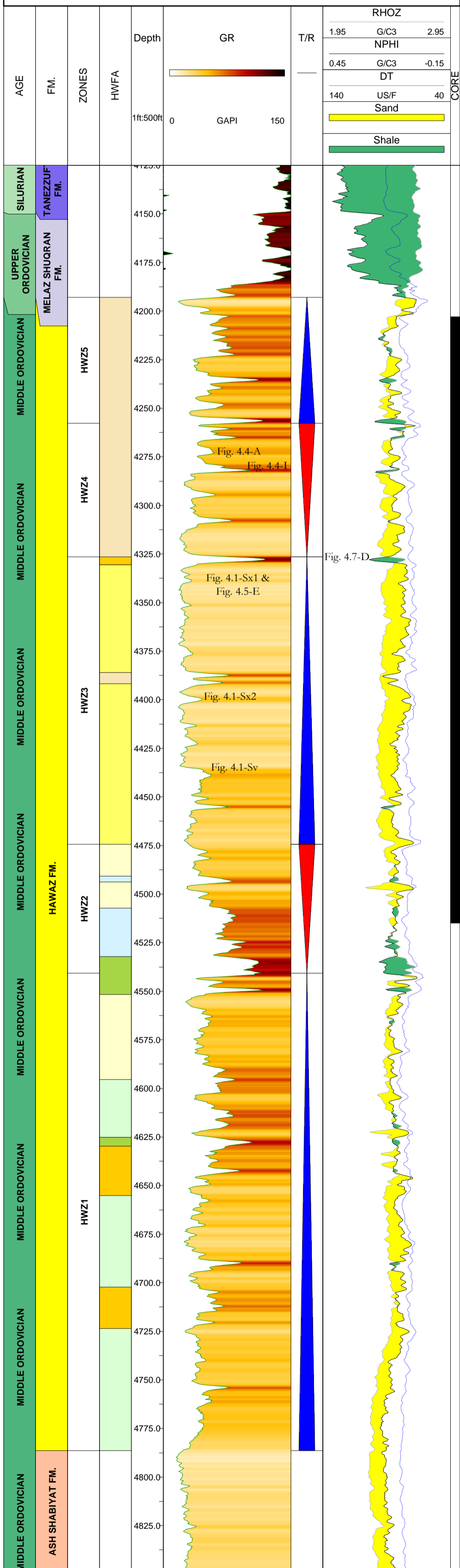
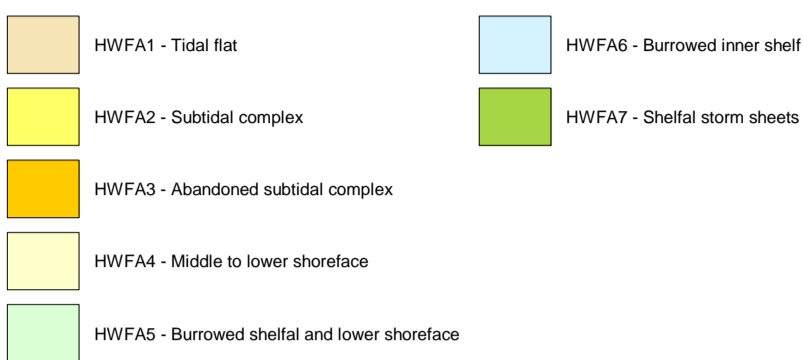
WELL:

W09

SCALE:

1:500

Hawaz Facies Associations



TITLE:

WELL SUMMARY CHART

WELL:

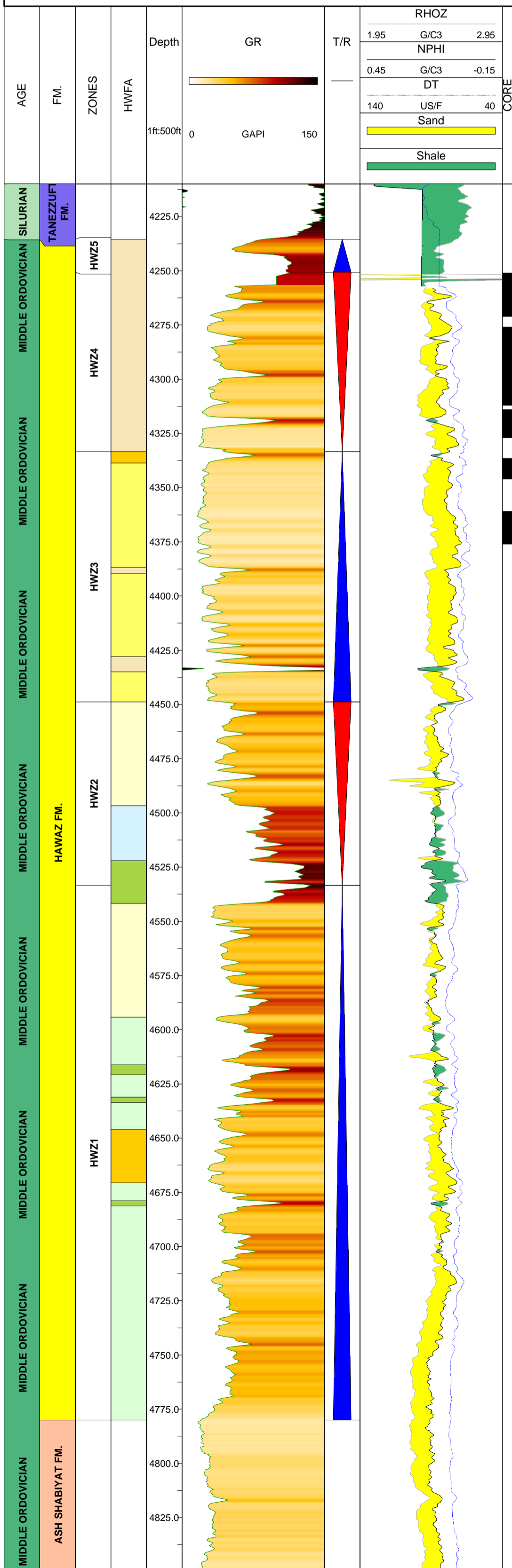
W10

SCALE:

1:500

Hawaz Facies Associations

- HWFA1 - Tidal flat
- HWFA6 - Burrowed inner shelf
- HWFA2 - Subtidal complex
- HWFA7 - Shelfal storm sheets
- HWFA3 - Abandoned subtidal complex
- HWFA4 - Middle to lower shoreface
- HWFA5 - Burrowed shelfal and lower shoreface



TITLE:

WELL SUMMARY CHART

WELL:

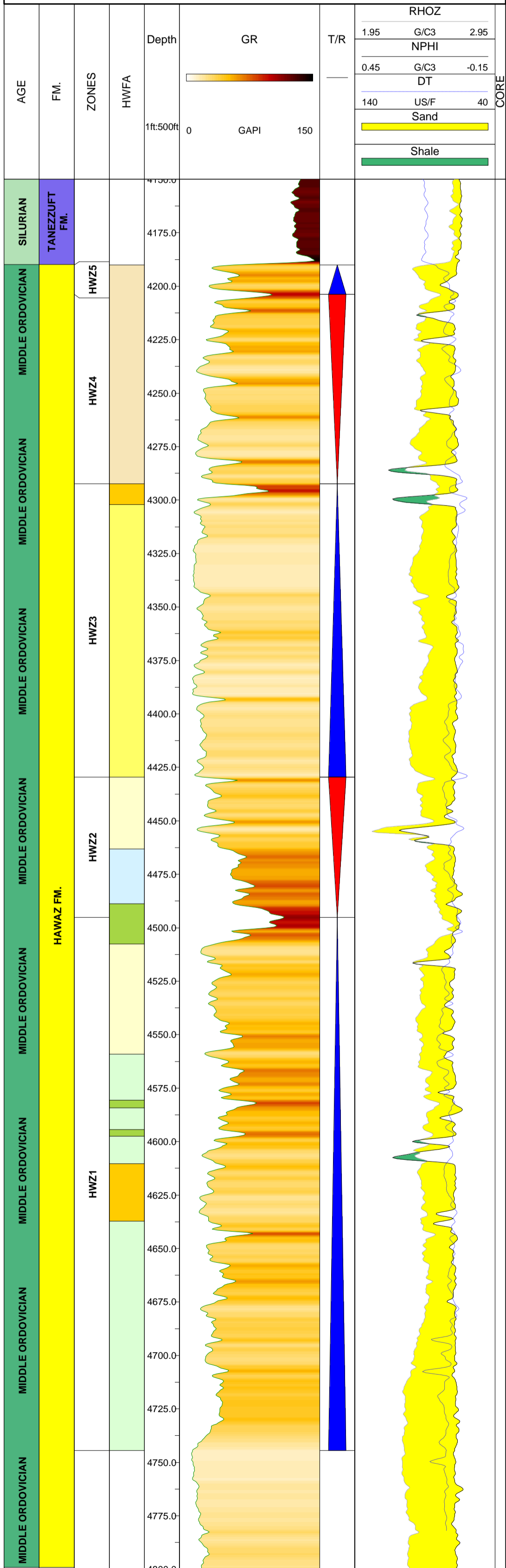
W11

SCALE:

1:500

Hawaz Facies Associations

- HWFA1 - Tidal flat
- HWFA6 - Burrowed inner shelf
- HWFA2 - Subtidal complex
- HWFA7 - Shelfal storm sheets
- HWFA3 - Abandoned subtidal complex
- HWFA4 - Middle to lower shoreface
- HWFA5 - Burrowed shelfal and lower shoreface



TITLE:

WELL SUMMARY CHART

WELL:

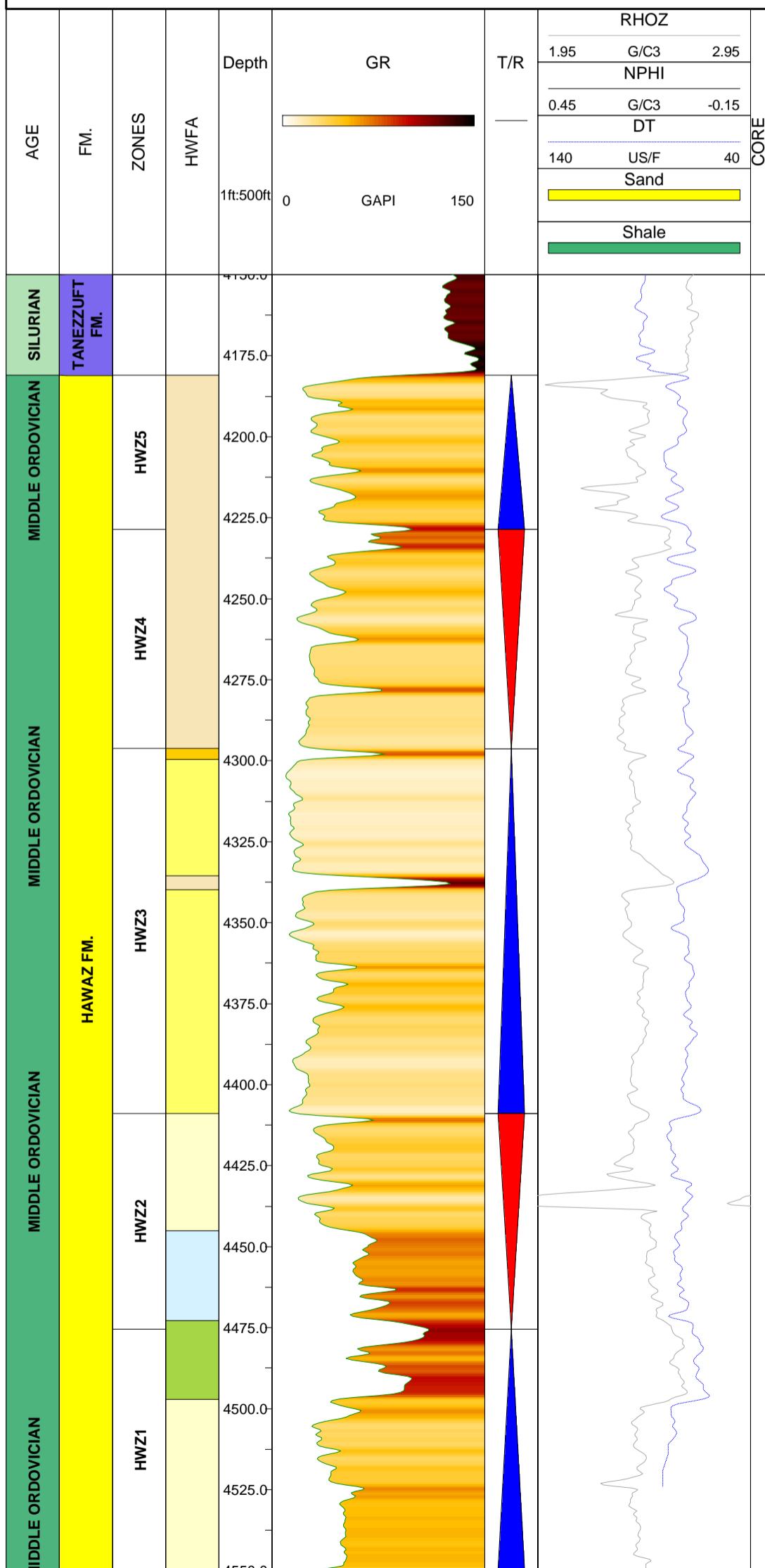
W12

SCALE:

1:500

Hawaz Facies Associations

- HWFA1 - Tidal flat
- HWFA6 - Burrowed inner shelf
- HWFA2 - Subtidal complex
- HWFA7 - Shelfal storm sheets
- HWFA3 - Abandoned subtidal complex
- HWFA4 - Middle to lower shoreface
- HWFA5 - Burrowed shelfal and lower shoreface



TITLE:

WELL SUMMARY CHART

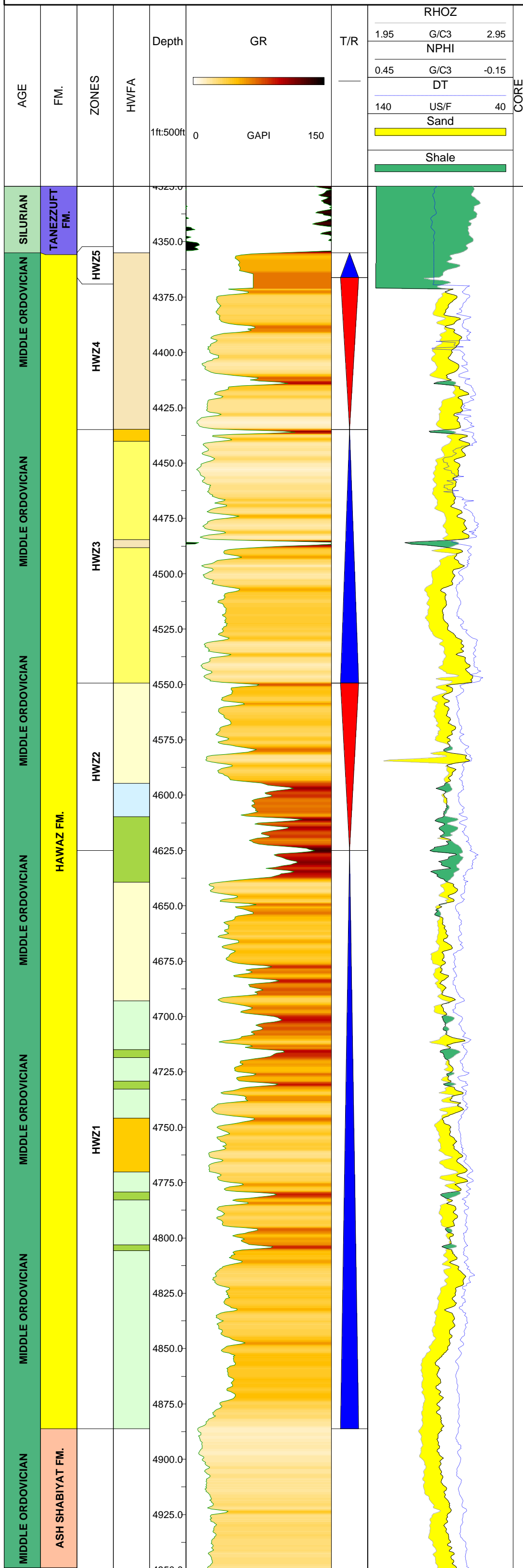
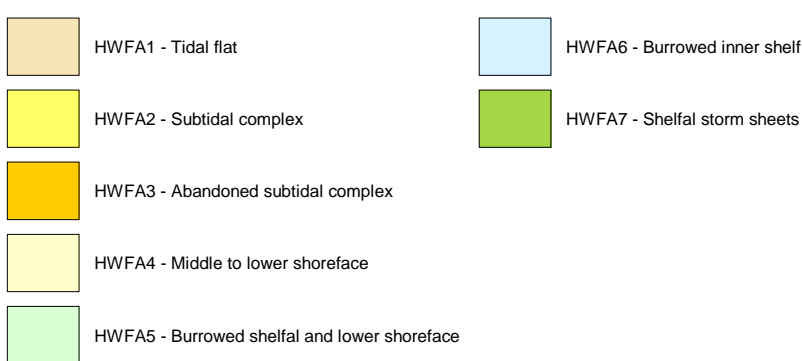
WELL:

W13

SCALE:

1:500

Hawaz Facies Associations



TITLE:

WELL SUMMARY CHART

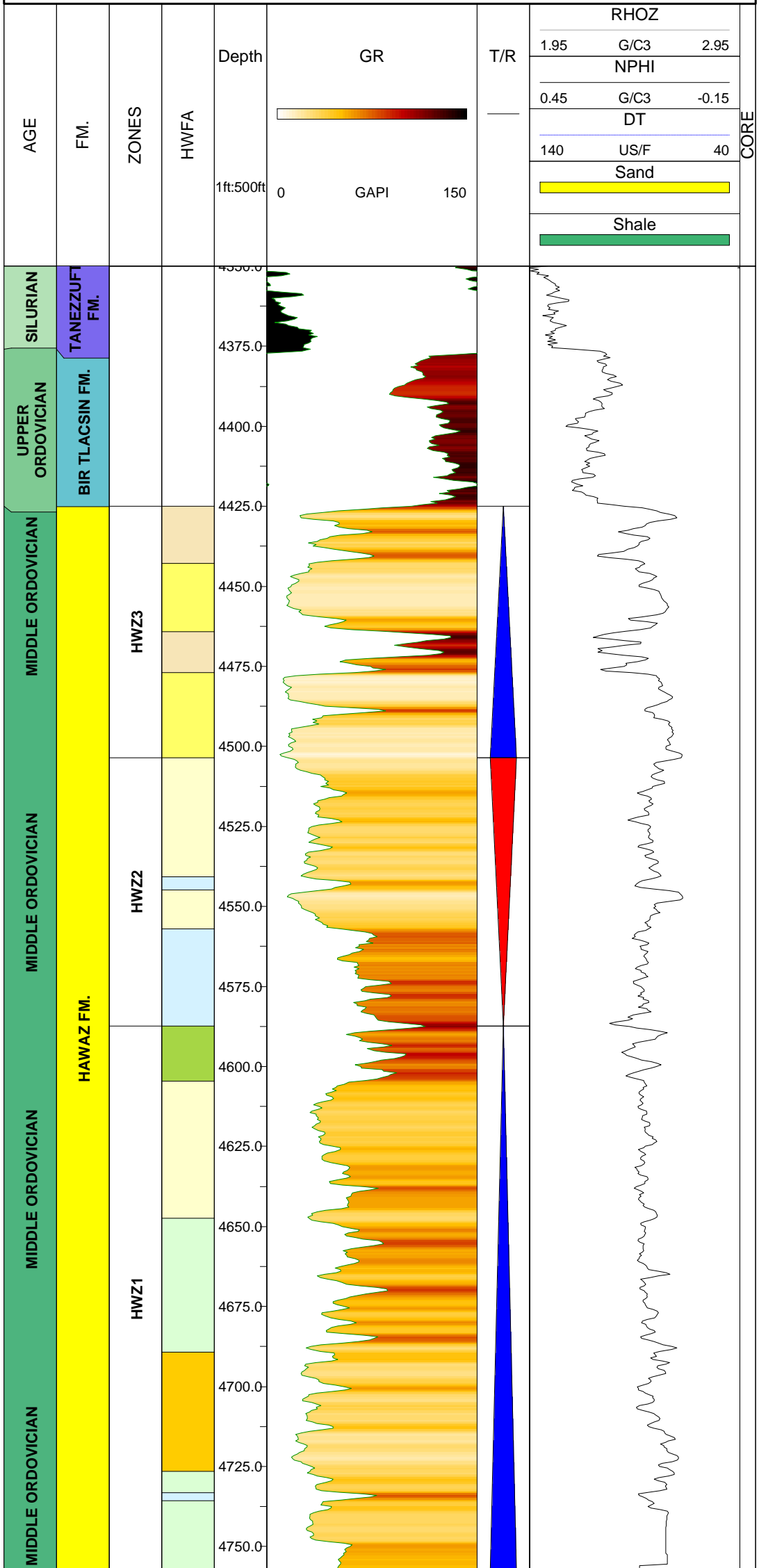
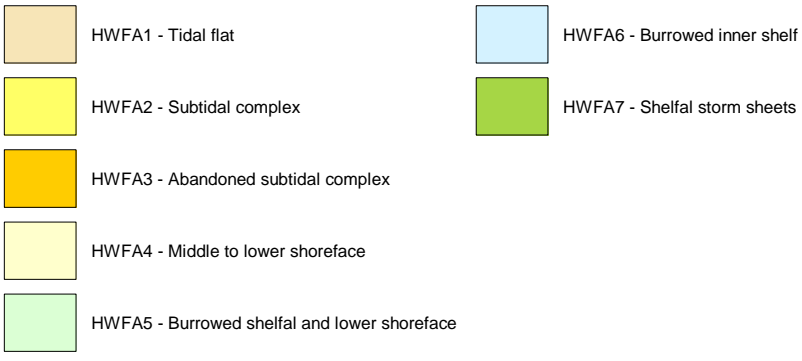
WELL:

W14

SCALE:

1:500

Hawaz Facies Associations



TITLE:

WELL SUMMARY CHART

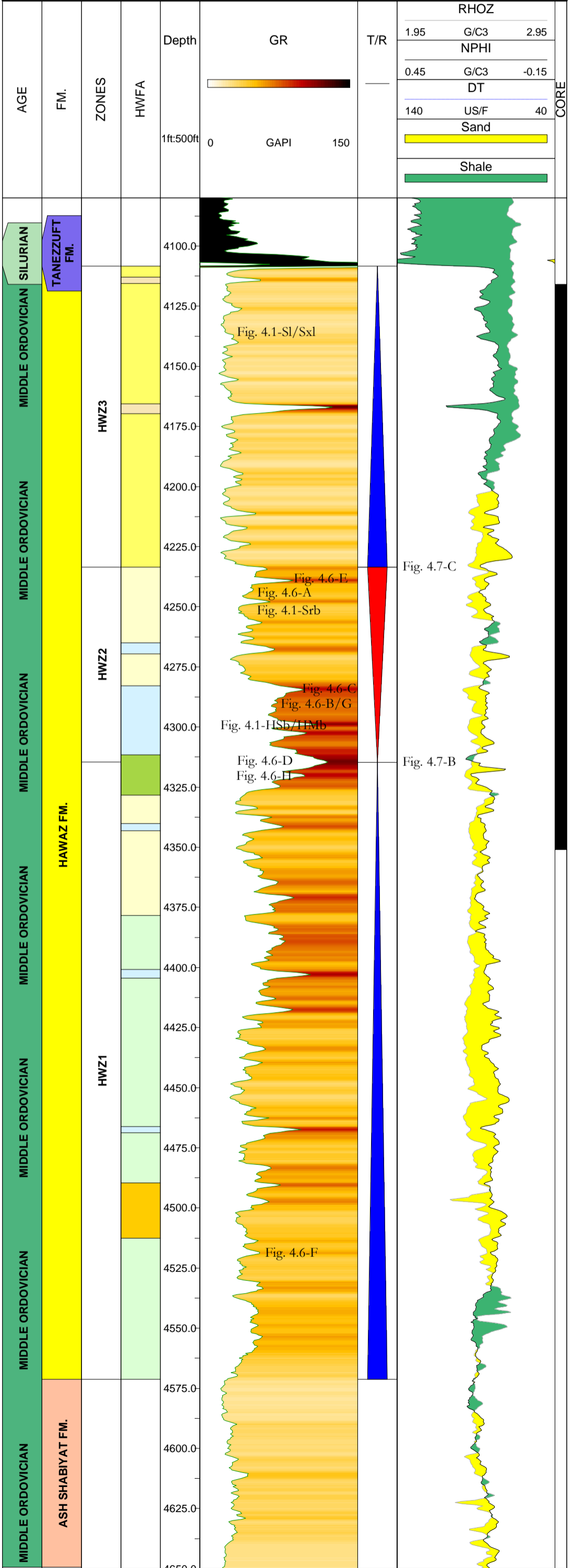
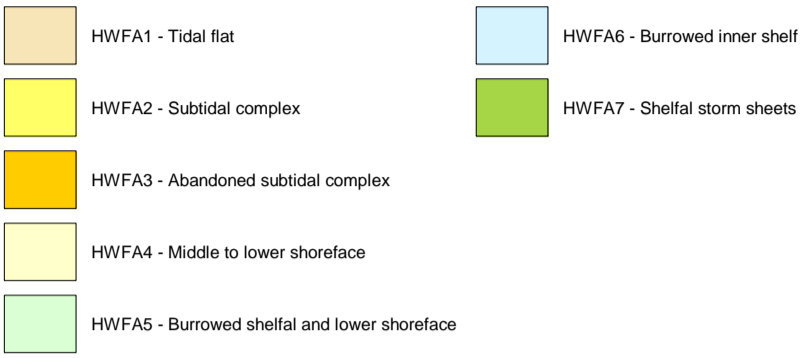
WELL:

W15

SCALE:

1:500

Hawaz Facies Associations



TITLE:

WELL SUMMARY CHART

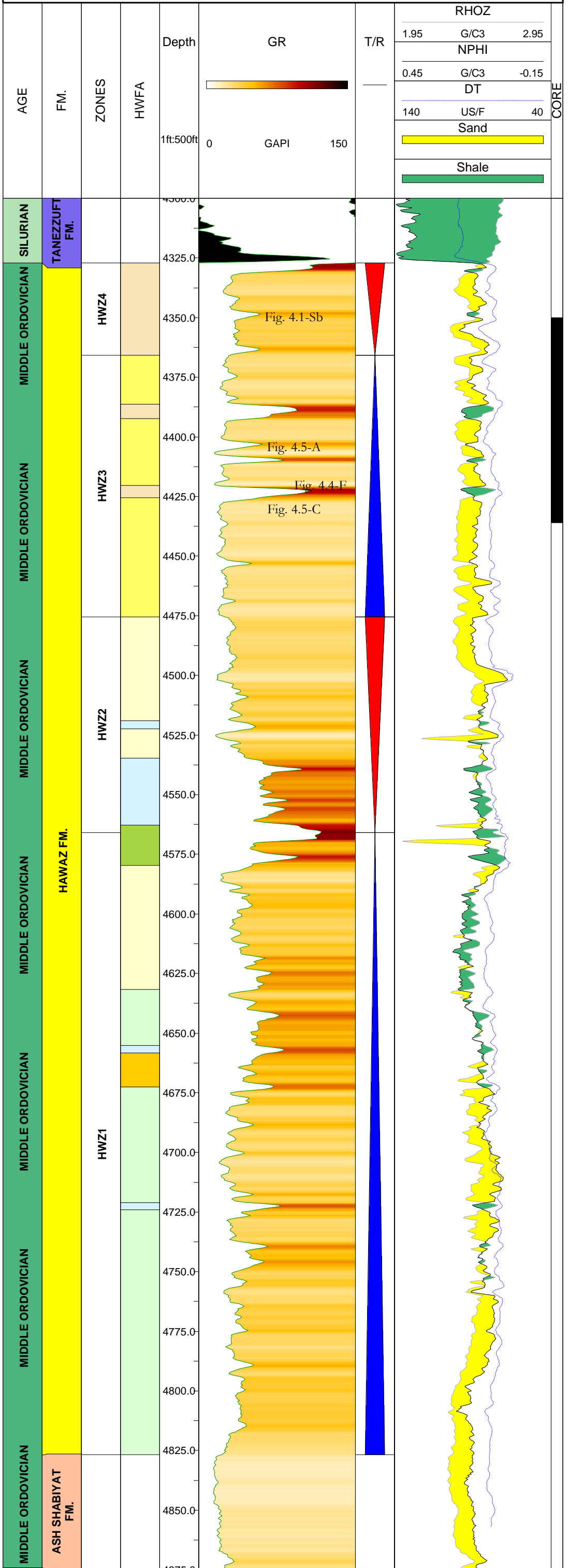
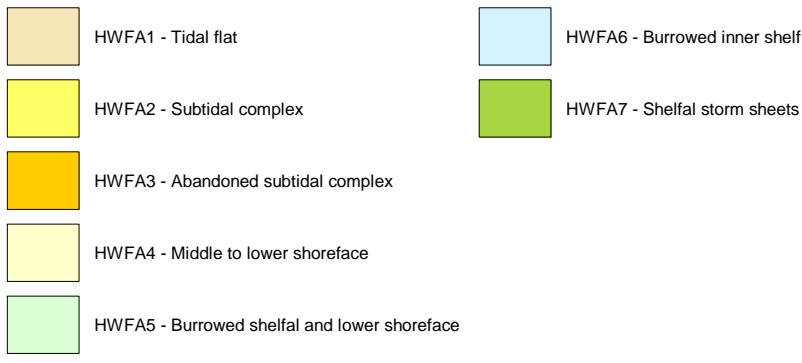
WELL:

W16

SCALE:

1:500

Hawaz Facies Associations



TITLE:

WELL SUMMARY CHART

WELL:

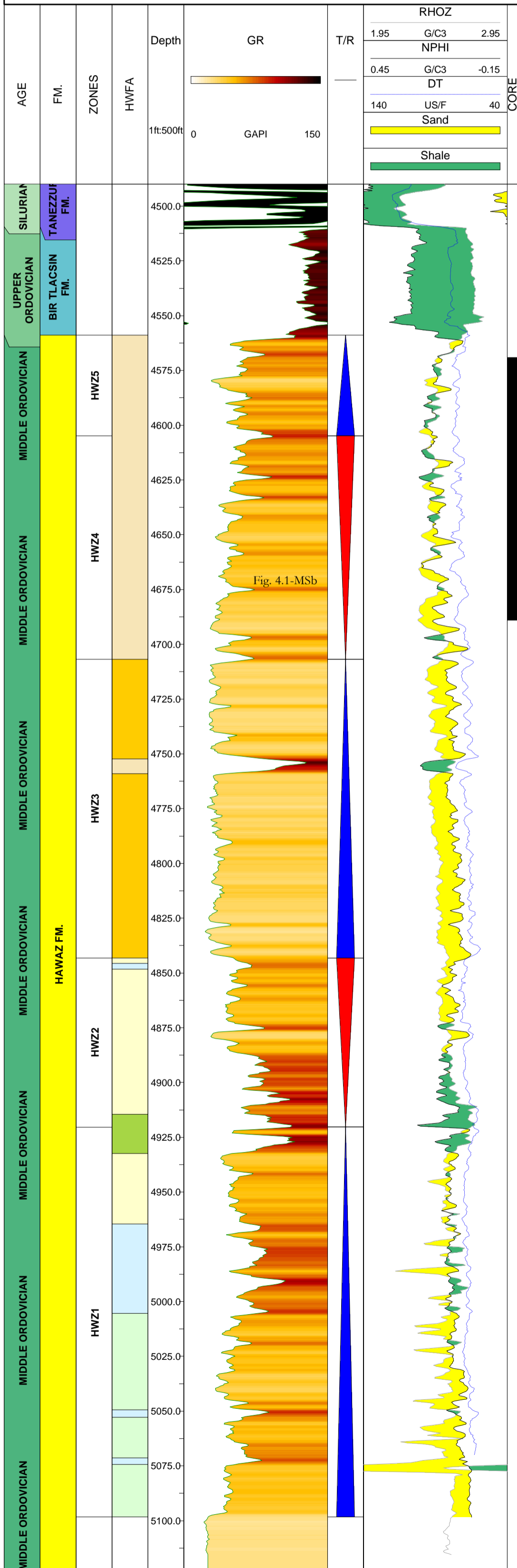
W17

SCALE:

1:500

Hawaz Facies Associations

- HWFA1 - Tidal flat
- HWFA6 - Burrowed inner shelf
- HWFA2 - Subtidal complex
- HWFA7 - Shelfal storm sheets
- HWFA3 - Abandoned subtidal complex
- HWFA4 - Middle to lower shoreface
- HWFA5 - Burrowed shelfal and lower shoreface



TITLE:

WELL SUMMARY CHART

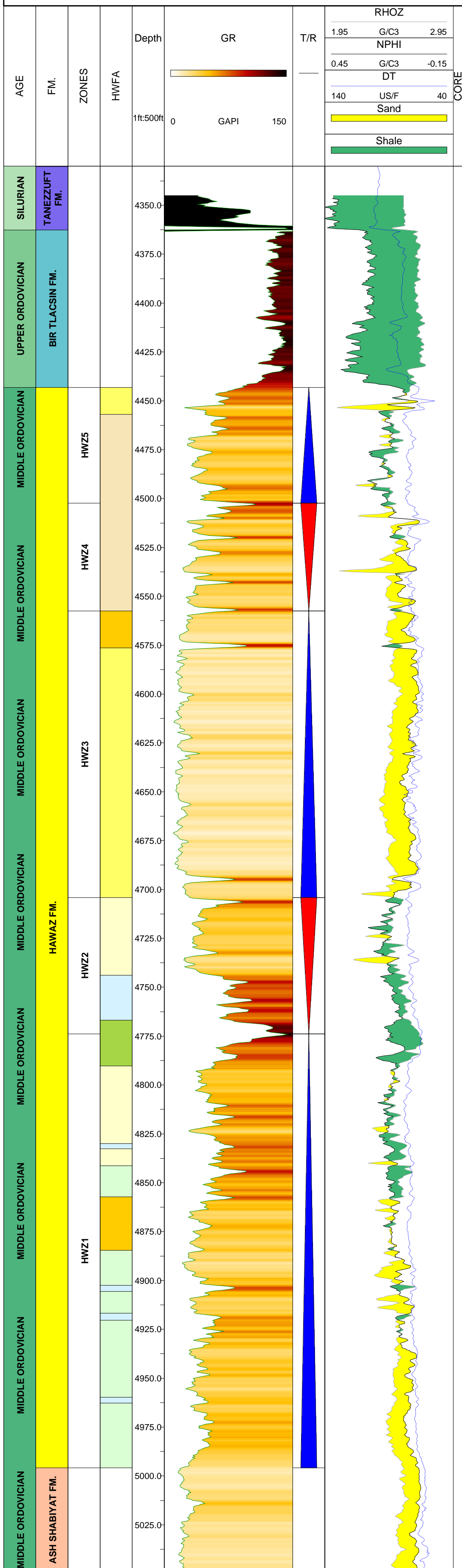
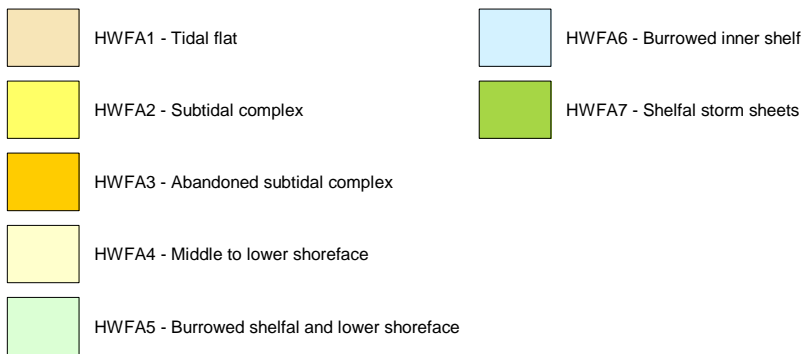
WELL:

W18

SCALE:

1:500

Hawaz Facies Associations



TITLE:

WELL SUMMARY CHART

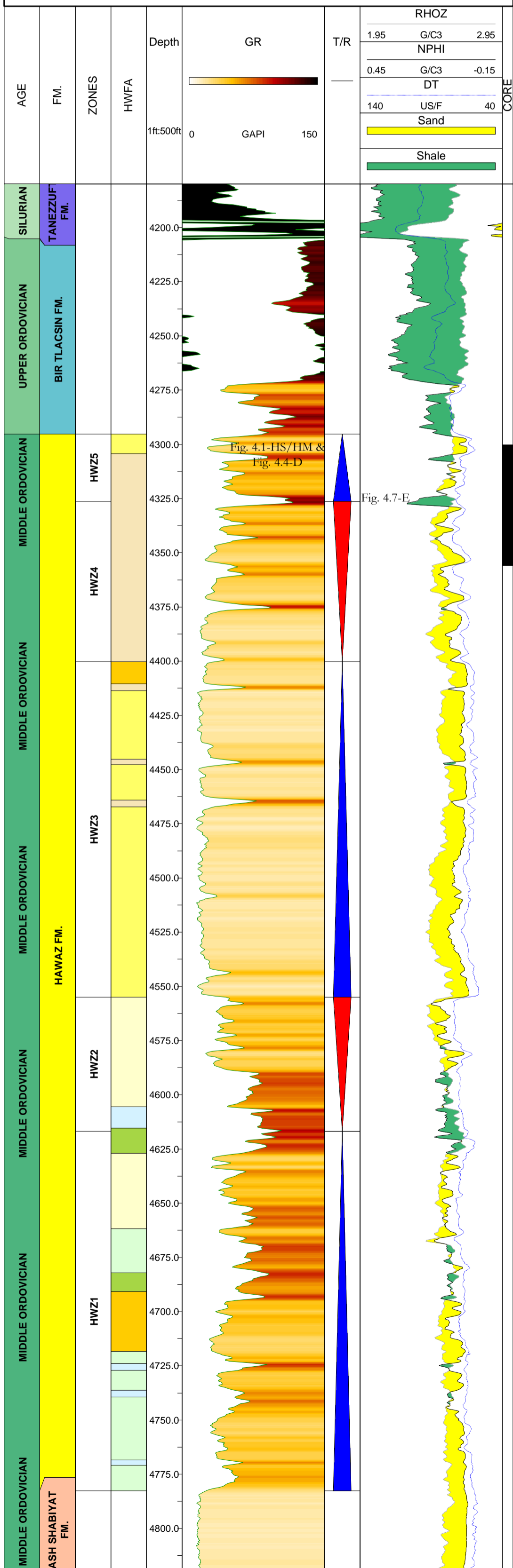
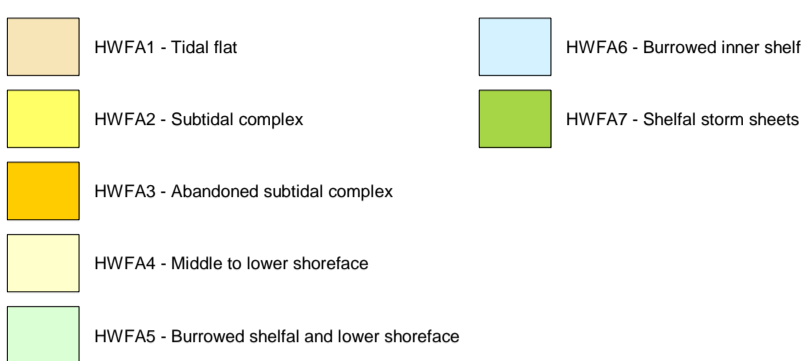
WELL:

W19

SCALE:

1:500

Hawaz Facies Associations



TITLE:

WELL SUMMARY CHART

WELL:

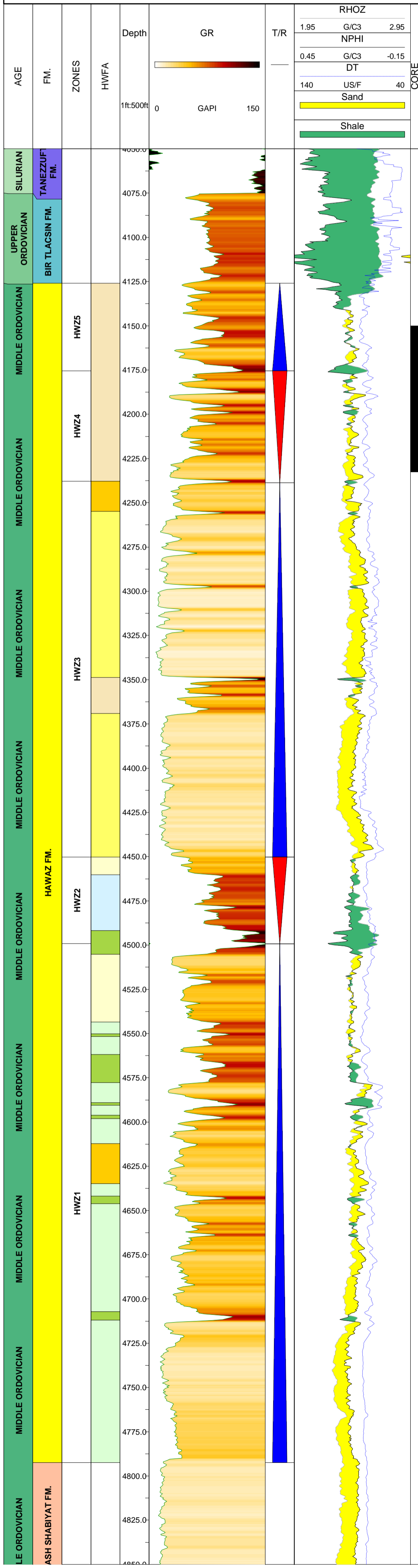
W20

SCALE:

1:500

Hawaz Facies Associations

- HWFA1 - Tidal flat
- HWFA6 - Burrowed inner shelf
- HWFA2 - Subtidal complex
- HWFA7 - Shelfal storm sheets
- HWFA3 - Abandoned subtidal complex
- HWFA4 - Middle to lower shoreface
- HWFA5 - Burrowed shelfal and lower shoreface



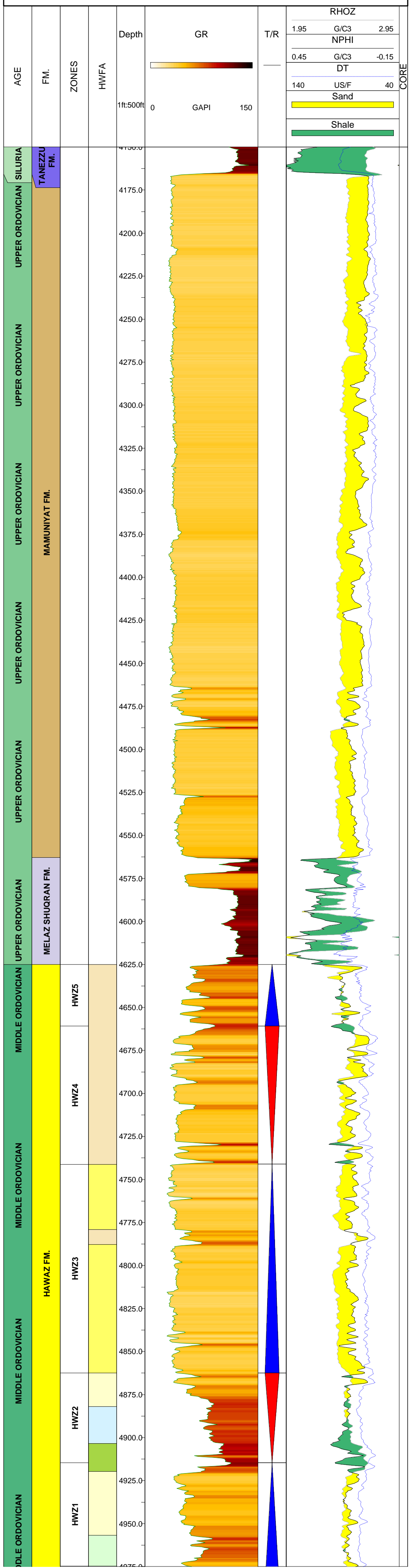
TITLE: **WELL SUMMARY CHART**

WELL: **W21**

SCALE: **1:500**

Hawaz Facies Associations

- HWFA1 - Tidal flat
- HWFA6 - Burrowed inner shelf
- HWFA2 - Subtidal complex
- HWFA7 - Shelfal storm sheets
- HWFA3 - Abandoned subtidal complex
- HWFA4 - Middle to lower shoreface
- HWFA5 - Burrowed shelfal and lower shoreface



TITLE:

WELL SUMMARY CHART

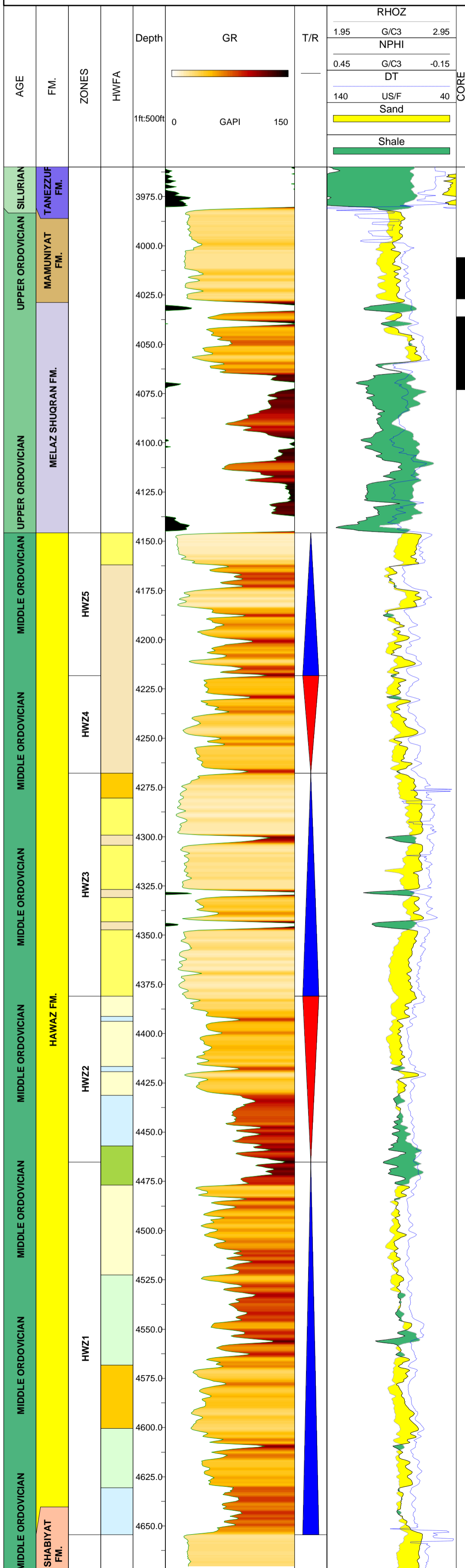
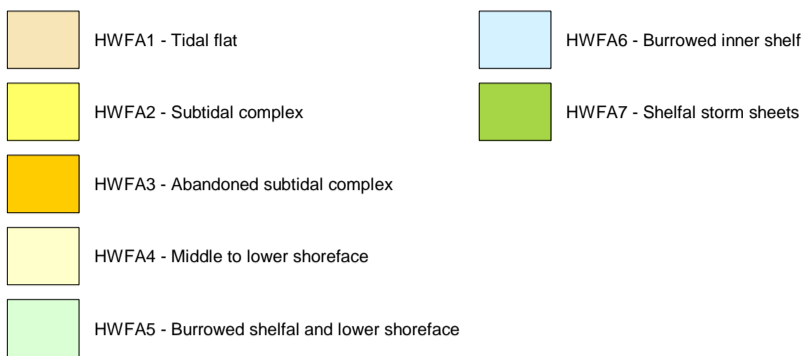
WELL:

W22

SCALE:

1:500

Hawaz Facies Associations



TITLE:

WELL SUMMARY CHART

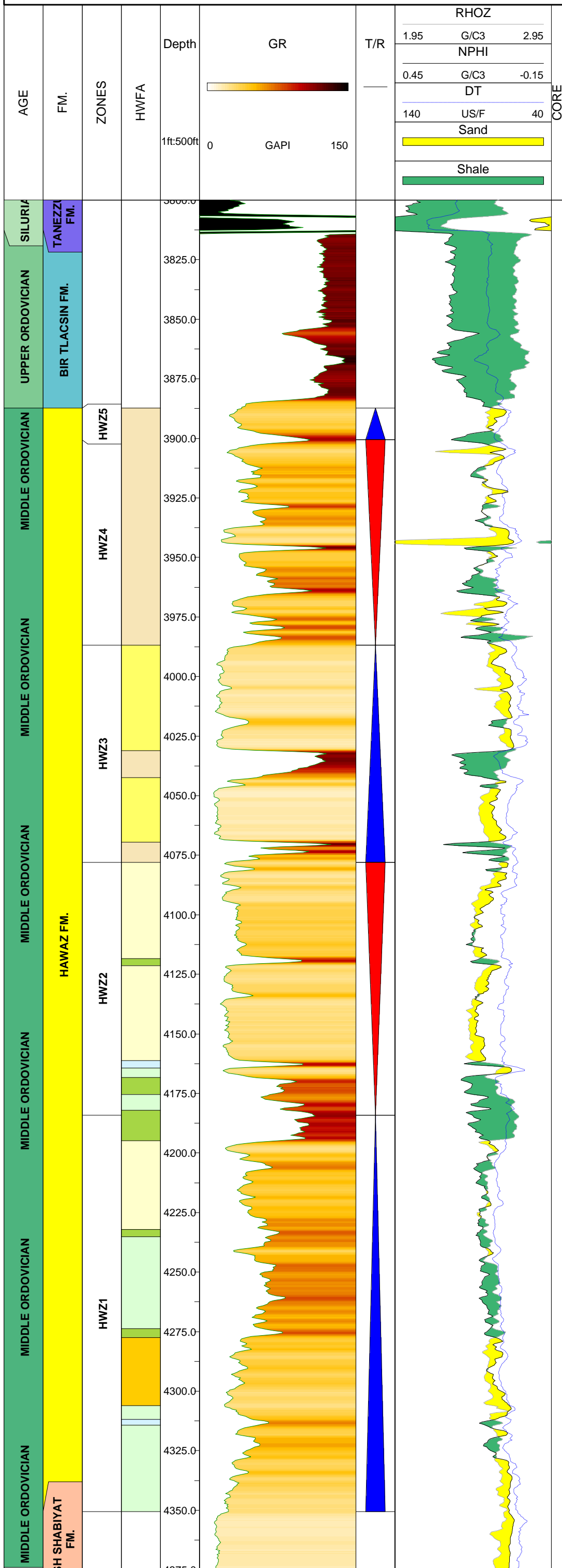
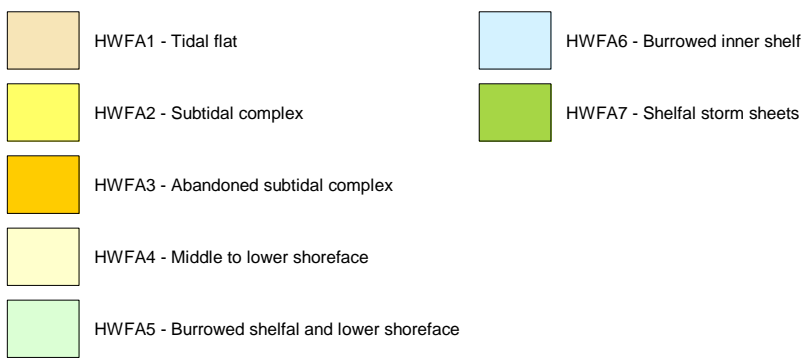
WELL:

W23

SCALE:

1:500

Hawaz Facies Associations



TITLE:

WELL SUMMARY CHART

WELL:

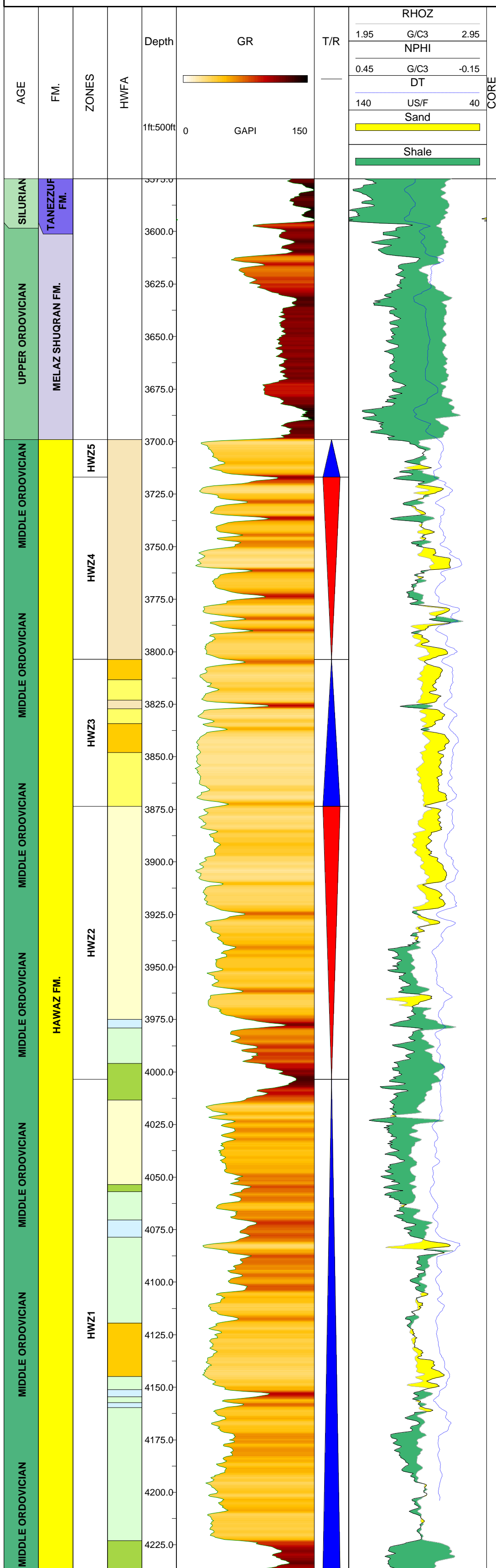
W24

SCALE:

1:500

Hawaz Facies Associations

- HWFA1 - Tidal flat
- HWFA6 - Burrowed inner shelf
- HWFA2 - Subtidal complex
- HWFA7 - Shelfal storm sheets
- HWFA3 - Abandoned subtidal complex
- HWFA4 - Middle to lower shoreface
- HWFA5 - Burrowed shelfal and lower shoreface



TITLE:

WELL SUMMARY CHART

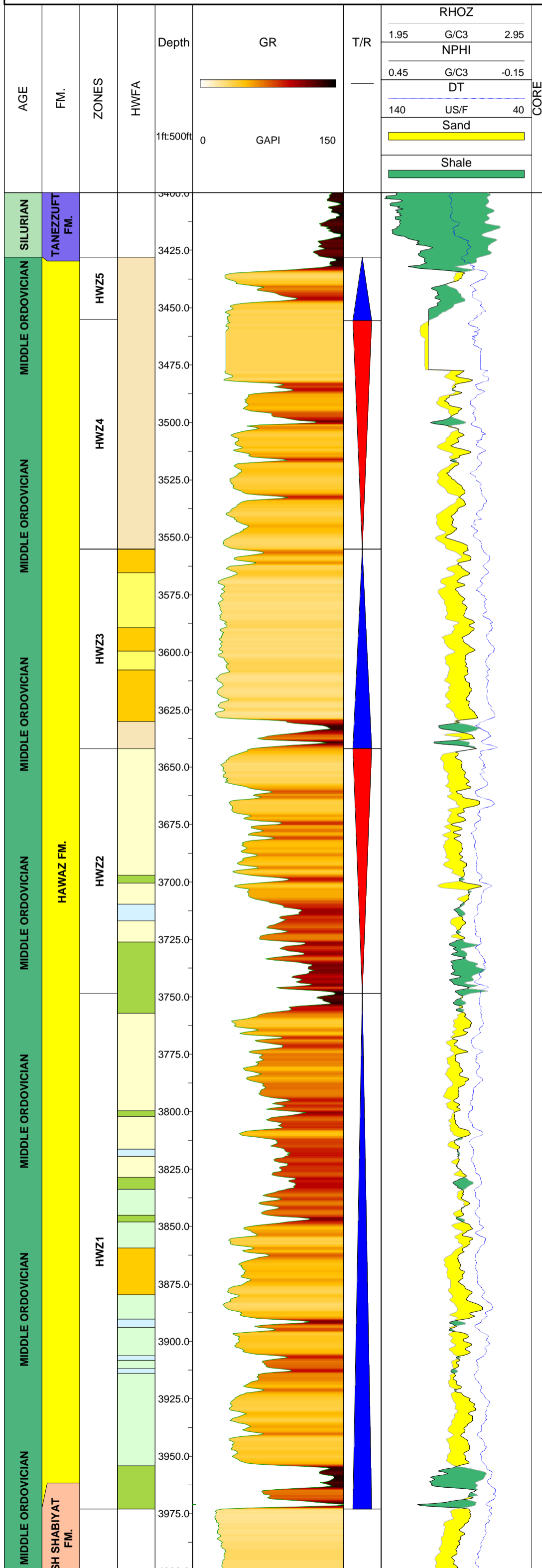
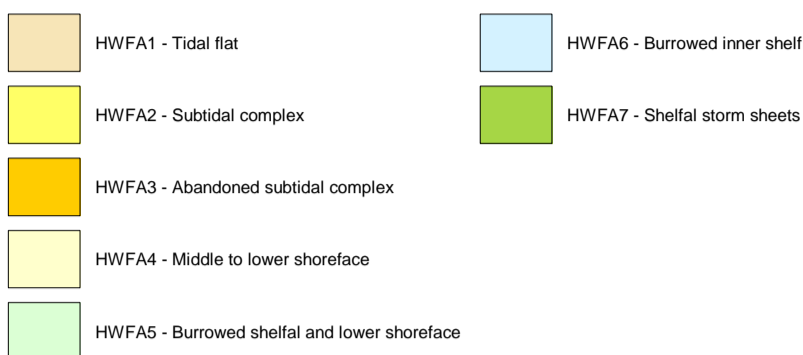
WELL:

W25

SCALE:

1:500

Hawaz Facies Associations



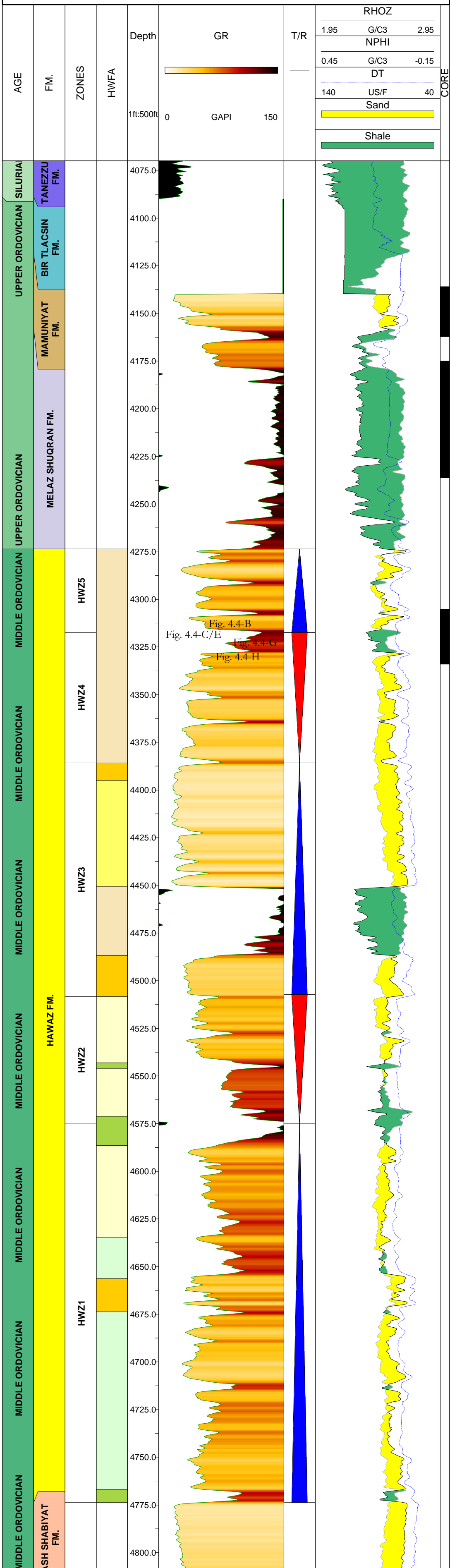
TITLE:
WELL SUMMARY CHART

WELL:
W26

SCALE:
1:500

Hawaz Facies Associations

- HWFA1 - Tidal flat
- HWFA6 - Burrowed inner shelf
- HWFA2 - Subtidal complex
- HWFA7 - Shelfal storm sheets
- HWFA3 - Abandoned subtidal complex
- HWFA4 - Middle to lower shoreface
- HWFA5 - Burrowed shelfal and lower shoreface



TITLE:

WELL SUMMARY CHART

WELL:

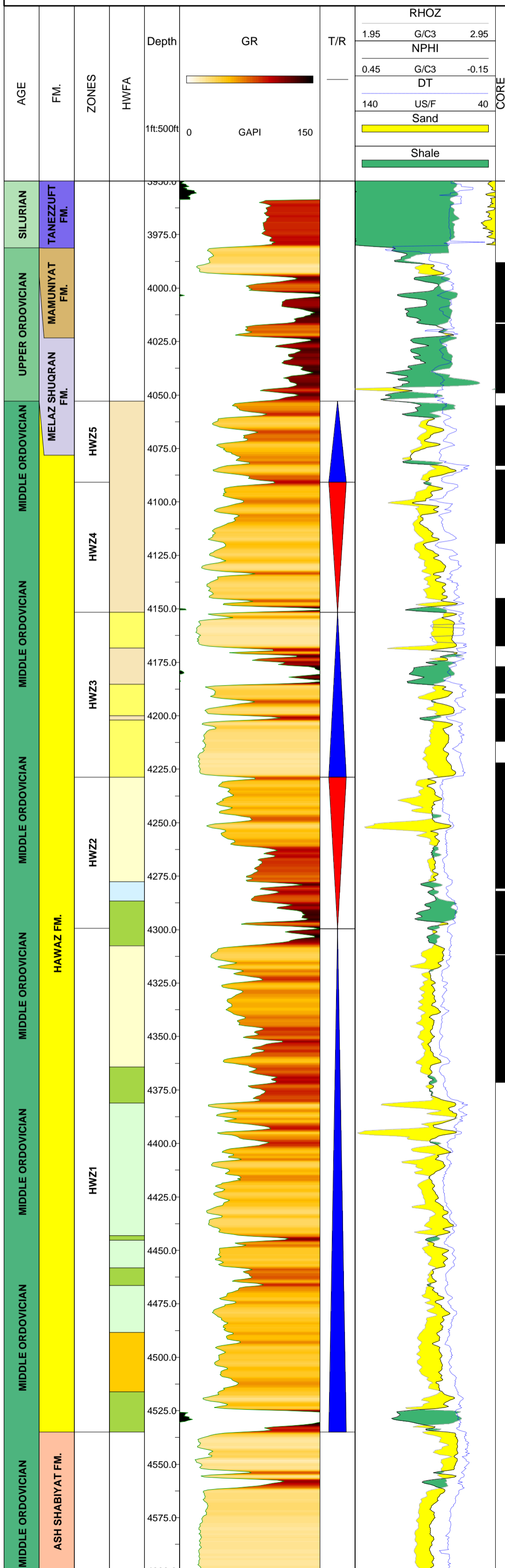
W27

SCALE:

1:500

Hawaz Facies Associations

- HWFA1 - Tidal flat
- HWFA2 - Subtidal complex
- HWFA3 - Abandoned subtidal complex
- HWFA4 - Middle to lower shoreface
- HWFA5 - Burrowed shelfal and lower shoreface
- HWFA6 - Burrowed inner shelf
- HWFA7 - Shelfal storm sheets



TITLE:

WELL SUMMARY CHART

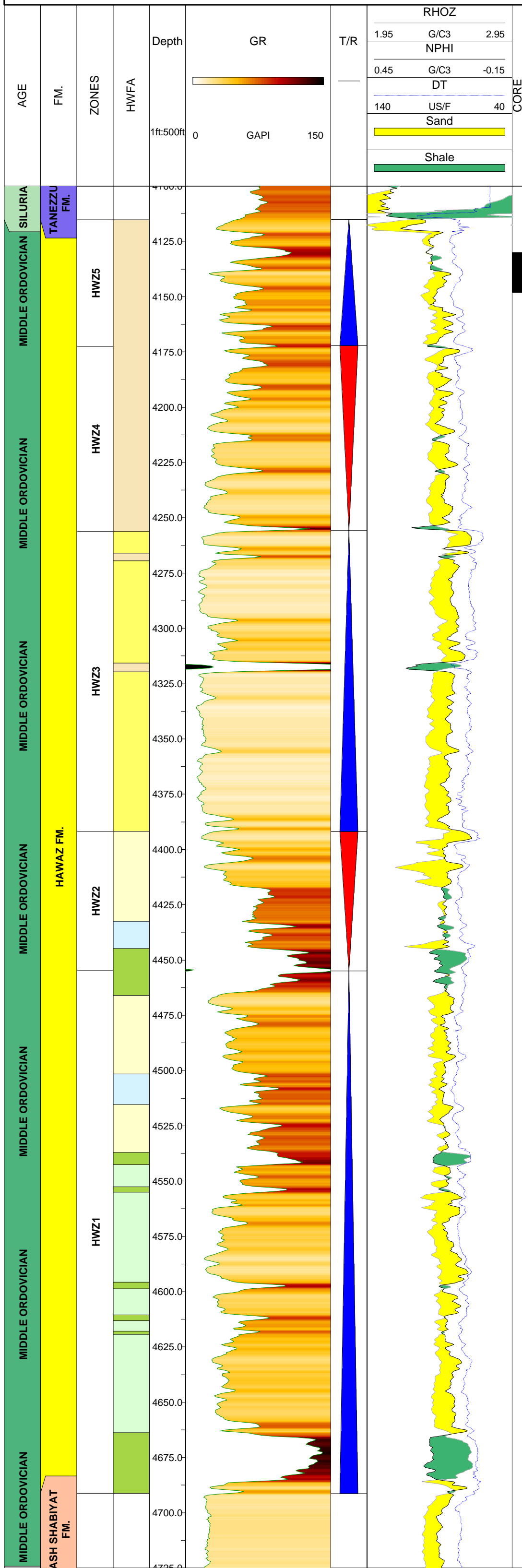
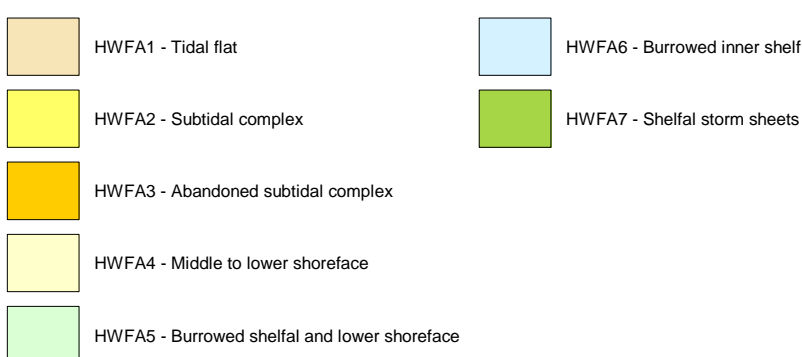
WELL:

W28

SCALE:

1:500

Hawaz Facies Associations



TITLE:

WELL SUMMARY CHART

WELL:

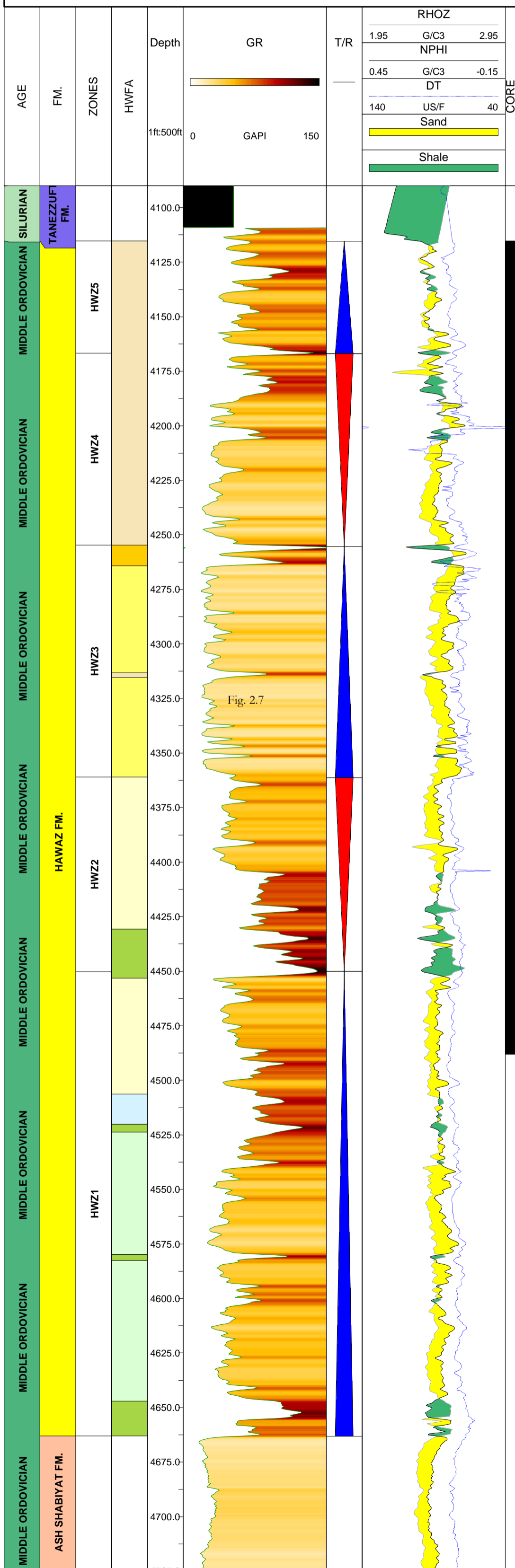
W29

SCALE:

1:500

Hawaz Facies Associations

- HWFA1 - Tidal flat
- HWFA6 - Burrowed inner shelf
- HWFA2 - Subtidal complex
- HWFA7 - Shelfal storm sheets
- HWFA3 - Abandoned subtidal complex
- HWFA4 - Middle to lower shoreface
- HWFA5 - Burrowed shelfal and lower shoreface



TITLE:

WELL SUMMARY CHART

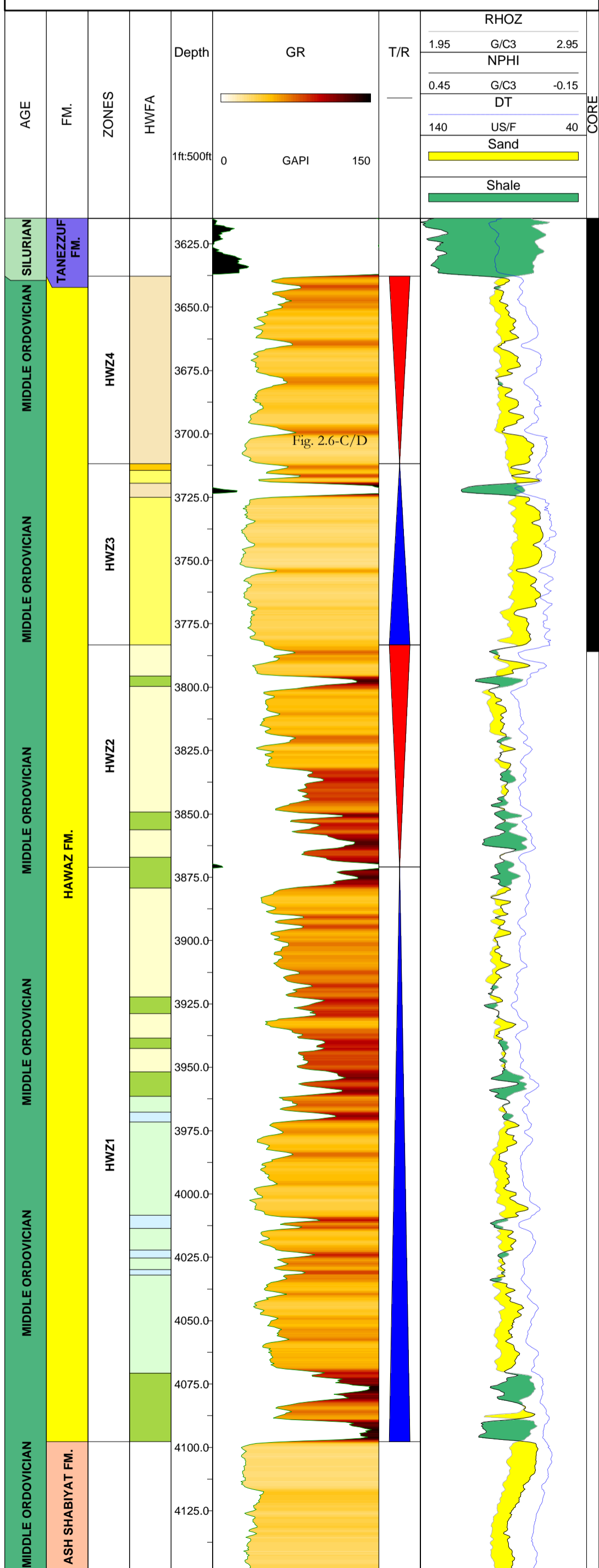
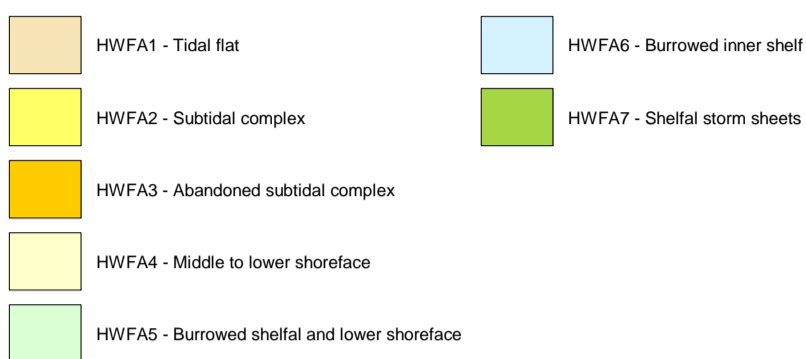
WELL:

W30

SCALE:

1:500

Hawaz Facies Associations



TITLE:

WELL SUMMARY CHART

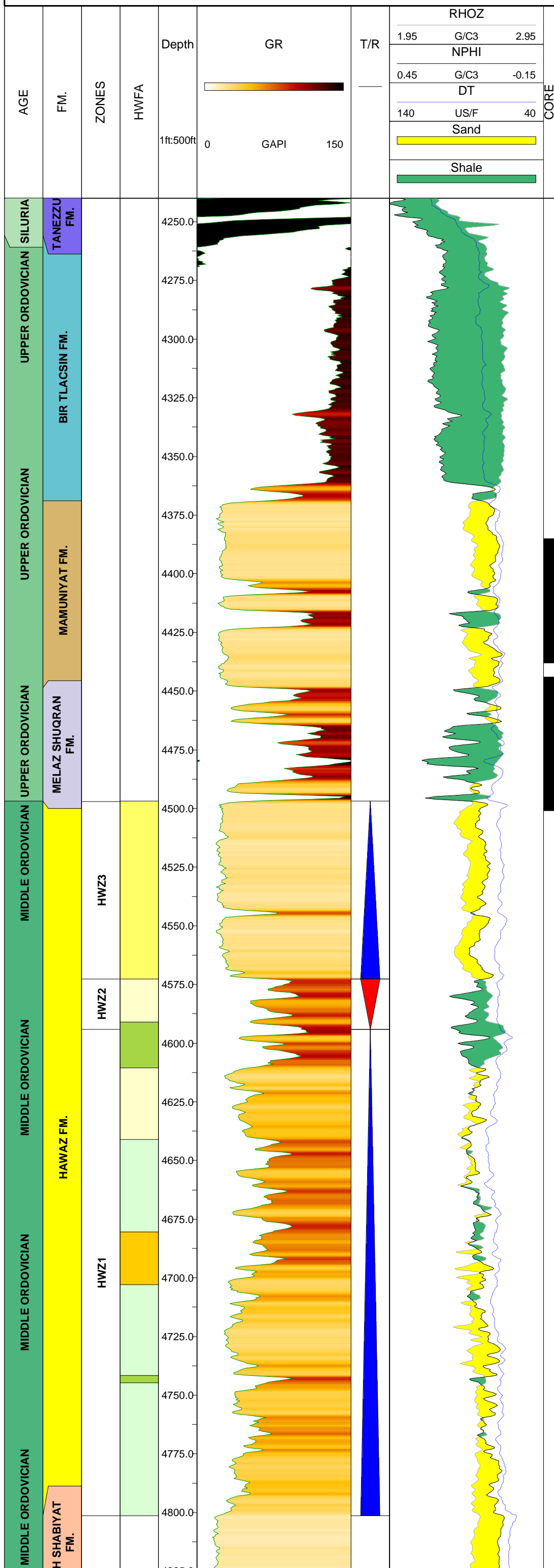
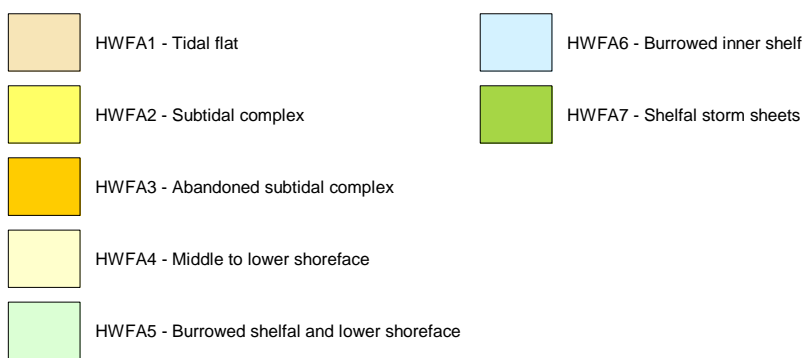
WELL:

W31

SCALE:

1:500

Hawaz Facies Associations



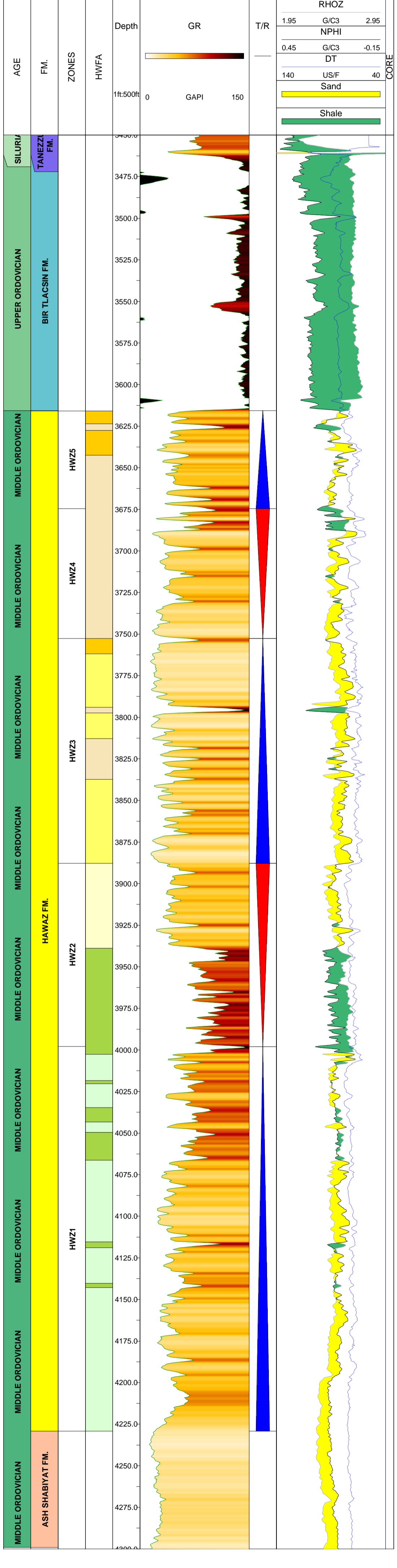
TITLE: **WELL SUMMARY CHART**

WELL: **W32**

SCALE: **1:500**

Hawaz Facies Associations

- HWFA1 - Tidal flat
- HWFA6 - Burrowed inner shelf
- HWFA2 - Subtidal complex
- HWFA7 - Shelfal storm sheets
- HWFA3 - Abandoned subtidal complex
- HWFA4 - Middle to lower shoreface
- HWFA5 - Burrowed shelfal and lower shoreface



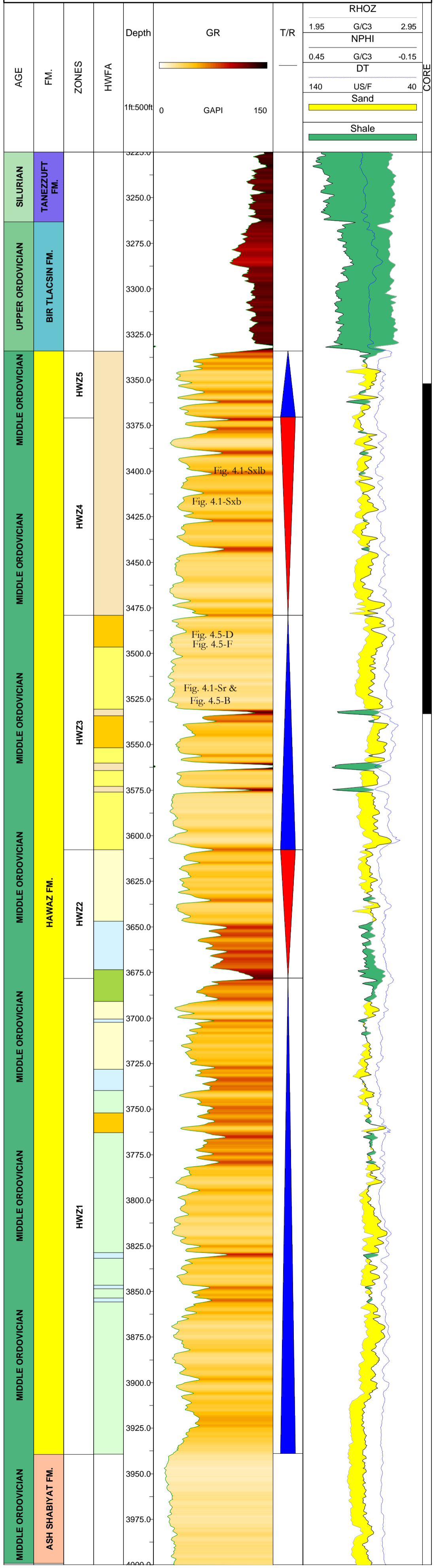
TITLE: **WELL SUMMARY CHART**

WELL: **W33**

SCALE: **1:500**

Hawaz Facies Associations

- HWFA1 - Tidal flat
- HWFA6 - Burrowed inner shelf
- HWFA2 - Subtidal complex
- HWFA7 - Shelfal storm sheets
- HWFA3 - Abandoned subtidal complex
- HWFA4 - Middle to lower shoreface
- HWFA5 - Burrowed shelfal and lower shoreface



TITLE:

WELL SUMMARY CHART

WELL:

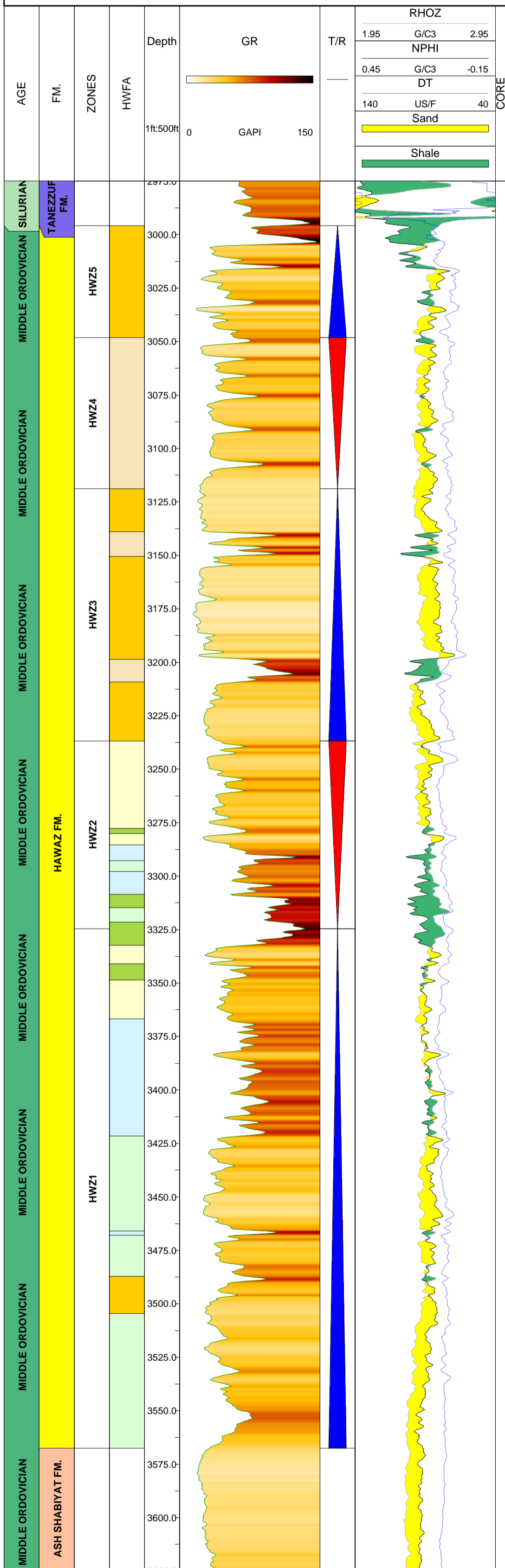
W34

SCALE:

1:500

Hawaz Facies Associations

- HWFA1 - Tidal flat
- HWFA6 - Burrowed inner shelf
- HWFA2 - Subtidal complex
- HWFA7 - Shelfal storm sheets
- HWFA3 - Abandoned subtidal complex
- HWFA4 - Middle to lower shoreface
- HWFA5 - Burrowed shelfal and lower shoreface



TITLE:

WELL SUMMARY CHART

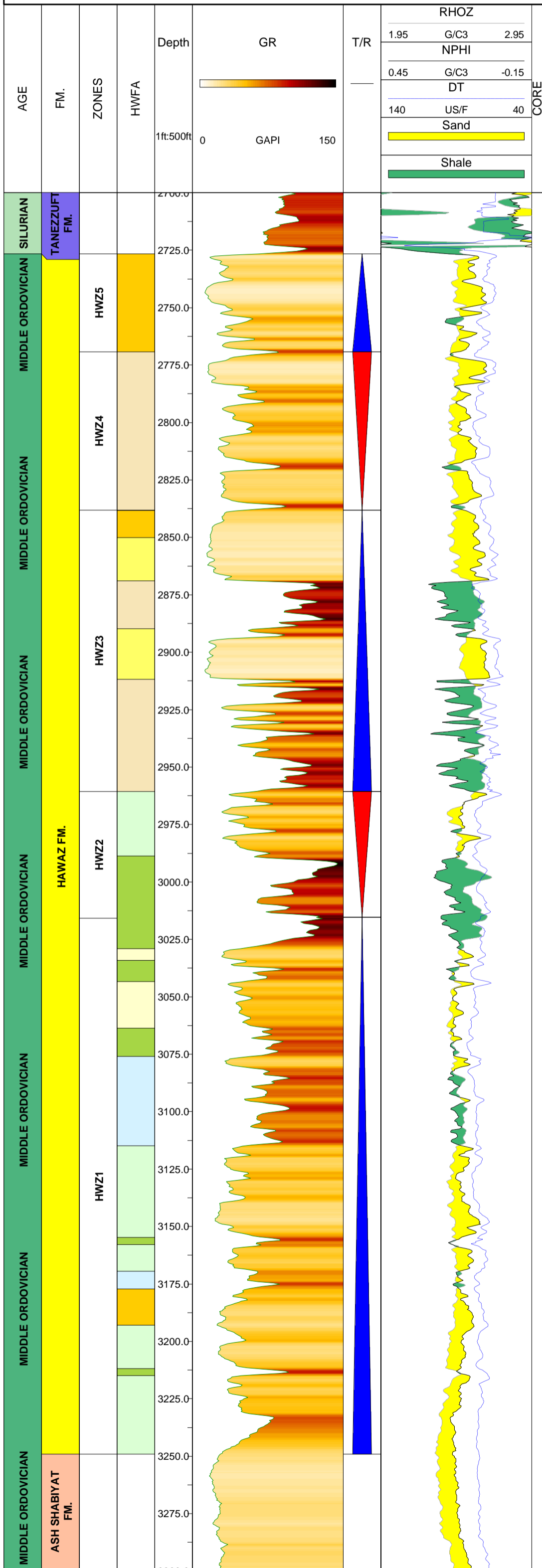
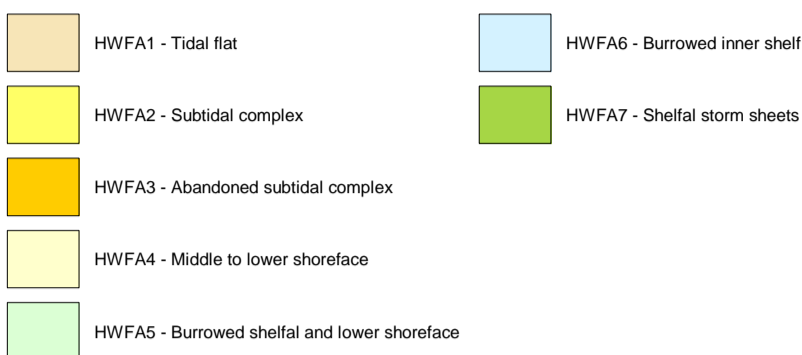
WELL:

W35

SCALE:

1:500

Hawaz Facies Associations





UNIVERSITAT DE
BARCELONA



geomodels
INSTITUT DE RECERCA